

การพัฒนากระบวนการสกัดแอนโดรกราโฟไลด์จากฟ้าทะลายโจรในคอลัมน์แบบพัลส์



นางสาว รัชฎาพร ว่องกิตติพงษ์

สถาบันวิทยบริการ

จุฬาลงกรณ์มหาวิทยาลัย

วิทยานิพนธ์นี้เป็นส่วนหนึ่งของการศึกษาตามหลักสูตรปริญญาวิทยาศาสตรดุษฎีบัณฑิต

สาขาวิชาเคมีเทคนิค ภาควิชาเคมีเทคนิค


คณะวิทยาศาสตร์ จุฬาลงกรณ์มหาวิทยาลัย

ปีการศึกษา 2546

ISBN 974-17-3981-8

ลิขสิทธิ์ของจุฬาลงกรณ์มหาวิทยาลัย

DEVELOPMENT OF ANDROGRAPHOLIDE EXTRACTION PROCESS FROM ANDROGRAPHIS  
PANICULATA NEES IN PULSED COLUMN



Miss Rutchadaporn Wongkittipong

สถาบันวิทยบริการ  
จุฬาลงกรณ์มหาวิทยาลัย

A Dissertation Submitted in Partial Fulfillment of the Requirements  
for the Degree of Doctor of Philosophy in Chemical Technology

Department of Chemical Technology

Faculty of science

Chulalongkorn University

Academic year 2003

ISBN 974-17-3981-8

Thesis Title                    DEVELOPMENT OF ANDROGRAPHOLIDE EXTRACTION  
PROCESS FROM *ANDROGRAPHIS PANICULATA* NEES IN  
PULSED COLUMN

By                                    Miss Rutchadaporn Wongkittipong

Field of Study                    Chemical Technology

Thesis Advisor                    Professor Somsak Damronglerd, Dr. Ing.

Thesis Co-advisor                Professor Christophe Gourdon, Dr. d'État.

Thesis Co-advisor                Associate Professor Lursuang Mekasut, Dr. d'Ing.

---

Accepted by the Faculty of Science, Chulalongkorn University in Partial Fulfillment  
of the Requirements for the Doctor's Degree

..... Dean of Faculty of Science  
(Professor Piamsak Menasveta, Ph.D.)

#### THESIS COMMITTEE

..... Co-chairs  
(Professor Gilbert Casamatta, Dr. d'État.)

..... Co-chairs  
(Associate Professor Tharapong Vitidsant, Dr. de l'I.N.P.T.)

..... Thesis Advisor  
(Professor Somsak Damronglerd, Dr. Ing.)

..... Thesis Co-advisor  
(Professor Christophe Gourdon, Dr. d'État.)

..... Thesis Co-Advisor  
(Associate Professor Lursuang Mekasut, Dr. Ing.)

..... Member  
(Professor Henry Angelino, Dr. d'État.)

..... Member  
(Associate Professor Woraphat Arthayukti, Dr. Ing.)

รศ.ดร. ว่องกิตติพงษ์ : การพัฒนากระบวนการสกัดแอนโดรกราโฟไลด์จากฟ้าทะลาย  
 โจรในคอลัมน์แบบพัลส์. (DEVELOPMENT OF ANDROGRAPHOLIDE  
 EXTRACTION PROCESS FROM *ANDROGRAPHIS PANICULATA* NEES IN  
 PULSED COLUMN) อ. ที่ปรึกษา : ศ.ดร. สมศักดิ์ ดำรงค์เลิศ, อ.ที่ปรึกษาร่วม : Prof.  
 Christophe Gourdon, รศ.ดร. เลอสรวง เมฆสุข, 175 หน้า. ISBN 974-17-3981-8.

งานวิจัยนี้เกี่ยวกับการสกัดของแข็ง-ของเหลวจากฟ้าทะลายโจร ซึ่งเป็นพืชสมุนไพรใน  
 ประเทศไทย ส่วนที่นำมาศึกษาคือใบและก้าน การศึกษาคุณลักษณะต่างๆเช่นความหนาแน่น  
 ขนาดอนุภาค ความพรุนและรูปร่างของก้านและใบ ขั้นตอนการศึกษาคือทำการทดลองครั้งแรก  
 ในรีแอกเตอร์แบบแบตเพื่อศึกษาอิทธิพลของตัวแปรต่อการสกัดสารแอนโดรกราโฟไลด์ เช่น  
 ปริมาณของของแข็ง เปอร์เซ็นต์สารละลายแอลกอฮอล์ที่ใช้ ขนาดอนุภาค อุณหภูมิ เกี่ยวกับไค-  
 เนติกของการสกัด ผลการสกัดที่ 70 และ 90 เปอร์เซ็นต์ ที่เวลา 20 และ 60 นาที ในการทดลอง  
 แบบแบตตามลำดับ โมเดลที่ใช้ในการถ่ายเทมวลอ้างอิงจากโมเดลที่มี 2 รูปทรง (ทรงกระบอก  
 แทนก้านและทรงแบนแทนใบของฟ้าทะลายโจร) ค่าสัมประสิทธิ์การแพร่ของแอนโดรกราโฟ  
 ไลด์ในสารละลายเอทานอล คือ  $8.43 \times 10^{-14}$  ตร.ซม/วินาที ที่อุณหภูมิห้อง และที่อุณหภูมิ 60  
 องศาเซลเซียส คือ  $52.1 \times 10^{-14}$  ตร.ซม/วินาที

สำหรับระบบการสกัดแบบต่อเนื่อง เป็นความพยายามครั้งแรกในการใช้ระบบพัลส์โดย  
 ใช้อากาศมาแทนที่ระบบพัลส์ แบบพิสตันในกระบวนการสกัดของแข็งและของเหลวในคอลัมน์  
 การสกัดเพื่อป้องกันและหลีกเลี่ยงสภาวะการท่วมภายในคอลัมน์สกัดเนื่องจากสาเหตุของส่วนที่  
 เป็นก้านของฟ้าทะลายโจรที่ไม่จมในสารละลายเอทานอล สุดท้ายงานวิจัยนี้ได้ทำการทดลอง  
 การสกัดกับอุปกรณ์ สกู – เอ็กทราเดอร์ ซึ่งเป็นอุปกรณ์ที่มีประสิทธิภาพสูงในการสกัดเพื่อเปรียบ  
 เทียบ เปอร์เซ็นต์การสกัดกับการทดลองแบบแบต

สถาบันนวัตกรรมการ  
 จุฬาลงกรณ์มหาวิทยาลัย

ภาควิชา.....เคมีเทคนิค.....	ลายมือชื่อนิติ.....
สาขาวิชา.....เคมีเทคนิค.....	ลายมือชื่ออาจารย์ที่ปรึกษา.....
ปีการศึกษา.....2546.....	ลายมือชื่ออาจารย์ที่ปรึกษาร่วม.....
	ลายมือชื่ออาจารย์ที่ปรึกษาร่วม.....

## 4273825823 : MAJOR CHEMICAL TECHNOLOGY

KEY WORD : SOLID-LIQUID EXTRACTION/ ANDROGRAPHOLIDE/  
MASS TRANSFER / MODELLING/ PUSED COLUMN

RUTCHADAPORN WONGKITTIPONG: DEVELOPMENT OF  
ANDROGRAPHOLIDE EXTRACTION PROCESS FROM *ANDROGRAPHIS  
PANICULATA* NEES IN PULSED COLUMN

THESIS ADVISOR : PROF. SOMSAK DAMRONGLERD, THESIS

COADVISOR : PROF. CHRISTOPHE GOURDON, ASSOC. PROF.

LURSUANG MEKASUT, 175 pp. ISBN 974-17-3981-8.

This work deals with the solid liquid extraction from the vegetal material. The characteristics (density, particle size, porosity and shape) of the *Andrographis paniculata* Nee which is a traditional plant in Thailand have been obtained. The extraction of andrographolide is first studied in a batch reactor. The influences of the operating conditions (initial mass, solvent concentration, particle size, temperature etc) on the kinetics of extraction have been investigated. An extraction yield of 70% to 90% has been reached at 20 to 60 min.

The mass transfer model based on the two-shape model is proposed. The diffusion coefficient of the andrographolide in the ethanol solution at the room temperature is  $8.43 \times 10^{-14} \text{ cm}^2 \cdot \text{s}^{-1}$ . It can be  $52.1 \times 10^{-14} \text{ cm}^2 \cdot \text{s}^{-1}$  at  $60^\circ\text{C}$ . Preliminary experiments with an air pulsing system have been performed in a continuous column in order to avoid the flooding due to floating particles at the top of the column.

The coupling of diffusion model with the mean residence time allows the design of the continuous process. Finally a twin screw extruder is used in order to compare the extraction yields with the batch experiments.

Department CHEMICAL TECHNOLOGY

Field of study CHEMICAL TECHNOLOG

Academic year 2003.

Student's signature.....

Advisor's signature .....

Co-advisor's signature .....

Co-advisor's signature .....

## ACKNOWLEDGEMENTS

There are numerous people whose their kind assistance is necessary to complete this thesis. First of all, I would like to express my gratitude to my co-advisors, Professor Somsak Damronglerd and Associate Professor Lursuang Mekasut for their helpful guidance, kindly advise and great support.

I also would like to extend my gratitude to Professor Christophe Gourdon who is my co-advisor for his hospitality and fruitful discussion throughout my study for 3 years in France. His laughs and sentences without “No” is forever recognized.

I would like to sincerely appreciate Professor Gilbert Casamatta and Associate Professor Tharapong Vitidsant for his duty to be the thesis defense co-chairs. Professor Henry Angelino and Associate Professor Woraphat Arthayukti, the examination committee members are acknowledged.

I would like to thank to Dr.Laurent Prat for his encouragement, supervision and contribution to help me many things about the research. His kindness and friendship is very recognized. The encouragement and practice from him can push me to complete this thesis.

The kind help from many technicians of Laboratory of chemical engineering, Toulouse (LGC) for extraction column installation and experiments are appreciated.

Many thanks to all my colleagues for their contributed suggestion, assistance, friendships and aids to help me studying French and English.

The great financial support from Thailand Research Fund and French Embassy is acknowledged. Finally, I am substantially indebted to my parents for their dedication and supports.

สถาบันวิทยบริการ  
จุฬาลงกรณ์มหาวิทยาลัย  
Rutchadaporn Wongkittipong

## CONTENTS

	PAGE
ABSTRACT (in Thai) .....	iv
ABSTRACT (in English) .....	v
ACKNOWLEDGMENTS .....	vi
CONTENTS .....	vii
LIST OF TABLES .....	x
LIST OF FIGURES .....	xi
NOMENCLATURES .....	xv
INTRODUCTION .....	1
CHAPTER I: INTRODUCTION .....	3
1.1 ANDROGRAPHIS PANICULATA NEES .....	4
1.1.1 Historical and traditional use of <i>Andrographis paniculata</i> (AP) .....	4
1.1.2 Culture .....	6
1.1.3 Harvesting and storage .....	6
1.1.4 General techniques for analysis .....	9
1.1.5 Chemical study .....	13
1.1.6 Safety .....	14
1.2 SOLID – LIQUID EXTRACTION PHENOMENA .....	15
1.2.1 Mass transfer model inside the solid particle .....	15
1.2.2 Mass transfer across the interface .....	17
1.2.3 Diffusion through cells .....	19
1.2.4 Example of tea infusion .....	21
1.3 FACTORS INFLUENCING THE EXTRACTION .....	24
1.3.1 Influence of the solid .....	24
1.3.2 Influence of the solute .....	25
1.3.3 Influence of the solvent .....	27
1.3.4 Influence of the temperature .....	28
1.3.5 Influence of agitation .....	28
1.3.6 Influence of humidity .....	28
1.4 METHODS OF EXTRACTION .....	28
1.4.1 Single stage or simple contact operation .....	28
1.4.2 Multiple stages operation .....	29
1.4.2.1 <i>Cross-current operation</i> .....	29
1.4.2.2 <i>Counter-current operation</i> .....	29
1.5 PULSED COLUMN EXTRACTION .....	30
1.5.1 General characteristics of pulsed columns .....	30
1.5.2 Air pulsed column .....	33
CONCLUSION .....	37
CHAPTER II: BATCH EXTRACTION EXPERIMENTS .....	38
INTRODUCTION .....	38
2.1 PLANT ANALYSIS .....	39
2.1.2 Plant Structure and geometrical characteristics .....	40
2.1.3 Porosity and apparent density of solid .....	41
Parameters .....	43
2.1.4 Calibration curve of andrographolide by HPLC .....	45
2.1.5 The Soxhlet Experiments .....	47
2.1.6 Solubility .....	49

## CONTENTS (continued)

	PAGE
2.2 KINETICS OF EXTRACTION.....	51
2.2.1 Batch reactor experiments.....	51
2.2.3 Effect of solvent concentration.....	54
2.2.4 Effect of particle size.....	56
2.2.5 Effect of Temperature.....	57
2.3.1 Effect of boiling point temperature of solvent.....	59
2.3.2 The influence of storage time on the herb quality.....	63
2.4 SOLVENT ABSORPTION IN PLANT.....	67
2.4.1 Solvent absorption.....	67
2.4.2 The relation of mass and volume of solid particle in the solution.....	69
CONCLUSION.....	71
CHAPTER III: MASS TRANSFER MODEL.....	72
INTRODUCTION.....	72
3.1 MODEL HYPOTHESIS.....	73
3.2 GENERAL EQUATIONS.....	74
3.2.1 Initial and boundary conditions.....	74
3.3 COMPARISON BETWEEN EXPERIMENTS AND MODEL.....	76
3.3.1 Numerical Treatment.....	76
3.3.2 Programming.....	78
3.3.3 Typical results of the simulation.....	79
3.4 IDENTIFICATION OF THE DIFFUSION COEFFICIENT.....	81
3.4.1 Influence of the solvent concentration.....	82
3.4.2 Influence of the particle size.....	82
3.4.3 Influence of the amount of solid.....	83
3.4.4 Influence of temperature.....	84
CONCLUSION.....	84
CHAPTER IV: CONTINUOUS PROCESS.....	85
INTRODUCTION.....	85
4.1 COLUMN AND PULSATION SYSTEM DESCRIPTION.....	86
4.1.1 Column.....	86
4.1.2 The pneumatic pulsation system.....	88
4.1.3 Calibration.....	90
4.1.3.1 Calibration curve of the liquid pump.....	90
4.1.3.2 Calibration curve of solid feed.....	91
4.1.4 Column operation.....	92
4.2 STEADY- STATE EXPERIMENTAL RESULTS.....	93
4.2.1 Liquid study without solids.....	93
4.2.2 Study of the solid at nominal conditions.....	97
4.2.2.1 Variations of $\frac{\dot{m}_{SO}}{\dot{m}_{SI}}$ and $\frac{\dot{m}_{SO}'}{\dot{m}_{SI}'}$ .....	98
4.2.2.2 Variations of $\alpha'_0$ .....	100
4.2.2.3 Conclusions.....	102
4.3 DYNAMIC EXPERIMENTAL RESULTS.....	103
4.3.1 Typical experimental results.....	103



## CONTENTS (continued)

	PAGE
4.3.2 Solid mass outlet.....	104
4.3.3 Transient regime (dynamic duration).....	105
4.3.4 Accumulated mass.....	106
4.3.5 Moving mass and dead mass.....	109
4.3.6 Mean residence time.....	112
4.4 EXTRACTION YIELDS AND RESIDENCE TIMES.....	113
CONCLUSION.....	117
CHAPTER V: TWIN SCREW EXTRUDER AND OPTIMIZATION.....	118
INTRODUCTION.....	118
5.1 TWIN-SCREW EXTRUDER.....	119
5.2 EXPERIMENT.....	120
5.2.1 Twin-screw extruder.....	120
5.3 OPTIMIZATION OF THE OPERATING CONDITIONS IN THE EXTRACTION COLUMN.....	124
5.3.1 Determination of the equation of $\dot{m}_{so}$ .....	125
5.3.2 Determination of the equation relative to the moving mass.....	126
5.3.3 Determination of the residence time.....	127
5.3.4 Determination of the extraction rate.....	128
5.3.5 Determination of the extraction yield.....	128
5.3.6 Determination of the equilibrium.....	129
5.3.7 Example of design.....	131
CONCLUSION.....	133
GENERAL CONCLUSIONS.....	134
APPENDICES.....	144
CURRICULUM VITAE.....	168

จุฬาลงกรณ์มหาวิทยาลัย

## LIST OF TABLES

TABLE	PAGE
1.1	Total percentage of diterpene lactone in AP at different growth periods.....7
1.2	Total percentage of diterpene lactones in the aerial part of AP after different periods of storage .....8
1.3	Published correlations relative to the diffusion coefficient .....26
2.1	Mass percentage of solid.....39
2.2	Determination of porosity and density by using solid: 0.45-0.6 mm, 5 g, solvent: 60% ethanol, $T_{\text{room}}$ : 20° C.....43
2.3	Determination of porosity and density by using mass of solid: 20 g, solvent: 60% ethanol, $T_{\text{room}}$ : 20°C .....43
2.4	Determination of porosity and density by using mass of solid 5 g, solvent: 30% ethanol, $T_{\text{room}}$ : 20°C .....44
2.5	Concentrations of andrographolide (mg/ml, mg/g) from soxhlet experiments (90% ethanol) .....48
2.6	Concentration of andrographolide (mg/g) from soxhlet experiment.....48
2.7	Experimental operating conditions .....52
3.1	Coefficients of diffusions obtained by optimization .....81
4.1	Experimental amplitudes in the column .....94
4.2	Operating conditions.....97
4.3	Results (Measurement).....98
4.4	Estimated data from the graph of the mass solid outlet at the bottom of the column as a function of time .....104
4.5	The residence time of the solid in the middle and at the bottom of the column .....116
5.1	Operating data of the experiments conducted with the twin screw extruder.121
5.2	Extraction yields from the twin screw extruder process.....123
5.3	Mass balance .....124
5.4	Solid output-solid input ratio according to the solid feed.....125
5.5	Experimental results on the moving mass .....126

จุฬาลงกรณ์มหาวิทยาลัย

## LIST OF FIGURES

FIGURE	PAGE
1.1	Andrographis paniculata Nees plant.....5
1.2	Leaves and stems of <i>Andrographis paniculata</i> Nees plant.....5
1.3	Seeds of <i>Andrographis paniculata</i> Nees .....5
1.4	Diagram of color test by using Kedde A and Kedde B (Standard of Thai Herbal Medicine: <i>Andrographis paniculata</i> (Burm.f.) Nees, 1999).....9
1.5	Diagram of color test using ethanolic potassium hydroxide (Standard of Thai Herbal Medicine: <i>Andrographis paniculata</i> (Burm.f.) Nees, 1999).....9
1.6	Method to identify the diterpene lactones of AP powder (Standard of Thai Herbal Medicine: <i>Andrographis paniculata</i> (Burm.f.) Nees, 1999).....12
1.7	The main active components in AP leaves .....14
1.8	Schematic concentration profiles during leaf infusion at (a) $t = 0$ ; (b) given $t$ ; (c) $t = \infty$ .....21
1.9	Cross-current extraction.....29
1.10	Counter-current extraction .....29
1.11	Different types of flow regimes in a pulsed column .....31
1.12	The pulsed flow regimes in the case of a solid-liquid counter-current application.....32
1.13	(a-d) show typical arrangements for air pulsing system (Baird, 1967): piston (a), rotary valve (b), self-triggered (c), and water-blow (d) (detail of pulsed leg only).....34
1.14	Water-blow pulsation apparatus (not at scale).....36
2.1	Distribution of mass percentage versus diameter of solid .....40
2.2	The structure of <i>Andrographis paniculata</i> (leaf and stem) from the Scanning Electronic Microscope.....40
2.3	Standard curve of andrographolide of 90% ethanol by HPLC .....46
2.4	Standard curve of andrographolide of 47.5%, 60% ethanol by HPLC.....46
2.5	Soxhlet Reactor .....47
2.6	Andrographolide concentrations as a function of the solid mass.....50
2.7	Andrographolide concentrations at the different times in vacuum evaporator.....51
2.8	Solid-liquid batch reactor .....52
2.9	Influence of initial solid mass on solute concentration (500 ml of 60% ethanol, $T_{\text{room}}$ : 22°C and solid diameter: 0.6-0.8 mm).....53
2.10	Influence of initial solid mass on solute mass percentage (500 ml of 60% ethanol, $T_{\text{room}}$ : 22°C and solid diameter: 0.6-0.8 mm).....53
2.11	Influence of initial solid mass on solute concentration (500 ml of water, $T_{\text{room}}$ : 22°C and solid diameter: 0.6-0.8 mm).....54
2.12	Influence of initial solid mass on solute mass percentage (500 ml of water, $T_{\text{room}}$ : 22°C and solid diameter: 0.6-0.8 mm).....54
2.13	Influence of percentage of ethanol on solute concentration (500 ml of ethanol solvent, $T_{\text{room}}$ : 22°C, solid mass: 10 g and solid diameter: 0.6-0.8 mm).....55
2.14	Influence of the percentage of ethanol on the solute mass percentage (500 ml of ethanol solvent, $T_{\text{room}}$ : 22°C, solid mass: 10 g and solid diameter: 0.6-0.8 mm).....55
2.15	Influence of percentage of ethanol on final solute concentration (500 ml of ethanol solvent, $T_{\text{room}}$ : 22°C, solid mass: 10 g and solid diameter: 0.6-0.8 mm).....56

## LIST OF FIGURES (continued)

FIGURE	PAGE
2.16 Influence of particle size on solute concentration (500 ml of 60% ethanol, $T_{\text{room}}$ : 22°C and solid mass: 10 g) .....	56
2.17 Influence of particle size on solute mass percentage (500 ml of 60% ethanol, $T_{\text{room}}$ : 22°C and solid mass: 10 g) .....	57
2.18 Influence of temperature on solute concentration (500 ml of 60% ethanol, solid mass: 10 g and solid diameter: 0.6-0.8 mm) .....	58
2.19 Influence of temperature on solute mass percentage (500 ml of 60% ethanol, solid mass: 10 g and solid diameter: 0.6-0.8 mm) .....	58
2.20 Concentration of andrographolide by varying boiling points of solvent (solid diameter: 0.6-0.8 mm).....	59
2.21 Andrographolide molecular structures .....	60
2.22 Possible mechanisms of the destruction of andrographolide .....	61
2.23 Reduction of andrographolide concentration as a function of time for different temperatures (initial kinetics) in logarithm scale .....	62
2.24 Influence of temperature on the constant of kinetics.....	62
2.25 Influence of storage time on the solute concentration 500 ml of water, solid mass: 10 g (Batch A).....	63
2.26 Influence of time on solute mass percentage 500 ml of water, solid mass: 10 g (Batch A).....	64
2.27 Influence of time on solute concentration 500 ml of 70% ethanol, solid mass: 10 g (Batch A).....	64
2.28 Influence of time on solute mass percentage 500 ml of 70% ethanol, solid mass: 10 g (Batch A).....	64
2.29 Solute concentration as function of time 500 ml of 70% ethanol, solid mass: 10 g by using the humid plant (Batch A).....	65
2.30 Solute mass percentage as function of time 500 ml of 70% ethanol, solid mass: 10 g by using the humid plant (Batch A).....	65
2.31 Solute concentration as a function of time 500 ml of 95% ethanol, solid mass: 10 g by using the humid plant (Batch A).....	66
2.32 Solute concentration as a function of time 500 ml of 95% ethanol, 10 g and 20g of new plant (Batch B) and 10g, 0.6-0.8 mm of Batch A.....	67
2.33 Solute mass percentage as a function of time 500 ml of 95% ethanol, 10g and 20g of new plant (Batch B) and 10 g, 0.6-0.8 mm of Batch A.....	67
2.34 The absorption of solid particles in the different ethanol solutions after 5 min .....	68
2.35 The floating and sinking volume percentages of solid particle in different ethanol solutions as a function of time .....	68
2.36 The dynamics of the floating solid as for a 95 % ethanol solution as a function of time.....	69
2.37 The mean $R_{95\%}$ as a function of the percentage of ethanol.....	69
2.38 The mass-volume relation of the floating solid (mostly stems).....	70
2.39 The mass-volume relation of the sinking solid (mostly leaves).....	70
3.1 Concentration profile for $\phi = 2$ (cylindrical shape).....	79
3.2 Concentration profile for $\phi = 1$ (plate shape).....	79
3.3 Geometric shape factor $\phi$ corresponding to the solid particle shape.....	80

## LIST OF FIGURES (continued)

FIGURE	PAGE
3.4 Comparison between experiments and model at $D = 5.06 \times 10^{-12} \text{ m}^2/\text{min}$ (solid diameter: 0.6-0.8mm, 60 % ethanol, Temp: 22°C, with $\phi$ : 1 and 2 respectively) .....	80
3.5 Comparison between experiments and model at $D = 5.06 \times 10^{-12} \text{ m}^2/\text{min}$ (solid diameter: 0.6-0.8 mm, 60 % ethanol and Temp: 22°C) .....	81
3.6 The diffusion coefficient as a function of percentage of ethanol (solid diameter: 0.6-0.8 mm, 500 ml of ethanol solution and Temp: 22°C) .....	82
3.7 The diffusion coefficient as a function of the diameter of particles (solid mass: 10g, 500 ml of 60%ethanol and Temp 22 °C) .....	83
3.8 The diffusion coefficient as a function of the amount of solid (solid diameter: 0.6-0.8mm, 500 ml of 60%ethanol, and Temp 22°C) .....	83
3.9 The diffusion coefficient as a function of temperature (solid diameter: 0.6-0.8mm, 500 ml of 60%ethanol, solid mass: 10g) .....	84
4.1 The schematic representation of the column .....	86
4.2 The phenomena within the column as a result of the pulsation system .....	88
4.3 Schematic of an air pulsing system .....	89
4.4 The operation function of ER3000 (Electronic Regulator) .....	89
4.5 The setpoint function .....	90
4.6 The calibration curve of the liquid flow .....	91
4.7 The calibration curve of the solid feed .....	91
4.8 The profile of the air pulsing at the lower set point is 80 to 100 psi .....	93
4.9 The profile of the air pulsing at the lower set point is 70 to 100 psi .....	93
4.10 The pressure profile .....	94
4.11 The relation between the level and the pressure of impulsion and pulsation in the column .....	95
4.12 The mass liquid outlet as a function of time at the set point is 80-100 psi .....	96
4.14 Solid flow rate ratio at the bottom and at the top of the column as a function of percentage of ethanol .....	99
4.15 Solid flow rate ratio at the bottom and at the top of the column as a function of mass inlet of solid .....	99
4.16 Experimental results of $\alpha_o$ ' function of percentage of ethanol when the mass solid input is $N^{\circ}1 = 11.33 \text{ g}/\text{min}$ .....	100
4.17 The experimental results of $\alpha_o$ ' as a function of the mass solid inlet when the initial level of the liquid is at the first plate .....	101
4.18 Experimental results of $\alpha_o$ ' as a function of the initial liquid level .....	102
4.19 A typical experiment showing mass solid outlet at the bottom of the column as a function of time .....	103
4.20 The rate of mass outer of the solid function of time for different mass solid input .....	105
4.21 The dynamic duration time function of mass solid outlet flow with 95% ethanol .....	105
4.22 The dynamic duration time as a function ethanol concentration of a rate mass solid inlet of $11.33 \text{ g} \cdot \text{min}^{-1}$ .....	106
4.23 The accumulated mass from the graph of rate of mass solid outlet at the bottom of the column $\dot{m}_{so}$ as a function of time .....	107

## LIST OF FIGURES (continued)

FIGURE	PAGE
4.24	The accumulated mass as a function of time when changing the mass solid input..... 107
4.25	The accumulated mass as a function of time $\dot{m}_{SI}$ is 11.33 g.min <sup>-1</sup> with the percentage of ethanol as parameter..... 108
4.26	The mean accumulated mass as a function of percentage of ethanol with the same mass solid input ..... 108
4.27	The mass solid outlet $M_{SO}$ as a function of time using 70% ethanol ..... 109
4.28	The moving mass from the graph of the mass solid outlet at the bottom of the column $\dot{m}_{SO}$ as a function of time ..... 109
4.29	The mean moving mass as a function of mass solid flow at the outlet with 95% ethanol..... 110
4.30	The mean moving mass as a function of percentage of ethanol $\dot{m}_{SI}$ is 11.33 g.min <sup>-1</sup> ..... 110
4.31	The dead mass as a function of mass flow rate of solid outlet with 95% ethanol..... 111
4.32	The dead mass as a function of percentage of ethanol $\dot{m}_{SI} = 11.33$ g.min <sup>-1</sup> ... 111
4.33	The mean residence time from the graph of the mass flow rate solid at the outlet at the bottom of the column $\dot{m}_{SO}$ as a function of time..... 112
4.34	The mean residence time as a function of mass flow rate of solid at the outlet for 95% ethanol..... 112
4.35	The mean residence time as a function of percentage of ethanol for $\dot{m}_{SI} = 11.33$ g/min ..... 113
4.36	The andrographolide concentration as a function of time with the recycled 95% ethanol..... 114
4.37	The andrographolide concentration as a function of time with the recycled 95% ethanol..... 114
4.38	The andrographolide concentration as a function of time with the recycled 95% ethanol..... 115
4.39	The andrographolide concentration at the middle of the column as a function of time..... 115
4.40	The andrographolide concentration at the bottom of the column as a function of time..... 116
5.1	Global process of the twin screw extruder ..... 120
5.2	The mass balance on the twin screw extruder..... 121
5.3	The percent of the outlet mass flow rate of solid at the bottom of the column with the inlet mass flow rate of the solid as a function of ethanol percentage ..... 126
5.4	The moving mass as a function of ethanol percentage ..... 127
5.5	The extraction yield as a function of time when using $C_1 = 80\%$ , $C_2 = 70\%$ and $C_{21} = 60\%$ ethanol respectively ..... 128
5.6	The percentage of extraction as a function of ethanol percentage ..... 129
5.7	The extraction yield as a function of the ethanol percentage with the 2.5 m column ..... 131
5.8	The extraction yield of the solid as a function of the column height ..... 133

## NOMENCLATURES

### CHAPTER I

$AP$	:	<i>Andrographis paniculata</i> Nees.
$a_m$	:	Surface of the membrane ( $m^2$ )
$A_p$	:	Pulse amplitude (m)
$A$	:	The specific surface area ( $m^2$ )
$c'$	:	The concentration of the particle in the centre of the leaf ( $mol\ m^{-3}$ )
$c'_1$	:	The concentrations on the solid side ( $mol\ m^{-3}$ )
$c_1$	:	The concentrations in solution side of the interface at any time t ( $mol\ m^{-3}$ )
$c'_\infty$	:	The concentrations in the leaf side at the equilibrium ( $mol\ m^{-3}$ )
$c_\infty$	:	The concentrations in liquid phase at the equilibrium ( $mol\ m^{-3}$ )
$C$	:	The concentration in the bulk fluid ( $mol\ m^{-3}$ )
$c_o$	:	The average concentrations in the bulk fluid ( $mol\ m^{-3}$ )
$c_{in}$	:	The average concentrations at the interface ( $mol\ m^{-3}$ )
$c$	:	The concentration in the solution at time t ( $mol\ m^{-3}$ )
$c_\infty$	:	The concentration in the solution at equilibrium ( $mol\ m^{-3}$ )
$D_{AB}$	:	Diffusion coefficient of solute A in the solvent B ( $m^2\ s^{-1}$ )
$D_x$	:	Molecular diffusivity ( $m^2\ s^{-1}$ )
$D_d$	:	Diffusivity (or diffusion coefficient) in dispersed phase ( $m^2\ s^{-1}$ )
$D$	:	The diffusivity ( $m^2\ s^{-1}$ )
$D_x$	:	The coefficient of molecular diffusion of the solute ( $m^2\ s^{-1}$ )
$D_c$	:	Diffusion coefficient in the solution ( $m^2\ s^{-1}$ )
$F$	:	The flux ( $m\ s^{-1}$ )
$f$	:	Pulse frequency ( $s^{-1}$ )
$f$	:	Friction coefficient
$K_B$	:	Boltzmann constant ( $kg\ m^2\ s^{-2}\ K^{-1}$ )
$K$	:	Partition coefficient (dimensionless)
$K_o$	:	Global coefficient of matter transfer ( $m\ s^{-1}$ )
$K_m$	:	Permeability of the membrane with respect to the solute ( $m\ s^{-1}$ )
$K_d$	:	Coefficients transfer matter in solid side of the membrane ( $m\ s^{-1}$ )
$K_c$	:	Coefficients transfer matter in liquid side of the membrane ( $m\ s^{-1}$ )
$k_1$	:	The rate constants at the interface from the leaf to solution ( $m\ s^{-1}$ )
$k_{-1}$	:	The rate constants at the interface from the solution to leaf ( $m\ s^{-1}$ )
$k_T$	:	The overall rate constant ( $m\ s^{-1}$ )
$M$	:	Molar mass (kg)
$p_c$	:	Critical pressure (Pa)
$Q_x$	:	Mass flow of solute crossing the membrane ( $m\ s^{-1}$ )
$r$	:	Radial coordinate (m)
$r_a$	:	Radius molecule (m)
$R$	:	Particle radius (m)

## NOMENCLATURES (continued)

$R_s$	:	The radius of the diffusing solute molecule (m)
$R_p$	:	Average radius of the pore (m)
T	:	Time (s)
T	:	Temperature (K)
V	:	Superficial liquid flow rate in column ( $\text{m}^3 \text{s}^{-1}$ )
$V_A$	:	Molar volume of the solute A ( $\text{m}^3 \text{mole}^{-1}$ )
$V_B$	:	Molar volume of the solution B ( $\text{m}^3 \text{mole}^{-1}$ )
X	:	Fraction mass of the solute in the solid
X	:	Local concentration in the particle ( $\text{kg m}^{-3}$ )
Y	:	Solute concentration in continuous phase ( $\text{kg m}^{-3}$ )
$\eta$	:	Viscosity ( $\text{kg m}^{-1} \text{s}^{-1}$ )
$\varepsilon$	:	The rate of interstitial emptiness or porosity (dimensionless)
$\delta$	:	Effective thickness (m)
$\delta_m$	:	Membrane thickness (m)
$\delta_{eff}$	:	The effective film thickness (m)
$\phi$	:	Particle porosity
$\Omega$	:	Volume fraction of porous of membrane
$\tau$	:	Tortuosity (m)
$\rho$	:	Density ( $\text{kg m}^{-3}$ )
<b>Subscripts</b>		
A	:	Solute
B	:	Solvent
c	:	Continuous phase
d	:	Dispersed phase
f	:	Value at flooding
$\infty$	:	Equilibrium



## NOMENCLATURES (continued)

### CHAPTER II

$E_a/R$	:	Activation energy/R (K)
HPLC	:	High Performance Liquid Chromatographic
K	:	Constant value
K	:	The pre-exponential factor ( $s^{-1}$ )
L	:	Length of solid (m)
$M$	:	Mass of solid (kg)
$M_{sol}$	:	The initial mass of solvent (ethanol) (kg)
$m_h$	:	Mass of humid solid (g)
$m_s$	:	Mass of dry solid (g).
R	:	The gas constant, 1.987 cal/ K-mole
SEM	:	Scanning Electronic Microscope
T	:	Temperature (K)
$V_{dry}$	:	Dry volume of sinking or floating part ( $m^3$ )
$V_{sol}$	:	Volume of sinking or floating part in the solvent ( $m^3$ )
$V_{sol}$	:	The initial volume of the solvent (ethanol) ( $m^3$ )
$V_0$	:	The initial total volume of the mixture solvent and solid ( $m^3$ )
V	:	The measured volume at the end of experiment ( $m^3$ )
$\varepsilon$	:	Porosity (dimensionless)
$\eta$	:	Viscosity ( $kg\ m^{-1}\ s^{-1}$ )
$\rho$	:	Density of solid ( $kg\ m^{-3}$ )
$\rho_{app}$	:	The apparent density of solid ( $kg\ m^{-3}$ )
$\rho_{net}$	:	The net density of solid ( $kg\ m^{-3}$ )
$\rho_{sol}$	:	Density of solvent (ethanol) ( $kg\ m^{-3}$ )
$\varphi$	:	Geometric shape factor (dimensionless)
$\omega$	:	The dry matter rate of the solid at the end of experiment ( $kg\ s^{-1}$ )

## NOMENCLATURES (continued)

### CHAPTER III

$A$	:	The specific area ( $m^2$ )
$C$	:	The concentration of andrographolide ( $kg\ m^{-3}$ )
$C_s$	:	The concentration of the solute in the solvent ( $kg\ m^{-3}$ )
$C_L$	:	The concentration of the solute in the liquid phase ( $kg\ m^{-3}$ )
$C_0$	:	The initial concentration of the solute ( $kg\ m^{-3}$ )
$Co_f$	:	Initial concentration of leaves ( $kg/kg$ of solid)
$Co_t$	:	Initial concentration of stems ( $kg/kg$ of solid)
$Ck(i,j)$	:	Concentration of solute/concentration of matter vegetable ( $kg\ m^{-3}$ )
$Ck(i,nx+1)$	:	Concentration of solute / concentration of solvent ( $kg\ m^{-3}$ )
$D$	:	The andrographolide diffusion coefficient ( $m^2s^{-1}$ )
$E$	:	The half of the thickness (or diameter) of the particle) (m)
$L$	:	Characteristic dimension of the particles (m)
$M$	:	Mass of the solid (kg)
$m_s$	:	Total mass of the solute in the solid phase (kg)
$m_0$	:	Initial total mass of the solute in the solid (kg)
$m_L$	:	Total mass of the solute in the liquid phase (kg)
$m$	:	Mass of solid (kg)
$N_p$	:	Number of solid particle contain in a M mass of solid for batch experiment
$N_x$	:	Number of numerical layer in particle
$t-final$	:	Final time of calculation (min)
$t$	:	Time (s)
$V_L$	:	The volume of the liquid phase ( $m^3$ )
$V$	:	The total volume of the solid ( $m^3$ )
$V$	:	The volume of the solid ( $m^3$ )
$V_p$	:	Volume of a particle ( $m^3$ )
$V$	:	Volume of the liquid ( $m^3$ )
$X$	:	Radial distance in the direction of material transfer from the centre of the symmetry(m)
$\Delta t$	:	Time step
$\phi$	:	Geometric shape factor
$\rho$	:	Density of the solid particle ( $kg\ m^{-3}$ )
$\alpha$	:	Ratio of leave/the total of solid

## NOMENCLATURES (continued)

### CHAPTER IV and V

$A_i$	:	The amplitude of the impulsion (psi)
$A_i'$	:	The amplitude of impulsion from the impulsion in the pulsed leg the column (m)
$A_i$	:	The amplitude of impulsion from impulsion in the body of the column (m)
$A_m$	:	The amplitude of the pulsation (psi)
$A_m'$	:	The amplitude of mixing from the pulsation in the pulsed leg of the column (m)
$A_m$	:	The amplitude of mixing from the pulsation in the body of the column (m)
$C_A$	:	Concentration of andrographolide in liquid phase ( $\text{kg m}^{-3}$ )
$C_i$	:	Initial concentration of andrographolide ( $\text{kg kg}^{-1}$ solid)
$\dot{m}_{LI}$	:	Mass liquid flow inlet ( $\text{kg s}^{-1}$ )
$\dot{m}_{SI}$	:	Mass solid flow inlet ( $\text{kg s}^{-1}$ )
$\dot{m}_{LO}'$	:	Mass liquid flow outlet at the top of column ( $\text{kg s}^{-1}$ )
$\dot{m}_{LO}$	:	Mass liquid flow outlet at the bottom of column ( $\text{kg s}^{-1}$ )
$\dot{m}_{SO}'$	:	Mass solid flow outlet at top column ( $\text{kg s}^{-1}$ )
$\dot{m}_{SO}$	:	Mass solid flow outlet at bottom column ( $\text{kg s}^{-1}$ )
$m_{acc}$	:	Accumulated mass (kg)
$m_{stoptime}$	:	Mass at the stopped time (kg)
$\dot{m}_{Andro}$	:	Mass flow of andrographolide in solid phase or in liquid phase ( $\text{kg s}^{-1}$ )
$M_s$	:	Mass of the solid (kg)
$M_L$	:	Mass of the liquid (kg)
$P_{low}$	:	The lower pressure set point (psi)
$Q_L$	:	The liquid flow rate ( $\text{kg s}^{-1}$ )
$Q_S$	:	The solid flow rate ( $\text{kg s}^{-1}$ )
TSE	:	Twin-screw extruder
$\alpha_o$	:	Sinking mass outlet / total solid mass outlet (at bottom of column)
$\alpha_o'$	:	Sinking mass outlet / total solid mass outlet (at top of column)
$\alpha_i$	:	Ratio of sinking mass and total solid mass in the sample
$\tau$	:	The residence time (s)

## INTRODUCTION

The therapies based on natural products have grown for last half of the 20<sup>th</sup> century in both industrial and developing countries. In particular, the pharmaceutical or pesticides industries often have to deal with the recovery of active products from plants. This operation is often costly because vegetal materials generally contain only a small amount of active products.

In Thailand, plants used medicinally are very popular and increasingly appreciated. This thesis focuses on the extraction process from the medical plant called *Andrographis Paniculata*, AP, which is a well known traditional medical plant in Thailand. *Andrographis* is grown extensively in China, Thailand and in a few others Asian countries. *Andrographis paniculata*, also known commonly as “King of Bitters” in Thailand, and has many native names such as Fah-Tha-Laai-Joan or Num-Lai-Pung-Porn. It is a species of the plant family Acanthaceae. According to Thai Pharmacopoeia its action is to reduce fever and to help treat the common colds, sore throat, and to induce subsidence of swelling, ulcers in the mouth or on the tongue, venomous snake bites, treat acute or chronic cough, colitis, dysentery, urinary infection with difficult painful urination, and carbuncles. It has been used for centuries in Asia to treat respiratory infections, fever, herpes, sore throat, and a variety of other chronic and infectious diseases. In traditional Chinese Medicine, *Andrographis* is an important "cold property" herb: it is used to rid the body of heat, as in fevers. In Scandinavian countries, it is commonly used to prevent and treat common colds. Research conducted in the 80's and 90's have confirmed that *Andrographis*, properly administered, has a surprisingly broad range of pharmacological effects, some of them extremely beneficial.

The goal of this research is to develop a continuous solid-liquid extraction from plant (AP) in a disc and doughnut pulsed column. The benefit from the study will be developed for related industries. Another objective is to test a non-sinusoidal pulsation mode in order to avoid flooding due to the floating particles in the pulsed pilot column. Finally, the results will be used to design an industrial installation and optimize its operating parameters.

The classical methodology for the development of a continuous process in a column, used as a solid-liquid contactor, starts with lab-scale batch experiments. This step allows choice of solvent and to identify the influence of the main operating parameters (such as operation time, solvent concentration, solid-liquid ratio, temperature, solid particle sizes and mixing). Then, the hydrodynamic conditions can be defined in the appropriate column. However this methodology encounters some difficulties due to the substantial heterogeneity of the plant. The process then has to be flexible enough to be adapted to the different periods of production and origins of the plant that can lead to major variations in the physico-chemical properties of the raw material.

In the **first chapter** a specific bibliography is presented on the plant material, the *Andrographis paniculata* and its history: cultivation, traditional use, chemical study, structure, effect and analytical techniques are presented. Then, the phenomenon

of mass transfer in plant extraction is explored through previous studies. The influences of the operating conditions on the extraction kinetics were investigated. Finally, the general characteristics of the pulsed column are described. In this work, a pneumatic pulsation has been used. This specific feature of the pulsing system is emphasized for this study.

In **Chapter II**, the characteristic of AP are detailed: physical structure, porosity and apparent solid volume. Soxhlet experimental results and the kinetics with batch studies are presented. Some of the main operating conditions were investigated: solid mass amount, particle size, ethanol percentage, temperature. Some information on the thermal stability of the product and on solvent absorption will be additionally given. The optimal extraction conditions have been derived from batch experiments.

**Chapter III** presents the mass transfer model inside the plant and the model hypothesis. The experimental data obtained in the **Chapter II** are compared with a mass transfer model: in order to measure the value of the diffusion coefficient  $D$ . The limiting steps are discussed according to the particles shapes ("2 shape model").

**Chapter IV** presents the results for the continuous process study in the column. The operation of the pneumatic pulsation cycle used to avoid flooding due to floating particles accumulated at the feed inlet is discussed. Particle residence times and extraction yields were determined. The coupling of the model with the mean residence time allows designing the continuous process.

Finally in **Chapter V**, extraction in a column and in a twin screw extruder is compared. Conclusions on some economical aspect on the process are made.

The overall methodology followed in this work is:

1. Study the influence of extraction parameters in a batch reactor.
2. Propose an extraction kinetics model and identify the diffusion coefficients.
3. Study the hydrodynamics (dynamic behaviour and residence times of solid particle) in the pulsed column.
4. Couple the diffusion model and the hydrodynamic characteristics of the plant in order to predict the extraction yields in the column.
5. Propose and design a process with a pulsed column.

The general conclusion summarizes the whole results as well as, the problems encountered in this work as well as the perspectives gained from this work. All the experimental results are gathered in the Appendices.

## CHAPTER I

### INTRODUCTION

The solid - liquid extraction is a fundamental operation in nuclear, metallurgical, food and pharmaceutical processes. For example, the extraction of coffee and tea (soluble preparation manufacture) is produced by treatment with boiling water, caffeine being extracted to the water from coffee and tea. The caffeine-free coffee is obtained by elimination of the caffeine of the green coffee bean by a treatment with chlorinated solvent. Natural perfumes are isolated from plants (flowers, roots, and stems) using alcohol. The solid may be contacted with the solvent in a number of different ways but traditionally part of the solvent retained by the solid is always referred as the underflow, the rich solvent being the overflow. The operation can be subdivided into two types: firstly, extraction occurs due to solubility of the solute in the solvent such as oilseed extraction; secondly, extraction occurs thanks to solvent reaction with a constituent of the solid material in order to produce a compound soluble in the solvent such as extraction of metals from ores. The two categories face different limiting steps, the first being rate-controlled by the diffusion phenomena whereas the second is more frequently controlled by the kinetics of the chemical reaction producing the solute. These differences are reflected into the different techniques used to carry out the operations. The present work aims with the extraction of solutes without the help of chemical reaction.

The solvent dissolves one (or several) components, crystallised and liquid, referred to as solutes. The extract is only composed of solvent and solute; the exhausted solid is called residual, inert or insoluble.

In this chapter, the solid phase is named *Andrographis paniculata*, the characteristics and properties of which will be described. Mass transfer being controlled by diffusion in our case, the diffusion modelling and the practical determination of the kinetic are presented as well.

Finally, among different types of solid-liquid extraction equipment, the pulsed column was chosen. A new technology of pulsation by air pulse has been implemented allowing for a non-sinusoidal pulsation cycle.

## 1.1 ANDROGRAPHIS PANICULATA NEES

### 1.1.1 Historical and traditional use of *Andrographis paniculata* (AP)

*Andrographis paniculata* (AP) is a plant in the *Acanthaceae* family. It is an ancient medicinal herb which grows widely in Asian tropical areas. Its common name is King of Bitter. There are many native names, one which is well known in Thai as Fah-Tha-laai-Joan or Num-Lai-Pung-Porn (Chanprasert and Pecharaply, 1988; Thai pharmacopoeia, 1997). It is an erect annual plant of 30-100 cm in height and 0.2- 0.6 cm in diameter (**Figure 1.1**). Stems are dark green, quadrangular with longitudinal furrows and wings on the angles of the younger parts, slightly enlarged at the nodes. The leaves are opposite, decussate, lanceolate, up to 8.0 cm long and 2.5 cm broad (**Figure 1.2**); the flowers are small, and the seeds numerous, yellowish brown. The fruits are small, 2-celled odourless capsules and extremely bitter. All parts of this plant have a bitter taste.

This plant was extensively used in traditional medicine. The herb is reported to possess astringent, anodyne, tonic properties and is reported helpful to treat dysentery, cholera, diabetes, influenza, bronchitis, piles, skin disorders, fever and worm infestation. It is useful for treating burning sensation, wounds, ulcers, chronic bronchitis, leprosy, flatulence, colic and diarrhea. In Thailand, (Thai pharmacopoeia, 1995) it is used in traditional medicine, against fever, dysentery, diarrhea, inflammation, and sore throat. To reduce diarrhea or sore throat, it was recommended (Division of medical plants research and development department of medical science ministry of public health, 1990) to take 2 capsules four times per day, each one being filled with 500 mg AP leaf powder. Another medication is to make use of AP leaf powder for reducing cough and sore throat (Office of medicinal plant data, 1989). It is a promising new way for the treatment of many diseases, including HIV, AIDS, and numerous symptoms associated with immune disorders (Weibo, 1995; Calabrese, 2000).

The known benefit of the AP plant for human has also led to its use in livestock production. For example, AP leaves or mixtures of AP and other leaves are fed to animals in a number of farms. Furthermore, farmers believe that by mixing AP leaves into chicken feed can reduce chicken mortality as well.

In China, AP has been claimed to be effective for dysentery upper respiratory tract infections, influenza, urinary tract infections and infectious wounds. The Chinese people used to boil roots and leaves of *Andrographis* and took the herbal soup to relieve symptoms of respiratory tract and lung infection, such as sore throat, cough, fever and etc. The herb was also commonly used to treat diarrhea and urinary tract infections. Other applications of *Andrographis* include treating skin infections, such as furuncle, carbuncle and eczema. For external treatment of the skin, ancient Chinese doctors applied fresh *Andrographis* paste to the infected areas. Chinese medical books also described *Andrographis* as a medicine to treat snakebites (Coloured atlas of the Chinese material medical specified in pharmacopoeia of the people's republic of China, 1995).



**Figure 1.1** *Andrographis paniculata* Nees plant

Source: <http://www.herblpg.com/thai>



**Figure 1.2** Leaves and stems of *Andrographis paniculata* Nees plant

Source: [www.herbalnet.org](http://www.herbalnet.org)



**Figure 1.3** Seeds of *Andrographis paniculata* Nees

Source: Standard of Thai Herbal Medicine: *Andrographis paniculata* (Burm.f.) Nees,(1999)



In Scandinavian countries, it is commonly used to prevent and treat common colds. Research conducted in the 80's and 90's have confirmed that *Andrographis*, properly administered, has a surprisingly broad range of pharmacological effects, some of them being extremely beneficial (Research review, 1997).

Finally, the extracted chemicals from *Andrographis paniculata* Nees is a medicine to cure diarrhea in pigs, pigs being considered to be the main source of proteins for Thai and Chinese people. The chemicals will increase productivity of pig farms scattered around the country.

### 1.1.2 Culture

*Andrographis* appears to grow best in the tropical and subtropical areas of China and Southeast Asia, India, Sri Lanka and Pakistan, Thailand (Gupta et al., 1990; Sandberg, 1994). Growing region and seasonality play both a role concerning with the plant composition. Normally grown from seeds (**Figure 1.3**), it grows in pine, evergreen and deciduous forest areas, and along roads and in villages (Standard of Thai Herbal Medicine: *Andrographis paniculata* (Burm.f.) Nees, 1999). It is also cultivated-quite easily, because it can grow in all of the ground types. Moreover, it grows in soil types where almost no other plant can be cultivated. However, it should not be cultivated in soil that is flooded or wet all year and also a serpentine soil will give very low production (Kasetklangklung, 1996).

The plant likes sunshine. The seeds are sown during May-June. The seedlings are transplanted in a distance of 60 cm x 30 cm grid. Two or three irrigations cycles may be scheduled during the day periods. It flowers during August - November, and the whole plant starts maturing during February-March when it is harvested for the drug. The plants used in this study were collected during November-January from Nakornpathom province in Thailand. The crude drug harvested for this study consists of dried or fresh leaves and the aerial parts of the plant.

### 1.1.3 Harvesting and storage

The highest concentration of active component occurs just before the plant blooms or at mid-way period between planting of blooming, making early fall the best time to harvest. It was (Suwanbareerak and Chaichantipyuth, 1991) reported that the highest amount of active component is in the mature plant. The age of the plant when their occurs is about 110-150 days.

The amount of diterpene lactones depend on both growing regions and seasons. The highest amount of active component is found in leaves. The lowest amount of active component is found in the stems (Standard of Thai Herbal Medicine: *Andrographis paniculata* (Burm.f.) Nees, 1999). The leaves contain the highest amount of andrographolide (2.39%), the most medicinally active phytochemical in the plant, while the seeds contain lower contents (Sharma, Krishan, and Handa, 1992). The highest percentages of active component are shown in the **Table 1.1**.

**Table1.1** Total percentage of diterpene lactone in AP at different growth periods

Sample	Period of harvesting	Total diterpene lactone (%)		
		Aerial part	Leaf	Stem
1	Before Blooming	6.09	6.80	2.28
	Blooming	7.31	9.81	2.06
	Young fruit	5.29	6.79	3.93
	Mature fruit	4.80	6.44	4.67
2	Before Blooming	7.05	9.54	3.02
	Blooming	9.79	12.52	5.81
	Young fruit	6.72	7.25	6.25
	Mature fruit	5.54	6.63	6.89

Source: Standard of Thai Herbal Medicine: *Andrographis paniculata* (Burm.f.) Nees, (1999).

The dried plant can be stored in airless plastic bags. It should be kept in a cool and clean place. The percentage of total diterpene lactone will decrease up to 25% after one year storage (Table 1.2) (Naiyana Tipakorn, 2002).

สถาบันวิทยบริการ  
จุฬาลงกรณ์มหาวิทยาลัย

**Table 1.2** Total percentage of diterpene lactones in the aerial part of AP after different periods of storage

Sample	Period of storage (Month)	Diterpene lactones Content (%)	Percentage decrease in Diterpene lactones content (%)
1	0	9.25	0.00
	3	9.13	1.30
	6	8.56	7.46
	9	7.99	13.62
	12	7.09	23.35
2	0	3.85	0.00
	3	3.58	7.01
	6	3.33	13.50
	9	3.18	17.40
	12	2.92	24.16
3	0	6.2	0.00
	3	6.03	2.74
	6	5.02	19.03
	9	4.18	32.58
	12	4.11	33.70
4	0	7.68	0.00
	3	7.32	4.69
	6	7.08	7.81
	9	6.78	11.72
	12	5.63	26.69
5	0	6.86	0.00
	3	6.44	6.12
	6	6.12	10.79
	9	5.78	15.74
	12	5.04	26.53

SOURCE: Standard of Thai Herbal Medicine: *Andrographis paniculata* (Burm.f.) Nees, (1999).

### 1.1.4 General techniques for analysis

*Andrographis* is commercially sold as a medicine. Subsequently, a large variety of laboratory methodologies have been developed to ensure a standardized level of andrographolide measurements: thin-layer chromatography (TLC), ultraviolet spectrophotometer, liquid chromatography, HPLC technique, and volumetric and colorimetric techniques.

One method used by Naiyana Tipakorn (2002) is to analyze the quality of the sample of AP leaves by means of a color test (preliminary test) and by thin-layer chromatography (confirmatory test).

#### Preliminary test

1 g of powdered AP leaves and 20 ml of ethanol is boiled into a water bath and then filtered. 300 mg of decoloring charcoal are added to the filtrate. The solution is stirred and filtered again (solution A) (Standard of Thai Herbal Medicine: *Andrographis paniculata* (Burm.f.) Nees, 1999).

#### Method 1 with Kedde reagent

In 1 ml of solution A, 2 drops are added to a 2% w/v solution of 3,5-dinitrobenzoic acid in methanol (Kedde A) and 2 drops are added to a 5.7% w/v of potassium hydroxide solution in methanol (Kedde B). Color changes to a purplish red color indicate that the sample has active compounds like AP (**Figure 1.4**) (Standard of Thai Herbal Medicine: *Andrographis paniculata* (Burm.f.) Nees., 1999).

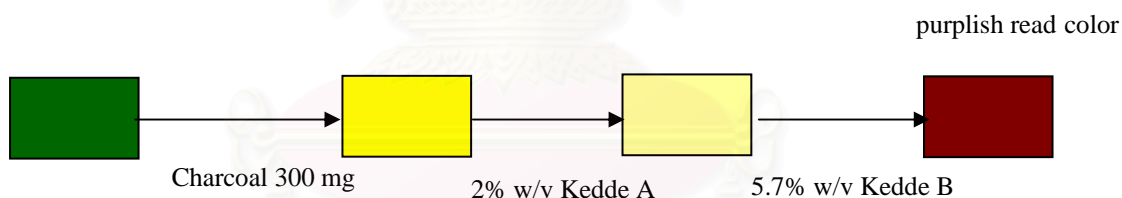


**Figure 1.4** Diagram of color test by using Kedde A and Kedde B (Standard of Thai Herbal Medicine: *Andrographis paniculata* (Burm.f.) Nees, 1999)

#### Method 2 with ethanolic potassium hydroxide

In 1 ml of solution A are added several drops of ethanolic potassium hydroxide until it turns to a red color. Then wait for 10-15 min. A color change to yellow indicates that the sample has active compounds such as AP (**Figure 1.5**) (Standard of Thai Herbal Medicine: *Andrographis paniculata* (Burm.f.) Nees, 1999).

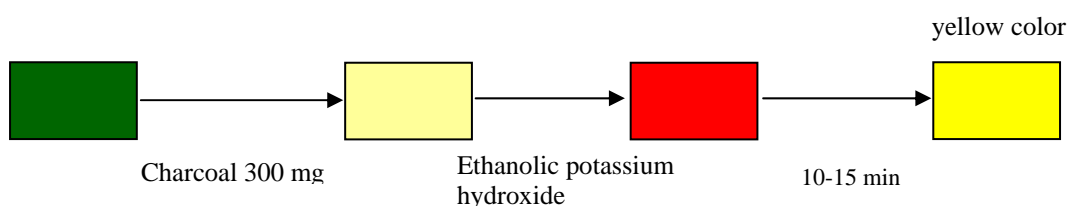


**Figure 1.5** Diagram of color test using ethanolic potassium hydroxide (Standard of Thai Herbal Medicine: *Andrographis paniculata* (Burm.f.) Nees, 1999)

The primary test is designed to test only for the existence of the AP active compound. The next method based on chromatography is normally used in Thai government laboratories which test and control the quality of medicinal plants.

### Confirmatory test

Thin layer chromatography analysis has to be performed after the color test to confirm the AP presence. 1 g of powdered AP leaves with 20 ml of ethanol are boiled in a water-bath for 5 minutes, then 300 mg of decolorizing charcoal is added, the mixture is stirred and filtered. The filtrate is evaporated under reduced pressure until dry and the residue dissolved in 1 ml of warm ethanol (80%). As standard, 2 mg of andrographolide, 2 mg of neoandrographolide and 4 mg of dehydroandrographolide are each dissolved in 1 ml of ethanol by using silica gel adsorbent GF254 and a chloroform mobile phase (absolute ethanol 85:15). 5 micro liter is used for each spot. The Migration path is 15 cm (ascending). The UV radiation ( $\lambda = 254$  nm) detection is made by spraying with 2% w/v 3,5- dinitrobenzoic acid in methanol (Kedde A) and excess of 5.7% w/v potassium hydroxide in methanol (Kedde B) (Standard of Thai Herbal Medicine: *Andrographis paniculata* (Burm.f.) Nees, 1999).

### Thin Layer Chromatography (TLC)

The experiment details are summarized as follows:  
Analytical Thin Layer

Technique: one way, ascending  
Adsorbents: Silica gels G (E. Merk), silica gel 60 F254, calcium sulphate binder 13%, 30g/60 ml of distilled water,  
Plate size: 20cm x 20cm, 20 cm x 5 cm,  
Layer thickness: 250 microns,  
Activation: air dried for 15 minutes and then at 105°C for 1 hour,  
Distance: 15 cm,  
Laboratory temperature: 25-30 °C.

#### Solvent system

System	Component	Ratio
1	Chloroform	-
2	Chloroform: Methanol	9: 1
3	Chloroform: Methanol	8: 1
4	Chloroform: Acetone	9: 1
5	Chloroform: Absolute ethanol	85: 15
6	Chloroform: Benzene	1: 1
7	Acetone: Methanol	8: 2
8	Ether: Methanol	7: 3
9	Benzene: Methanol	1:1
10	Ethyl acetate: Methanol	8: 2

### Detection of compound on TLC plate

a) Ultraviolet light at the wavelength 254 nm

Unsaturated organic compounds could be fluorescent under UV light. Diterpenoid lactone compounds presented violet spots.

b) Iodine vapour for unsaturated organic compounds.

Reagent : Iodine crystal

Note : The chromatographic plate is placed into a closed vessel containing some crystal of Iodine. Iodine vapour generated bind to the spot of organic compound presented as brown spots.

Other methods of the general isolation techniques, like open column chromatography, quick column chromatography and crystallisation, have been described in the work of Nanthakarn Mahaverawat (1992) (**Appendix I**).

### Total lactones or diterpene lactones

The method to identify the active constituents (diterpene lactones) of AP powder is detailed elsewhere (Standard of Thai Herbal Medicine: *Andrographis paniculata* (Burm.f.) Nees, 1999). The total percentage of diterpene lactones is calculated from the dry matter weight of AP leaves. 1 ml M of NaOH solution is equal to 35.04 mg of andrographolide. The total diterpene lactones of andrographolide is 7.3% (Naiyana Tipakorn, 2002).

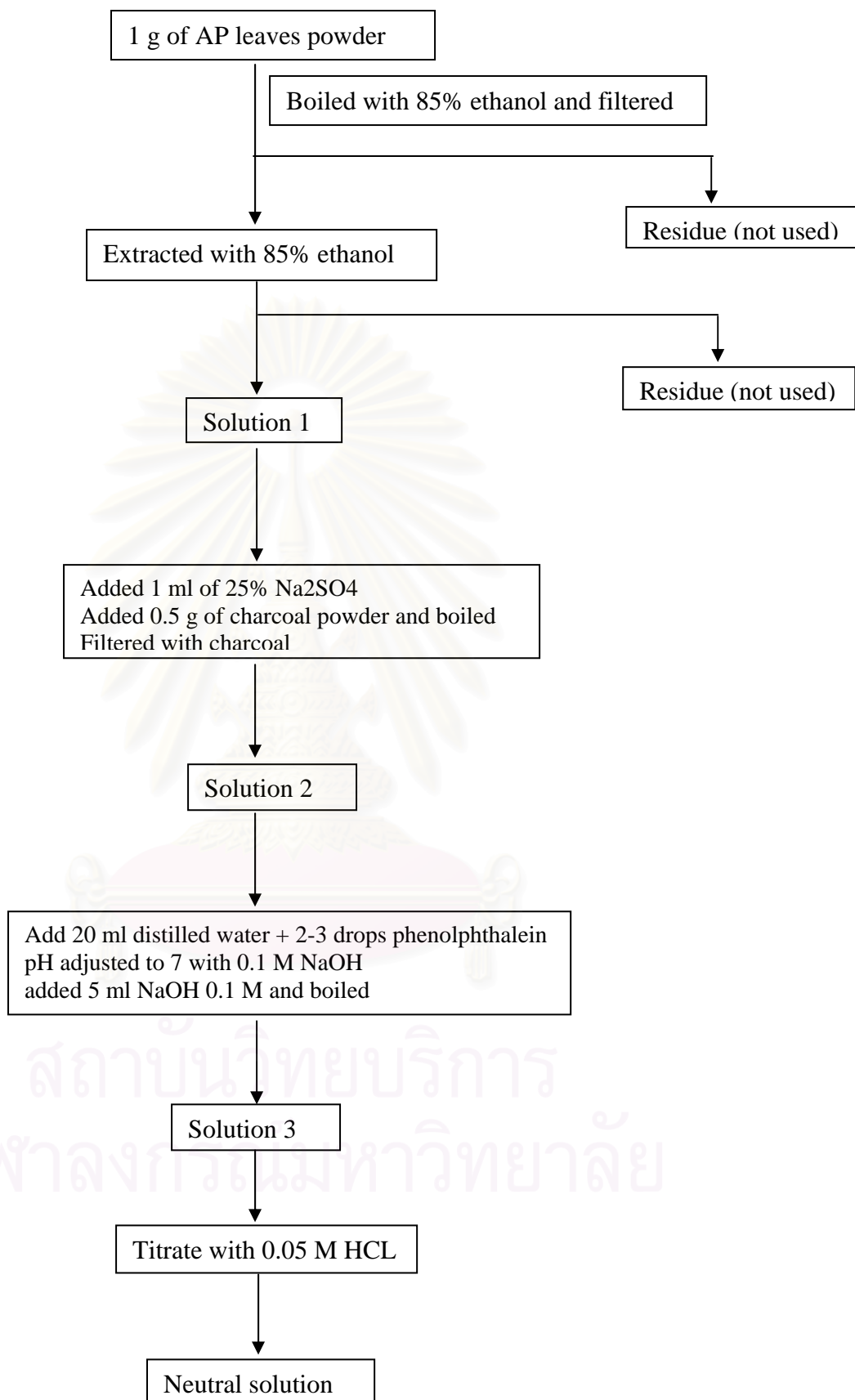


**Figure 1.6** Method to identify the diterpene lactones of AP powder (Standard of Thai Herbal Medicine: *Andrographis paniculata* (Burm.f.) Nees, 1999)

A rapid method for isolation of andrographolide from the leaves of *Andrographis paniculata* is reported elsewhere (Rajani, 2000). The leaf powder is extracted by cold maceration in a 1:1 mixture of dichloromethane and methanol and isolation of andrographolide is obtained directly from the resulting extract by recrystallisation. The methods work well with IR, UV, mass and melting point and co-chromatography with a reference standard on TLC. UV absorption spectrum, TLC, HPLC and differential scanning calorimeter validate the purified compound.

### 1.1.5 Chemical study

A crystal compound, andrographide, was first isolated from *Andrographis* by Boorsma in 1896. In 1911, Corter identified this compound as a Lactone (Sichuan Chinese herb research institute, 1973). Later studies showed that active chemical components in *Andrographis paniculata* (AP) are andrographolide and neo-andrographolide. Chemical constituents isolated from this plant have been reported such as diterpenoid lactones of a paniculata Nees: andrographolide, neo-andrographolide, deoxyandrographolide and 14-deoxy-11, 12-didehydroandrographolide (Sichuan Chinese Herb Research Institute, 1973). Andrographolide and total lactones are the common forms used in clinics. Animal studies on rats and mice conclude that all four lactones have anti-inflammatory and anti-pyretic effect. Since the herb shows no effect in treating infected animals when adrenal glands of the animals were totally removed, this suggested that *Andrographis* might exert anti-inflammation through stimulatingly the adrenal glands. It can be seen that the main constituents of this plant are diterpenoid lactone with ethanol solution extracts, 4 lactone constituents were obtained which is an unsaturated trihydroxy lactone. It is freely soluble in methanol, ethanol, pyridine, acetic acid, sparingly soluble in benzene, chloroform and acetone, insoluble in ether and water.

A systematic study on the chemistry of *Andrographis paniculata* has been carried out by various researchers at various times. The reviews of such compounds are illustrated in the work of (Srisomporn Preeprame, 1992; Saxena, 1998).

Analysis of the whole plant gave the following lactones: (1) andrographolide ( $C_{20}H_{30}O_5$ ; mp 230-239°C), 0.6%; (2) 14-deoxy-11-oxoandrographolide ( $C_{20}H_{28}O_5$ , mp 98-100°C), 0.12%; (3) 14-deoxy-11, 12-didehydroandrographolide ( $C_{20}H_{30}O_4$ , mp 203-204°C), 0.06%; (4) 14-deoxyandrographolide ( $C_{20}H_{30}O_4$ , mp 175°C), 0.02%; and a non-bitter constituent, (5) neoandrographolide ( $C_{26}H_{40}O_8$ , mp 167-168°C), 0.005%. The leaves contain andrographolide (yield, 1%). From the petroleum ether extract of the leaves from Bangladesh, the following components have been isolated:  $\alpha$ -,  $\beta$ -unsaturated lactone, andrographosterol ( $C_{23}H_{38}O$ , mp 135°C), homoandrographolide ( $C_{22}H_{32}O_9$ , mp 115°C), andrographane ( $C_{40}H_{82}$ , mp 67-68°C), andrographone ( $C_{32}H_{64}O$ , mp 85°C), a wax and two esters containing hydroxy groups.

Nanthakarn Mahaverawat (1992) has reported the chemical properties of *Andrographis*. Its physical properties were as follows: m.p. is 228-230°C, ultraviolet spectrum in ethanol:  $\lambda_{max}$  223 nm, deoxyandrographolide ( $C_{20}H_{30}O_4$ , m.p. is 173 - 176 °C,  $\lambda_{max}$  248 nm), neoandrographolide ( $C_{20}H_{40}O_8$ , m.p. is 170-172°C,  $\lambda_{max}$  205 nm) and 14-Deoxy-11, 12-dedehydroangrapholide ( $C_{20}H_{30}O_4$ , m.p. 203-204°C). It was found that the ethanol extract yield was higher than the aqueous extract. The highest composition of the extract is andrographolide.



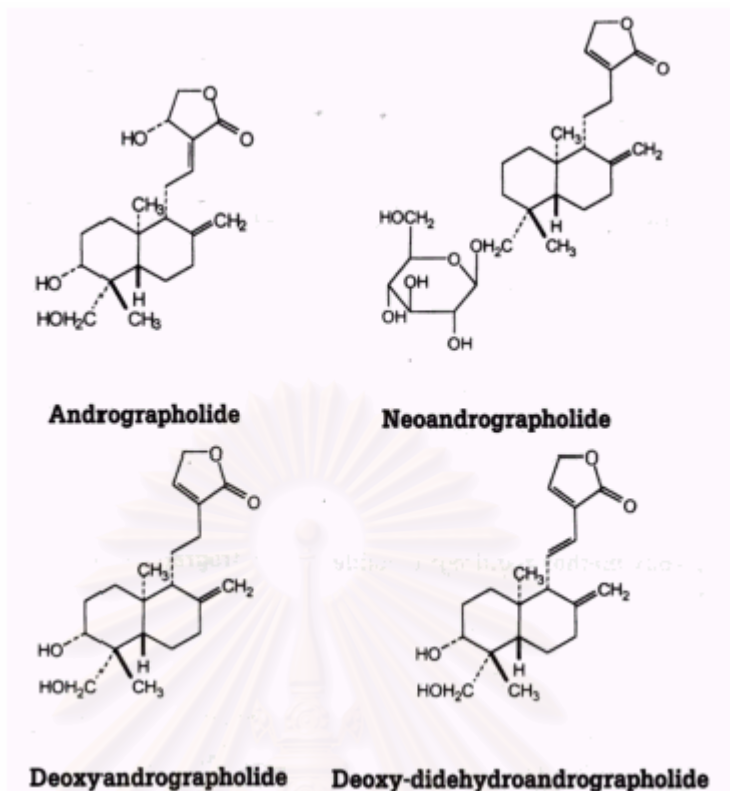


**Figure 1.7** The main active components in AP leaves

### 1.1.6 Safety

In Traditional Chinese Medicine and in systems of healing in Thailand and India, AP has been perceived as safe going back a long time. Although trial and error in humans may not be considered scientific, it is a way of determining whether a substance is effective or harmful. When scientists began to investigate the safety of AP, formal toxicological studies in animal models and in animal and human clinical trials confirmed that andrographolide and other members of this AP family of compounds have very low toxicity. In other tests for toxicity, rats or rabbits received 1 g/kg orally of andrographolide or neoandrographolide for seven days. This amount did not affect body weight, blood counts, liver or kidney function, or other important organs (Akbarsha et al., 1990; Yin and Guo, 1993).

After AP ingestion, people rarely experienced dizziness and heart palpitations. As with all herbs, some people will have an allergic reaction to AP. The other side effect, as discussed above, is antifertility. Overall, evidence up to date indicates that andrographolides are naturally occurring compounds with low toxicity when used appropriately.

#### Warning:

Although *Andropogonis paniculata* is known to have very low toxicity, it should, like *sanguinaria* (bloodroot), be avoided by women who are pregnant or who wish to become pregnant. It exhibits antifertility effects.

## 1.2 SOLID – LIQUID EXTRACTION PHENOMENA

The solute transfers from the solid substrate into an appropriate solvent. Four main steps may be distinguished: the penetration of the solvent into the solid phase, the chemical reaction or the solubilization of the solute, the diffusion of the solution inside the solid, the solute diffusion from the solid phase towards the outer liquid phase (Lalou, 1995).

- The penetration of the solvent into the solid phase is generally fast enough in comparison with the other ones. Therefore, it can be disregarded in the global kinetic model.

- The chemical reaction occurring between the solvent and the solute, when it takes place, can be instantaneous or relatively slow. In the first case, the kinetics are driven by diffusion while in the second one, the mass transfer is chemically driven. In the present case, we have to focus only on a solubilization step and not on a chemical one. Solubilization being generally fast, it can be neglected.

- The diffusion of the solution inside the solid is usually the limiting step as it has been exhibited in (Bichsel, 1979; Spiro and David, 1982; Spiro and Selwood, 1984).

- The diffusion of the solute from the solid phase towards the outer liquid phase can be slowed by a layer of liquid stagnating at the interface of the solid (Boundary layer of film theory). The effect of this layer can be limited when the solution is sufficiently agitated to permit a permanent renewal of the solvent in order to accelerate the global phenomena.

At every step, a mathematical model can be established from the physical and chemical knowledge of the phenomena: reaction model, model of transfer inside the solid and the film model.

### 1.2.1 Mass transfer model inside the solid particle

The rate concept of mass transfer within a solid substrate is difficult to study because it is impossible to define accurately the actual progress inside the solid.

Diffusion inside solid particles is generally described by the Fick's second differential equation:

$$\frac{\partial X}{\partial t} = -D_x \nabla^2 X \quad (1.1)$$

where  $X$  : The mass fraction of the solute in the solid,  
 $D_x$  : The coefficient of molecular diffusion of the solute.

This equation is valid for solute diffusion in rigid porous bodies at the condition that their structure is considered as quasihomogeneous and macroscopically isotropic. In our case, the coefficient of molecular diffusion of the solute  $D_x$  has to be replaced by the apparent diffusivity  $D_{xa}$ , which accounts with the porosity and the tortuosity of the solid particle.

Equation 1.1 can be written in spherical coordinates , as follows:

$$\frac{\partial X}{\partial t} = -D_{xa} \left[ \frac{\partial^2 X}{\partial r^2} + \frac{2}{r} \frac{\partial X}{\partial r} \right] \quad (1.2)$$

The initial condition is

$$X(r, 0) = X_{in} = \text{constant} \quad \forall r \quad (1.3)$$

Two standard boundary conditions can be written:

$$\text{At } r=0 \quad \left. \frac{\partial X}{\partial r} \right|_{r=0} = 0 \quad \text{from the assumption of particle symmetry} \quad (1.4)$$

The other one (at the solid-liquid interface) depends on the type of process applied. When the ratio between the volume of the outer solvent  $V_y$  and that of the pores in the solid phase  $\phi V_x$  is very high or when a fast chemical transformation of the solute takes place in the external medium, the continuous phase mass transfer resistance can be neglected. It is then possible to write

$$\left. X \right|_{r=R} = Y / \phi = \text{constant} \quad (1.5)$$

- X : Local solute concentration in the particle ( $\text{kg/m}^3$ ),
- r : Radial coordinate (m),
- R : Particle radius (m),
- Y : Solute concentration in continuous phase ( $\text{kg/m}^3$ ),
- $\phi$  : Particle porosity,
- $D_{xa}$  : Apparent diffusivity ( $\text{m}^2/\text{s}$ ),
- t : Time (sec).

In the case of a one-dimensional system, Equation (1.1) may be simplified as:

$$\frac{\partial X(t, x)}{\partial t} = D_d \frac{1}{x^{\phi-1}} \frac{\partial}{\partial x} \left( x^{\phi-1} \frac{\partial C(t, x)}{\partial x} \right) \quad (1.6)$$

- X : Fraction mass of the solute in the solid,
- x : Space coordinate,
- t : Time,
- $D_d$  : Diffusivity (or diffusion coefficient) in the dispersed phase (solid),

$\varphi$ : Being a shape factor according to the particle geometry (cylindrical or spherical).

### 1.2.2 Mass transfer across the interface

Many industrial processes in which mass transfer is important involve transport of a solute from the bulk fluid of one phase at the interface and then from the interface to the bulk of the second phase. The diffusing solute transfers from phase 1, where its concentration is higher than at equilibrium, into phase 2. In the interior of bulk fluids, mass flux is accomplished by mixing due to turbulent fluctuation, and the concentration of the solute concentration in the interiors is practically constant.

Mass transfer resistance is concentrated in the boundary layer near the interface where the concentration gradient is the steepest. Mass transfer stops when equilibrium is established between the bulk fluids. The most common approach to this problem is to develop a theoretical model for mass transfer in the interface region and to see if the results of such an analysis are consistent with the experimental overall mass-transfer results.

Several different theoretical models have been developed in the past, most of the models being based on the following assumptions:

- First, the total resistance to mass flux is the sum of the resistances relative to each phase including the resistance at the interface. However, in many cases the interface resistance may be considered as being negligible, and in this case, the total resistance to mass transfer may be restricted as the sum of the phase resistance (resistance additivity rule).
- Secondly, at the interface the two phases are assumed to be at equilibrium, and this equilibrium is established more rapidly than the change of average concentration in either bulk fluid (Azbel, 1981).

The two major models of the mechanism of mass (and also heat) transfers between two phases are the film theory and the penetration theory. The film theory assumes that there is a region in which steady-state molecular diffusion is the prevailing transfer mechanism, while the penetration theory assumes that the interface is continuously impinged by eddies, that is to say that mass transfer is controlled by unsteady molecular diffusion.

#### The Film model

The first hydrodynamics model that has been proposed for the investigation of the transport process both of heat and mass transfer is the so-called film-theory model. According to this model, steady-state mass transfer occurs by molecular diffusion across a stagnant, or laminar-flow film at the interface between the phases, in which the fluid is turbulent. All the resistance is assumed to be confined inside the film, and therefore mass concentration gradients arise only inside this film. In the bulk fluids, the concentration is assumed to be constant and equal to some average values. With

this system it is logical to treat mass transfer at a phase boundary by use of the equations of molecular diffusion.

The mass, per unit time,  $\dot{m}'$  transferred across a unit area of interface is proportional to the concentration gradient between the bulk fluid and the interface, so that

$$\dot{m}' = \frac{-D}{\delta_{eff}} (c_o - c_{in}) = -k(c_o - c_{in}) \quad (1.7)$$

where  $c_o$  and  $c_{in}$  are the average concentrations in the bulk fluid and at the interface, respectively  $D$  is the diffusivity, and  $\delta_{eff}$  is the effective film thickness. For the phase on the other side of the interface  $\dot{m}'$  is similarly proportional to the concentration gradient between the interface and the bulk fluid.

In equation (1.7)  $k = D/\delta_{eff}$  is a mass transfer coefficient that characterizes the rate of mass flux, and the value  $\delta_{eff}$  is, by definition, the thickness of some boundary layer in which molecular diffusion has the same effective flux resistance as that actually determined by the convective diffusion. The equation reveals a major error of the theory that indicates linearity between mass flux and the molecular diffusion coefficient  $D$ . In practice, turbulence in the bulk of the fluid diminishes only gradually as the film surface is approached, and consequently transition from eddy diffusion to molecular diffusion. The weakest element of the theory is the positioning of a stagnant film of a definite (but unknown) thickness, this thickness being evaluated in light of experimental results (Azbel, 1981).

### The Penetration model

In the penetration or surface-renewal model, mass transfer is observed as an unsteady time-dependent process. In the Higbie penetration model (1935), mass transfer is assumed to take place during brief, repeated contacts of mass (gas or solid) with the interface, this motion being generated by turbulent fluctuations in the bulk fluid. Fresh liquid elements continually replace those interacting with the interface (Danckwerts, 1951), and consequently mass transfer is effected by the interface being systematically renewed.

The exposure time of such fluid elements to mass-transfer effects at the interface is so short that steady-state characteristics do not have time to develop, and any transfer that does take place is due to unsteady molecular diffusion. Each element of liquid, as long as it stays on the surface, may be considered to be stagnant, and the concentration of the dissolved gas in the element may be considered to be everywhere equal to the bulk-liquid concentration when the element is brought to the surface. Hanraty (1951) showed that the model was applicable to the transfer between a liquid and a solid.

### Mass transfer with chemical reaction

Mass transfer typically takes place on the surface of active particles when they are dispersed and suspended in a continuous phase. For the determination and quantitative evaluation of the influence of the various parameters that are presented in each system, It is necessary to know the rates of both, the chemical transformation and the physical transfer of mass, as well as the effects of interaction between the two processes.

A phenomenon of mass transfer with chemical reaction (Giovammo, 1967) takes place whenever two phases which are not at chemical equilibrium with one another are brought into contact. Such phenomena are made of a number of elementary steps that can be summarized follow:

(i) Diffusion of one or more reactants from the bulk of phase 1 to interface between the two phases, physical equilibrium being assumed to be reached at the interface; whenever the concentration of the reactants at interface is finite in one phase, it is also finite in the other.

(ii) Diffusion of the reactant from the interface towards the bulk of phase 2.

(iii) Chemical reaction within phase 2.

(iv) Diffusion of reactants initially presents within phase 2, and/or of reaction products, within phase 2 itself, due to concentration gradients which are set up by the chemical reaction.

Step (ii), (iii) and (iv) may take place simultaneously, and thus mutually interfere. The overall phenomenon resulting from steps (ii), (iii) and (iv) takes place in series with step (i). If step (i) is rate-controlling, the overall rate is not influenced by the chemical reaction, and the process may be regarded as a simple mass transfer phenomenon which is not influenced by the reaction rate. Of course, the chemical reaction may itself be the cause of an overall high mass transfer rate within phase 2, and therefore for step (i) being rate-controlling.

The analysis of mass transfer with chemical reaction is of interest when the overall phenomenon resulting from steps (ii), (iii) and (iv) is rate-controlling. The two phase involved may be either both fluid, or one fluid and one solid (such as a porous catalyst as phase 2, or a dissolving solid as phase 1). If phase 2 is fluid, the problem to be considered is far more complicated, because the fluid mechanics of that phase needs to be considered.

#### **1.2.3 Diffusion through cells**

In the plant material, the solute is imbedded into the plant cells from where it is extracted by a mechanism of dialysis through the cellular partitions.

The diffusion through a membrane, or dialysis, is a significant phenomenon for many processes of solid- liquid extraction. By definition, it is the transfer of a

solution through a membrane by diffusion starting from a solution concentrated towards a dilute solution. At the same time, a diffusion of solvent is observed through the membrane in the opposite direction. In the case of a dilute solution, the integration of Fick's law on the diffusion, with the condition that there is no volume variation of each side of membrane and that the transfer coefficient be constant on the diffusion, leads to the following transfer equation (Lane and Riggle, 1959; Tuwiner, 1962; Sprigs and Li, 1976):

$$Q_s = K_o a_m \delta x_{lm} \quad (1.8)$$

$Q_x$ : Mass flow of solute crossing the membrane,

$K_o$ : Global coefficient of mass transfer,

$a_m$ : Surface of the membrane ,

$\delta x_{lm} = \frac{x_1 - x_2}{\ln(x_1 / x_2)}$ : Mean logarithmic difference of concentration on both

sides of the membrane.

The global coefficient of mass transfer is function of the transfer resistances relative to the two liquid films and to the membrane:

$$\frac{1}{K_o} = \frac{1}{K_m} + \frac{1}{K_d} + \frac{1}{K_c} \quad (1.9)$$

$K_m$ : Permeability of the membrane with respect to the solute,

$K_d$  and  $K_c$ : Mass transfer coefficients apart the membrane.

The permeability of membrane with respect to the solute can be estimated using the next relationship (Lane and Riggle, 1959):

$$K_m = D_c F \Omega / H \delta_m \quad (1.10)$$

$D_c$ : Diffusion coefficient in the solution,

$F$ : Resistance factor,

$\Omega$ : Volume fraction of membrane pores,

$H$ : Factor of tortuosity or capillary length to the thickness of the membrane,

$\delta_m$ : Membrane thickness.

The resistance factor F can be evaluated, according to (Bacon, 1936) as:

$$F = 1 - 2.104 \frac{R_s}{R_p} + 2.09 \left( \frac{R_s}{R_p} \right)^3 - 0.95 \left( \frac{R_s}{R_p} \right)^5 \quad (1.11)$$

$R_s$ : The radius of the diffusing molecule (solute),

$R_p$ : Average radius of the pore.

### 1.2.4 Example of tea infusion

Spiro and Siddique (1981); Spiro and Jago (1981) have studied the kinetics and equilibria of tea infusion. It is composed of 3 main contributions, which arise from the diffusion of the constituent through the leaf: its transfer across the leaf/solvent at the interface, and its diffusion through the Nernst layer.

In order to determine the extraction rate of all soluble material from plant substrates, a simple kinetic equation for the infusion of a single constituent is:

$$\ln\left(\frac{c_\infty}{c_\infty - c}\right) = k_T t \quad (1.12)$$

$c$  : Solute concentration in the solution at time  $t$ ,

$c_\infty$  : Solute concentration in the solution at equilibrium,

$k_T$  : The overall rate constant.

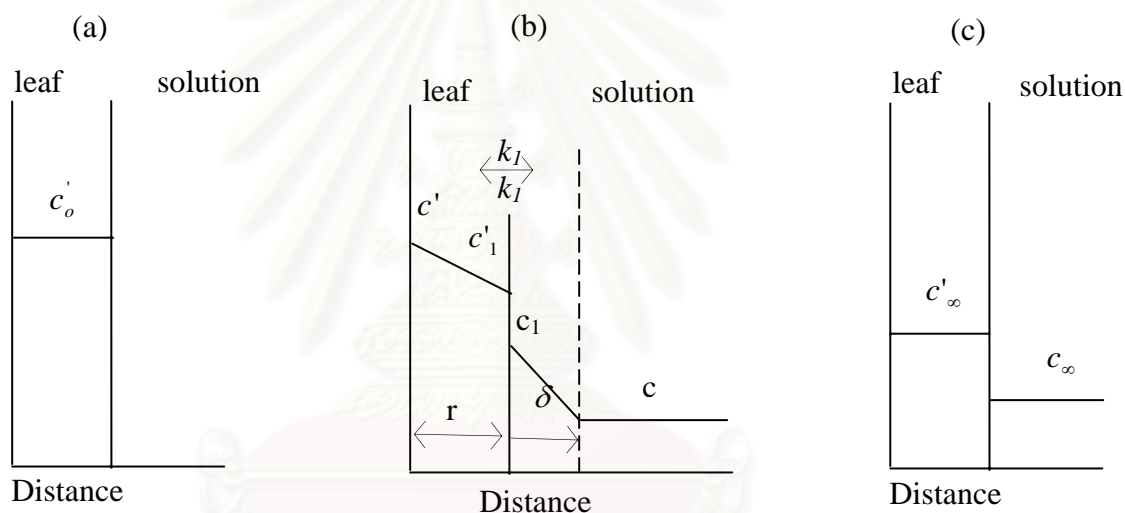


**Figure 1.8** Schematic concentration profiles during leaf infusion at (a)  $t = 0$ ; (b) given  $t$ ; (c)  $t = \infty$

**Figure 1.8** illustrates the profiles of the concentration before ( $t = 0$ ) and during diffusion ( $t$ ) and after the system has reached equilibrium ( $t = \infty$ ). All the values,  $c$ , are volume concentration ( $\text{kg m}^{-3}$  or  $\text{mol m}^{-3}$ ). Each particle is surrounded by a Nernst diffusion layer (Levich, 1962) of effective thickness  $\delta$  which decreases with increased stirring.

$c'$  is the concentration of the particular constituent in the centre of the leaf lamina.

$c'_1$  and  $c_1$  are respectively their concentrations on the leaf side (solid) and on the solution side of the interface at any time  $t$ .

$c'_\infty$  and  $c_\infty$  are their concentrations in the leaf side and liquid phase equilibrium is reached.



$c$  is the concentration in the bulk solution, outside the Nernst diffusion layer of effective thickness  $\delta$ .

The first-order rate constants for the transfer of the constituent across the interface are  $k_1$  ( $\text{m s}^{-1}$ ) from the leaf to solution and  $k_{-1}$  in the opposite direction ( $\text{m.s}^{-1}$ ).

To apply an analogous steady-state treatment for a liquid - liquid system, a partition coefficient  $K$  can be introduced. The partition coefficient  $K$  is therefore given by:

$$K = \frac{k_1}{k_{-1}} = \frac{c_\infty}{c'_\infty} \quad (1.13)$$

At steady state, the flux  $F$  (the net amount of a soluble constituent leaving the leaf per unit time) is given by the following kinetics equations:

$$F = AD_{leaf}(c' - c'_1)/d \quad (1.14)$$

$$= A(k_1c'_1 - k_{-1}c_1) \quad (1.15)$$

$$= AD_{soln}(c_1 - c)/\delta \quad (1.16)$$

$$= d(cV)/dt \quad (1.17)$$

where equation (1.14) and (1.16) are applications of Fick's first law and the diffusion coefficients of constituents are relative to each medium with the appropriate subscripts.  $D_{leaf}$  is likely to be dependent of either distance or concentration or both. Equation (1.17) expresses the fact that this flux also equals the amount of constituent entering the bulk solution per unit time.

The aim of such an approach is the derivation of a kinetics equation with  $c$  as the unique concentration variable because it is only the concentration in the bulk solution that can be experimentally followed. Combination of equations (1.14), (1.15) and (1.16) allows us to express each of the three unknown concentration  $c'$ ,  $c'_1$  and  $c_1$  as a function of  $c$ . The elimination of the unknown concentration  $c'_1$  and  $c_1$  between equation (1.14) and (1.16) now leads to:

$$k_1c' - k_{-1}c = \frac{F}{A} \left( 1 + \frac{k_1d}{D_{leaf}} + \frac{k_{-1}\delta}{D_{soln}} \right) \quad (1.18)$$

Incorporation of equation (1.14) gives the following equation:

$$k_1(c' - c'_\infty) + k_{-1}(c_\infty - c) = \frac{F}{A} \left( 1 + \frac{k_1d}{D_{leaf}} + \frac{k_{-1}\delta}{D_{soln}} \right) \quad (1.19)$$

If  $T$  is the total amount of the soluble constituent in the system, then at times  $t = 0$ ,  $t = \infty$  and  $t$ , respectively:

$$T = V'c'_0 = V'c'_\infty + Vc_\infty = c_\infty \left( \frac{V'}{K} + V \right) \quad (1.20)$$

In an infusion experiment, leaf material of mass  $w$  is immersed in a volume  $V$  of solution. Swelling of the leaf is taken to be essentially complete before significant solute extraction has occurred.

The swollen leaf may be conveniently regarded as a collection of lamina of width  $2d$  and total surface area  $A$ . If the small area around the edges of the lamina is neglected, the leaf volume  $V_{\text{leaf}}$  equals  $2d(A/2) = Ad$ . However, to eliminate  $c'$ , the conservation equation is drawn which expresses the fact that the total amount of constitute in the system is conserved.

$$T = Adc'_\infty + Vc_\infty \quad (1.21)$$

solvent: 
$$T = Ad \left( \frac{c' + c'_1}{2} \right) + Ad \left( \frac{c_1 + c}{2} \right) + (V - A\delta)c \quad (1.22)$$

Combination of equation (1.21) and (1.22), with the removal of  $c'_1$  and  $c_1$  by means of equations (1.15) and (1.16), gives:

$$Ad(c' - c'_\infty) = V(c_\infty - c) + \frac{F}{2} \left( \frac{d^2}{D_{\text{leaf}}} - \frac{\delta^2}{D_{\text{soln}}} \right) \quad (1.23)$$

This makes possible elimination  $(c' - c'_\infty)$  from equation (1.19):

$$(c_\infty - c) \left( k_{-1} + \frac{k_1 V}{Ad} \right) = \frac{F}{A} \left( 1 + \frac{k_1 d}{2D_{\text{leaf}}} + \frac{k_{-1} \delta}{D_{\text{soln}}} + \frac{k_1 \delta^2}{2D_{\text{soln}} d} \right) \quad (1.24)$$

Dividing through by  $k_{-1}$  and making use of equations (1.13) and (1.14):

$$\begin{aligned} (c_\infty - c) \left( 1 + \frac{KV}{Ad} \right) &= \frac{F}{A} \left( \frac{1}{k_{-1}} + \frac{Kd}{2D_{\text{leaf}}} + \frac{\delta}{D_{\text{soln}}} + \frac{K\delta^2}{2D_{\text{soln}} d} \right) \\ &= \frac{F}{Ak'} \text{ (for short)} \\ &= \frac{V}{Ak'} \left( \frac{dc}{dt} \right) \end{aligned} \quad (1.25)$$

Finally, the overall first-order rate constant  $k_T$  of equation (1.12) is given by:

$$\frac{1}{k_T} \left( \frac{A}{V} + \frac{K}{d} \right) = \frac{1}{k'} = \frac{1}{k_{-1}} + \frac{Kd}{2D_{leaf}} + \frac{\delta}{D_{soln}} + \frac{K\delta^2}{2D_{soln}d} \quad (1.26)$$

The last term on the right-hand side of equation (1.26) can usually be neglected as it will almost always be much smaller than the  $\delta / D_{soln}$  term. There are 3 special cases according to the relative sizes of the other terms on the right-hand side:

- (i) If  $1/k_{-1}$  is the largest term,  $k' \approx k_{-1}$  and the infusion is surface-controlled. It is worth noting that the relevant rate constant is that of the re-absorption of the constituent into the leaf.
- (ii) If the second term is the largest,  $k' \approx 2D_{leaf} / Kd$  and the rate-controlling step is diffusion of the constituent through the swollen leaf.
- (iii) If  $\delta / D_{soln}$  is the largest term so that  $k' \approx D_{soln} / \delta$ , the infusion is controlled by diffusion of the constituent across the Nernst layer.

### 1.3 FACTORS INFLUENCING THE EXTRACTION

Phenomena of mass transfer in the solid, in particular from a plant material, are affected by several parameters that can be distinguished into two groups: constitutive parameters and operating parameters.

The constitutive parameters group is composed of factors nearly constant during the extraction process and their influences cannot be controlled by the operator.

On the contrary, the operating parameters condition the process. Their influences on the apparent kinetics of extraction may be controlled by the operator. Belonging to this group are classically the temperature, the concentration of solvent, the agitation, the diameter of particle size, the solid-liquid ratio, etc (Poole, 1966).

#### 1.3.1 Influence of the solid

The structure of the plant material is complex. The classical descriptions used in chemical engineering cannot claim to cover all plant structures. The characteristics of particles are usually determined by:

- The porosity ( $\epsilon$ ),
- The tortuosity ( $\tau$ ) defined by the real length of pores in relation to the straight line along the direction of the main flux of diffusion (Lalou, 1995),
- The size and the shape of particles,
- The specific surface area (A).

The porosity of the plant substrate is relatively high. The tortuosity ( $\tau$ ) classically being comprised between 2 and 6 may be more important in the case of

plants with compact structure. It is possible to measure the porosity, while it remains difficult to measure the tortuosity ( $\tau$ ).

Simeonov, Tsibranska and Minchev (1999) have studied the kinetics and structural changes for the tobacco leaves (*Nicotiana tabacum* L.) - water and oak bark (*Quercus frainetto* Ten) - water systems. The variable effective diffusivity and porosity have been derived from a numerical approach being compared to experimental results.

Indeed, the determinations of these factors are not so easy to solve since the plant material structure is often very complex. Besides, particle sizes and shapes are most of the time non-uniform.

### 1.3.2 Influence of the solute

The solute extracted acts on the diffusion by its molecular structure, size, localization, distribution and link into the plant material with other compounds. The various solutes extracted from fruits and vegetables permitted to show that the diffusion rate decreases when the molecular size increases (Dousse, 1978). The extraction rate of hydro-soluble material increases according to this order: organic acid > sugar > phenol (Lalou, 1995).

Many authors have attempted to propose correlations for diffusion coefficients. **Table 1.3** presents some of the equations used to calculate the diffusion coefficient of molecules in the liquid phase at different conditions.

Equation	Application domain	Reference
Einstein: $D_{AB} = \frac{K_B \cdot T}{f} \quad (1.27)$		Anderson, 1973 ; Einstein, 1956; Ghai et al., 1973
Stokes-Einstein: $D_{AB} = \frac{K_B \cdot T}{6\pi r_{aA}\eta_B} \quad (1.28)$	Spherical solute of large size in relation to the solvent	Li and Change, 1955
$D_{AB} = \frac{K_B \cdot T}{4\pi r_{aA}\eta_B} \quad (1.29)$	Solute particle equal size to the solvent	Li and Change, 1955
Wilke-Chang $D_{Am} = 7.4 \cdot 10^{-8} \frac{(\phi M)^{\frac{1}{2}} \cdot T}{\eta_m \cdot V_A^{0.6}} \quad (1.30)$	large size spherical solute particle in relation to the solvent	Perry et al.; Wilke and Chang, 1955
$D_{AB} = \frac{k \cdot T}{\eta_B \cdot V_A^{\frac{1}{3}}} \quad (1.31)$		
$k = 8.2 \cdot 10^{-8} \left[ 1 + \left( \frac{3V_B}{V_A} \right)^{\frac{2}{3}} \right] \quad (1.32)$	If solvent is H <sub>2</sub> O and V <sub>A</sub> <V <sub>B</sub> , k=25.2 10 <sup>-8</sup>	Scheibel, 1954
$D_{AB} = \frac{10 \cdot 10^{-8} M_B^{\frac{1}{2}} \cdot T}{\eta V_A^{\frac{1}{3}} \cdot V_B^{\frac{1}{3}}} \quad (1.33)$		
$D_{AB} = \frac{8.5 \cdot 10^{-8} M_B^{\frac{1}{2}} \cdot T}{\eta V_A^{\frac{1}{3}} \cdot V_B^{\frac{1}{3}}} \quad (1.34)$		
	$\frac{V_B}{V_A} \leq 1.5$	Skelland, 1974
	$\frac{V_B}{V_A} > 1.5$	

A: solute; B: solvent; D<sub>AB</sub>: Diffusion coefficient of solute A in the solvent B; K<sub>B</sub>: Boltzmann constant; T: Temperature; f: friction coefficient; r<sub>a</sub>: radius molecule; η: viscosity; M: molar mass; V<sub>A</sub>: molar volume of the solution A at the normal boiling point temperature V<sub>B</sub>: molar volume of the solution B at the normal boiling point temperature.

**Table 1.3** Published correlations relative to the diffusion coefficient

### 1.3.3 Influence of the solvent

As in the case of the solute, the nature and the molecular size of the solvent affects the diffusion rate. The smaller the size of the solvent molecule, The higher the diffusion. (Leybros and Fremeaux, 2002). The choice of solvent is first determined by the chemical structure of the material to be extracted. Since the vegetal oils consist essentially of triglycerides of fatty acids, they are normally extracted with hexane whereas for the free fatty acids, which are more polar than the triglycerides, more polar alcoholic solvents are used.

Some classical criteria help in the selection of solvent:

Selectivity: Selectivity of the solvent is of great importance. The purity of the recovered extract will have consequences on the possible further upgrading steps. Maximum selectivity consistent with solvent capacity is desirable. This concept has been extensively applied in liquid-liquid extraction (Treybal, 1963).

A good solvent, selective and volatile, provides some rich solutions while reducing the operation of evaporation and purification (recovery).

Physical Properties: The choice of a solvent with low viscosity and of density relatively low is recommended to facilitate the diffusion of solvent, agitation and mechanical separation. Low surface tension facilitates wetting of the solids in the first extraction stage. A high boiling solvent with a high latent heat of evaporation requires recovery conditions that may be adverse for thermally sensitive extracts and will increase the cost of solvent recovery.

Thermal stability: At the processing temperature the solvent should be completely stable in order to avoid expensive solvent purification and losses. Contamination of the solvent-free solute with any solvent breakdown products must be avoided, especially in food products.

Hazards: The solvent should be as much as possible non-toxic and non-hazardous (i.e. non-flammable and non-explosive).

Cost: The cost of fresh solvent has to be as low as possible.

Besides, in the case of aqueous extraction, pH measurement gives some control on selectivity (Hildebrandt et al, 1970).

Except for hexane (aliphatic hydrocarbon) previously mentioned, the short-chain alcohols are also an important class of solvents. They are generally used in admixture with water and a large range of compositions is therefore available. Another large class of extraction solvents are the halogenated hydrocarbons. A solvent of promising interest is liquid or supercritical carbon dioxide that appears to be suitable for extracting flavour components from plants (Laws, 1977). However it requires operation under pressure of up to 7 MPa (70 atm) (critical pressure,  $p_c = 7.3$  MPa) which affects the cost of the extraction unit, although solvent recovery seems likely to be more economical than in the case of conventional solvents.

In conclusion, the principal solvents used are water, alcohols (methanol, ethanol), and hydrocarbons (hexane).

#### **1.3.4 Influence of the temperature**

A higher temperature generally increases as well as solubility and the diffusivity of the solution and reduces the viscosity of the solution. Operational temperature is limited by the risks of extracting harmful compounds as well as the risks of thermal degradation of the solute, and by the security of the installation (fire hazard).

#### **1.3.5 Influence of agitation**

The mechanical agitation of particles in the solvent, that permits their maintenance in suspension and the homogenization of the medium, has an effect still favourable on the operation. Furthermore, agitation will have great influence on mass transfer at the solid – liquid interface.

#### **1.3.6 Influence of humidity**

In the utilization of a hydrophobic solvent, the diffusivity is inversely proportional to the water content of solid (Leybros and Fremaux, 2002).

### **1.4 METHODS OF EXTRACTION**

Selection of methods of solid-liquid extraction depends on the answer to the following question: how much extraction time is required to approach equilibrium? Particularly, when a low extraction rate requires an extended residence time or when the nature of the solid material does not facilitate the continuous transport. If the extraction is accompanied by a chemical reaction, a stagewise operation is preferred, the residence time being determined by the reaction rate.

The methods of recovery depend largely on the solute and to some extent on the solvents. Solvent recovery is often energy consuming and a complete process energy analysis is recommended to reduce the costs.

#### **1.4.1 Single stage or simple contact operation**

This is the simplest way to operate, but it assumes that extraction is restricted to one theoretical stage. It generally involves a large amount of solvent, so that the solvent is never saturated and it generally corresponds to a batch process with large contact times to allow the diffusion of the solvent and the solubilization of the solute. In a continuous process, it corresponds to a co-current operation.

## 1.4.2 Multiple stages operation

### 1.4.2.1 Cross-current operation

The cross-current operation is illustrated by the **Figure 1.9**:

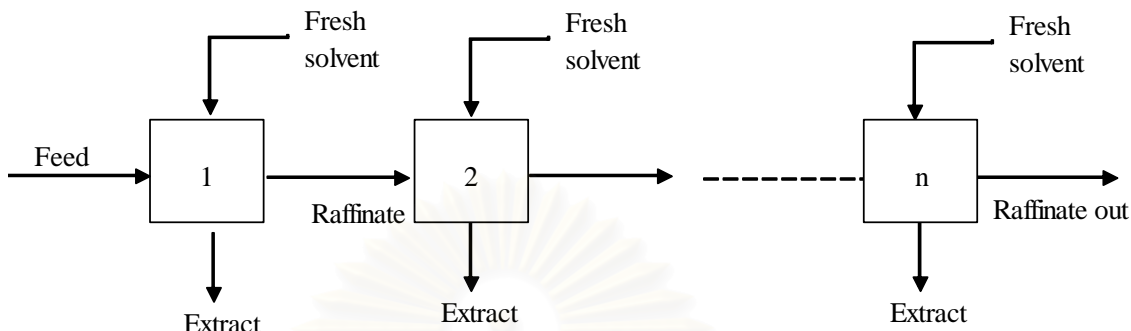


**Figure 1.9** Cross-current extraction

The feed is contacted with a fresh solvent. It corresponds to the first stage, that is similar to a simple contact. Then the raffinate coming out the first stage is contacted again with fresh solvent. This operation is repeated  $N$  times, performing by this way  $N$  theoretical stages. This operation may be achieved in a Soxhlet for instance, at the laboratory scale.

This method ensures that the solid feed is exhausted at the end of the process, but the main disadvantage lies in the fact, that a huge amount of fresh solvent is required. Subsequently, a counter-current operation is most of the time preferred to a cross-current process.

### 1.4.2.2 Counter-current operation

In counter-current extraction the solid feed and solvent enter at opposite ends of the extractor so that the raffinate and extract flow counter currently, as shown in **Figure 1.10**. By this means the rich extract is brought into contact with entering feed containing the highest concentration of solute, thus achieving a constant driving force along the process a low solvent consumption and a high extract concentration.

For these reasons, it is probably one of the most popular way of operating separation processes. But in the case of solid-liquid flows, the counter-current operation is not simple to manage, since the hydrodynamics often not favorable. The density difference between the solid phase and the solvent are often so low that it does not allow simple counter-current flow.

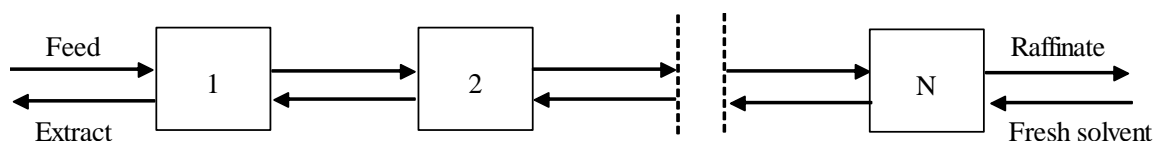


**Figure 1.10** Counter-current extraction



## 1.5 PULSED COLUMN EXTRACTION

One of the requirements for effective solid-liquid extraction is through mixing of the two phases. In a batch extraction this is easily accomplished by agitating the two phases then allowing both phases to settle and the separate both phases. By a suitable arrangement of mixing vessels and settling tanks it becomes possible to operate stagewise and countercurrent. However, if many repeated extractions are necessary this method is likely to be awkward and expensive. In order to reduce the number of pieces of equipment for countercurrent extraction, it has become more practical to use packed columns. Many studies have been made and proposed the use of agitation to help mass transfer. A classical method is based on the pulsation of the liquid to improve turbulence throughout the column.

Liquid-liquid extraction in pulsed columns is today a classic unit operation. The principles of pulsed columns were established by Van dijck (1935) who described two methods of pulsation. One involved the use of horizontal perforated plates that were mechanically moved up and down, while liquids passed through the extractor. The other involved keeping the internals of the extractor stationary, while the liquids were to be pulsed by an outside mechanism, the motion of which was transmitted to the liquid hydraulically. In pulsed plate or packed columns, mass transfer rates are enhanced without much axial mixing, permitting lower column heights. This has led to wide applications, particularly in the solvent extraction of radioactive materials where the possibility of creating the pulsing action remotely is an advantage. Classically, pulsation is transmitted directly from a piston to the continuous phase in the column filled with stationary packing or plates.

The amplitude and the frequency of pulsation are the parameters that control either the residence time of the phases or the turbulence level inside the compartments. In the case of liquid-liquid flow, it allows to control the droplet size, and consequently, the interfacial area.

Choice of packing and plates depend on the system chosen and on the process flexibility needed. This choice can be perforated plates, sieve plates or discs and doughnuts. The latter one is particularly well adapted to solid flow.

### 1.5.1 General characteristics of pulsed columns

The fluid dynamic characteristics of pulsed plate columns in the case of liquid dispersions have been described by Sege and Woodfield, (1954); Chantry, (1955); Edwards, (1956); Geier, (1957); Richardson, (1961) and Berger, (1978). **Figure 1.11** shows five distinct types of flow regimes that have been observed in pulsed columns as a function of throughput and pulsating conditions, characterized by the product of amplitude by frequency of pulsation.

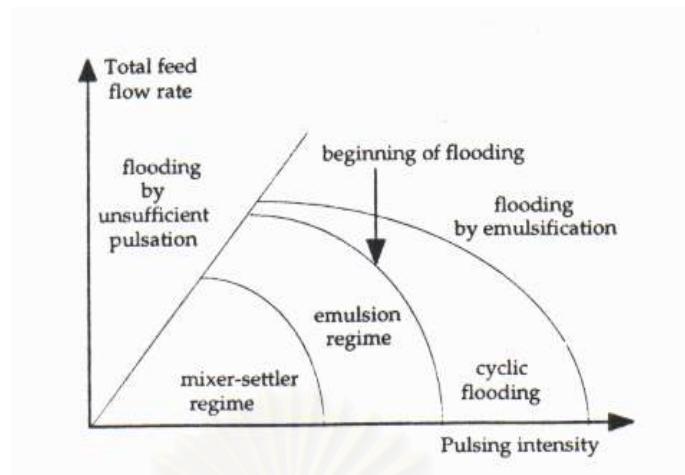


**Figure 1.11** Different types of flow regimes in a pulsed column

The flow regimes are called:

- Flooding by insufficient pulsation
- Mixer - settler type operation
- Emulsion type operation
- Cyclic flooding
- Flooding by emulsification.

At low pulsation and low flow rates the dispersed phase coalesces under the plate (or above, depending on which phase is dispersed). This region is called the **mixer-settler regime** since the liquids are mixed and allowed to settle as in mixer-settler contactors. Occurring at low flow rates and frequencies, as indicated, this regime is characterized by the separation of the light and heavy phase during the quiescent portion of the pulsation. The column operation is very stable but inefficient, in terms of mass transfer performance, compared with the operation in the emulsion regime.

For higher flowrates, but still low pulsing condition, the mixer-settler regime is so much enhanced that the dispersed phase accumulates close to the plates leading to local flooding. The phases are no longer able to flow counter-currently and the regime corresponds to a global **flooding of the column by insufficient pulsation**. This regime is obviously disregarded.

At higher flowrates, but now at higher pulsing conditions, the dispersed phase is dispersed homogeneously inside each compartment of the column, with uniform droplet sizes. This regime is called the **emulsion regime**, well adapted to stable conditions and to efficient mass transfer rates.

The **cyclic flooding** region occurs at even higher throughputs and frequencies. It is characterized by a mixture of coarse and fine droplets of dispersed phase, forming large irregular shaped particles of dispersed phase by coalescence with fines and rising periodically throughout the column. This region corresponds to an unstable operating region and the efficiency of the column is generally poorer than in the emulsion regime.

The **flooding by emulsification** is encountered by increasing both flowrates and pulsation intensity beyond the cycle flooding region. Counter-current flow throughout the column no longer exists and there is even some probability of phase inversion. Generally, it leads to dramatic phase entrainment. This regime is obviously disregarded.

Considering now the application to solid-liquid processes, the need for a continuous liquid-solid contactor was primarily developed for processes involving radioactive material. (Grimmett and Brown, 1962) have presented a column which consists of five contact stages with solid, stainless steel balls, accumulated on each stage, each stage allowing a 1 inch bed of solid to be accumulated. The solid and liquid phases flow counter-currently, the solid flowing down, the liquid up. The hydraulic pulse was introduced at the bottom of the column. From the bottom of the column, the solid is air-lifted as a slurry into a liquid-solid separator. The column is pulsed by a piston pulser with a 2 inches diameter piston. A variable speed motor allows the amplitude to vary from 0 – ½ inches and the frequency from 0-2000 cycles per minute.

**Figure 1.12** shows the observed operating characteristics of the contactor. Assuming that the liquid flow rate and pulse amplitude have been fixed, at zero pulsing frequency, a small solid flow rate can usually be maintained. However when the pulsing frequency is increased, a corresponding increase in solid flow rate is possible. This trend continues until a frequency of about 600 cycles per minute is reached, at this point the maximum solid flow rate is reached. A further increase in frequency decreases the allowable solid flow rate.

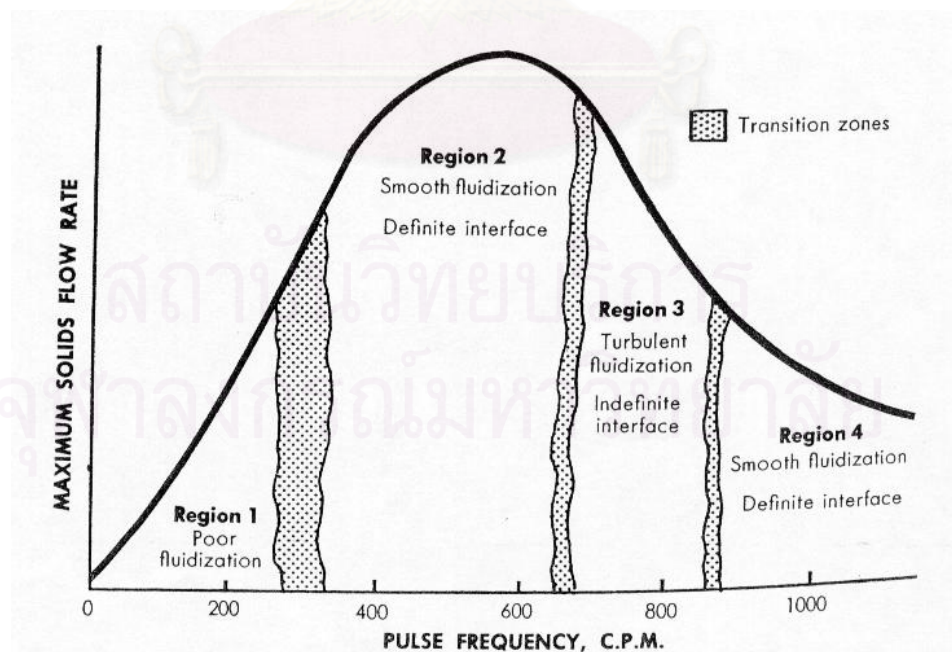


**Figure 1.12** The pulsed flow regimes in the case of a solid-liquid counter-current application

According to frequency used, four characteristic operating regions can be observed. Region 1 is equivalent to a **Poor fluidization** with the liquid-solid interface rising and falling with the applied pulse. Region 2 is **Smooth fluidization** with a definite liquid-solid interface. The transition between these two regions is not sharp. Transition to Region 3 is sharp, this region is equivalent to **Turbulent fluidization** and an indefinite liquid solid interface. Region 4 represents a smooth fluidization, a definite liquid-solid interface and a sharp transition from Region 3. The upper boundary of the region, if one exists, has not been observed.

**Figure 1.12** shows that the boundaries are universal. They are influenced by the pulsation amplitude, the physical properties of the solids, the configuration and dimensions of the column, and to some extent by the liquid flow rate. Generally, an increase in liquid flow decreases the maximum solid flow.

In our laboratory, (Sutham Sukmanee, (1984); Galaya Srisuwan, (1988); Haunold, (1991)) have studied for many years the exploitation of a disc and doughnut pulsed column for solid-liquid contact purposes. They have considered the solid phase as a population of different sized particles, circulating by gravity counter-currently to the solvent. This procedure makes possible and ensures a perfect impregnation of the particles by the solvent and an effective control of the driving force. Thus, they can reach efficiencies close to that obtained in a batch, although phase contact times are not at all the same orders of magnitude in the two cases (some minutes in columns against some hours in agitated vessels).

More recently, Somkiat Ngamprasertsith (1993) has considered the optimizing exchange conditions between the two phases while trying to minimise the consumption of solvent. Additionally, some points of disagreement between experience and simulation that subsisted after the work of (Sutham Sukmanee, (1984); Galaya Srisuwan, (1988); Haunold, (1991)) have been solved in this work.

But, some difficulties have been also exhibited. Practically, the counter-current flow between small, light particles and the solvent dictates some conditions on the throughput. Generally low flowrates are recommended so that the risk of solid phase entrainment interesting is reduced. This observation has led us also to a new consideration on the way of pulsating the column.

The objective is to have at our disposal a more flexible system than the piston way of pulsing which only permits a regular sinusoidal motion of the phases, leading to a kind of fluidization for the small particles. Therefore, we became interested in the air pulsating systems.

### 1.5.2 Air pulsed column

Air pulsed columns have been developed on a large scale for over one century in the coal mining industry. In 1954, Thornton was the first author to propose the advantages of isolating the pulser from the liquid contents in the column extraction by using an air space. The air pulsing technique acts as a barrier between the process liquid and any moving parts (piston or bellow) and prevents rapid changes in pressure. The pulsing device acts on the air column, which transmits the pulsation to the continuous phase. The air pulsing offers the main advantage of isolating the pulser

from the process liquid and for this reason has been widely used in the nuclear industry. It has been estimated (Weech and Knight, 1967) that the cost of an air pulsation system with injection and exhaust valves is only 12 percent of that of an equivalent piston pulsator, so it seems likely that air pulsing has to be used in new applications where investment cost is an important criterion. Jealous and Johnson (1955) had calculated the power required by a sieve plate column assuming that each perforation behaved as an orifice with a non-recoverable pressure drop. They found that the non-recoverable power was but a small fraction of the power required to accelerate and decelerate the pulsing liquid, so that piston power ratings had to be as much as fifty times the actual power dissipation. This disadvantage can be eliminated by air-pulsing at the resonant frequency of the air-liquid system. However it should be noted that if the system is non-resonant, air-pulsing consumes more power than direct pulsing (Thornton, 1954).

The commercial extraction equipment surveys, (Akell and Reman, 1966) had described that pulsed columns are currently used only at a small scale and to a limited extent. One problem is the distribution of the pulsation uniformly across a large cross-sectional area. The pulsation generators involving moving parts (pistons) tend to become very costly as the displacement volume requirement is raising. A solution to this problem is to apply the pulsation to the liquid indirectly, through an air column (Thornton, 1954).

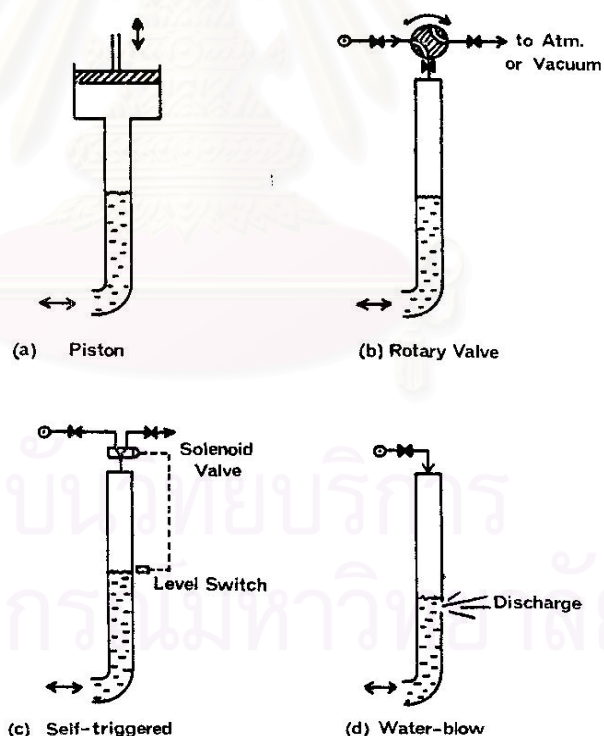


**Figure 1.13** (a-d) show typical arrangements for air pulsing system (Baird, 1967): piston (a), rotary valve (b), self-triggered (c), and water-blow (d) (detail of pulsed leg only).

Weech and Knight (1967) successfully studied a pulsed column of 26 cm in diameter and 12.4 m in height by using a pair of air injection and exhaust valves controlled by rotating cams. The work of Baird (1966, 1967) developed an air pulse

technique, which requires no mechanical moving parts to pulse a solvent extraction column at low amplitudes. As the operating frequency is close to the natural frequency of the system, the power consumption for given intensity is quite minimal. The advantages of the air pulsing technique are the relatively low capital costs of the equipment, their applicability to large columns, and a higher flexibility than a mechanical moving piece (Milburn and Baird, 1970).

The main suggestion is that the column should be operated at its natural frequency. The advantages are minimum energy and air consumption for given pulse intensity, sinusoidal and therefore reproducible and smooth waveform and finally energy and air requirements are simpler to predict.

An operating method of the column at its natural frequency with self-triggered control system was chosen. The column is controlled by a solenoid valve that could be linked electrically to a liquid level-sensing device (**Figure 1.13.c**), to ensure operation at the natural frequency by Baird (1965). However a large air control valve would need to be operated for the pilot scale and the control system would require an automatic shut-off in case of failure of one component (Baird, 1967). The maintenance problem with self-triggering system was the main reason for the preference to a rotary valve drive for the pulser, as described by Weech and Knight (1967). The simplest air pulsing system, involving no moving parts or valves and the energy source is compressed gas, called the "water blow" system (**Figure 1.13d**). The pulse leg is provided with a small discharge orifice and air is constantly supplied to it. With proper sizing of the discharge orifice, air and liquid discharge from it alternatively, and the liquid level surges up and down at the natural frequency.

Baird (1967) had studied the air pulsing column of water (water blow) in column of 1 inch, 3 inches and 6 inches in diameter. The basic principle of water blow is simple and will be explained in **Figure 1.14a**. **Figure 1.14a** shows a column of liquid in a U-tube, one leg of which is open to the atmosphere and the other closed. A gas supply G enters the closed leg and leaves by way of a small discharge tube set in the side of the leg. Simultaneously a liquid supply L enters the U-tube. After a time, the liquid level rising in both arms of the U-tube causes the liquid level to rise in both legs of the U-tube. Then after, the liquid column is unbalanced as shown in **Figure 1.14a**, with liquid and gas competing to get out of the discharge. This situation is unstable, because if the liquid momentarily blocks the discharge it allows the gas pressure in the closed leg to rise and push the liquid column downwards. The inertia of the liquid is such that it continues downwards after clearing the discharge, allowing the gas pressure in the closed leg to fall nearly to atmospheric pressure. As the liquid column is unbalanced, it then moves back down the open leg and up the closed leg until the discharge is again blocked by liquid. Thus it will be seen that the liquid column continues to oscillate, being alternately subject to gas pressure and to the static pressure due to its own imbalance. The alternating liquid flow discharge is normally much less than the gas flow because of the higher density of the liquid.

The name "water-blow pulsation" has been given to the above technique because of the characteristic noise and appearance of the discharge (Baird, 1967). Although the principle of operation is simple, the underlying theory is not completely understood. The various flow rates and various apparatus designs are shown in (**Figs. 1.14a to 1.14d**).

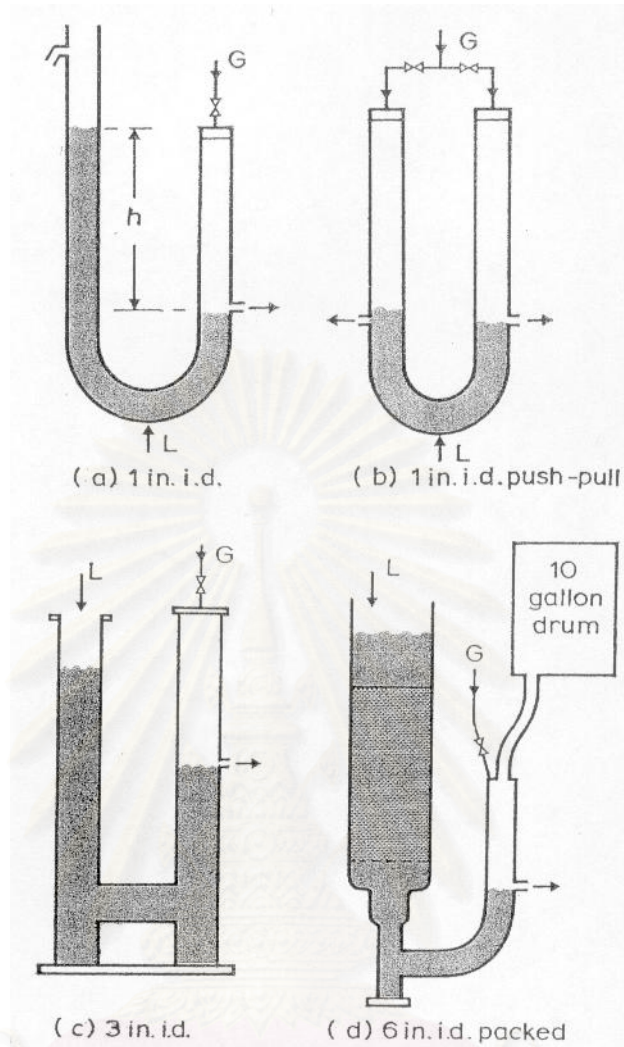


**Figure 1.14** Water-blow pulsation apparatus (not at scale)

For obvious reasons of cost and space, the pulse leg is close to the column with a smaller diameter than the column: pulse leg to column diameter ratios have been reported between 0.29 (Weech, 1967) and 0.5 (Uhle, 1965). However if the pulse leg is very narrow, the velocities in it can become so large that friction losses in the pulsed leg can exceed those in the main column. The use of long radius bends, diffusers, etc. can reduce losses but the most effective parameter is the pulse leg diameter. For a given design there will be an optimum diameter determined by a balance between higher friction losses at small diameter and higher piping cost and space requirement at large diameter ratios.

## CONCLUSION

This chapter has presented the material, the methods and the equipment of the present study.

First, *Andrographis paniculata* is a widely used traditional plant in Thailand. The botanical characteristics, the properties of the plant, the historical and traditional use, the cultivation, the harvesting-storage conditions, including the chemical study on the active principle of this plant have been detailed.

Second, the mass transfer mechanism has been reviewed and the difficulties arising from the plant morphology have been emphasized.

Finally, the general characteristics of pulsed columns have been reviewed. In this work, we have focused our attention on the pneumatic pulse system with air, which seems to be more flexible and appropriate to the solid-liquid flows than the mechanical system. The reasons for that choice are purely hydraulic in nature. Because of the low density difference between a plant material and a solvent, it is sometimes difficult to operate continuously and the smaller particles tend to fluidize in the column, before being either entrained by the continuous flow or highly accumulated at the feed, hindering phase flow.



สถาบันวิทยบริการ  
จุฬาลงกรณ์มหาวิทยาลัย



## CHAPTER II

### BATCH EXTRACTION EXPERIMENTS

#### INTRODUCTION

This chapter presents some of the preliminary experiments performed on *Andrographis paniculata* in order to obtain the characteristics required by the solid-liquid extraction process.

The first part aims with plant characteristics such as determination of size, shape, structure and initial concentration of solute obtained in soxhlet experiments.

The second part is devoted to the batch extraction experiments, leading to an analysis of the influence of the main operating parameters such as mass of solid, percentage of ethanol solution, size of particles and temperature.

The third part is devoted to the destruction of the active principle due to temperature, age and storage.

The last part will give information on the hydrodynamic behaviour of the solid in the solvent.



สถาบันวิทยบริการ  
จุฬาลงกรณ์มหาวิทยาลัย

## 2.1 PLANT ANALYSIS

The plant is analysed in order to determine plant characteristics such as: size class, shape, structure and initial concentration of solute.

### 2.1.1 Material

The raw material is sieved into six parts according to the following distribution of particle sizes:

- 1 particle size less than 0.1 mm
- 2 particle size from 0.1 to 0.3 mm
- 3 particle size from 0.3 to 0.45 mm
- 4 particle size from 0.45 to 0.6 mm
- 5 particle size from 0.6 to 0.8 mm
- 6 particle size larger than 0.8 mm

After every sieving, each particle class was weighed. The distribution in mass of the size fractions of the raw material is illustrated in **Table 2.1**.

Diameter	Mass of solid (g)				% mass
d<0.1	5.8	16.9	23.6	15.13	5.00
0.1<d<0.3	17.4	49.4	62.8	43.2	14.28
0.3<d<0.45	18.8	51.5	68.55	46.28	15.30
0.45<d<0.6	15.7	45.1	59.3	40.03	13.23
0.6<d<0.8	17.5	51.4	71.2	46.7	15.43
d>0.8	46.3	125.6	161.8	111.23	36.76

**Table 2.1** Mass percentage of solid

**Figure 2.1** shows the distribution of mass percentage of the plant according to the diameter. This figure shows that there are quite the same percentage on class size 0.1-0.3 mm, 0.3-0.45 mm, 0.45-0.6 mm and 0.6-0.8 mm. All the class sizes (except d < 0.1 mm and d > 0.8 mm) will be used in the batch reactor experiments.

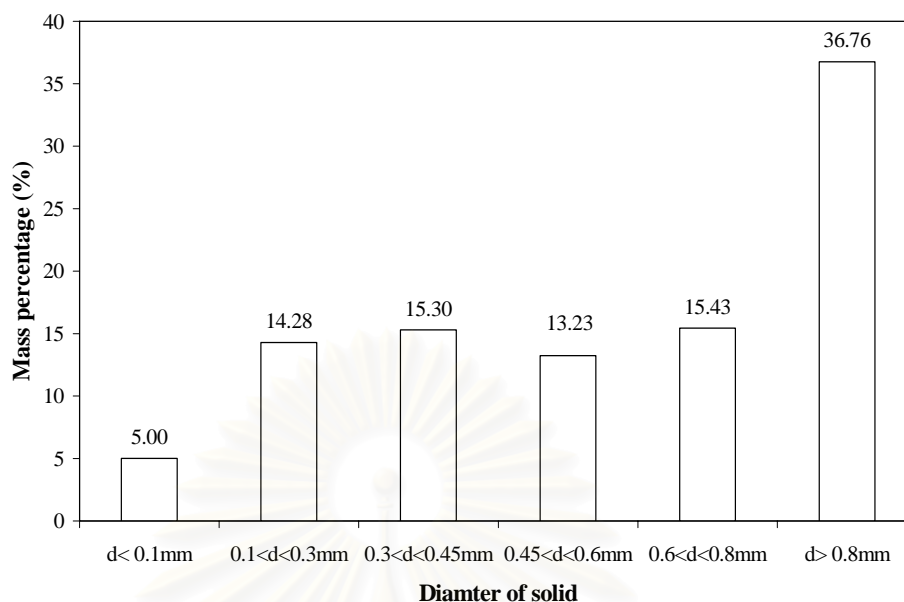


**Figure 2.1** Distribution of mass percentage versus diameter of solid

### 2.1.2 Plant Structure and geometrical characteristics

*Andrographis paniculata* samples were scanned with a Scanning Electronic Microscope (SEM) in order to obtain visual observations of its structure, especially the thickness and the shape of the plants. As a result of the observations, the particles can be separated into two shapes (cylinder refers to stems and plate refers to leaves). The thickness of leaves can be considered as  $35\ \mu\text{m}$  and the diameter of stem is  $900\ \mu\text{m}$ . The pictures of leaf and stem of *Andrographis paniculata* from SEM are presented in **Figure 2.2**.

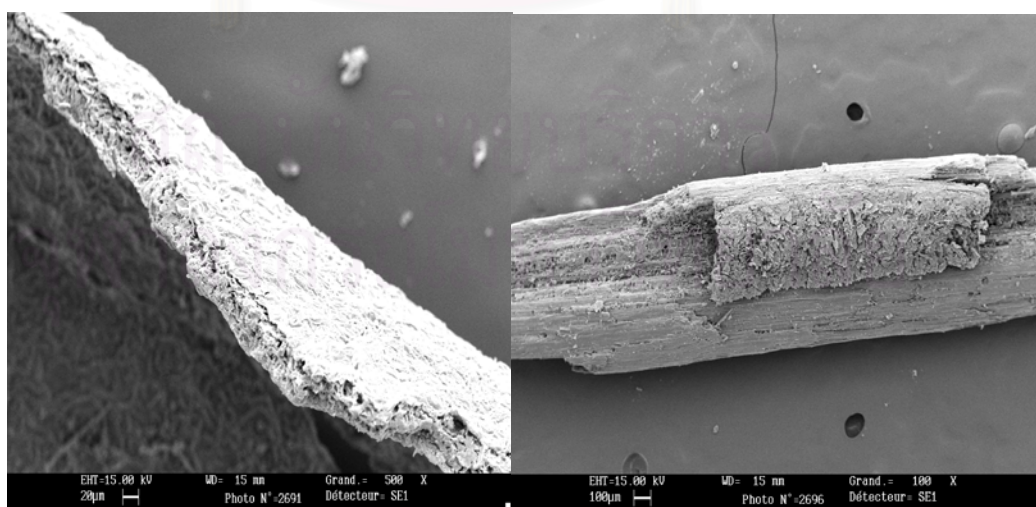


**Figure 2.2** The structure of *Andrographis paniculata* (leaf and stem) from the Scanning Electronic Microscope

### 2.1.3 Porosity and apparent density of solid

Experiments were performed as follows:

A known mass  $M$  of solid was introduced in a test-tube. Then a known mass of  $M_{sol}$  corresponding to  $V_{sol}$  was introduced. The initial total volume of the solid-liquid mixture was noted as  $V_0$ . The test-tube was closed in order to avoid evaporation and was allowed to rest for one day (24 hours is generally sufficient). The final total volume  $V$  was measured. Then, we separated out the solid and weighed the isolated humid solid  $m_h$ , then dried it in an oven at temperature of about  $60^\circ\text{C}$ . During drying, the solvent absorbed in pores of the solid were vaporized and a mass of dry solid  $m_s$  was obtained.

We used two methods to determine the porosity and apparent density of the solid:

**Method 1:** determination  $\varepsilon$  and  $\rho_{app}$  by variation of volume

The experiment is as follows:

- We define the total volume of the solid (volume taking into account the pores):

$$V_t = V_0 - V_{sol} \quad (2.1)$$

- We define the empty volume in the solid (volume of pores):

$$V_p = V_0 - V \quad (2.2)$$

From the definition of the porosity:  $\varepsilon = \text{empty volume of pores} / \text{total volume of the solid}$

We can calculate the porosity of the solid, then:

$$\varepsilon = \frac{V_p}{V_t} \quad (2.3)$$

However, it is necessary to understand that we can never be certain that all the restrained air in pores has been replaced by solvent; then we cannot be sure we have reached a reasonable approximation of the porosity (Lalou, 1995).

To determine the apparent density, we use a simple method based on the measurement of the volume occupied by a solid mass.

Experimentally, we have:

$$\rho_{app} = \frac{M}{V_t} \quad (2.4)$$

**Method 2:** to determine  $\varepsilon$  and  $\rho_{app}$  based on the rate of the dry material  $\omega$  and  $\rho_{net}$

-We define a net density of the solid without pores:

$$\rho_{net} = \frac{M}{V - \frac{M_{sol}}{\rho_{sol}}} \quad (2.5)$$

$V$  : The measured volume at the end of experiment,

$M$  : Mass of solid,

$M_{sol}$  : The initial mass of solvent (ethanol),

$\rho_{sol}$  : Density of solvent (ethanol),

- We defined an apparent density of a solid particle of  $\varepsilon$  porosity:

$$\rho_{app} = \frac{\rho_{net} \cdot (1 - \varepsilon)}{\omega} \quad (2.6)$$

$\omega$  : The dry matter rate of the solid at the end of experiment.

- We define a dry matter rate  $\omega$  corresponds to a particle of which pores are filled entirely by solvent

$$\omega = \frac{\text{mass of dry solid}}{\text{mass of dry solid} + \text{mass of absorbed solvent}}$$

$$\omega = \frac{m_s}{m_s + m_{sol}} = \frac{1}{1 + \frac{\rho_{sol}}{\rho_{net}} \cdot \left( \frac{\varepsilon}{1 - \varepsilon} \right)} \quad (2.7)$$

The experiment then leads to:

$$\omega = \frac{m_s}{m_h} \quad (2.8)$$

Porosity

$$\varepsilon = \frac{1}{1 + \frac{\rho_{sol}}{\rho_{net}} \cdot \frac{\omega}{1 - \omega}} \quad (2.9)$$

**Tables 2.2, 2.3 and 2.4** present the results of the experiments for two solid diameters (0.45-0.6mm and 0.6-0.8mm) with variations of 60% and 30% ethanol concentration and mass solid (20 g for 200 ml solvent and 5g for 100 ml).

**Table 2.2** Determination of porosity and density by using solid: 0.45-0.6 mm, 5 g, solvent: 60% ethanol,  $T_{\text{room}} : 20^{\circ} \text{C}$

Parameters	Experiments									
	1.1	1.2	1.3	2.1	2.2	2.3	3.1	3.2	3.3	Average
$M$ (g)	5.05	5.05	5.05	5.01	5.01	5.01	5.01	5.01	5.01	5.02
$M_l$ (g)	88.67	88.67	88.67	88.73	88.73	88.73	88.28	88.28	88.28	88.56
$V_l$ (ml)	99	99	99	99	99	99	99	99	99	99
$V_0$ (ml)	1052	105	105	105	105	105	105	105	105	105
$V$ (ml)	103	103	103	103	103	103	103	103	103	103
$m$ (g)	0.57	0.56	0.57	0.55	0.56	0.57	0.54	0.57	0.56	0.56
$m_h$ (g)	2.86	3.07	2.55	2.76	2.81	2.77	2.98	2.57	2.79	2.80
$m_s$ (g)	0.84	0.90	0.77	0.84	0.87	0.89	0.93	0.82	0.91	0.86
METHOD 1										
$\varepsilon$	0.33	0.33	0.33	0.33	0.33	0.33	0.33	0.33	0.33	<b>0.33</b>
$\rho_{app}$ (kg/m <sup>3</sup> )	841.67	841.67	841.67	835.00	835.00	835.00	835.00	835.00	835.00	<b>837.22</b>
METHOD 2										
$\omega$	0.29	0.29	0.30	0.30	0.31	0.32	0.31	0.32	0.33	0.31
$\rho_{net}$ (kg/m <sup>3</sup> )	1436.71	1436.71	1436.71	1453.16	1453.16	1453.16	1267.54	1267.54	1267.54	1385.80
$\varepsilon$	0.79	0.80	0.79	0.79	0.78	0.77	0.76	0.75	0.75	0.78
$\rho_{app}$ (kg/m <sup>3</sup> )	294.63	294.01	303.98	307.44	313.48	326.99	306.55	314.13	321.87	309.23

**Table 2.3** Determination of porosity and density by using mass of solid: 20 g, solvent: 60% ethanol,  $T_{\text{room}} : 20^{\circ} \text{C}$

Parameter	Solid 0.45-0.6mm				Solid 0.6-0.8mm		
	(1)	(2)	(3)	average	(1)	(2)	average
$M$ (g)	20	20	20	20	20.01	20.03	20.02
$M_l$ (g)	176.6	176.6	176.47	176.56	179	177.6	178.3
$V_l$ (ml)	200	200	200	200	203	202	202.5
$V_0$ (ml)	212	214	214	213.33	217	218	217.5
$V$ (ml)	208	210	210	209.33	212	213	212.5
$m$ (g)	100.07	85.04	31.71	72.27	49.35	47.68	48.52
$m_1$ (g)	120.03	95.08	36.8	83.97	59.35	57.68	58.52
$m_2$ (g)	103.84	87.09	32.86	74.6	51.34	49.82	50.58
$m_h$ (g)	19.96	10.04	5.09	11.7	10	10	10
$m_s$ (g)	3.77	2.05	1.15	2.32	1.99	2.14	2.07
Method 1							
$\varepsilon$	0.33	0.29	0.29	0.3	0.36	0.31	0.33
$\rho_{app}$ (kg/m <sup>3</sup> )	1666.67	1428.57	1428.57	1507.94	1429.29	1251.88	1340.58
Method 2							
$\omega$	0.19	0.2	0.23	0.21	0.2	0.21	0.21
$\rho_{net}$ (kg/m <sup>3</sup> )	2028.35	1686.31	1665.82	1793.49	1791.81	1457.97	1624.89
$\varepsilon$	0.91	0.88	0.86	0.88	0.89	0.86	0.87
$\rho_{app}$ (kg/m <sup>3</sup> )	188.28	201.37	225.16	204.94	197.08	208.04	202.56

**Table 2.4** Determination of porosity and density by using mass of solid 5 g, solvent: 30% ethanol,  $T_{\text{room}} : 20^{\circ}\text{C}$

Parameters	Solid 0.45-0.6mm			Solid 0.6-0.8mm		
	1	2	average	1	2	average
$M$ (g)	5	5	5	5	5.01	5.01
$M_1$ (g)	94.4	94.06	94.23	94.97	96.13	95.55
$V_1$ (ml)	100	100	100	100	101	100.5
$V_0$ (ml)	106	105	105.5	106	107	106.5
$V$ (ml)	104	104	104	104	104	104
$m$ (g)	0.73	0.76	0.75	0.74	0.75	0.75
$m_1$ (g)	4.32	4.51	4.42	4.6	4.05	4.33
$m_2$ (g)	1.64	1.64	1.64	0.98	1.65	1.32
$m_h$ (g)	3.59	3.75	3.67	3.86	3.3	3.58
$m_s$ (g)	0.91	0.88	0.9	0.24	0.9	0.57
Method 1						
$\varepsilon$	0.33	0.2	0.27	0.33	0.5	0.42
$\rho_{app}$ (kg/m <sup>3</sup> )	833.33	1000	916.67	833.33	835	834.17
Method 2						
$\omega$	0.25	0.23	0.24	0.06	0.27	0.17
$\rho_{net}$ (kg/m <sup>3</sup> )	989.84	924.61	957.22	1122.62	1547.27	1334.94
$\varepsilon$	0.77	0.77	0.77	0.95	0.82	0.89
$\rho_{app}$ (kg/m <sup>3</sup> )	231.78	210.94	221.36	56.14	274.86	165.5

Note:  $m$ : weight of the paper filters

$m_1$ : weight of (wet solid + paper filters)

$m_2$ : weight of (dry solid + paper filters)

By comparing the experimental results derived from the two methods, we can notice that the second method, which was used by Prat in 1998, appears less accurate for our plant material. Values of apparent density that we obtained are very different relative to the possible real values. However, the first method used in this work, which is simpler, leads to more acceptable values. 60% ethanol is better absorbed in the plant than 30% ethanol.

During the experiments to determine  $\varepsilon$  and  $\rho_{app}$ , we have two main remarks that can explain our observation:

- The solid diameter that we chose to treat essentially corresponds to leaves. At the humid state, leaf particles glue themselves together easily (even with a good technique to separate solid-liquid) and keep a considerable quantity of liquid therefore on their contact surfaces. It may be the reason for erroneous value of  $m_h$ , therefore, it affects the values of  $\omega$ ,  $\varepsilon$  and  $\rho$  (method 2).

- While treating too large a mass of solid (20 g), two things are observed. First agitation is difficult when the solid rests; it remains a volume of restrained air in spaces between the particles. It creates erroneous value of  $V_0$  and  $V$ . The second reason: the height of the solid in the test-tube is important. As the height of the solid is

higher, the absorption of the liquid throughout the solid is difficult. It may explain why the  $V$  value is less precise in the experiments of **Table 2.3**.

## Results

The following result is obtained for the porosity  $\varepsilon$  and the density  $\rho$  of *Andrographis paniculata*:

$$\rho_{net} = 837 \text{ kg.m}^{-3}$$

$$\varepsilon = 0.33$$

### 2.1.4 Calibration curve of andrographolide by HPLC

The objective for creating a standard curve of andrographolide is to link the HPLC area to the quantity of andrographolide that appears in the solution. The experiment is as follows: first, the standard pure crystals of andrographolide are dissolved to the exact concentration of 2.50 mg/ml in a 90 % ethanol solution, then the solution is diluted by 50% several time to obtain the concentrations of 1.25, 0.625, 0.3125, 0.156, 0.078 and 0.039 mg/ml, respectively. The solutions are analyzed using HPLC (High Performance Liquid Chromatographic) to determine the relationship between the area under the curve and the concentration of andrographolide.

#### Method of HPLC

- Column: LICHROSORB RP18,
- Size of column: 123 × 4.6 mm,
- Mobile phase is methanol-water (50%-50% volume),
- Volume injection: 25  $\mu$ l,
- Flow rate of mobile phase: 1.00 ml/min,
- Detector wavelength: 223 nm,
- Final time: 20 min.

**Figure 2.3** shows that the andrographolide concentration linearly increases with the area under the curve of the HPLC

สถาบันวิทยบริการ  
จุฬาลงกรณ์มหาวิทยาลัย



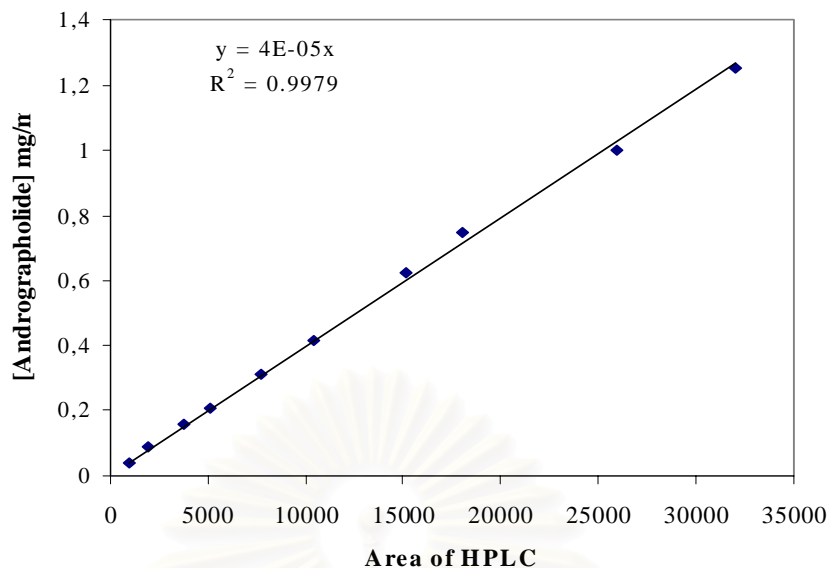


**Figure 2.3** Standard curve of andrographolide of 90% ethanol by HPLC

The experiments are also repeated in order to determine the standard curve of andrographolide by varying the percentage of ethanol with the aim to confirm the relation between the concentration and the area under the curve.

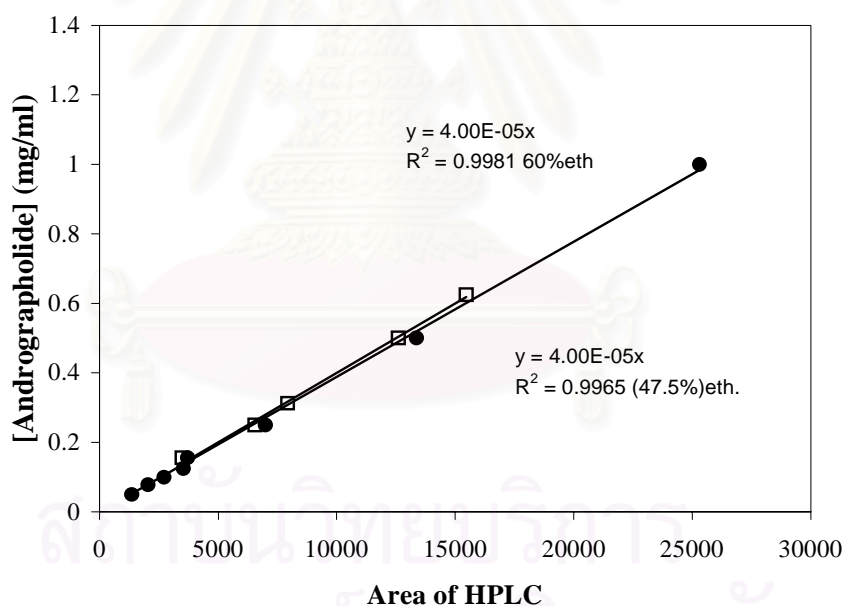


**Figure 2.4** Standard curve of andrographolide of 47.5%, 60% ethanol by HPLC

It is obvious that the relation between the concentration and the area under the curve is linear for the different concentrations of ethanol solutions. There is no effect of percentage of ethanol for this relation. Accordingly, the linear model can be applied in this circumstance.

$$\text{Equation is } C = 4.00 \times 10^{-5} \text{ Area under curve.}$$

### 2.1.5 The Soxhlet Experiments

The soxhlet reactor is presented in **Figure 2.5**. This device is often used to obtain a reference for the initial composition of the solid phase.

The goal of the soxhlet experiment is to determine the maximum quantity of andrographolide contained in the *Andrographis paniculata*. The soxhlet reactor permits multiple contact of the solid content in the extraction thimble with pure solvent at the temperature of condensation. The total solute contained in the solid can be extracted after a long enough time. The method corresponds to a cross-current contract method (**Chapter I**).

This experiment is as follows: a 10 g mass of dry herb was introduced in an extraction thimble, then put into the soxhlet. Then 500 ml ethanol solvent was poured in the ball glass. This ball was heated by an electric oven and the temperature was kept constant during the experiment. The solvent was transferred by evaporation and condensation towards the upper part where it accumulated around and inside the extraction thimble, when the solution reached the level of siphon, the solvent flowed out back to the ball, where it was evaporated again.

In this work, the experiments were done for different sizes of solid: 10 g of *Andrographis paniculata* of different sizes with 500 ml of 90% ethanol (solvent). Then, the soxhlet extraction products were analysed by HPLC to get the concentration of active ingredients in the raw material.

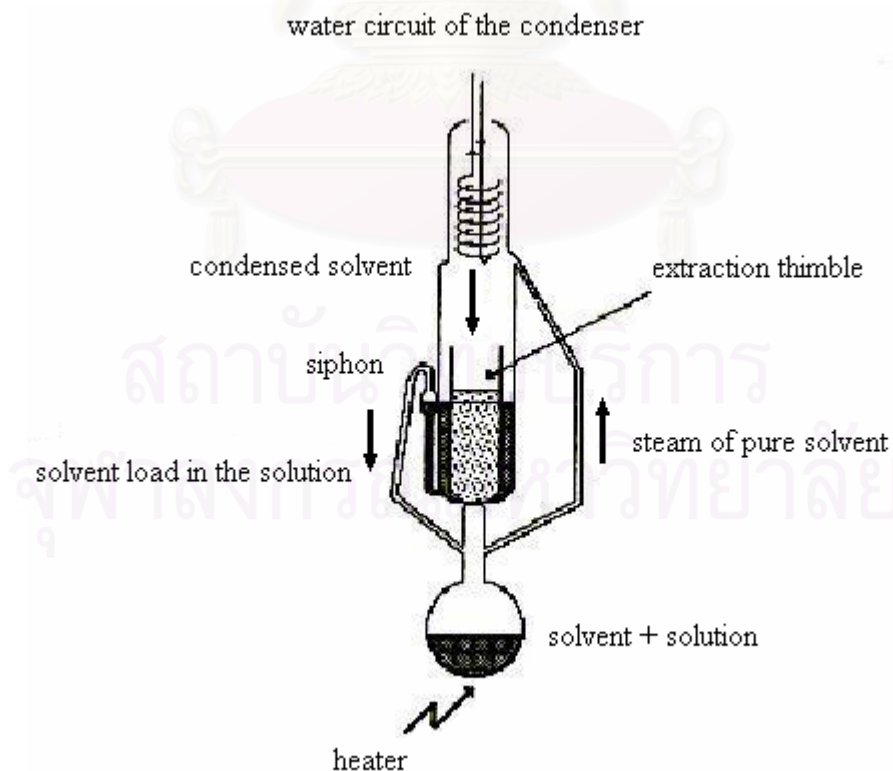


**Figure 2.5** Soxhlet Reactor

The concentrations of andrographolide in the extracted solution are presented in **Table 2.5**.

Number of exp.	diameter (mm)	[Andro.] in solvent (mg/ml solvent)	[Andro.] in particle (mg/g solid)	Stems (%m)	Leaves (% m)
1	Only leaves	0.888	44.38	0.00	100.00
2	Only stems	0.304	15.20	100.00	0.00
3	d<0.1	0.598	29.88	49.68	50.32
4	0.1<d<0.3	0.751	37.57	23.32	76.68
5	0.3<d<0.45	0.795	39.73	15.93	84.07
6	0.45<d<0.6	0.765	38.23	21.08	78.92
7	0.6<d<0.8	0.766	38.30	20.83	79.17

**Table 2.5** Concentrations of andrographolide (mg/ml, mg/g) from soxhlet experiments (90% ethanol)

The content of andrographolide in leaves is 3 times more than in the stems. Concentration in stems is 15.2 mg/g and concentration in leaves is 44.38 mg/g solid.

The concentration is slightly different when using particle sizes of 0.1 to 0.8 mm. This result shows that the concentration is also similar and the amounts of stems and leaves have a similar ratio. However, for solid particle size less than 0.1 mm (the fine particles) the concentration is smaller (certainly due to a different ratio of stems and leaves).

The mass fractions of the stems and the leaves in each solid diameter were calculated. The results show a mass fraction of leaves of 50% in the fine particle class (d<0.1 mm). For the other classes, the mass fractions of leaves and stems are nearly the same (20% of stems and 80% of leaves).

Based on the experimental result, the initial concentration of solute was studied for different diameters with 90% ethanol. In **Table 2.5**, we found that the initial concentration is independent of the diameter. The next experiment will be done in order to study the influence of the percentage of ethanol solvent with the initial concentration.

Number of exp.	Diameter (mm)	% of ethanol (solvent)	% of ethanol (condensed)	[Andrographolide]	
				mg/ml	mg/g
1	0.6-0.8	15	60	0.609	30.45
2	0.45-0.6	15	60	0.619	30.95
3	0.45-0.6	0	0	0.184	9.2
4	0.45-0.6	4	30	0.307	15.35

**Table 2.6** Concentration of andrographolide (mg/g) from soxhlet experiment

**Table 2.6** shows the andrographolide concentration using 10g of solid with 500 ml of ethanol solution in the soxhlet experiment with different ethanol concentrations. Experiments 1 and 2 confirm that the diameter has no influence on the concentration of andrographolide. Experiments 3 and 4 show a lower concentration of andrographolide.

This can be due to a direct influence of the solvent: with less ethanol, the solvent cannot reach all the andrographolide inside the solid. This can also be due to an indirect influence: with less ethanol, the boiling point increases and consequently the extraction in the soxhlet is performed at a higher temperature. The molecules can be destroyed by the high temperatures or another substance can be extracted. More experiments will be done in **Chapter 2.4** to verify which hypothesis is more plausible.

### 2.1.6 Solubility

The experiments for the solubility were done by preparing one litre of ethanol solution, and then a powder of known solid mass is introduced into the mechanically agitated batch reactor. The experiments are done for 3 hours in order to ensure that maximum andrographolide is extracted. Then, the solid is separated and the solute is analyzed by HPLC. After separating the solid, a known mass of fresh solid is introduced into the ethanol solvent again. The experiments are done continuously until there is no longer any solvent for the fresh solid mass (there are some liquid losses by the absorption of the solid and filtration in each step). **Figures 2.6 and 2.7** indicate that andrographolide concentrations increase with the solid mass.

**Figure 2.6** shows the concentration of andrographolide when ethanol is evaporated at different times. For experiment 1 which uses 260 g of solid, the amount of solute is not sufficient to determine the evolution of concentration in the vacuum evaporator. However an idea is to put the solid into the fresh solvent for experiment 2.

Then the experiment 2 started with 200 g of solid in one litre of ethanol solvent. Experiment 2 showed that the andrographolide concentration linearly increases when the mass of solid increases. This graph is unable to present the solubility of andrographolide with ethanol.

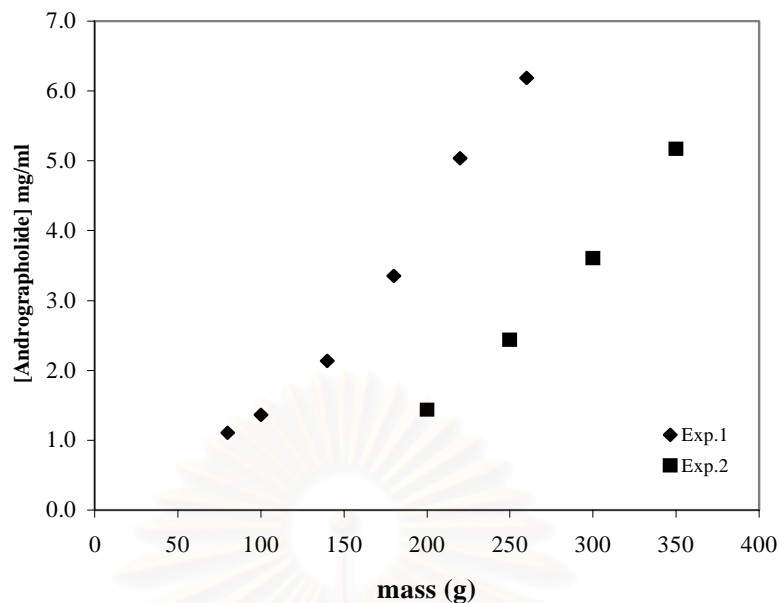


**Figure 2.6** Andrographolide concentrations as a function of the solid mass

The next experiment was done in a vacuum evaporator in order to evaporate the ethanol at low temperatures. The samples are taken at different times until almost the ethanol was evaporated. The result is presented in **Figure 2.7**.

**Figure 2.7** shows that the andrographolide concentrations continuous increase until the last sample. Since there is only a little amount of active principle in the plant material, it is very difficult to study the maximum concentration that can be extracted from the matter because a large amount of solid will be used in the reactor. However this result confirms that the ethanol solvent has a high capacity of solubilization of the andrographolide from *Andrographis paniculata*.

The concentration of andrographolide in ethanol increased up to 35 mg/ml but that does not yet seem to be the upper limit. More experiments are to be performed in order to obtain the solubility. One way can be to start from crystals.

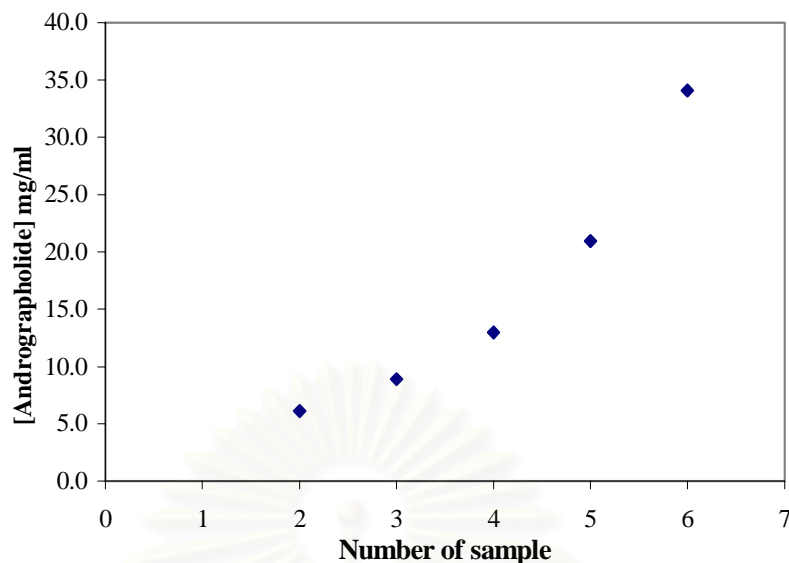


**Figure 2.7** Andrographolide concentrations at the different times in vacuum evaporator

## 2.2 KINETICS OF EXTRACTION

The objective of the batch experiments was to measure global kinetics of extraction and to analyze the influence operating parameters was. The results will be used to prepare the continuous process in the disc and doughnut pulsed column.

### 2.2.1 Batch reactor experiments

The batch reactor is shown in **Figure 2.8**. It is a very useful type discontinuous contactor for studying mass transfer and the kinetics of the extraction. The batch reactor is a glass container, temperature controlled, equipped with a syringe, which is used to sample the solvent during the experiment. An agitation by motor and a control of the temperature by a thermostat bath were well controlled during the experiment. A condenser situated at the top of the container permitted operation at atmospheric pressure.

500 ml of an aqueous ethanol solution was introduced in the one litre reactor. At time zero, a known mass of a particular class size of *Andrographis paniculata* was introduced in the reactor. The agitation ensured a good solid-liquid contact. Liquid samples were taken at different times 2, 4, 7, 10, 15, 20, 25, 30, 40, 60, 80, 100, 120, and 150 minutes, respectively. And the andrographolide concentration in the liquid phase was then measured by HPLC. As the analytic volume sample was 1 ml (compared with a total of 500 ml) the measurement was assumed to have no influence on the process.

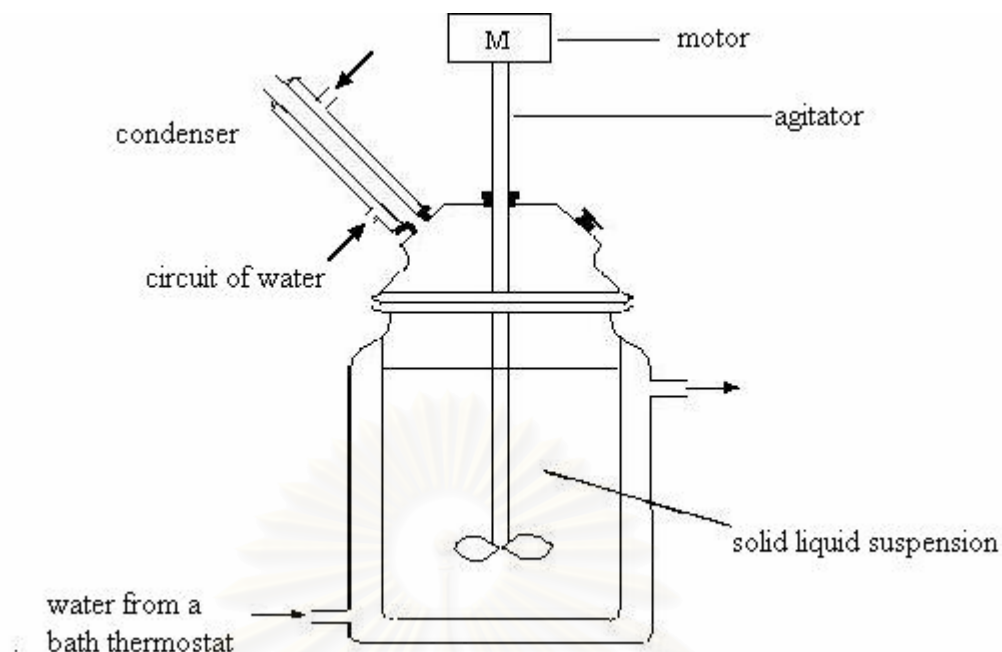


**Figure 2.8** Solid –liquid batch reactor

The objective of batch experiments is to study the influence of the initial mass of solid, the diameter of particle size, the concentration of ethanol solution and the temperature. All the results are illustrated in **Appendix II.I**.

Fourteen experiments series are represented in **Table 2.7**. They were done under different operation conditions.

Experiment number	Temp °C	Mass solid (g)	Diameter (mm)	% ethanol
1. (C1)	22	10	0.6-0.8	80
2. (C2)	22	10	0.6-0.8	70
3. (C15)	22	20	0.6-0.8	60
4. (C21)	22	20	0.6-0.8	0
5. (C5)	22	10	0.45-0.6	60
6. (C17)	22	10	0.1-0.3	60
7. (C25)	40	10	0.6-0.8	60
8. (C26)	50	10	0.6-0.8	60
9. (C27)	60	10	0.6-0.8	60
10 (C14)	22	10	0.6-0.8	60
11 (C16)	22	5	0.6-0.8	60
12 (C11)	22	10	0.6-0.8	0
13 (C12)	22	20	0.6-0.8	0
14 (C13)	22	30	0.6-0.8	0

Experiments (C25), (C26) and (C27) were done performed in Thailand

**Table 2.7** Experimental operating conditions

### 2.2.2 Effect of initial mass

Figures 2.9 and 2.11 show the concentration of andrographolide versus time for different amounts of solid particles with 60% ethanol and water respectively. The andrographolide concentration in the extracted solvent is nearly linear proportional to the mass of solid that has been used. These results show that within the experimental range, there are no solubility limits in the solvent at 22°C.

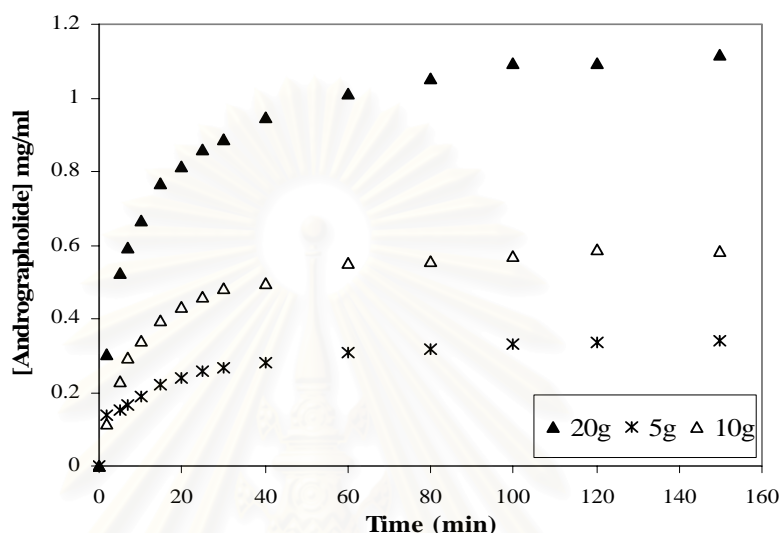


**Figure 2.9** Influence of initial solid mass on solute concentration (500 ml of 60% ethanol,  $T_{\text{room}}$ : 22°C and solid diameter: 0.6-0.8 mm)

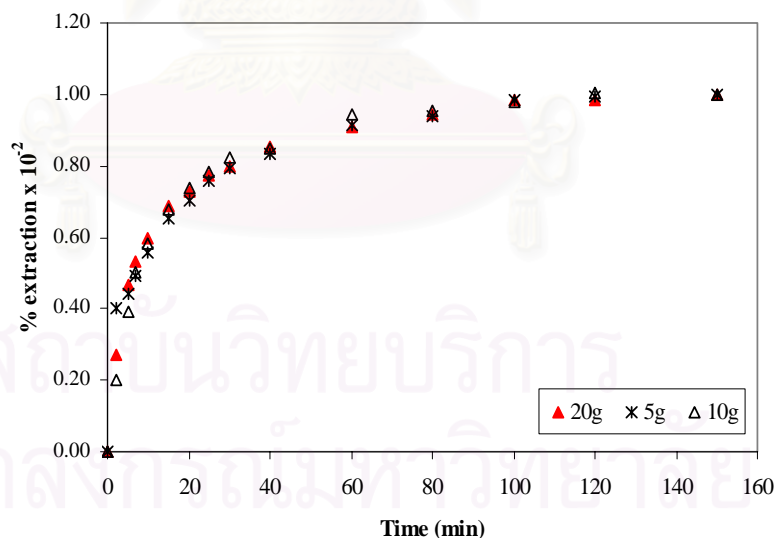


**Figure 2.10** Influence of initial solid mass on solute mass percentage (500 ml of 60% ethanol,  $T_{\text{room}}$ : 22°C and solid diameter: 0.6-0.8 mm)

Figures 2.10 and 2.12 show final concentration extracted as percentages as function of time for different amount of solid particles with 60% ethanol and water respectively. The percentage of extraction is determined by dividing each concentration at different times with the concentration at the final time (at 150 min). The curves show that the initial mass has no significant influence on the kinetics of extraction.



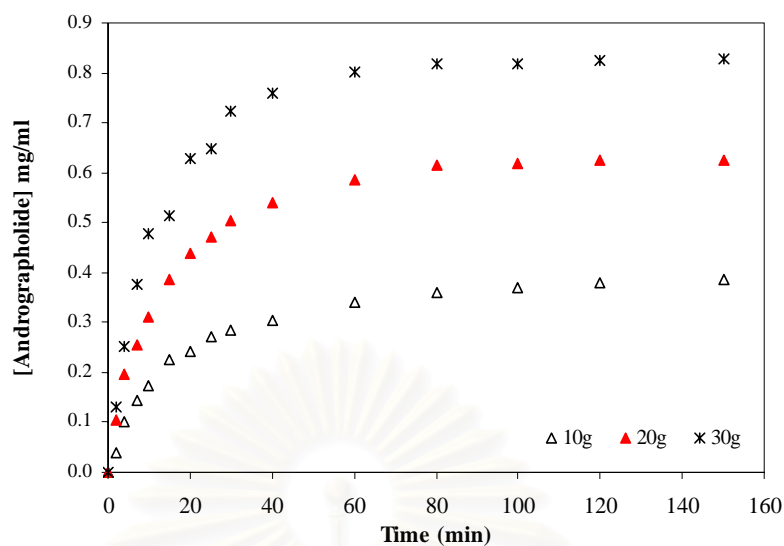


**Figure 2.11** Influence of initial solid mass on solute concentration (500 ml of water,  $T_{\text{room}}$ : 22°C and solid diameter: 0.6-0.8 mm)

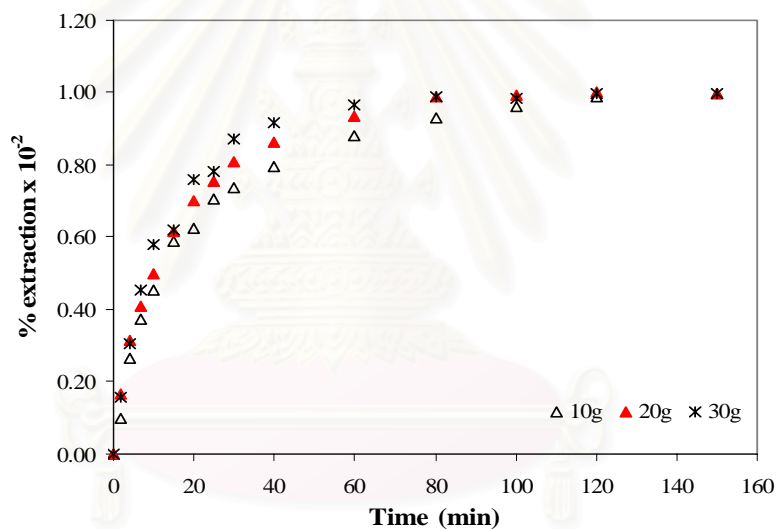


**Figure 2.12** Influence of initial solid mass on solute mass percentage (500 ml of water,  $T_{\text{room}}$ : 22°C and solid diameter: 0.6-0.8 mm)

### 2.2.3 Effect of solvent concentration

**Figure 2.13** shows the evolution of extracted andrographolide as function of time for experiments 1, 2, 3 and 4. The final concentration increases with percentage of ethanol.

Ethanol and water have similar solubility properties because they contain an hydroxyl group which is hydrophilic. Since ethanol is an organic solvent whereas water is an inorganic solvent, andrographolide ( $C_{20}H_{30}O_5$ ) which is a large hydrocarbon molecule can be better dissolved in ethanol although andrographolide is more polar (Wede, 1987).

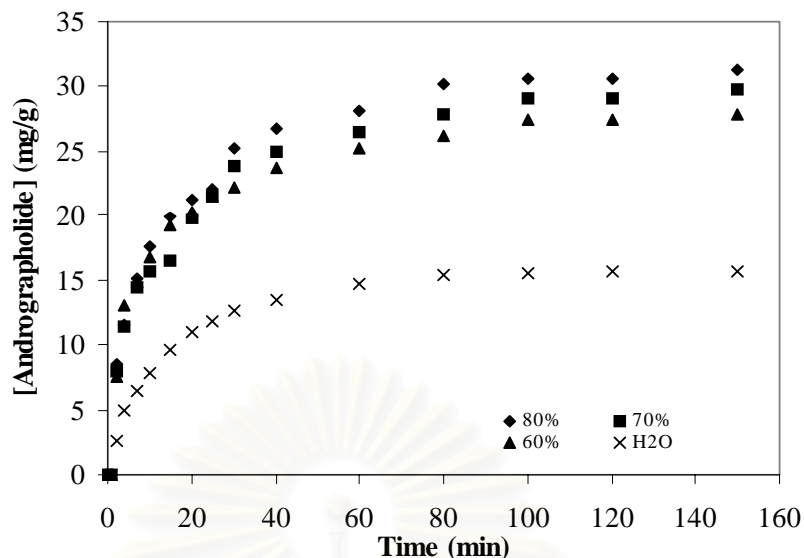


**Figure 2.13** Influence of percentage of ethanol on solute concentration (500 ml of ethanol solvent,  $T_{\text{room}}$ : 22°C, solid mass: 10 g and solid diameter: 0.6-0.8 mm)

**Figure 2.14** shows the percentage of final extracted concentration as a function of time. The percentage of extraction is determined by dividing each concentration for different times with the concentration at final time (at 150 min). The curves show that the percentage of ethanol has no significant influence on the kinetics of extraction (ethanol slightly increases the kinetics)

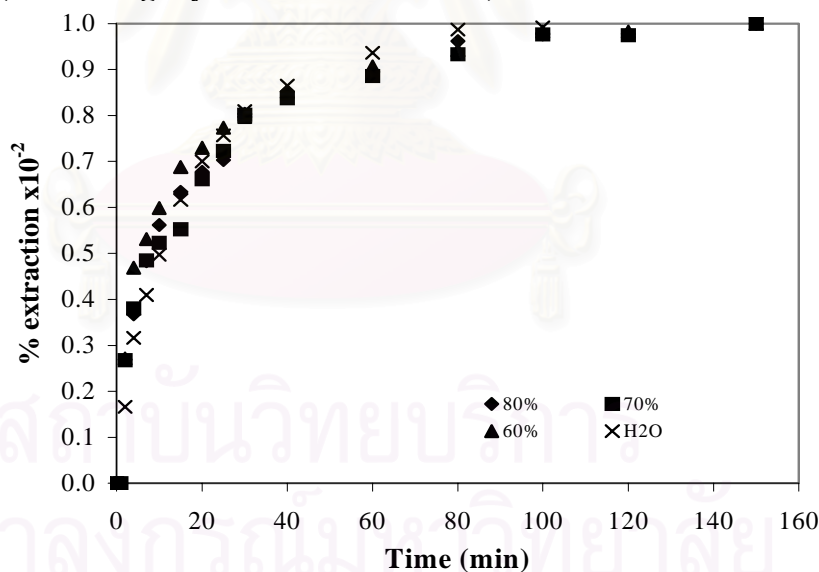


**Figure 2.14** Influence of the percentage of ethanol on the solute mass percentage (500 ml of ethanol solvent,  $T_{\text{room}}$ : 22°C, solid mass: 10 g and solid diameter: 0.6-0.8 mm)

**Figure 2.15** shows the final extracted concentration as function of percentage of ethanol. The experiment results show that the final concentration of andrographolide increases linearly with the percentage of ethanol.

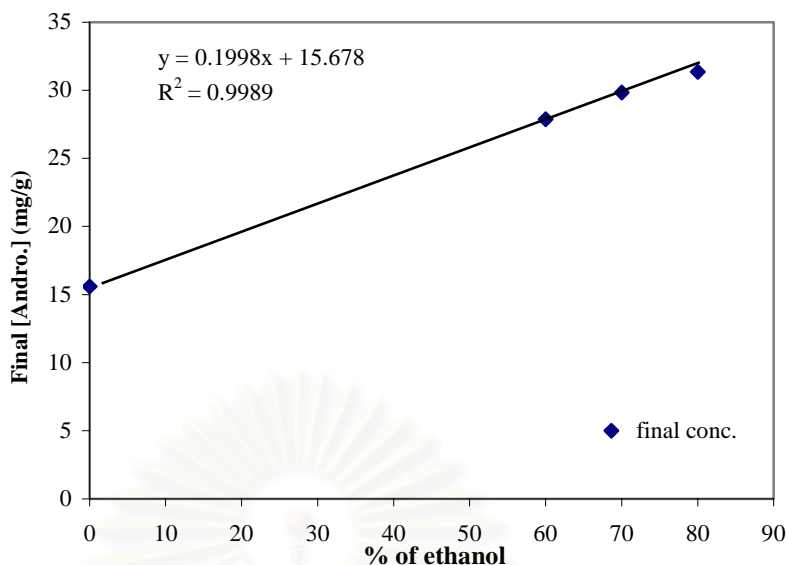


**Figure 2.15** Influence of percentage of ethanol on final solute concentration (500 ml of ethanol solvent,  $T_{\text{room}}$ : 22°C, solid mass: 10 g and solid diameter: 0.6-0.8 mm)

#### 2.2.4 Effect of particle size

The graph in **Figure 2.16** shows the evolution of extracted andrographolide as function of time for experiments 3, 5, 6 and 10 of **Table 2.7**. The differences in the final concentrations in the experiments are not significant enough to be analyzed as an effect of particle size. This difference can be due to the stems to leaves ratio in the samples.

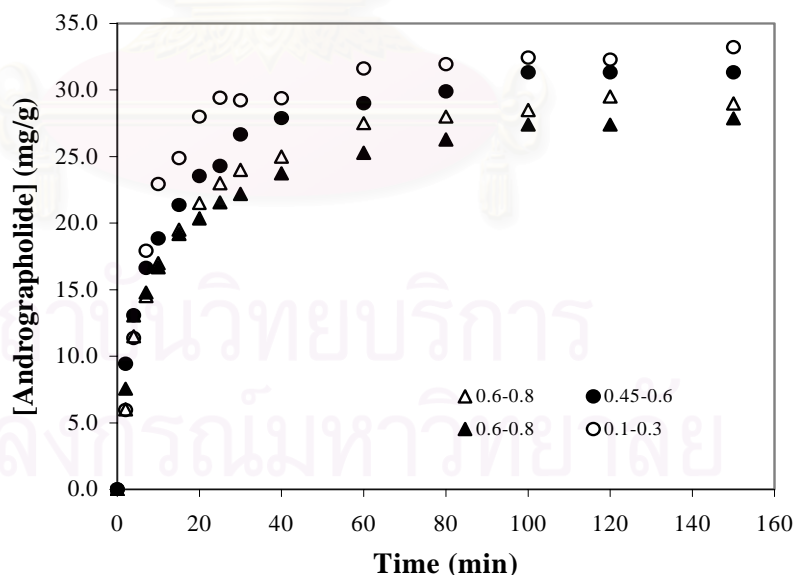


**Figure 2.16** Influence of particle size on solute concentration (500 ml of 60% ethanol,  $T_{\text{room}}$ : 22°C and solid mass: 10 g)

**Figure 2.17** shows the percentage of final extracted concentration as a function of time for experiments 3, 5, 6 and 10. The curves show that the rate of extraction slightly increases with the decrease in the size of the particles.

This is a classical result since the pore diffusion path increases with particle size. But as the particles are sieved, the size classes obtained depend on the diameter for the stem (cylindrical shape) and on the width for the leaves (plate shape). Since, in the case of the leaves that contain the main amount of solute, the relevant dimension for the diffusion is the thickness, the effect of the size is expected to be not overly important in the experimental results.

In the case of the diameter variation, there are many reasons why the concentration at the final time (150 min) is not exactly the same but similar. The ratio of the stem and the leaf in each experiment is not identical, the extraction rate is also different (at the same volume, a cylinder has more surface area than a plate) and the initial stem concentration is lower than in leaf.

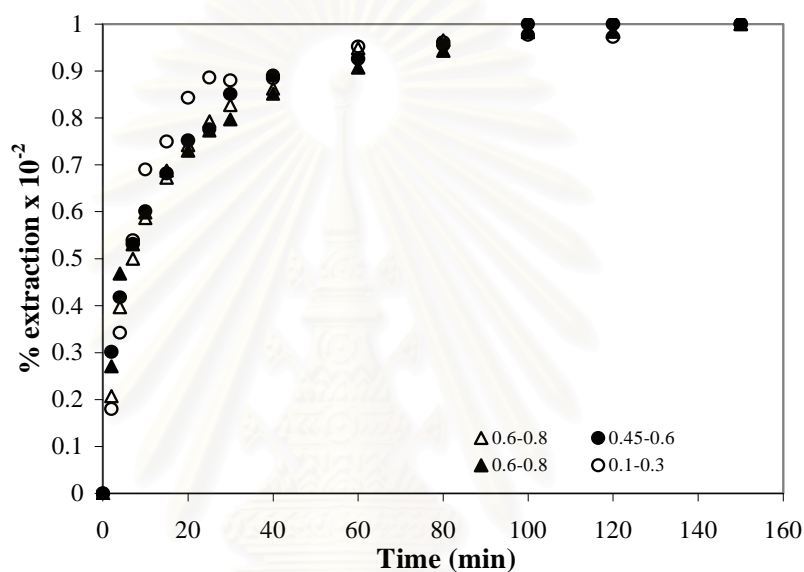


**Figure 2.17** Influence of particle size on solute mass percentage (500 ml of 60% ethanol,  $T_{\text{room}}$ : 22°C and solid mass: 10 g)

### 2.2.5 Effect of Temperature

**Figure 2.18** shows the evolution of extracted andrographolide as a function of time for experiment 7, 8 and 9 (experiment 3 does not appear on this figure because the plant used has a different origin and subsequently did not have the same initial concentration, see **Chapter 2.3.2**). The curves show that the final concentration increases with temperature. This can be due to the effect of temperature on the penetration of solvent inside the solid and on the thermodynamic effect on solubility, but further experiments should be done in order to confirm this result as the raw plant used did not have the same origin and consequently, the observed phenomena could come from differences in samples.

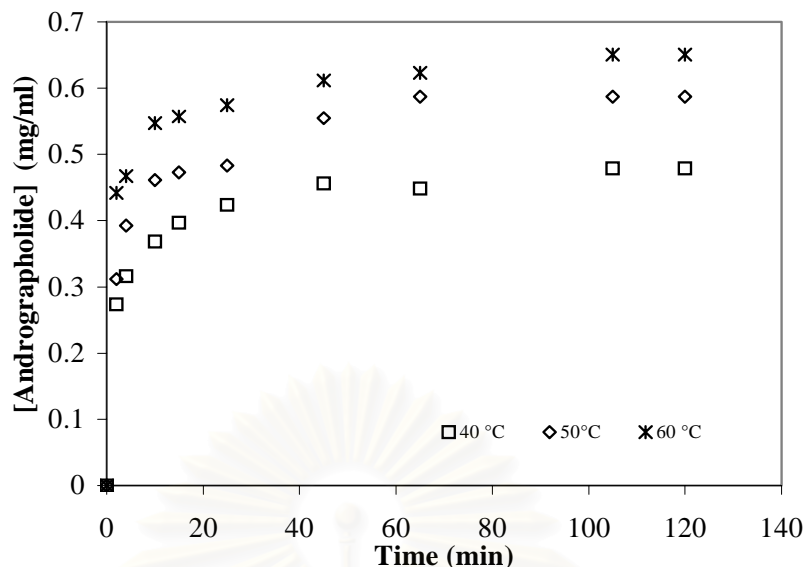


**Figure 2.18** Influence of temperature on solute concentration (500 ml of 60% ethanol, solid mass: 10 g and solid diameter: 0.6-0.8 mm)

**Figure 2.19** shows the percentage of final extracted concentration as a function of time for experiments 3, 7, 8 and 9. The curve shows that the temperature has some influence on the kinetics of extraction. The curves from 40°C to 60°C seem to be similar but a significant difference can be noticed with the experiments at 22°C. Since the coefficient can be written as a function of the temperature and the viscosity (Lalou, 1995):  $D = f\left(K \frac{T}{\eta}\right)$ , the coefficient of diffusion  $D$  is expected to increase with the temperature.

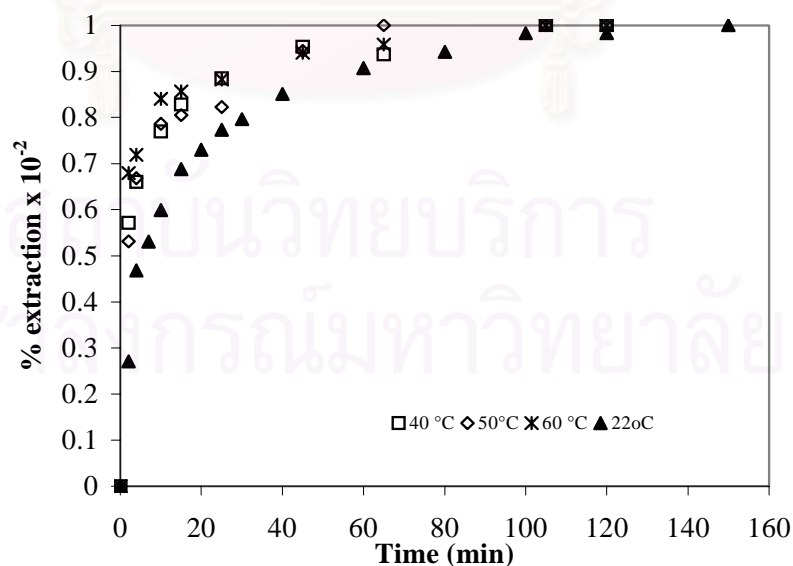


**Figure 2.19** Influence of temperature on solute mass percentage (500 ml of 60% ethanol, solid mass: 10 g and solid diameter: 0.6-0.8 mm)

## 2.3 KINETICS OF DESTRUCTION

Since the andrographolide concentration decreases with the ethanol-water solution to a value less than 0.20 mg/ml (**Table 2.6**) with the water, the following experiment will be done in order to find the rate of destruction of the andrographolide.

### 2.3.1 Effect of boiling point temperature of solvent

The experiment was prepared in a one litre batch reactor, equipped with a mechanical agitation and a jacket in which, 500 ml of an aqueous ethanol solution was introduced. At time zero, a known mass of *Andrographis paniculata* was introduced in the reactor and the extraction was performed at 22°C for 3 hours. Solid and liquid phases were then separated. The solution was then heated to its boiling point and samples were taken and analyzed in order to obtain the kinetics of destruction of andrographolide. Three initial solutions were studied: 100% of water, 7.5% and 15% of ethanol. Consequently the destruction was done at three different temperatures: 97°C, 92°C and 86°C, and measured in the reactor. The reduction of the concentration of andrographolide is illustrated in the **Figure 2.20**. It shows the concentration of andrographolide as a function of the reaction time at the boiling point of the solvent.

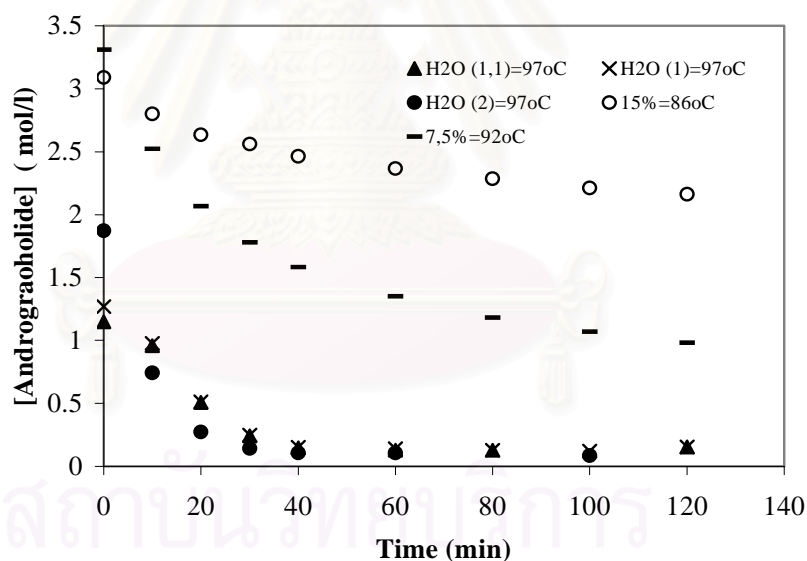


**Figure 2.20** Concentration of andrographolide by varying boiling points of solvent (solid diameter: 0.6-0.8 mm)

It might seem that raising the temperature would always be a good way to save time by making the kinetics of diffusion goes faster. However the problem with raising the temperature is that all kinetics are accelerated, including all the unwanted side reactions. Since andrographolide is a lactone, the opening of the lactone ring could be the most likely destruction mechanism. However, the lactone ring would react in a different manner either with water or ethanol. The former will open the ring by hydrolysis, whereas the latter will do it by trans-esterification. Hydrolysis is expected to be a much faster reaction compared to trans-esterification. Then the rate of destruction should be a function of both, the temperature and the composition of the solvent.

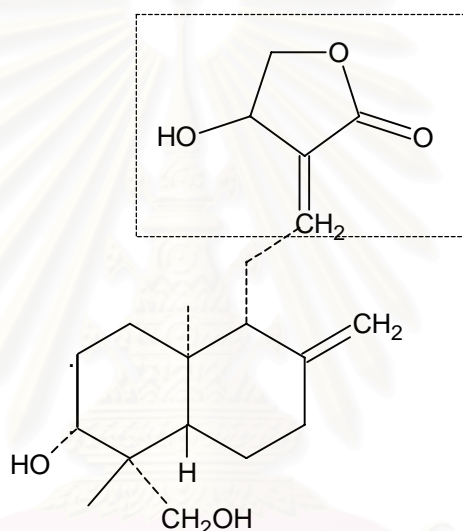


**Figure 2.21** Andrographolide molecular structures

สถาบันวิทยบริการ  
จุฬาลงกรณ์มหาวิทยาลัย

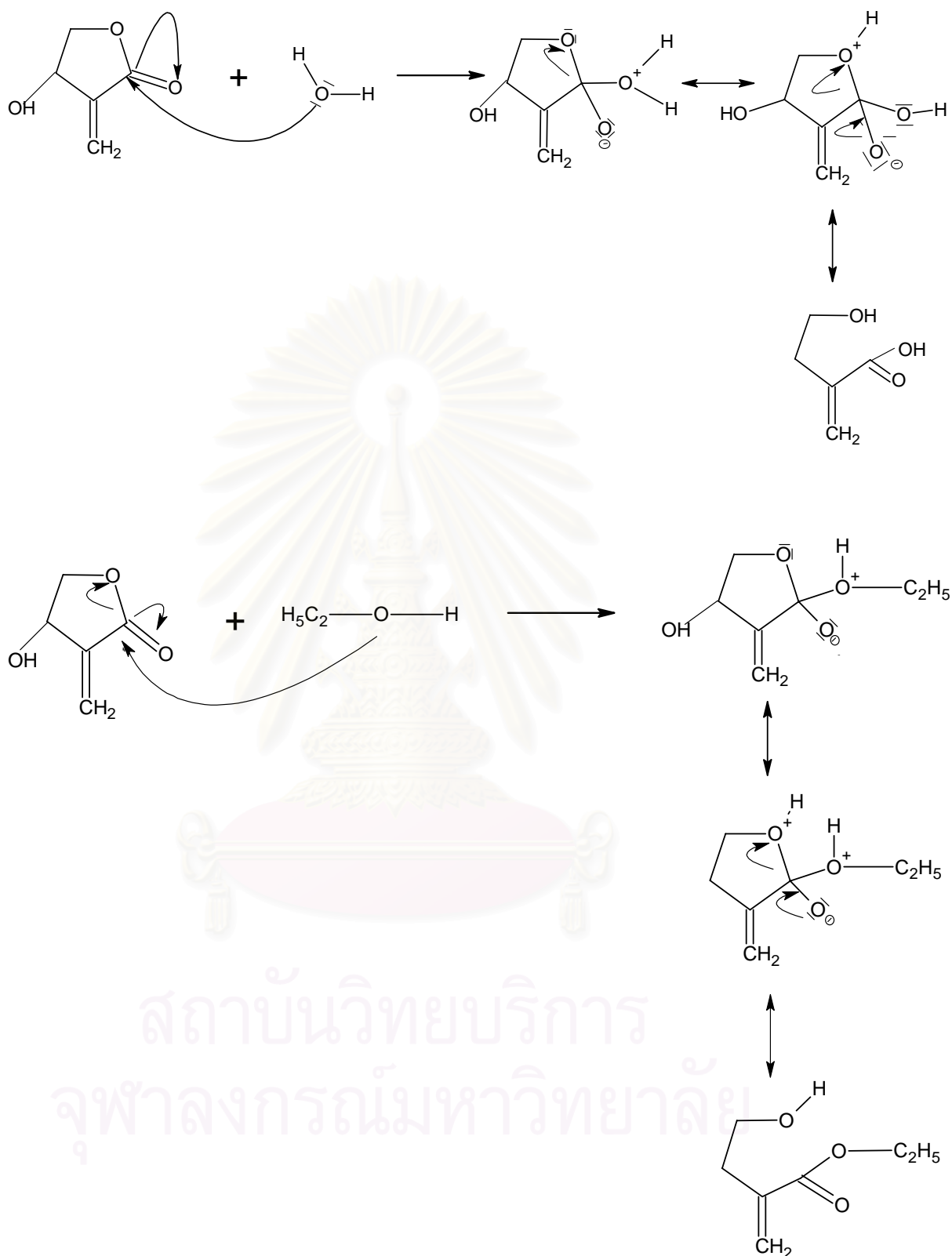


**Figure 2.22** Possible mechanisms of the destruction of andrographolide



Then, the order of the reaction rate with respect to the andrographolide concentration has been determined by a series of experiments. **Figure 2.23** shows the reduction of andrographolide as a function of time in logarithm scale.

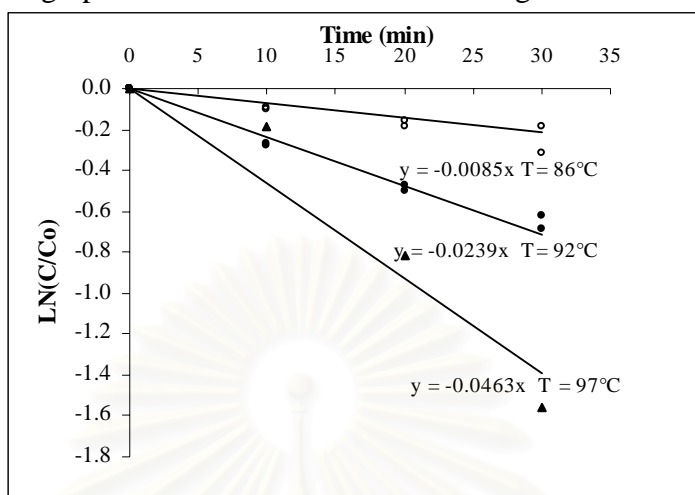


**Figure 2.23** Reduction of andrographolide concentration as a function of time for different temperatures (initial kinetics) in logarithm scale

$\ln(C/C_0)$  as a function of time seems, in a first approach, to be linear. The kinetics can then be approached by a first order system in respect with the andrographolide concentration. The rate constant generally depends on absolute temperature  $T$  following the law first proposed by Arrhenius:

$$\ln k = \ln k_0 - \frac{E_a}{RT} \quad (2.10)$$

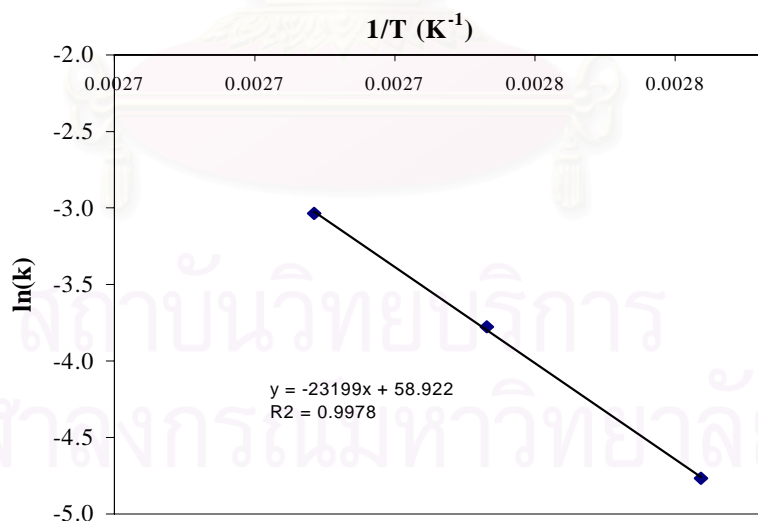


**Figure 2.24** Influence of temperature on the constant of kinetics

$k_0$  and  $E_a/R$  are determined by drawing  $\ln(k)$  as function of  $1/R$  (**Figure 2.24**):

$$k_0 = 3.89 \cdot 10^{25} \text{ min}^{-1}$$

$$E_a/R = 23200 \text{ K}$$

With these parameters it is possible to determine the percentage of andrographolide destroyed in the solution after 3 hours as a function of the temperature. The maximum temperature to have a percentage inferior to 98% is 66.5°C.

Since the rate of destruction should be a function of both the temperature and the composition of the solvent, this first approach can certainly not be reproduced in all the experiments (as for the 97°C points).

The objective in this part is not to make a complete study of the rate of destruction but to explain the observed phenomena in soxhlet experiments (i.e. the very low amount of extracted andrographolide with low percentage of ethanol or pure water solvent) and consult on the choice temperature for the industrial implementation of the process. A simple first order reaction will then be assumed in respect to andrographolide concentration to represent the global kinetics of destruction.

### 2.3.2 The influence of storage time on the herb quality

Two different main batches of herbs were used in this thesis. The first batch (Batch A) was harvested in 2001 and used in the experiments until January 2003. Second batch (Batch B) was harvested in 2003.

**Figures 2.25 to 2.28** show the apparent kinetics of extraction for batch A in 2001 and batch B in 2003.

In January 2003, we found that andrographolide concentrations decreased from 0.39 mg/ml to 0.15 mg/ml in water and from 0.60 mg/ml to 0.39 mg/ml in 70% ethanol, respectively. However, **Figures 2.26 and 2.28** show that there is no major effect of age on the diffusion coefficient.

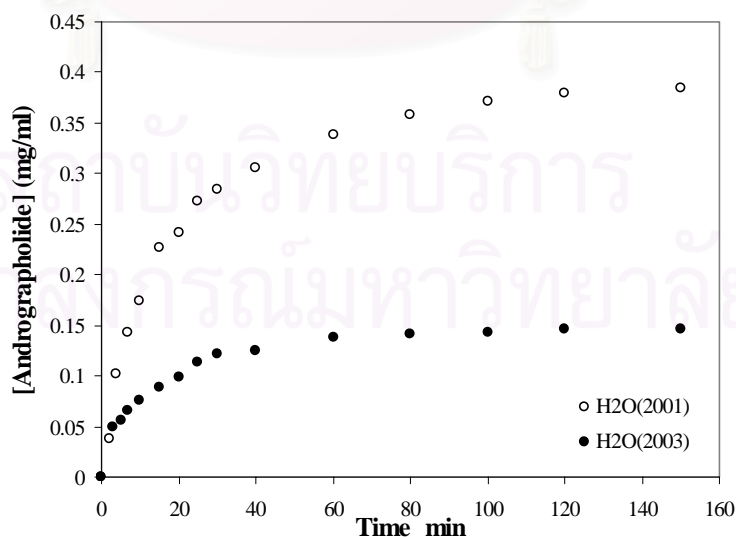


**Figure 2.25** Influence of storage time on the solute concentration 500 ml of water, solid mass: 10 g (Batch A)

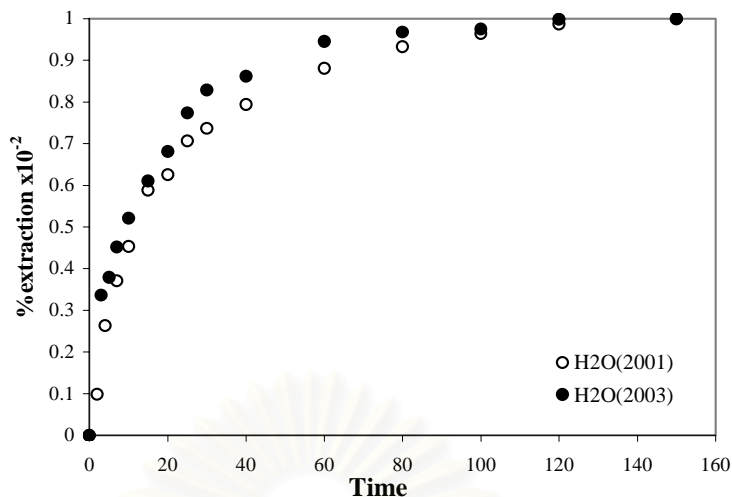


**Figure 2.26** Influence of time on solute mass percentage 500 ml of water, solid mass: 10 g (Batch A)

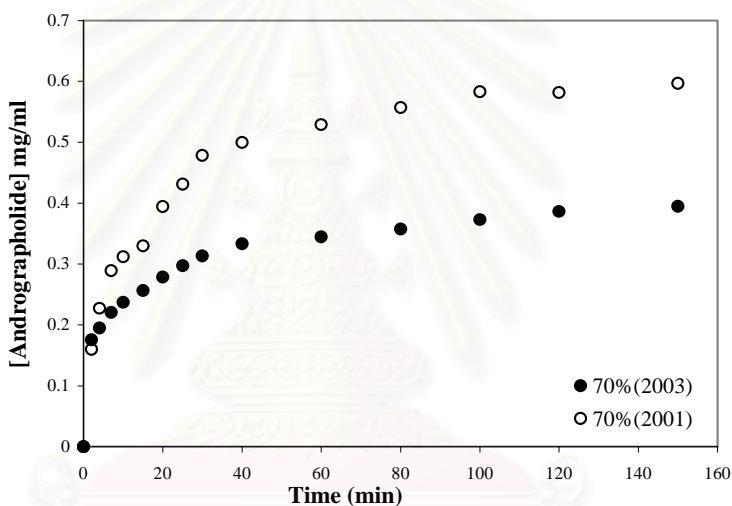


**Figure 2.27** Influence of time on solute concentration 500 ml of 70% ethanol, solid mass: 10 g (Batch A)

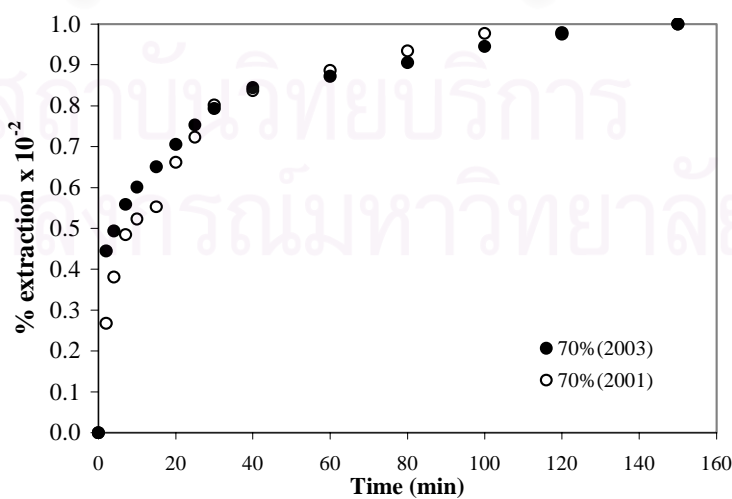


**Figure 2.28** Influence of time on solute mass percentage 500 ml of 70% ethanol, solid mass: 10 g (Batch A)

Furthermore, parts of these plants had been in contact with humidity for 6 months. The moist plants gave off strong odours due to fermentation. Next kinetics experiments were performed as shown (Figures 2.29 and 2.30) with 70% ethanol and in Figure 2.31 with 95% ethanol.

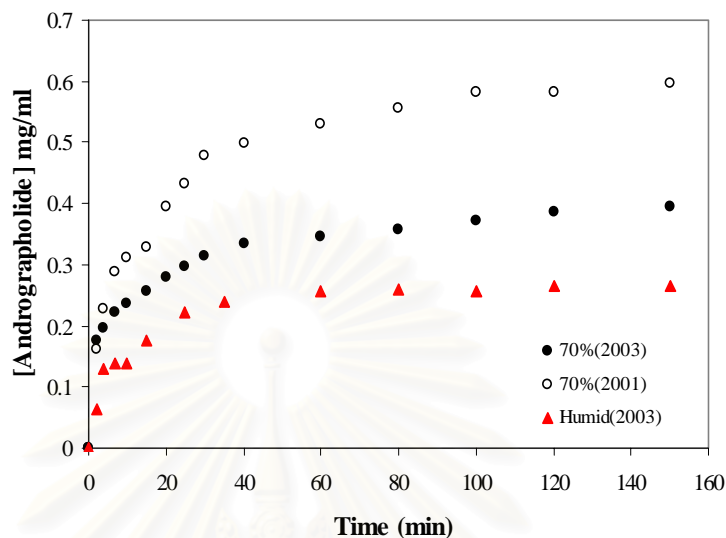


**Figure 2.29** Solute concentration as function of time 500 ml of 70% ethanol, solid mass: 10 g by using the humid plant (Batch A)

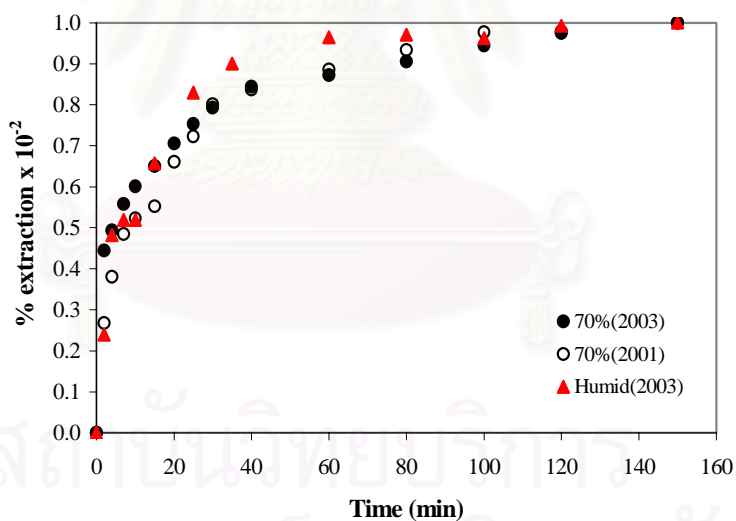


**Figure 2.30** Solute mass percentage as function of time 500 ml of 70% ethanol, solid mass: 10 g by using the humid plant (Batch A)

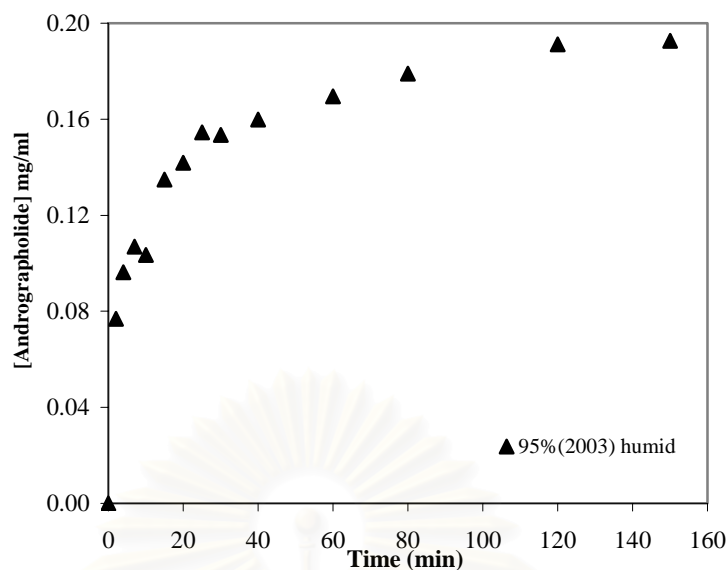


**Figure 2.31** Solute concentration as a function of time 500 ml of 95% ethanol, solid mass: 10 g by using the humid plant (Batch A)

The andrographolide concentration decreases from 0.62 mg/ml to 0.19 mg/ml using 95% ethanol and 0.39 mg/ml to 0.27 mg/ml extracted using 70% ethanol, respectively with the humid plant. The andrographolide concentration in plant decreases by about 40% within two years. The storage of plant must be done in an area without humidity to avoid deterioration.

A new batch of plant was purchased in January 2003 (Batch B) for the experiments in the extraction column. The solid plant was used directly without any sieving or separating. The plant was allowed to contain smaller as well as larger sized particles. Additional experiments were performed in soxhlet and batch reactors in order to characterize the new batch of solid.

The soxhlet experiment was done with 95% ethanol. The obtained andrographolide concentration was 28 mg/g of *Andrographis paniculata*. **Figures 2.32** and **2.33** show the andrographolide concentration and the percentage of extraction with 500 ml of 95% ethanol.

**Figures 2.32** and **2.33** show that the final concentration and the evolution of the new plant (Batch B) was less than with (Batch A) because there are some variations in particle sizes and the percentage of stem is greater than in Batch A. The andrographolide concentration results of Batch B are presented in **Appendix II.II**.

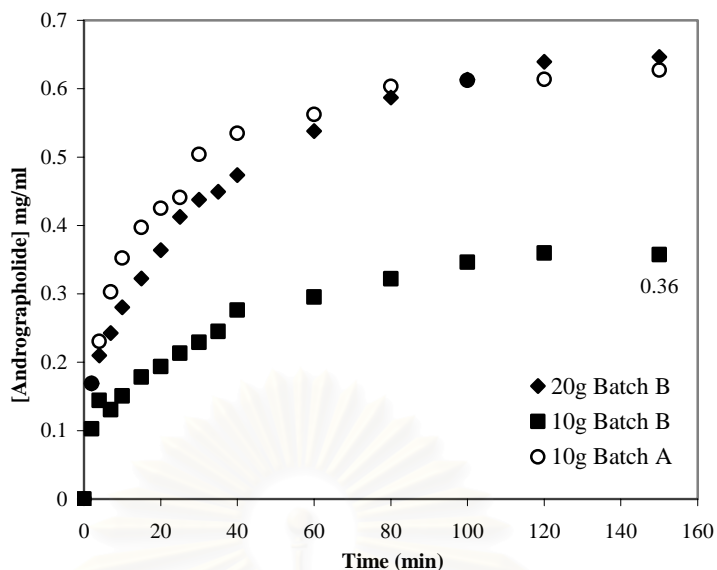


**Figure 2.32** Solute concentration as a function of time 500 ml of 95% ethanol, 10 g and 20g of new plant (Batch B) and 10g, 0.6-0.8 mm of Batch A

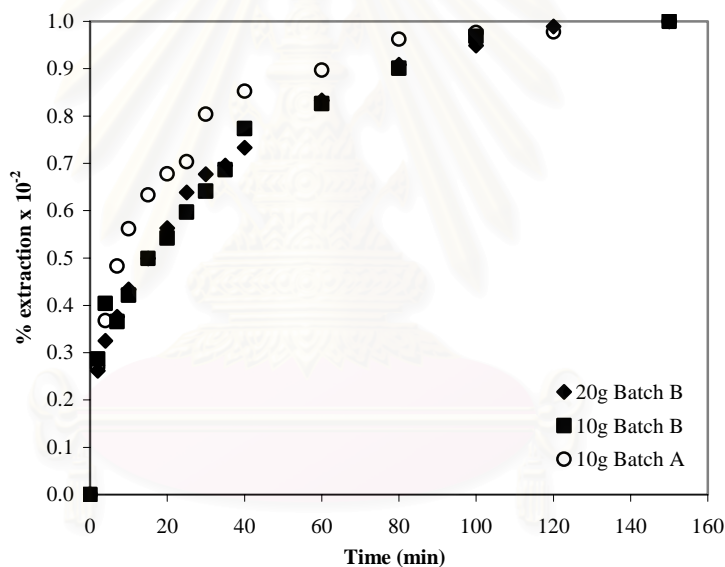


**Figure 2.33** Solute mass percentage as a function of time 500 ml of 95% ethanol, 10g and 20g of new plant (Batch B) and 10 g, 0.6-0.8 mm of Batch A

## 2.4 SOLVENT ABSORPTION IN PLANT

### 2.4.1 Solvent absorption

In order to prepare for the column experiments, the phenomena and characteristics of the plants in the solvent were observed. The experiment is done by first preparing 95 %, 70%, 50% and 0% ethanol solution in a measuring cylinder. The solid particle is measured and placed into the solution. Next the mixed solution is agitated for 3 min and allowed to it sink alone for 2 min. The volume occupied by the sinking and floating solid were then measured at each time, the experiment was done for 360 min.

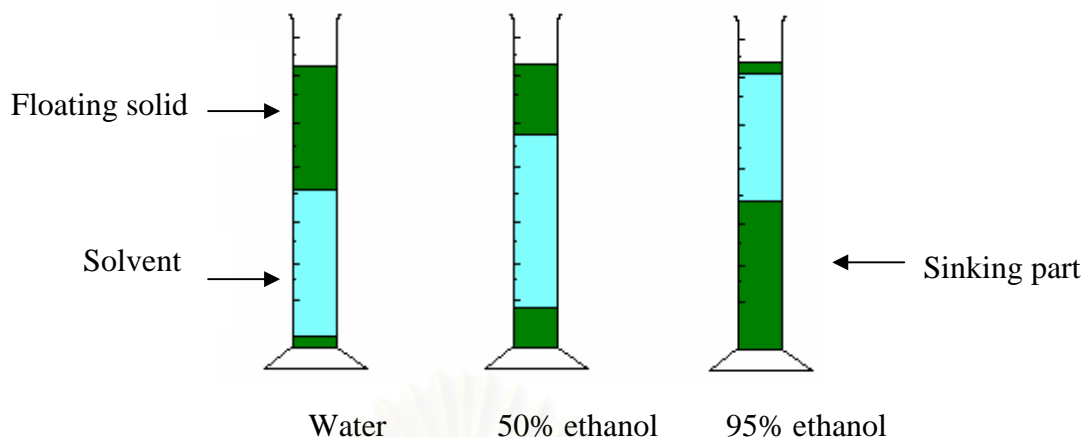


**Figure 2.34** The absorption of solid particles in the different ethanol solutions after 5 min

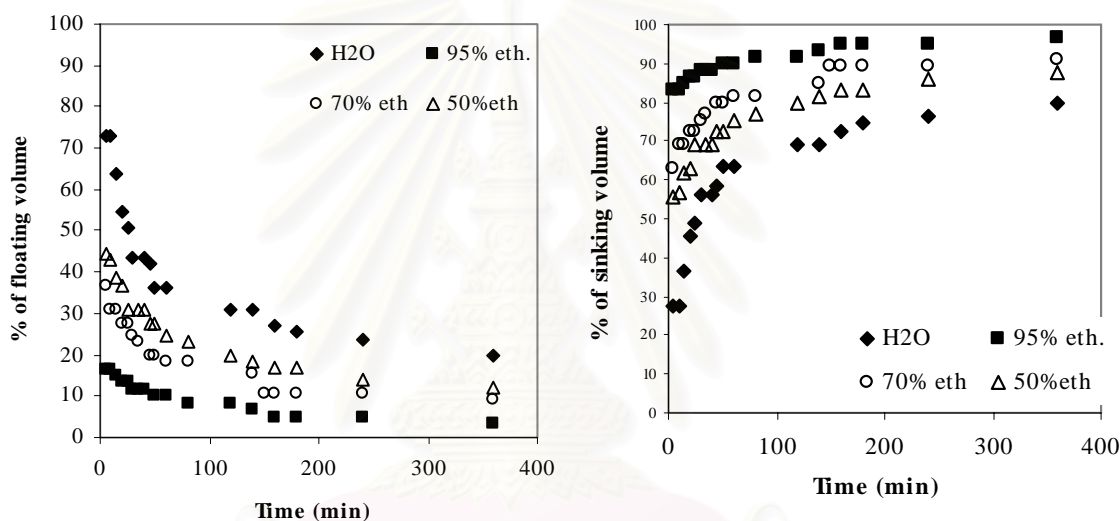


**Figure 2.35** The floating and sinking volume percentages of solid particle in different ethanol solutions as a function of time

**Figure 2.35** shows that during the early minutes, the floating part decreases quickly to 17, 37, 45 and 73% for the 95, 70, 50 and 0 % ethanol solutions respectively. Then this percentage decreases more slowly until a final value is reached (which depends on the nature of the solvent) after about 6 hours.

The process involved the absorption of solvent into the solid. As the porosity is filled up, the apparent density increases then the solid sinks.

**Figure 2.36** shows the ratio of percentage of floating material compared to the 95% ethanol experiments:

$$R_{95\%} = \frac{\text{Volume \% floating for specific solvent}}{\text{Volume \% floating for 95\% ethanol}}$$

In a first approach we will consider that the kinetics is the same, but the final state depends on the percentage of ethanol due to tension surface and the difference in density.

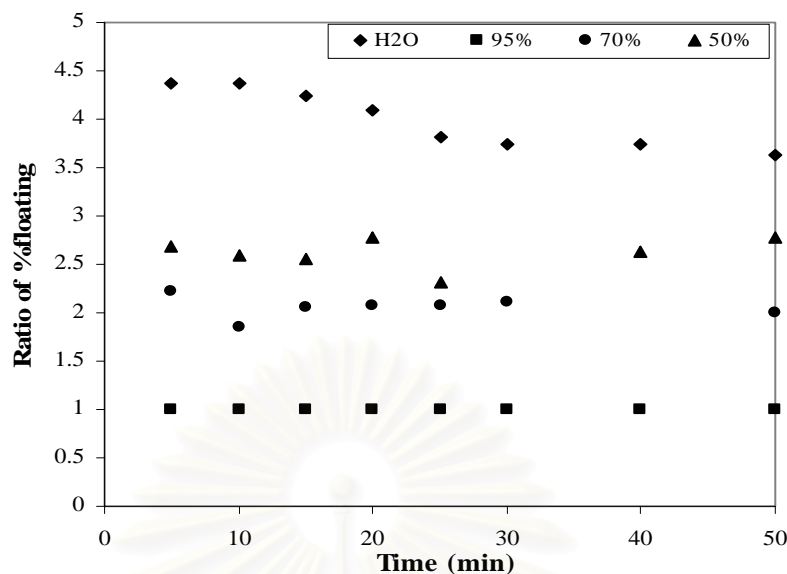


**Figure 2.36** The dynamics of the floating solid as for a 95 % ethanol solution as a function of time

**Figure 2.37** shows that the equilibrium is linked to the percentage of ethanol through the following relation:  $y = -0.0308(\text{percent of ethanol}) + 4.075$ . This equation has no physical meaning but will be useful for the industrial design of the process.

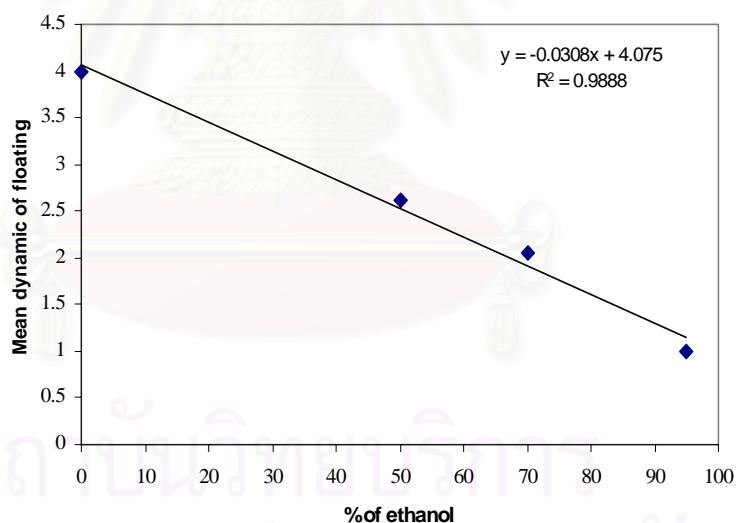


**Figure 2.37** The mean  $R_{95\%}$  as a function of the percentage of ethanol

#### 2.4.2 The relation of mass and volume of solid particle in the solution

In the pulsed extraction column, only volume is easily measurable. The volume-mass curves must be studied for both stems and leaves. The experiment was undertaken by first separating the floating and sinking parts of the dry solid particles. Both parts of the solid were introduced in different graduated cylinders to measure dry volume of floating and sinking solid ( $V_{\text{dry}}$ ). Then 95% ethanol was poured in the cylinder. Finally the volume of solid in the solvent ( $V_{\text{sol}}$ ) was measured.



**Figures 2.38** and **2.39** show the relation of mass and volume of solid in the solvent ( $V_{sol}$ ) for the floating and sinking parts respectively. The wet volume ( $V_{sol}$ ) of floating (stems) and sinking (leaves) solid are 7.92 and 4.31 times the dry mass solid respectively.

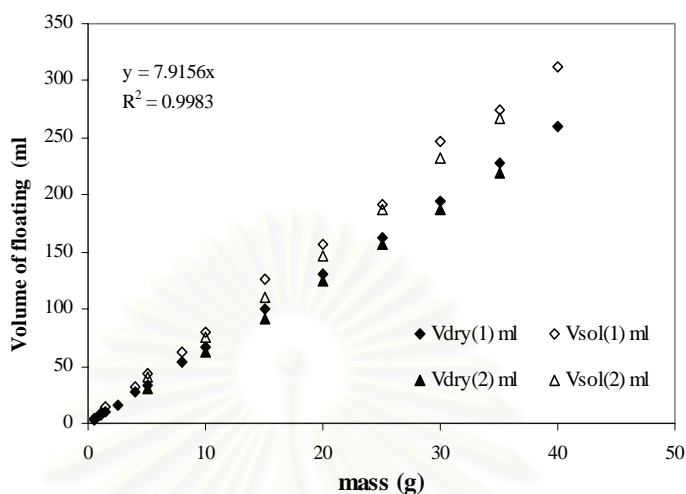


**Figure 2.38** The mass-volume relation of the floating solid (mostly stems)

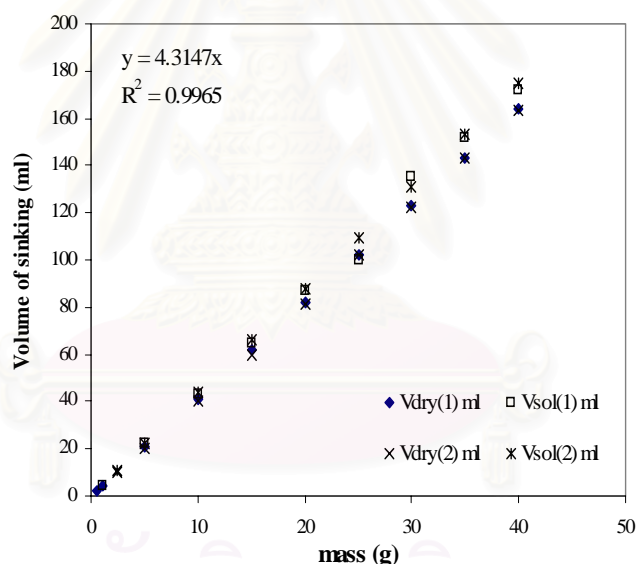


**Figure 2.39** The mass-volume relation of the sinking solid (mostly leaves)

**Figure 2.39** shows the dry volume of the sinking solid ( $V_{dry}$ ) is close to the wet volume (volume in the solvent,  $V_{sol}$ ) of the sinking solid because most of the particle are made up of leaves which have a plane shape and sink readily in the solvent. The volume of the sinking solid in the solvent will be measured in the pulsed column to allow to find the mass of the solid which sinks in the solvent.

## CONCLUSION

In our study, *Andrographis paniculata* samples were scanned with a Scanning Electronic Microscope in order to have visual observations on the structure of the solid particles, especially the characteristic dimensions. As a result of the observations, the solid can be separated into two groups in term of differences in structure, shape and characteristic dimensions (stems and leaves). For each group, soxhlet experiments were performed to obtain initial concentration.

Batch extraction experiments were then performed in order to study influence of operating parameter such as ethanol concentration, particle size and temperature. In this investigation, it was found that the sizes of the particle have very little effect on both extraction kinetics and final concentration. The percentage of ethanol in the solvent has also no effect on the kinetic of extraction but the final concentration increases with the percentage of ethanol. Then a reaction of degradation of the solute which is activated at high temperature (from about 70°C upward) was characterized. Next, the influence of the time after harvesting (storage time) was studied. The andrographolide decreases after 2 years of storage time and dramatically decreases after 4 months fermentation occurs. Finally, experiments on the absorption of solid in the solvent were conducted in order to see the hydrodynamic behaviour of the stems and of the leaves separately, including the percentage of absorption.

Consequently, subsequent modelling steps had to consider the difference in particle shape. The experimental results will then be used to identify the diffusion coefficients for all experiments. The comparison between model and experiment will be presented in **Chapter III**.

The influence of the operating parameters presented in this chapter will allow for a choice of process conditions to be made in terms of solvent quality and temperature, based on economics or safety criteria.

## **CHAPTER III**

### **MASS TRANSFER MODEL**

#### **INTRODUCTION**

In the case of traditional solid-liquid extraction a monodispersed porous solid phase is the norm, assuming uniform particle shapes and sizes. However plants are heterogeneous in size and in shape as a result of the necessary mechanical pre-treatment (size- reduction and fractionation of plants).

Often in solvent extraction systems, the diffusion of the solute inside the particle is the rate-controlling step. This is caused by the particle structure (void fraction, pore diameter and tortuosity etc.) or to the existence of membranes or cells. In our case, no chemical reaction occurs.

In this chapter a model of the diffusion mechanism is developed, taking into account the heterogeneity of the material in particular the plant shape applied to the extraction andrographolide from leaves and stems.



สถาบันวิทยบริการ  
จุฬาลงกรณ์มหาวิทยาลัย

### 3.1 MODEL HYPOTHESIS

The objective is to establish a mass transfer model and to compare experimental results with the model. It should then be possible to identify the diffusion coefficients as a function of ethanol percentage, particle size and temperature.

In order to describe the andrographolide transfer, the following assumptions are made:

1. The solid particles are presented in two shapes: a plane shape corresponding to the leaves and a cylindrical shape corresponding to the stems. The solute diffusion takes place in the transverse direction and is monodirectional.
2. Every particle is symmetrical and homogeneous.
3. The diffusion coefficient is constant throughout the experiment. The andrographolide concentration in a particle depends only on position and time.
4. The solvent in the batch reactor is perfectly mixed. The transfer resistance in the liquid phase is negligible and the andrographolide concentration in the bulk phase depends only on time.
5. The transport of the andrographolide particles is diffusional. It is described by a diffusion coefficient assumed to be constant for a set of conditions.
6. At the interface, the concentrations of every species in solution between the internal liquid (in pores) and external to particles are supposed to be equal.
7. Initial concentration in each experiment is calculated using the experiment at 150 min because the ability of extraction for each solvent is different.
8. The mass percentage of leaves in all samples was assumed to be about 80%.  
**(Chapter 2.2.2).**

These assumptions led to a simplified diffusion model for mass transfer andrographolide from the solid.

### 3.2 GENERAL EQUATIONS

The general diffusion model for solid-liquid extraction (Prat et al., 1999; Seikova et al., 1999; Simesov, Tsibranska, and Minchev, 1999) with one space variable is:

$$\frac{\partial C(t, x)}{\partial t} = D \cdot \frac{1}{x^{\varphi-1}} \frac{\partial}{\partial x} \left( x^{\varphi-1} \frac{\partial C(t, x)}{\partial x} \right) \quad (3.1)$$

Where t: Time,  
 x: Radial distance in the direction of mass transfer from the centre of the symmetrical particle,  
 $\varphi$ : Geometric shape factor. It may take values of 1, 2 and 3 respectively corresponding to particles shape (plates, cylindrical and spherical),  
 C : The concentration of andrographolide IN SOLID,  
 D: The diffusion coefficient of andrographolide.

**For the leaves:** ( $\varphi = 1$ )

$$\frac{\partial C_1}{\partial t} = D \cdot \frac{\partial^2 C_1(t, x)}{\partial x^2} \quad (3.2)$$

**For the stems:** ( $\varphi = 2$ )

$$\frac{\partial C_2(t, x)}{\partial t} = D \cdot \left( \frac{1}{x} \cdot \frac{\partial C_2(t, x)}{\partial x} + \frac{\partial^2 C_2(t, x)}{\partial x^2} \right) \quad (3.3)$$

#### 3.2.1 Initial and boundary conditions

**a) Initial conditions ( $t = 0$ ):**

- For the continuous phase:  $C_s = 0$  (concentration of solute in the solvent)
- For the dispersed phase:  $C(x) = C_0, \forall x$

**b) Boundary conditions:**

At the center of a particle, ( $x = 0$ )

$$\left( \frac{\partial C(t, x)}{\partial x} \right)_{x=0} = 0 \quad \forall t \quad (3.4)$$

- At the interface ( $x = e$ ), equality of flux of andrographolide:

The retiring flux from the solid:

$$F = -D \cdot A \left( \frac{\partial C(t, x)}{\partial x} \right)_{x=e} \quad (3.5)$$

The incoming flux into the liquid:

$$F = V_L \frac{dC_L(t)}{dt} \quad (3.6)$$

Where  $V_L$ : The solvent volume,

A: The specific area.

The equality of flux from equations (3.5) and (3.6) is written as:

$$\frac{dC_L(t)}{dt} = -D \cdot \frac{A}{V_L} \left( \frac{\partial C(t, x)}{\partial x} \right)_{x=e} \quad (3.7)$$

### c) The mass balance

The concentration of the mass of solute can be written as

$$\forall t, \quad C_L(t) \cdot V_L + \int_0^V C(t, x) dV = C_0 V \quad (3.8)$$

Where

$C_L$ : The concentration of the solute in the liquid phase,

$V_L$ : The volume of the liquid phase,

$V$ : The total volume of the solid,

$C_0$ : The initial concentration of the solute.

And  $dV$  can be expressed by:

$$dV = N_p \cdot dV_p = \varphi \frac{M}{\rho \cdot e^\varphi} \cdot x^{\varphi-1} \cdot dx \quad (3.9)$$

$$V = \int dV = \frac{M}{\rho} \quad (3.10)$$

Where:

$V$ : The volume of the solid,

$N_p$ : Number of solid particles contained in a mass  $M$  of solid for batch experiment,

$V_p$ : Volume of a particle,

$\rho$ : Apparent mass volume of a solid particle,

$e$ : The half of the thickness (or diameter) of the plate particle (or cylinders),

$M$ : Mass of the solid,

$\varphi$ : Geometric shape factor.

### 3.3 COMPARISON BETWEEN EXPERIMENTS AND MODEL

#### 3.3.1 Numerical Treatment

The equations are discretized using finite differences.

Equation (3.1) is developed as follows:

$$\begin{aligned}
 \frac{\partial C(t, x)}{\partial t} &= D \cdot \frac{1}{x^{\varphi-1}} \frac{\partial}{\partial x} \left( x^{\varphi-1} \frac{\partial C(t, x)}{\partial x} \right) \\
 &= D \cdot \frac{1}{x^{\varphi-1}} \cdot x^{\varphi-1} \frac{\partial^2 C(t, x)}{\partial x^2} + D \frac{1}{x^{\varphi-1}} (\varphi-1) \cdot x^{\varphi-2} \cdot \frac{\partial C(t, x)}{\partial x} \\
 &= D \cdot \frac{\partial^2 C(t, x)}{\partial x^2} + D \frac{(\varphi-1)}{x} \cdot \frac{\partial C(t, x)}{\partial x}
 \end{aligned} \tag{3.11}$$

then:

$$\frac{\partial C(t, x)}{\partial t} = D \cdot \left[ \frac{(\varphi-1)}{x} \cdot \frac{\partial C(t, x)}{\partial x} + \frac{\partial^2 C(t, x)}{\partial x^2} \right] \tag{3.12}$$

The resolution of this equation is done through the explicit Crank-Nicholson method.

The thickness  $e$  (or diameter) of the solid particle (in the direction of the diffusion) is discretized according to  $n$  discretizations at constant  $\Delta x$ . The time interval of the calculation ( $0 \leq t \leq t\text{-final}$ ,  $t\text{-final}$  is the final time of the calculation) is discretized according to  $m$  time discretizations at constant  $\Delta t$ .  $i$  and  $j$  are indexed with respect to time  $t$  and to position  $x$  ( $i = 1 \rightarrow m$ ;  $j = 1 \rightarrow n$ ) in the finite different method calculation where:

$$\begin{aligned}
 \frac{\partial C}{\partial t} &= \frac{C(i, j) - C(i-1, j)}{\Delta t} \\
 \frac{\partial C}{\partial x} &= \frac{C(i, j) - C(i, j-1)}{\Delta x} \\
 \frac{\partial^2 C}{\partial x^2} &= \frac{C(i-1, j+1) - 2C(i-1, j) + C(i-1, j-1)}{\Delta x^2}
 \end{aligned} \tag{3.13}$$

By substituting equations (3.13) into equation (3.12), we obtain:

$$\begin{aligned}
 C(i, j) &= C(i-1, j) + D \cdot (\varphi-1) \frac{\Delta t}{j \Delta x^2} \cdot (C(i-1, j) - C(i-1, j-1)) \\
 &\quad + D \cdot \frac{\Delta t}{\Delta x^2} (C(i-1, j+1) - 2C(i-1, j) + C(i-1, j-1))
 \end{aligned} \tag{3.14}$$

We can calculate values of  $C$  for all points  $(i, j)$  using the following discretized boundary conditions:

$$\begin{aligned}
 i = 1 (t = 0): \quad C(1, j) &= C_0 \quad \forall j \\
 C_L(0) &= 0
 \end{aligned} \tag{3.15}$$

$$j = 1 (x = 0): \quad \frac{C(i, j+1) - C(i, j)}{\Delta x} = 0 \quad \forall i$$

$$\text{then:} \quad C_1(i, 1) = C_1(i, 2) \quad (3.16)$$

Using the conservation of the mass principle we write:

$$m_s + m_L = m_0 \quad \forall t \quad (3.8)$$

Where

$m_s$ : Total mass of the solute in the solid phase,

$$m_s(t) = \int_0^V C(t, x) dV \quad (3.8)$$

$m_0$ : Initial total mass of the solute in the solid,

$$m_0 = C_0 \cdot V \quad (3.8)$$

$V$ : Total volume of the solid,

$m_L$ : Total mass of the solute in the liquid phase.

The concentration of solute in the liquid phase is given by

$$C_L(t) = \frac{m_L(t)}{V_L} = \frac{m_0 - m_s(t)}{V_L} \quad (3.8)$$

At  $t = i$ : equations (3.8) and (3.9) give:

$$m_s = \sum_j \left( \varphi \cdot \frac{M}{\rho e^\varphi} \cdot (j\Delta x)^{\varphi-1} \cdot \Delta x \right) \cdot C(i, j) \quad (3.17)$$

Equation (3.8) and (3.10) give:

$$m_0 = C_0 \frac{M}{\rho} \quad (3.18)$$

From equation (3.8), we may write:

$$C_L(i) = \frac{1}{V_L} \left[ C_0 \cdot \frac{M}{\rho} - \sum_j \left( \varphi \cdot \frac{M}{\rho e^\varphi} \cdot (j\Delta x)^{\varphi-1} \cdot \Delta x \right) \cdot C(i, j) \right] \quad (3.19)$$

The coefficient of diffusion  $D$  which is the only parameter can be identified using a simple dichotomy method based on a quadratic criterion.



### 3.3.2 Programming

The model is programmed under the software Scilab 2.6.

The data used in this calculation program are:

- $m$ : Mass of solid (kg),
- $e$ : Half of thickness (m),
- $L$ : Characteristic dimension of the particles (m),
- $\rho$ : Density of the solid particle ( $\text{kg/m}^3$ ),
- $V$ : Volume of the liquid (L),
- $Co_f$ : Initial concentration of leaves (g/g),
- $Co_s$ : Initial concentration of stems (g/g),
- $t\text{-final}$ : Final time of calculation correspondent to the final time of batch experiment (min),
- $D$ : Diffusion coefficient (Trial and error for the initial value),
- $\phi$ : Geometrical shape factor stems = 2 and leaves = 1,
- $Ck(i, j)$ : Concentration of solute (g)/concentration of plant matter (L),
- $Ck(i, nx+1)$ : Concentration of solute (g) / solvent concentration (L),
- $\Delta t$ : Time step,
- $nx$ : Number of numerical layers in particle.

We started our program of modelling with the value of  $\Delta t = 0.05$  minutes and  $nx = 22$ .

### 3.3.3 Typical results of the simulation

The concentration profiles for the stems ( $\phi = 2$  cylindrical shape) and the leaves ( $\phi = 1$  plane shape) are presented in the **Figures 3.1** and **3.2** respectively. The calculations were made with the same value coefficient of diffusion  $D$ .

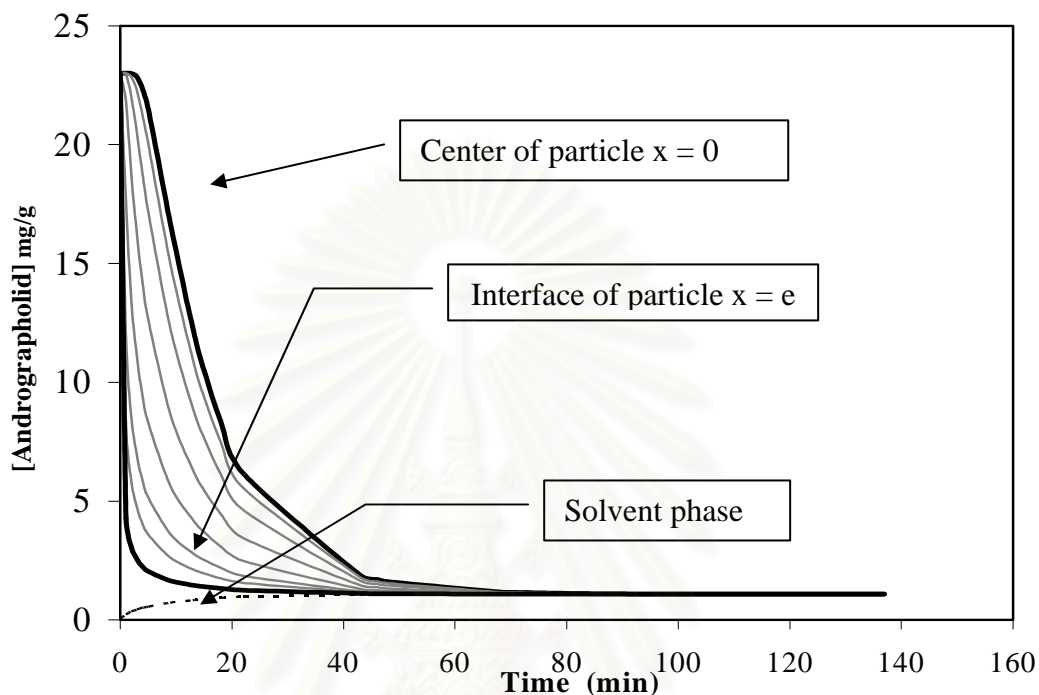


**Figure 3.1** Concentration profile for  $\phi = 2$  (cylindrical shape)

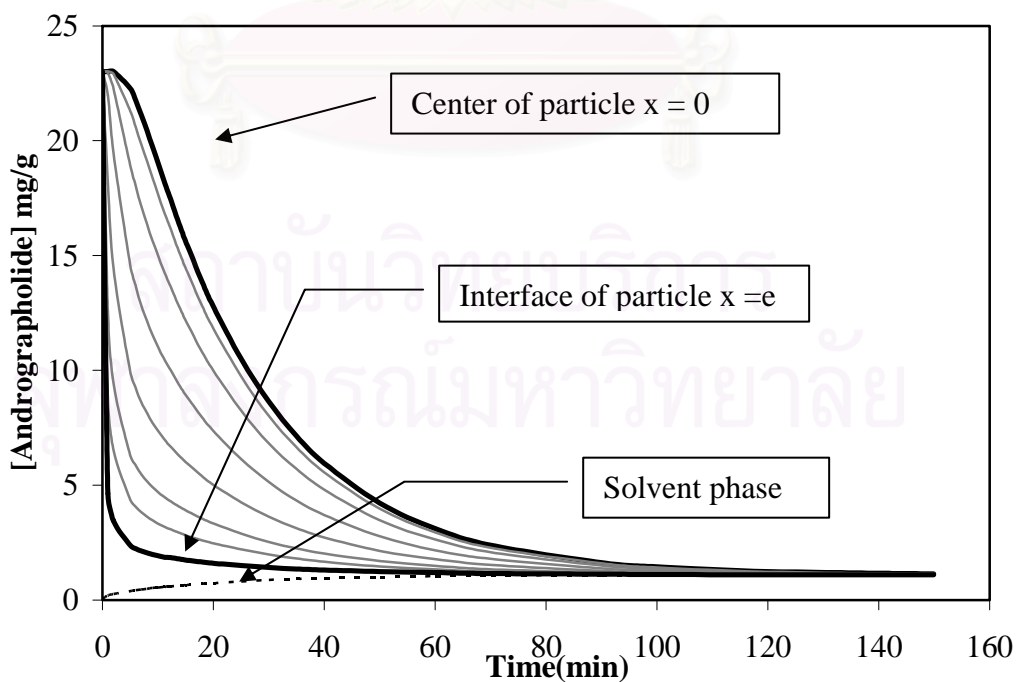


**Figure 3.2** Concentration profile for  $\phi = 1$  (plate shape)

The concentration profile of the solid particle for the stem decreases more quickly than the concentration profile for the leaves, because at the same volume, the cylinder has a larger diffusion surface area than the plate shape. The surface area of a cylinder is eight times the plate surface area for the same volume.

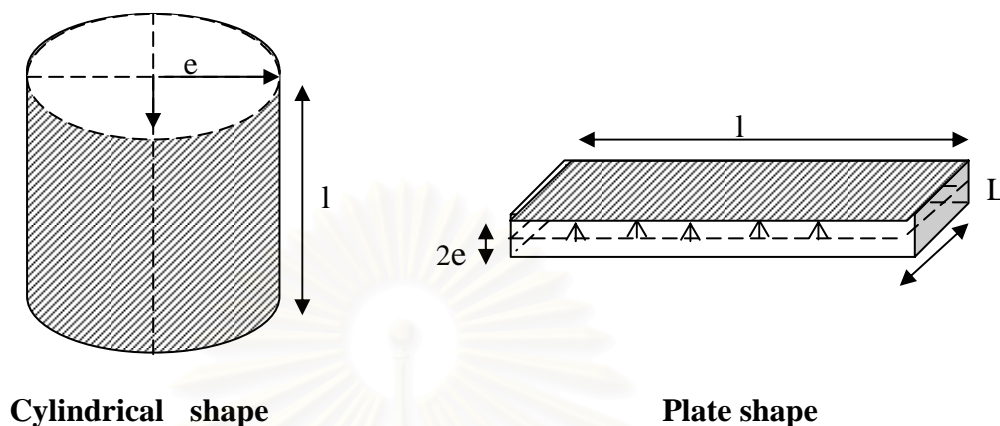


**Figure 3.3** Geometric shape factor  $\phi$  corresponding to the solid particle shape

As an example, the diffusion coefficient  $D$  that fits the experimental values for experiment number 3 is shown in **Figure 3.4**. The figure shows that the proposed model, with the identified value of  $5.06 \times 10^{-12} \text{ m}^2/\text{min}$  for  $D$ , describes fairly well the extraction phenomena for both geometric shape. However using only one particle shapes (plate or cylinder) does not describe accurately the experimental data (Seikova et al, 1999).

Since in the batch experiments, 0.6-0.8 mm size class particles are used, (soxhlet experiments giving a percentage of leaves of 80%), the extraction is then simulated taking into account the two different shapes. **Figure 3.5** demonstrates now a better agreement with the experimental results.

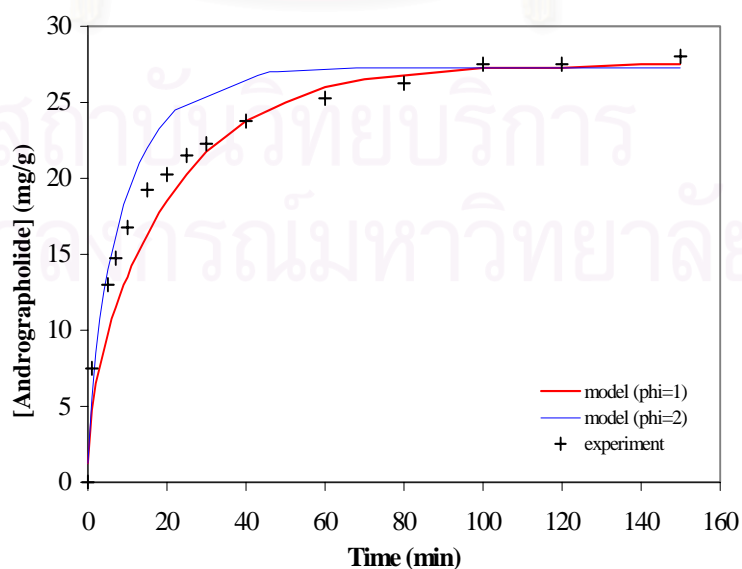


**Figure 3.4** Comparison between experiments and model at  $D = 5.06 \times 10^{-12} \text{ m}^2/\text{min}$  (solid diameter: 0.6-0.8mm, 60 % ethanol, Temp: 22°C, with  $\phi$ : 1 and 2 respectively)

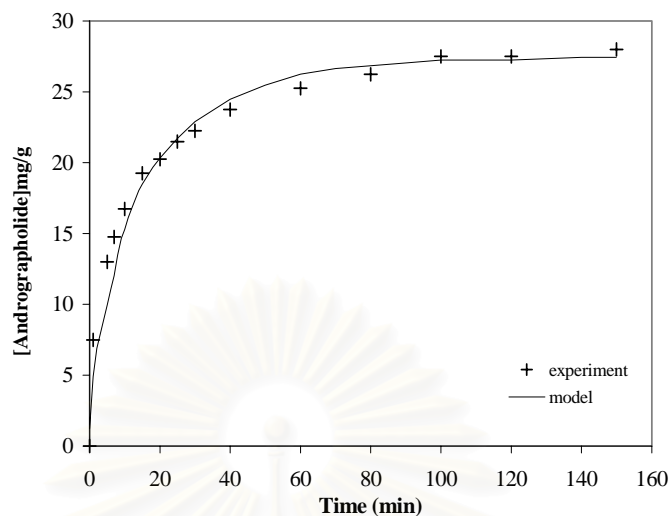


**Figure 3.5** Comparison between experiments and model at  $D = 5.06 \times 10^{-12} \text{ m}^2/\text{min}$  (solid diameter: 0.6-0.8 mm, 60 % ethanol and Temp: 22°C)

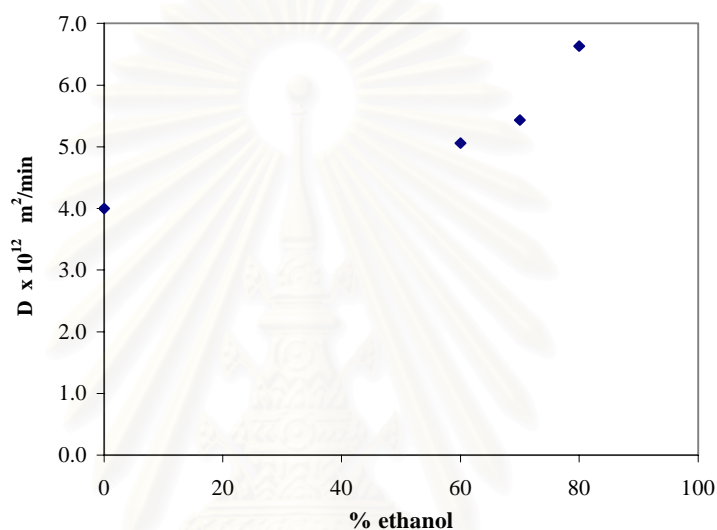
### 3.4 IDENTIFICATION OF THE DIFFUSION COEFFICIENT

By applying this 2-shaped approach, a good fitting between experimental and numerical data is obtained. The identified values of the coefficient of diffusion for all the experiments are shown in Table 3.1, including the values of the identification criterion. The coefficient of diffusion varies from  $5.0 \times 10^{-12}$  to  $7.5 \times 10^{-12} \text{ m}^2/\text{min}$  in ethanol solution at 22°C. Temperature can increase this value to  $31 \times 10^{-12} \text{ m}^2/\text{min}$  at 60°C. The results confirm the experimental observations of the influence of the main parameters (**Figures 3.6, 3.7 and 3.8**).

Temp °C	Diameter (mm)	% ethanol	Mass solid (g)	$D \times 10^{12} \text{ m}^2 \cdot \text{min}^{-1}$	Criteria
22	0.6-0.8	80	10	6.63	6.26E-07
22	0.6-0.8	70	10	5.43	1.72E-07
22	0.6-0.8	60	20	5.06	6.60E-07
22	0.6-0.8	0	20	0.95	8.01E-07
22	0.1-0.3	60	10	7.37	6.51E-07
22	0.45-0.6	60	10	7.31	6.09E-07
22	0.6-0.8	60	10	5.56	1.50E-07
40	0.6-0.8	60	10	23.55	7.99E-07
50	0.6-0.8	60	10	17.17	1.30E-07
60	0.6-0.8	60	10	31.26	9.09E-07
22	0.6-0.8	60	5	6.25	4.24E-07
22	0.6-0.8	0	10	3.79	2.73E-07
22	0.6-0.8	0	20	4.87	2.55E-07
22	0.6-0.8	0	30	5.35	2.30E-07

**Table 3.1** Coefficients of diffusions obtained by optimization**3.4.1 Influence of the solvent concentration**

**Figure 3.6** shows the diffusion coefficient with varying percentages of ethanol on the solute concentration for diameters of solid between 0.6-0.8 mm, a mass of particle of 10g, and temperature from 20-22°C. We found that the diffusion coefficient increases when the percentage of ethanol increases. Since the higher percentage of ethanol is a stronger organic solvent, the rate of diffusion increases with the percentage of ethanol (Treybal, 1963; Wede, 1987).

**Figure 3.6** The diffusion coefficient as a function of percentage of ethanol (solid diameter: 0.6-0.8 mm, 500 ml of ethanol solution and Temp: 22°C)**3.4.2 Influence of the particle size**

**Figure 3.7** shows the diffusion coefficient as a function of diameter of particles for a mass of solid of 10g, a 500 ml 60% ethanol solution, and temperature between 20-22°C. The graph shows that the diffusion coefficient increases slightly when the particle size decreases. It is found that the particle size has a slight influence on the rate of extraction, knowing that the pore diffusion resistance depends on particle size (the larger the size, the longer the pore diffusion path is longer). However, the diffusion coefficient is also quite small with values of  $5.0 \times 10^{-12}$  to  $7.5 \times 10^{-12}$  m<sup>2</sup>/min in an ethanol solution at 22°C.

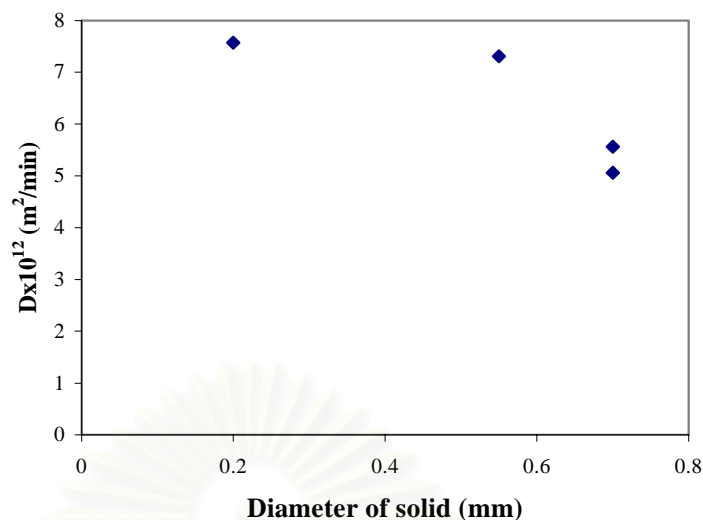


**Figure 3.7** The diffusion coefficient as a function of the diameter of particles (solid mass: 10g, 500 ml of 60% ethanol and Temp 22 °C)

### 3.4.3 Influence of the amount of solid

**Figure 3.8** shows that the diffusion coefficient is nearly the same when varying the amount of solid in the ethanol solution. The diffusion coefficient can be varied between  $5.05 \times 10^{-12} - 6.27 \times 10^{-12} \text{ m}^2/\text{min}$ .

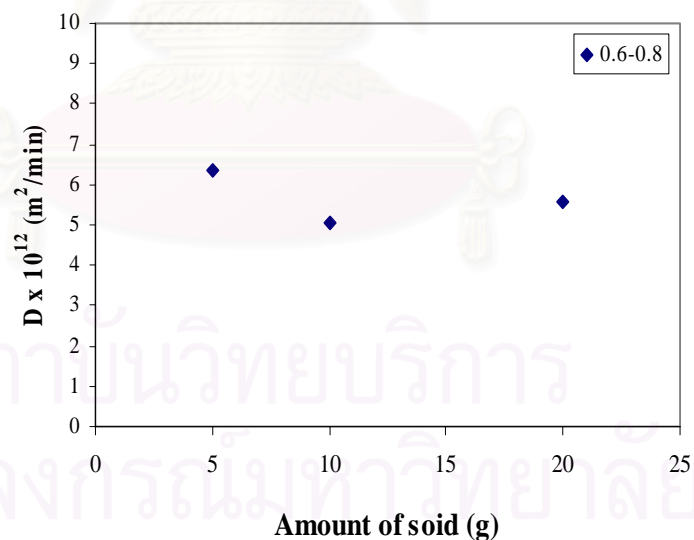


**Figure 3.8** The diffusion coefficient as a function of the amount of solid (solid diameter: 0.6-0.8mm, 500 ml of 60% ethanol, and Temp 22°C)

### 3.4.4 Influence of temperature

**Figure 3.9** shows the diffusion coefficient as a function of temperature. From the graph, the diffusion coefficient increases with the temperature up to  $31 \times 10^{-12} \text{ m}^2/\text{min}$  for  $60^\circ\text{C}$ . But for the  $50^\circ\text{C}$  the diffusion coefficient is shown to be smaller than at  $40^\circ\text{C}$ , this result can be explained from the problem of stems to leaves ratio in each experiment. We have to add that these experiments have been done previously in Thailand which the raw plants not from the same origin.

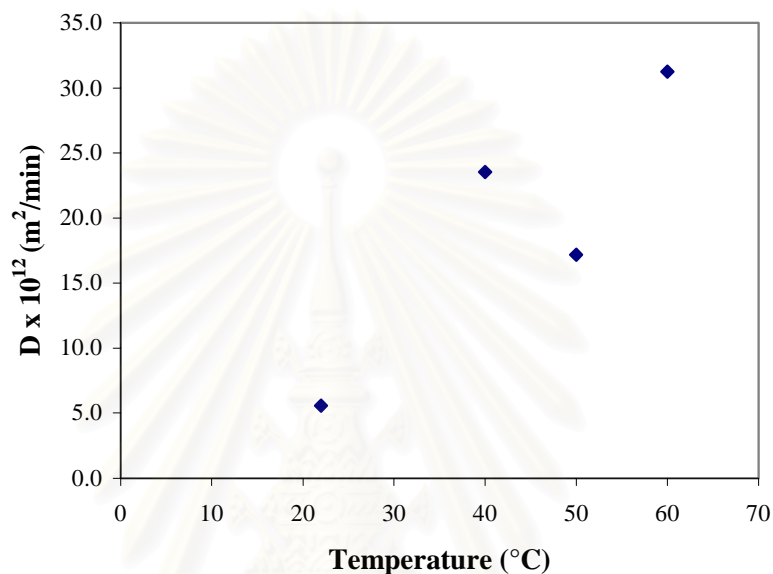


**Figure 3.9** The diffusion coefficient as a function of temperature (solid diameter: 0.6-0.8mm, 500 ml of 60% ethanol, solid mass: 10g)

## CONCLUSION

A mass transfer model has been proposed, taking into account the difference in shape of the particles. The experimental results were used to identify the diffusion coefficients for all experiments. The value of the coefficient varied from  $5.0 \times 10^{-12}$  to  $31 \times 10^{-12} \text{ m}^2 \cdot \text{min}^{-1}$  or  $8.43 \times 10^{-14} - 52.1 \times 10^{-14} \text{ cm}^2 \cdot \text{s}^{-1}$  in ethanol solution as a function of the temperature. The coefficient of diffusion  $D$  increases when  $T$  increases.

These results will now be used in the design of an industrial pilot column. The planned apparatus will be a disc and doughnut pulsed column. The influences of the operating parameters presented in this work will allow process conditions to be chosen in terms of solvent quality, temperature, and based on economical or safety criteria for the continuous process.

The following chapter will describe a continuous process for the hydrodynamic study, using a pulsed extraction column.

## CHAPTER IV

### CONTINUOUS PROCESS

#### INTRODUCTION

This chapter presents a continuous process for solid-liquid extraction from plant material in a disc and doughnut pulsed column with a pneumatic non sinusoidal pulsation cycle. In the case studied, the difficulty lies in the totally different hydrodynamic behaviour of two classes of particles in the raw plant substrate. One class of particles tends to float and the other to sink. In addition, the hydrodynamic characteristics of the solid particles also depend on the solvent concentration.

With the use of a more flexible system than a mechanical pulsation which only allows a regular sinusoidal motion of the phases, the aim was to avoid flooding due to floating particles accumulating at the feed inlet. Therefore, an air pulsating system was used in the column chosen.

The first part describes the operation of the extraction column as well as the pneumatic pulsation.

In the second part, experiments were undertaken to present the global characteristics of the steady state process in an extraction column aimed at studying out, the influence on the solid-liquid separation.

The third part dealt with the dynamic experimental results. In addition particle residence times and extraction yields were also determined.



## 4.1 COLUMN AND PULSATION SYSTEM DESCRIPTION

### 4.1.1 Column

The column is composed of a vertical cylindrical body 5.4 cm in diameter and 2.5 m in height of Pyrex glass and the disc and doughnut packing were arranged and maintained by braces of constant length. The column consisted of a series of differential compartments with a distance between disc and doughnut of 2.5 cm. A disc is 2.5 cm in diameter and the aperture of a doughnut is 1.4 cm. A schematic presentation of disc and doughnut plate is shown in Figure 4.1a.

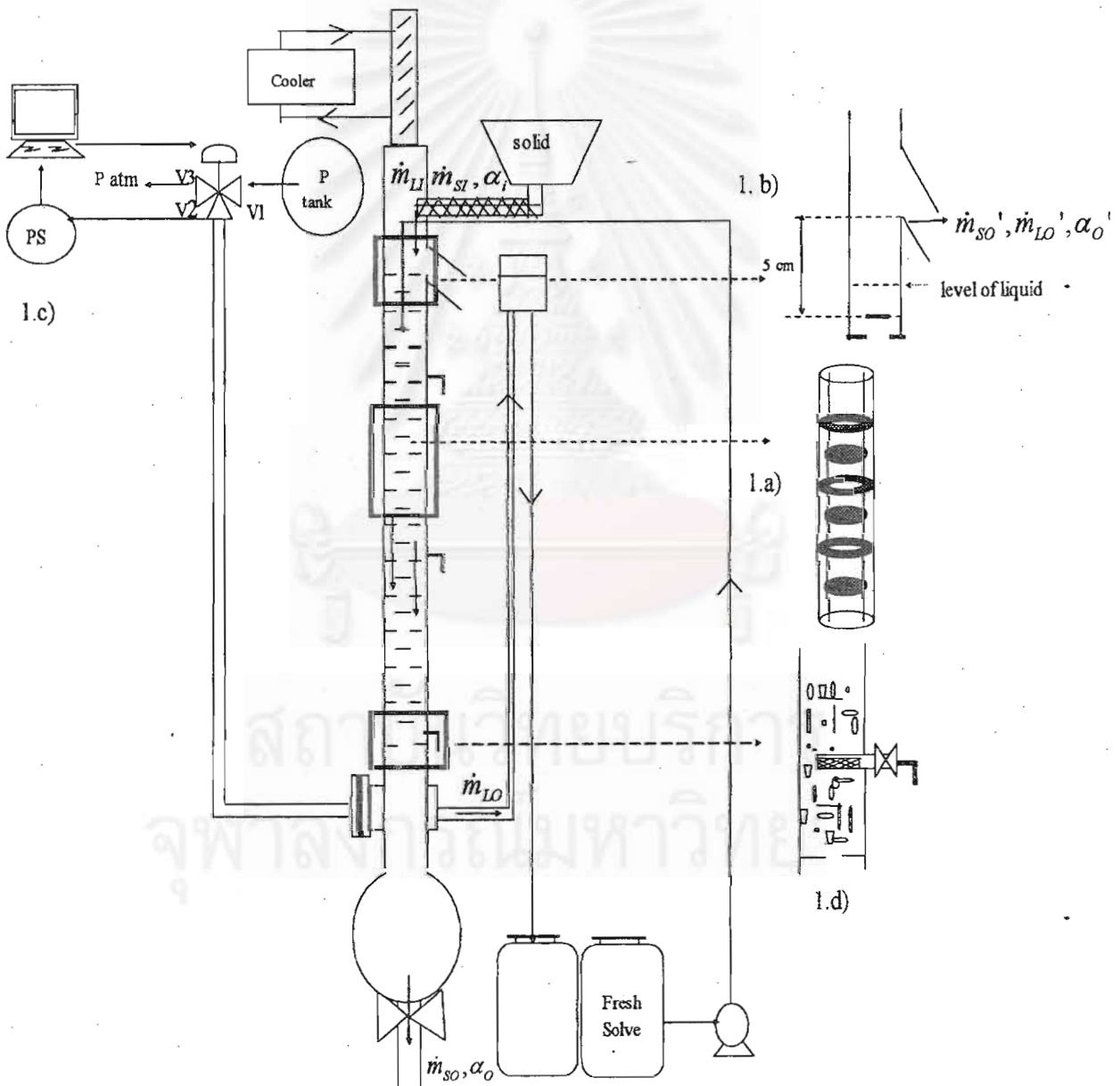


Figure 4.1 The schematic representation of the column

The parameters used are as follows:

- $\dot{m}_{LI}$ : Mass liquid flow inlet (g/min),
- $\dot{m}_{SI}$ : Mass solid flow inlet (g/min),
- $\dot{m}_{LO}'$ : Mass liquid flow outlet at the top of column(g/min),
- $\dot{m}_{LO}$ : Mass liquid flow outlet at the bottom of column (g/min),
- $\dot{m}_{SO}'$ : Mass solid flow outlet at top column (g/min),
- $\dot{m}_{SO}$ : Mass solid flow outlet at bottom column (g/min),
- $\alpha_o$ : Sinking mass outlet/ total solid mass outlet (at bottom of column),
- $\alpha_o'$ : Sinking mass outlet/ total solid mass outlet (at top of column),
- $\alpha_i$ : Ratio of sinking mass and total solid mass in the sample.

Two main modifications have been made on this pilot compared with a classical column:

### **The upper part of the column**

At the upper part of the column, a 5 cm diameter Tee element was added to allow a supplementary outlet at the top of the column (Figure 4.1.b). This was used to evacuate the floating solid.

### **The pulsating system**

An air pulsing system (Figure 4.1c) was chosen that allowed for variation in the pulsation policy. The air pulser components consisted of a vertical riser adjacent to the column called a pulsed leg. Air pulsing is carried out by means of a three ways solenoid valve. The first valve ( $V_1$ ) admits air pressure to the pulsed leg and the second valve ( $V_2$ ) allows air from the pulsed leg to exit. Air storage was added to smooth out fluctuations in the air pressure supplied to  $V_1$ . The exhaust air from valve ( $V_3$ ) was discharged to the atmospheric.

Despite its pulsing energy limits (in terms of amplitude and frequency), the proposed system gives the opportunity to have non-sinusoidal forms of pulsation. The movement of the liquid is separated into two steps. The first step is a classical sinusoidal pulsation in order to mix the two phases in the column (pulsation step). The second step allows for a short increase of level inside the column in order to purge the floating solid though the top outlet tube (impulsion step).

A classical policy used in this work is described in Figure 4.2 the two steps where can be observed. Between the pulsation and the impulsion, there is a transitory step corresponding to the filling up of the column after the column has been purged.

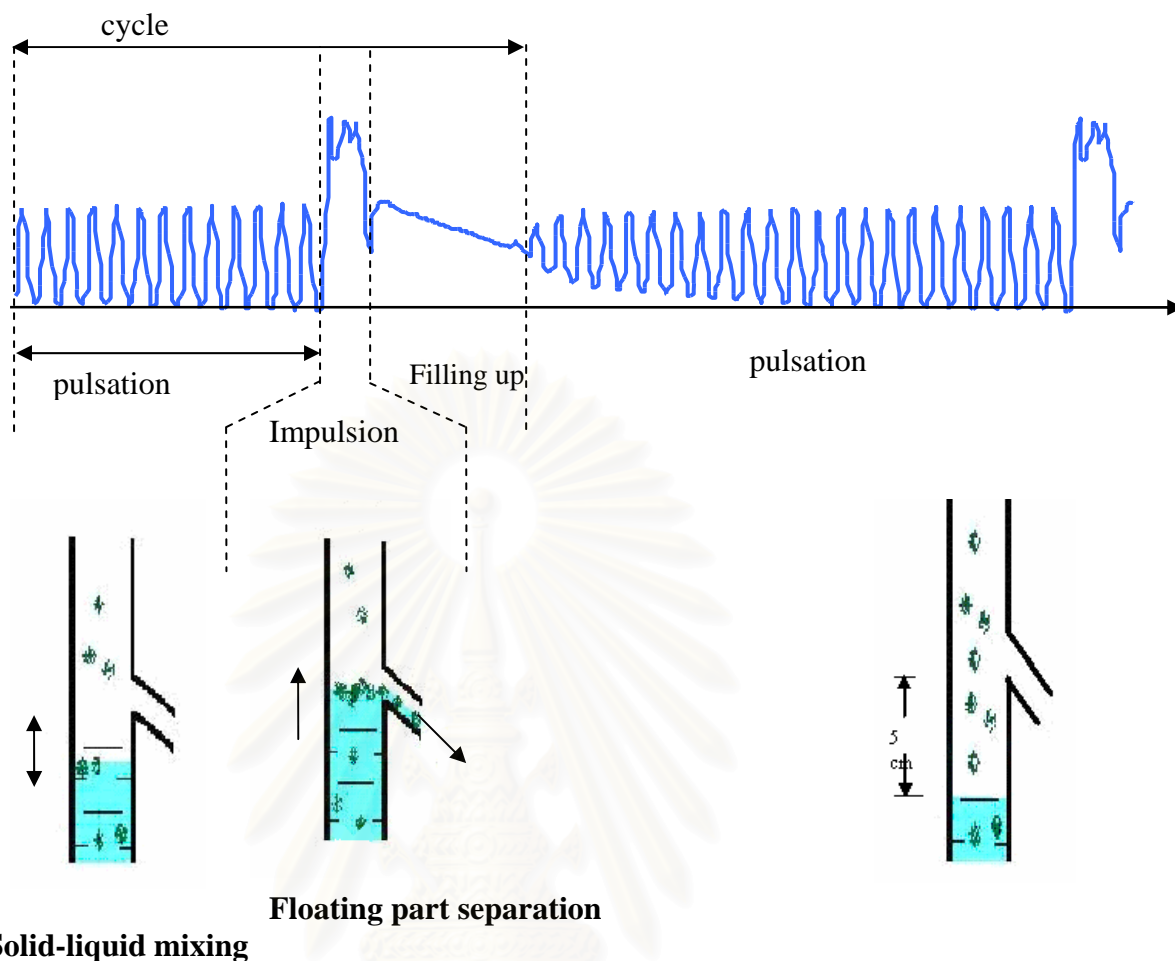


**Figure 4.2** The phenomena within the column as a result of the pulsation system

#### 4.1.2 The pneumatic pulsation system

**Figure 4.3** illustrates the typical pressure and signal (analogic) connections for the pulsation system. It is composed of a three-way valve linked on one hand to a storage tank set a 2 bars pressure and on the other hand to the atmosphere (1 bar pressure). The delivery pressure is then connected to the pulsed leg of the column and the active range is then 1 to 2 bars.

A computer is used for the supervision of the cycle and allows to deliver the setpoint (in pressure) to the PID regulator. The feedback is assured by an external pressure sensor situated in the pulsed leg.

The ER3000 is a microcontroller based device that implements a digital control algorithm to regulate pressure. Supply pressure is allowed into the ER3000 via a pulse width modulated solenoid valve at the inlet port, and pressure is reduced via a similar valve at the exhaust port (normally the exhaust vents to ambient). The ER3000 is a 0-100 psi pressure controller (0-6.80 atm).

In a typical application, the ER3000 compares the feedback signal to the set point every 25 milliseconds. If the feedback is lower than the set point, the ER opens its inlet valve, allowing pressure to flow onto the dome of a pressure reducing regulator. This opens the main valve of the regulator, increasing pressure downstream. The ER3000 will continue to increase pressure on the dome of the regulator, increasing downstream pressure until the feedback signal is equal to the set point. If the set point is lowered, so that the feedback is now higher than the set point, the ER3000 will cause the regulator to self vent, thus lowering downstream pressure. The ER3000 will continue to reduce pressure on the dome of the regulator until the feedback signal is equal to the set point. The regulation system is described in **Figure 4.4**.

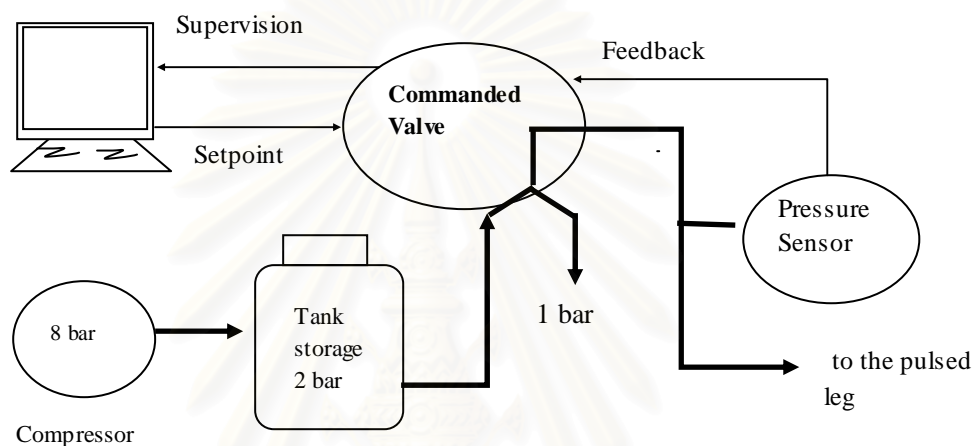


**Figure 4.3** Schematic of an air pulsing system

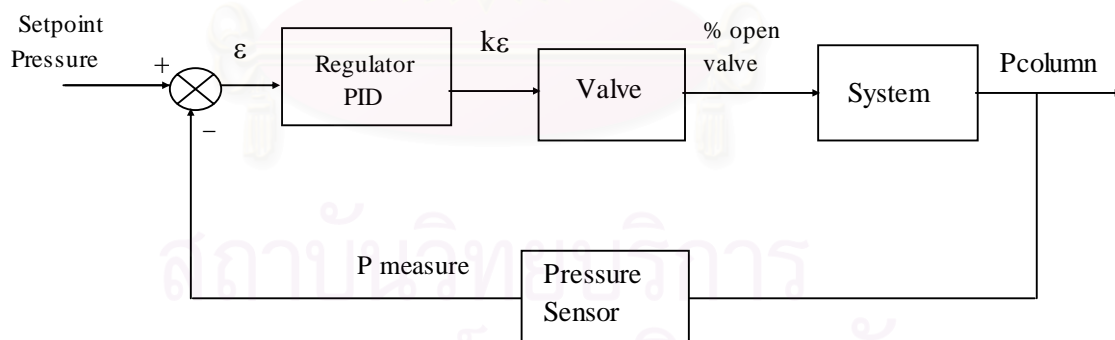


**Figure 4.4** The operation function of ER3000 (Electronic Regulator)

Supplied external transducer was used to measure the process pressure in the pulsed leg. Then using the ER3000 control of the actual pressure was obtained by installing a pressure transducer at the output of the regulator or valve to provide the feedback signal to the ER3000.

The computer is used to relay the set point to the ER3000. This setpoint can be constant or can vary with time. A typical way to described this function is:

1. Step to 80 PSI
2. DWELL for 0.6 sec
3. Step to 0.00 PSI
4. DWELL for 0.6 sec
5. Loop to step No.1, 30 times
6. Step to 100.00 PSI
7. DWELL for 2.0 Sec
8. Loop to step No.1 always
9. End.

**Figure 4.5** shows the setpoint function generated from the typical way.

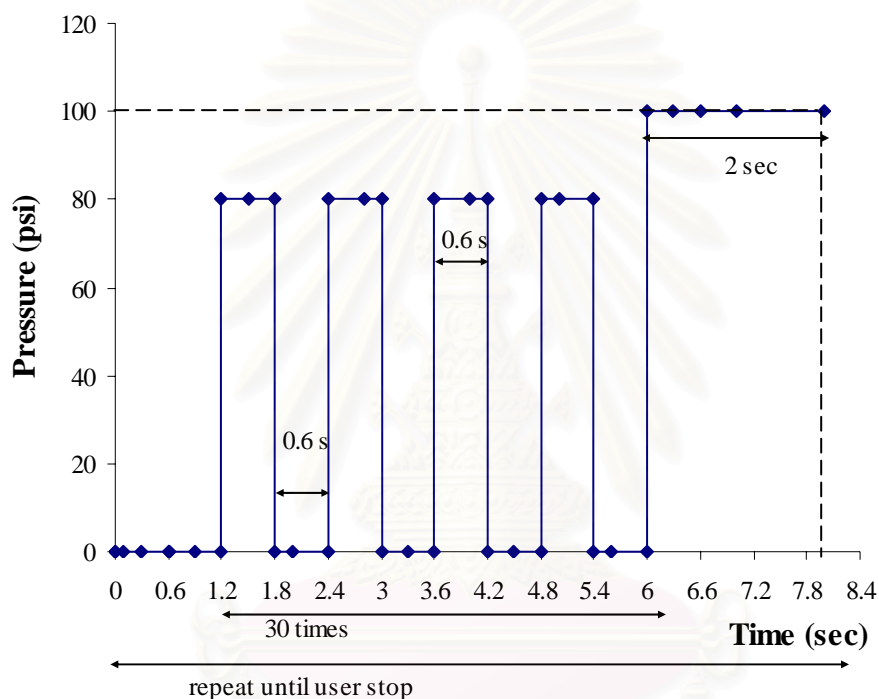


**Figure 4.5** The setpoint function

### 4.1.3 Calibration

#### 4.1.3.1 Calibration curve of the liquid pump

The liquid is fed into the column using a piston pump. The experiments are undertaken by measuring the liquid flow rate at the outlet of the column while varying the percentage of the open pump value in order to obtain a calibration of the liquid pump. **Figure 4.6** shows that the liquid flow linearly increases with the percentage open pump. The straight line correlation found is

$$\text{Flow rate} = 0.725 \times \text{of \% open pump valve.}$$

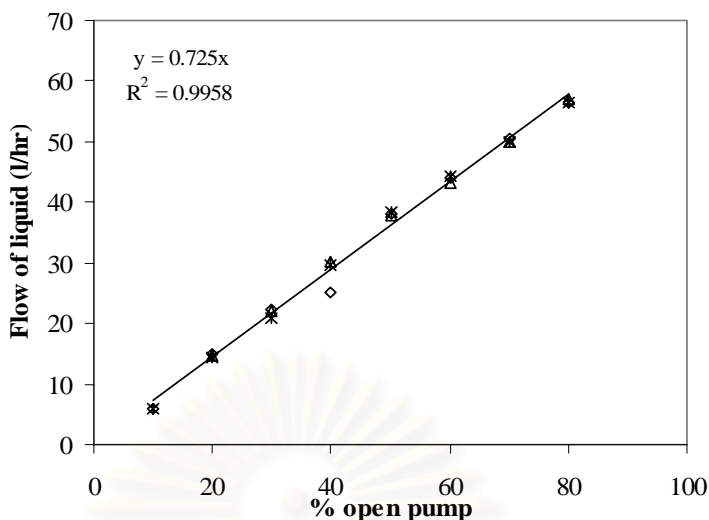


**Figure 4.6** The calibration curve of the liquid flow

Before doing any experiments the liquid flow rate is measured for every run in order to know the exact amount of liquid feed flow.

#### 4.1.3.2 Calibration curve of solid feed

The solid is fed into the column using an endless screw at the top of the column which simultaneously makes it possible to press and tap the solid. The solid feed is measured by changing the speed number of the screw. **Figure 4.7** shows solid feed flow rate increasing when increasing the speed number of the screw. The correlation is flow of liquid =  $0.486e^{0.425(\text{speed number})}$ .

Problems encountered are that the solid feed is not uniform either when there is high flow rate of solid is humid. The screw becomes plugged if there is too much humidity.

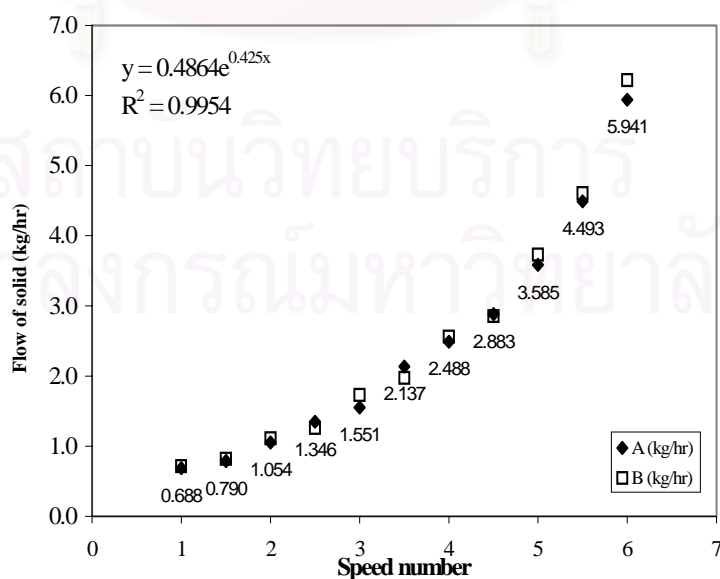


**Figure 4.7** The calibration curve of the solid feed

#### 4.1.4 Column operation

At the start of each experiment the compressor is turned on. The 8 bars in the air pressure is connected to a monometer that reduce the pressure down to 2 bars storage tank.

The column is filled with solvent and the level of liquid in the column is adjusted while changing the level of the counter-pressure leg. The set point profile is then prepared and the ER3000 system is turned on. In order to minimize energy and air consumption, operation is undertaken at the natural frequency of the column (Thornton, 1954 ; Weech and Knight, 1967). On this column, this corresponds to a frequency of  $1.67 \text{ sec}^{-1}$ .

*Andrographis paniculata* is then fed continuously along with the ethanol solution at the top column and the solution is removed continuously from the column. Consequently, the phases are forced to flow co-currently. This way of functioning is linked to the low density difference between both phases, which is not sufficient to allow a counter-current operation. Besides, in this study, there is no practical need to perform an extraction in excess of 1 theoretical stage.

The entire flow system oscillates by means of the external pulsation imposed by the pneumatic action. The two phases are mixed due to pulsation, usually sinusoidal, so that a vertical pressure action is imposed on the co-current flow of the two phases. The impulsion action aims at eliminate the floating solid particles (especially the stems) at the top of the column, while obtaining a good level of mixing inside the column (**Figure 4.2**). At the very top of the column, a cooler has been installed in order to avoid the ethanol evaporation.

The experimental system is a semi-continuous process because the entire solid particle is collected in the glass balloon at the bottom of the column, which has no effect both on the air pressure in the column and on the extraction process. Subsequently, experiments cannot be undertaken for too long a time, the time limits being around 3 hours of operation.

The difficulties arising during the experiments are described as follows:

- The upper part of the column: the diameter of the floating solid column (T column) was not large enough for the floating solid when purged by the impulsion. There are some solid blocks at this level resulting in clogging. It was made larger to allow for more floating solids to exit there.

- In order to sample the solution in the pulsed column, there was a problem with the solid clogging the sampling valve. Consequently, a steel tube diameter (4x6mm) was connected with the valve and span in the column. Half of the tube was cut and replaced with a grid steel. To set up the tube, the grid steel side was located at the lower part in order to avoid small solid particles setting into the tube and allowing only the liquid to pass through the valve (**Figure 4.1d**). Besides, the air pressure can flush out some of the smaller particles from the valve.

## 4.2 STEADY- STATE EXPERIMENTAL RESULTS

### 4.2.1 Liquid study without solids

Experiments were performed without solid inlet in order to observe liquid behaviour as a function of the pressure profile set point and the liquid level.

Figures 4.8 and 4.9 show the profile of the pressure when the lower set point is set at 80 psi and 70 psi respectively and the upper setpoint at 100 psi. The amplitude of pulsation is the same for both experiments. The lower value of the pressure changes function of the lower set point value (62.94 for 80 psi and 50.06 for 70 psi).

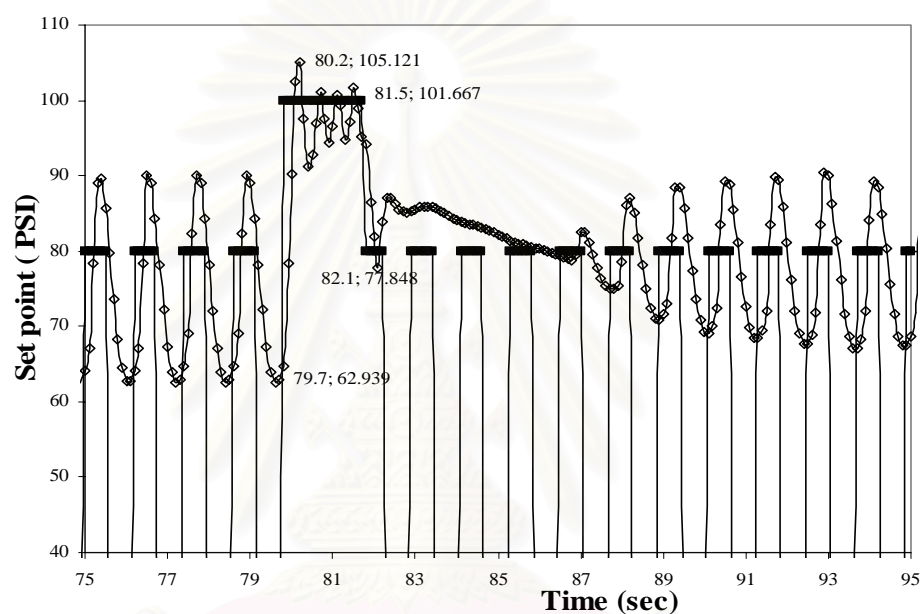


Figure 4.8 The profile of the air pulsing at the lower set point is 80 to 100 psi

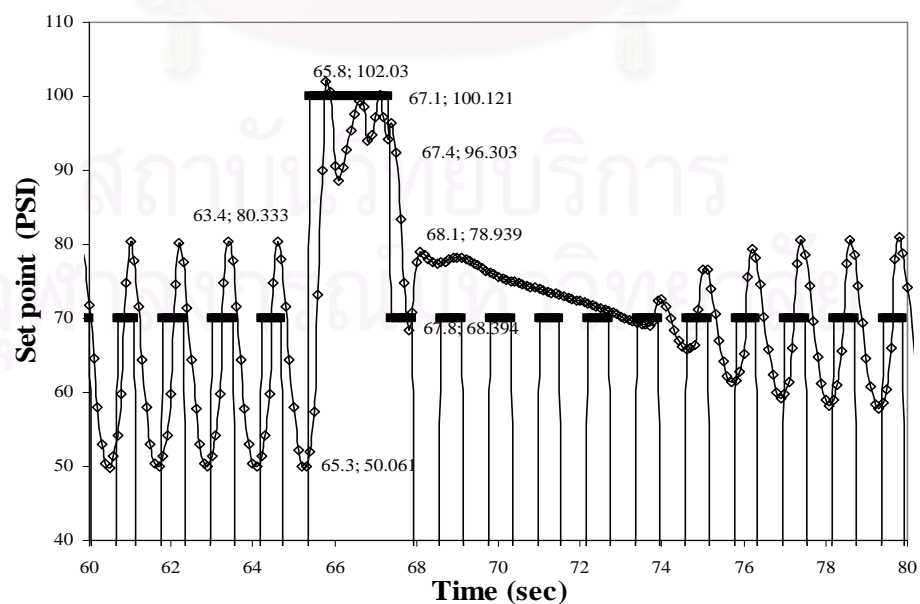
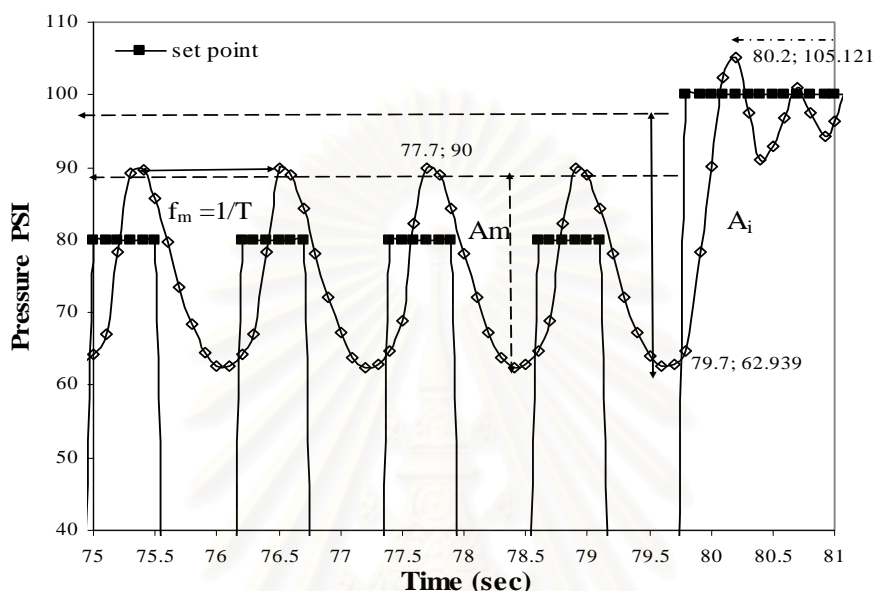


Figure 4.9 The profile of the air pulsing at the lower set point is 70 to 100 psi



**Figure 4.10** shows an example of the pressure profile. The amplitudes of the impulsion and the pulsation were measured directly from the pulsed leg column. **Table 4.1** shows the amplitude of the impulsion and the pulsation according to the lower pressure set point. The experiment was done by changing the lower set point from 40 to 80 psi. The level of liquid in the pulsed leg was then measured. The initial level of liquid is 0 (at the first plate).



**Figure 4.10** The pressure profile

$P_{low\ set\ point}$	$A_i$ (psi)	$A_i'$ (cm)	$A_i$ (cm)	$A_m$ (psi)	$A_m'$ (cm)	$A_m$ (cm)
80	42.18	14	5.55	26.82	1.3	0.515
70	51.97	18	7.14	30.39	1.4	0.555
60	61.00	21	8.33	31.21	1.45	0.575
50	67.70	22.5	8.92	32.49	1.5	0.595
40	67.06	23	9.12	26.61	1.3	0.515

**Table 4.1** Experimental amplitudes in the column

All the following variables were measured:

$A_i$  : The amplitude of the impulsion (psi),

$A_i$  : The amplitude of impulsion from the impulsion in the body of the column (cm),

$A_i'$  : The amplitude of impulsion from the impulsion in the pulsed leg column (cm),

$A_m$  : The amplitude of the pulsation (psi),

$A_m$  : The amplitude of mixing from the pulsation in the body of the column (cm),

$A_m'$  : The amplitude of mixing from the pulsation in the pulsed leg of the column (cm),

$P_{low}$  : The lower pressure set point (psi).

The relation between the pressure (psi) and the amplitude of the liquid level (cm) was investigated.

Figure 4.11 shows the relation between the amplitude level and the amplitude pressure in the pulsed leg column as a function of the impulsion and the pulsation level. The experiments show that the relation between level and pressure of the impulsion is 10 times higher than the pulsation. At the same amplitude pressure (psi), the amplitude of the impulsion is higher than the amplitude of pulsation.

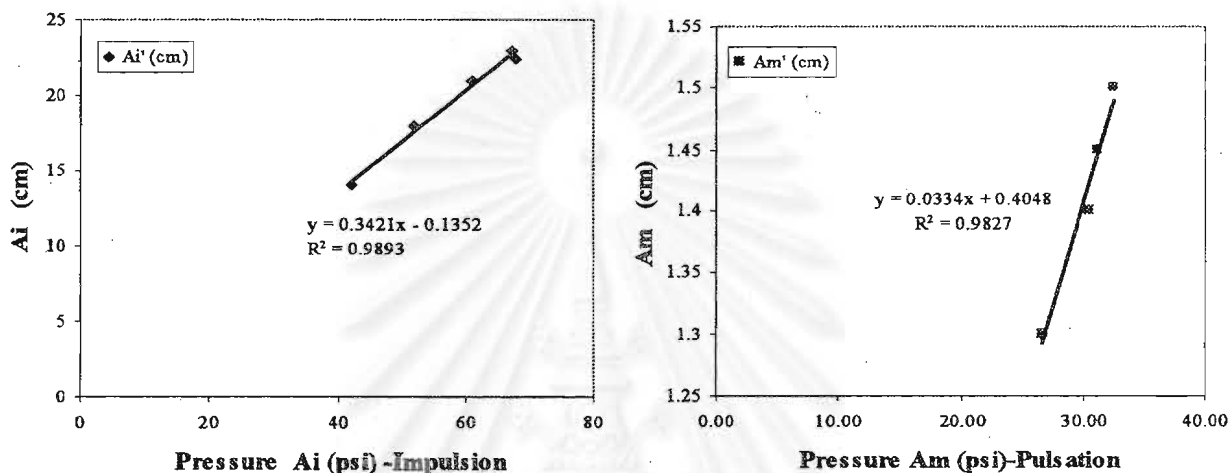


Figure 4.11 The relation between the level and the pressure of impulsion and pulsation in the column

The liquid outlet as a function of impulsion was studied by changing the initial level of the liquid in the column. The objective was to find the proper level of liquid in the column before starting the air pulsing. During the experiment, we need a minimum of solvent that gets out at the column to help the solid to get out too.

The experiment was done by filling up the column with water, adjusting and changing the level of the liquid by changing the level of the counter-presume leg. Then the same profile set point pressure was launched and the  $m_{LO}$  was measured as a function of time.

Figure 4.12 shows the mass of the liquid outlet as a function of time while the set point is 80 to 100 psi by changing the level of the liquid. During the experiment, there is some loss in liquid feed  $m_{LI}$  through the Tee column. At liquid levels of 3 cm and 4 cm, the liquid loss is reduced. The volume of the liquid outlet in Figure 4.12 is the sum of the liquid losses from the liquid feed inlet and the impulsion as a function of time.

The appropriate level of the liquid should be set near the Tee column (opening of the column) without any liquid losses due to pulsation. Besides, it allows a small impulsion in order to purge the solid and minimize solvent loss.

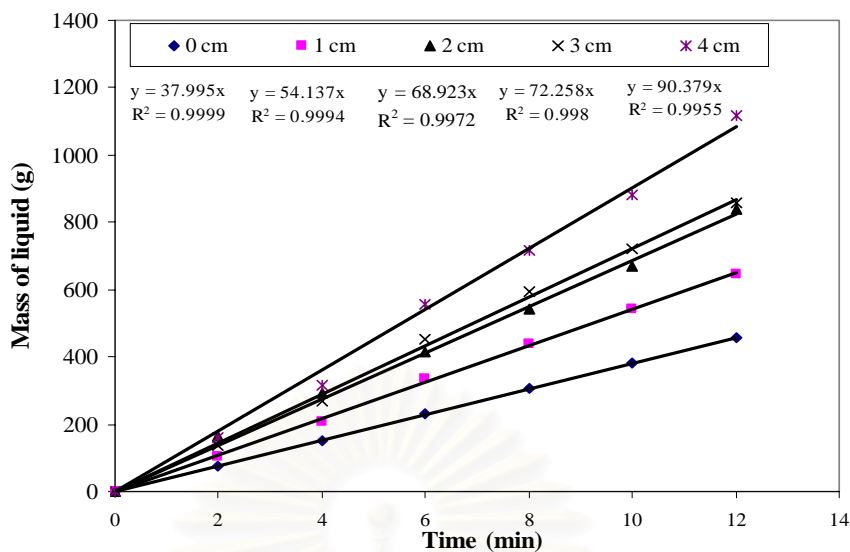


**Figure 4.12** The mass liquid outlet as a function of time at the set point is 80-100 psi

**Figure 4.13** shows the mass flow of liquid that leaves the column and the calculation function of the initial level of the liquid (level equal to zero corresponds to the first plate) while the pressure setpoint is 80 to 100 psi. From **Table 4.2** the amplitude of the liquid from the impulsion in the column is 5.5 cm. The distance between the first plate and the opening of the column is 5 cm. The difference between the amplitude and the impulsion is higher than 0.5 cm. This value allows the calculation of the liquid mass outlet  $\left( liquid\ mass = \frac{\pi D^2 \Delta h}{4} \right)$  when changing the level of the initial liquid level. The amounts of liquid that leaves the column increases when increasing the liquid level in the column. The experimental results confirm this calculation.

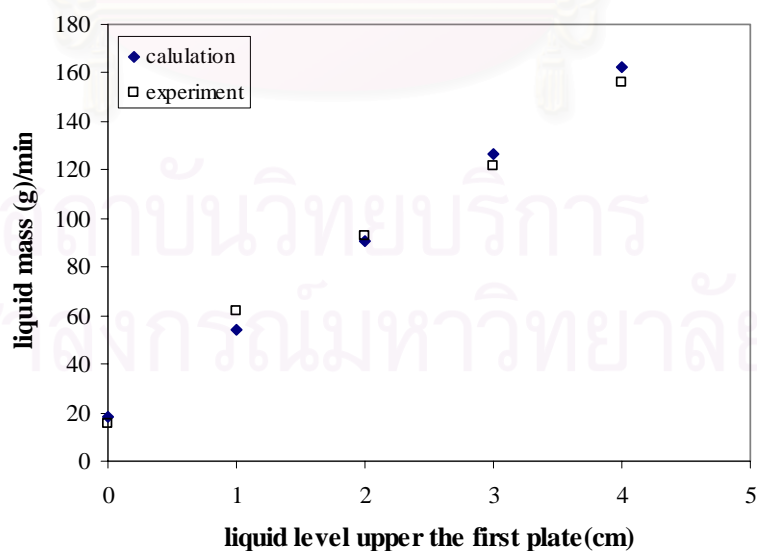


**Figure 4.13** The mass liquid outlet as a function of initial liquid level in the column at the set point is 80-100 psi

#### 4.2.2 Study of the solid at nominal conditions

The objectives are on one hand to study the behaviour of the solid particles as a function of the operating parameters and on the other hand to characterize the floating/sinking solid separation at the top of the column.

At the top of the column, the solid in contact with the liquid absorbs the solvent. As shown in **Chapter 2.4.1**, even after a long time of contact (5 hours) parts of the solid are still floating. In the column, the time of contact depends on  $f_i$ . Furthermore, if the solid flow rate reaches a certain level, some solid does not reach the liquid and remains dry.

Two main values will then characterize the efficiency of the floating/sinking separation at the top of the column:

-  $\frac{\dot{m}_{SO}}{\dot{m}_{SI}}$  which represents the part of the solid going through the column (and for which solid liquid extraction occurs),

-  $\alpha_o' = \frac{\dot{m}_{\text{sin king}}}{\dot{m}_{\text{total}}}$  the sinking ratio of the solid going out at the top of the column.

These two values are related via the global mass balance. The operating conditions of the experiments are presented in **Table 4.2**. This work does not focus on the analysis of the influence of the frequency and of the amplitude during the mixing period of the pulsation (sinusoidal part). The only objective is that  $f_m$  and  $A_m$  permit sufficient level of mixing in the column to be reached. All experiments are presented in **Appendix III**.

Exp. N°	Ethanol %	level cm	$f_m$ min <sup>-1</sup>	$A_m$ psi	$f_i$ min <sup>-1</sup>	$A_i$ psi	$\dot{m}_{SI}$ g.min <sup>-1</sup>	$\dot{m}_{LI}$ g.min <sup>-1</sup>
1	95	0	50.42	25	1.58	33.5	11.33	431.6
2	95	0	52.63	25	1.58	33.5	11.33	431.6
3	95	0	52.63	25	1.58	33.5	17.57	431.6
4	95	0	60	21	2.33	33.5	25.85	452.35
5	95	1.5	52.17	21	1.57	22	11.33	419.15
6	95	1.5	52.17	21	1.57	22	17.57	431.6
7	70	1.5	52.63	23.5	1.58	22	11.33	368.28
8	70	3	52.17	21	1.57	22	17.57	547.35
9	70	1.5	52.17	21	1.57	22	11.33	431.6
10	70	2	52.17	21	1.57	22	11.33	431.6
11	50	3.5	52.17	21	1.57	22	11.33	501.4
12	50	3.5	52.17	21	1.57	22	11.33	501.4
13	50	3.5	52.17	21	1.57	22	11.33	482.54
14	30	3.5	52.17	21	1.57	22	11.33	456.01
15	30	3.5	52.17	21	1.57	22	11.33	463.18

**Table 4.2** Operating conditions

Once the steady state is reached, the flow rates are measured.

The volumes  $V_{SO}$  and  $V_{SO}'$  were directly measured (at the bottom and at the top respectively). The relation between mass and volume (**Chapter 2.4.2**) was used to calculate the flow rates  $\dot{m}_{SO}$  and  $\dot{m}_{SO}'$ . Furthermore, the solid bottom outlet was separated into a sinking and floating part (of course, the solid top outlet should be only composed of floating particles). All the results are gathered in **Table 4.4**.

$V_{SO}$  : The volume of the solid in the solvent at the bottom of the column (ml),

$V_{SO}'$  : The volume of the solid in the solvent at the top of the column (ml).

Exp. N°	Ethanol %	$\dot{m}_{LO}'$ g.min <sup>-1</sup>	$\dot{m}_{SO}$ g.min <sup>-1</sup>	$\dot{m}_{SO}'$ g.min <sup>-1</sup>	$\dot{m}_{SI}$ g.min <sup>-1</sup>	$\frac{\dot{m}_{SO}}{\dot{m}_{SI}}$	$\frac{\dot{m}_{SO}'}{\dot{m}_{SI}}$	% error of mass balance	$\alpha'$
1	95	45.87	8.83	1.79	10.62	0.83	0.17	6.3	0.32
2	95	45.87	7.79	2.50	10.29	0.76	0.24	9.2	0.35
3	95	45.87	11.26	5.84	17.10	0.66	0.34	2.7	0.53
4	95	67.03	15.44	12.58	28.02	0.55	0.45	-8.4	0.72
5	95	45.90	8.27	1.68	9.95	0.83	0.17	12.2	0.15
6	95	49.50	11.43	2.2	13.63	0.84	0.16	22.4	0.31
7	70	46.25	7.96	2.72	10.68	0.75	0.25	5.8	0.22
8	70	49.18	10.39	3.79	14.18	0.73	0.27	19.3	0.28
9	70	50.84	7.44	-	-	-	-	-	0.25
10	70	50.84	6.04	-	-	-	-	-	0.27
11	50	50.84	5.94	4	9.94	0.60	0.40	12.3	0.35
12	50	50.84	8.04	3.31	11.35	0.71	0.29	-0.2	0.35
13	50	51.15	5.82	2.32	8.14	0.71	0.29	28.2	0.32
14	30	52.81	4.45	3.56	8.01	0.56	0.44	29.3	0.35
15	30	52.81	6.09	2.78	8.87	0.69	0.31	21.7	0.35

**Table 4.3** Results (Measurement)

$$\% \text{ error of mass balance} = \frac{\dot{m}_{SI} - \dot{m}_{SI}(\text{measurement})}{\dot{m}_{SI}} \times 100$$

#### 4.2.2.1 Variations of $\frac{\dot{m}_{SO}}{\dot{m}_{SI}}$ and $\frac{\dot{m}_{SO}'}{\dot{m}_{SI}}$

**Figure 4.14** shows the ratio of the mass flow rates at the bottom and at the top of column as a function of the percentage of ethanol, the mass solid input being fixed to 11.33 g/min.

$\dot{m}_{SO}$  increases when the percentage of ethanol increases. This confirms that the solid particles sink easily and faster at higher ethanol concentrations as shown in **Chapter 2.4.1**. Furthermore, the mass of floating parts leaving the column  $\dot{m}_{SO}'$  decreases when the percentage of ethanol increases.

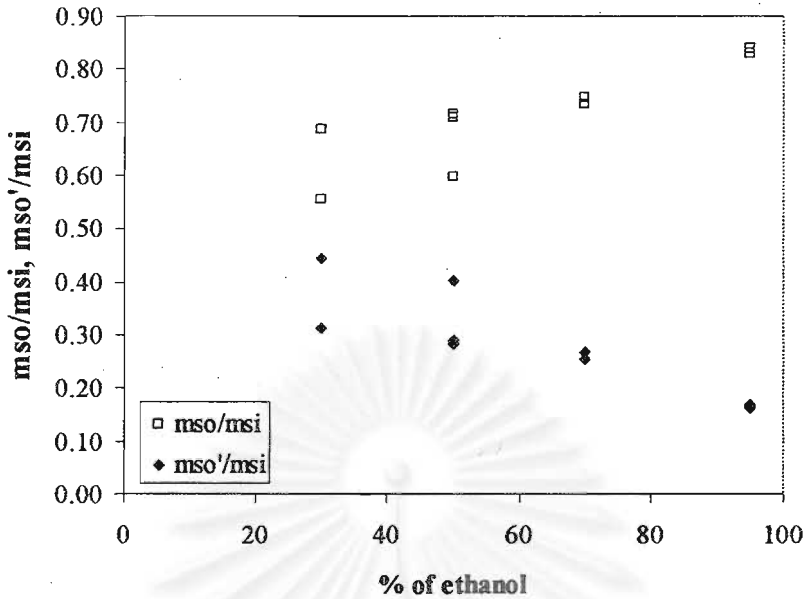


Figure 4.14 Solid flow rate ratio at the bottom and at the top of the column as a function of percentage of ethanol

Figure 4.15 shows the ratio of the mass flow of solid at the bottom and at the top of the column with a mass solid flow input at 95% ethanol (Experiments 1, 2, 3 and 4 in Table 4.4).

$\frac{\dot{m}_{SO}}{\dot{m}_{SI}}$  decreases when the mass solid inlet increases and  $\frac{\dot{m}'_{SO}}{\dot{m}'_{SI}}$  increases when

the mass solid inlet increases. The separation of the solid is more efficient when the mass of solid at the inlet is small because some of the solid remain dry with high  $\dot{m}_{SI}$ .

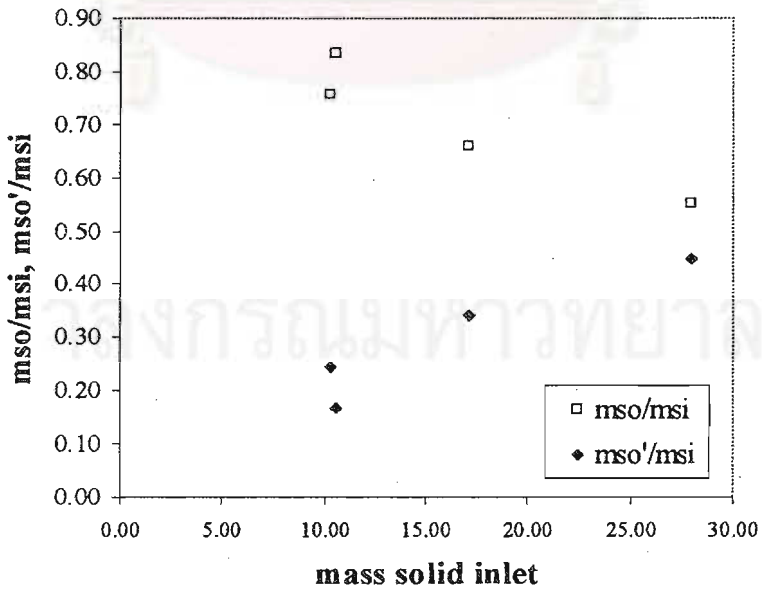


Figure 4.15 Solid flow rate ratio at the bottom and at the top of the column as a function of mass inlet of solid

#### 4.2.2.2 Variations of $\alpha'_o$

The objective is to investigate the effect of ethanol concentration on the separation of floating solid and sinking solid at the top of the column and to compare the experimental data with one another.

$\alpha'_o$  is the characteristic efficiency of the separation between the floating and sinking solids, defined by the ratio of sinking solid and the total solid in the outlet mass flow at the top of the column. If  $\alpha'_o$  tends to 0, it means that the outlet is only composed of floating particles, separation between the floating and sinking part being assumed perfect. The maximum value of  $\alpha'_o$  should be 0.8 because the ratio of leaves and stems in the sample is 0.8.

**Figure 4.16** shows that  $\alpha'_o$  decreases as percentage of ethanol increases for the same mass solid inlet ( $11.33 \text{ g}\cdot\text{min}^{-1}$ ). The separation is due to solvent absorption into the particles during contact time. In **Chapter 2.4.1**, it has been shown that the kinetics of solvent absorption increase with the percentage of ethanol.

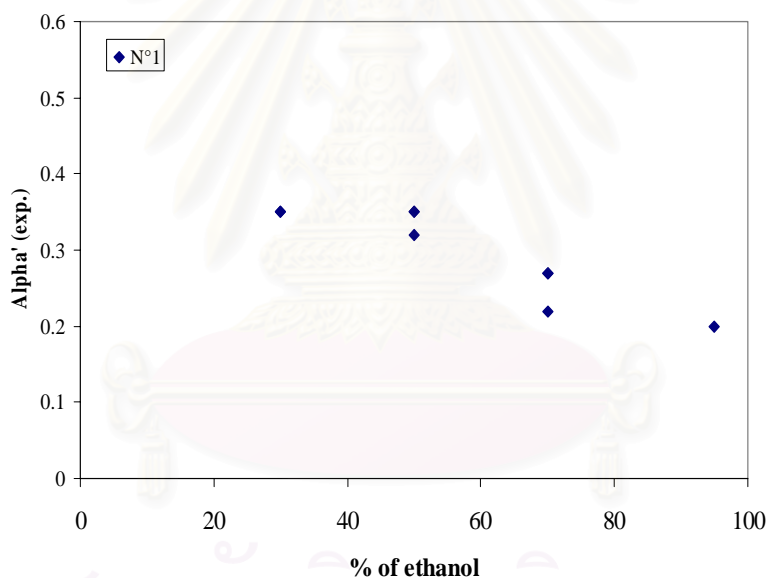


**Figure 4.16** Experimental results of  $\alpha'_o$  function of percentage of ethanol when the mass solid input is  $N^{\circ}1 = 11.33 \text{ g}/\text{min}$

**Figure 4.17** shows  $\alpha'_o$  as a function of mass solid inlet.  $\alpha'_o$  significantly increases with increasing mass solid inlet (initial level of liquid equals, to zero with the percentage of ethanol being 95%). When the mass solid inlet increases, the volume occupied by the solid at the top of the column increases and part of the volume is no larger in contact with the solvent. Consequently, the apparent efficiency of the separation decreases.

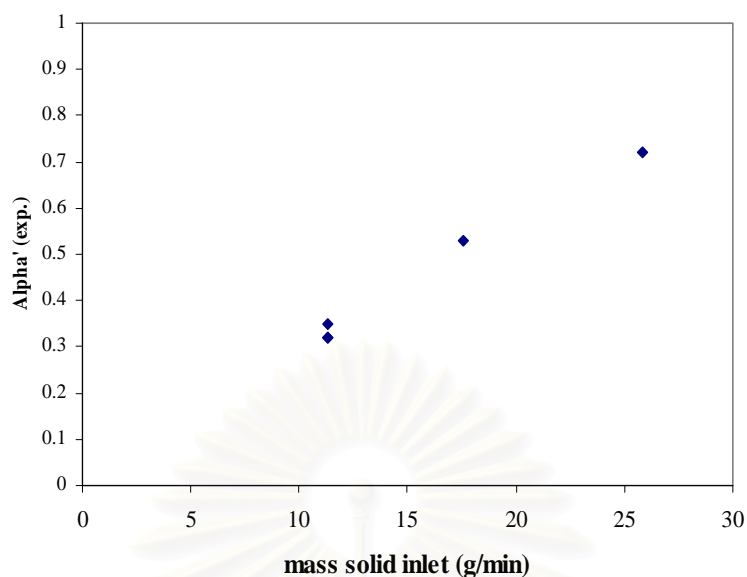


**Figure 4.17** The experimental results of  $\alpha_o'$  as a function of the mass solid inlet when the initial level of the liquid is at the first plate

**Figure 4.18** shows that  $\alpha_o'$  slightly increases with increasing liquid level. As the liquid level is above the first plate level, the solid feed stays in the liquid and thanks to the liquid the solid is removed from the column easily.

With the initial liquid level at the first plate, the liquid level will be below the first plate after the impulsion. Accumulated solids will then be stored on the plate. Therefore, when the next impulsion occurs, the solid that is accumulated on the disc prevents fresh solid from getting into the column. Consequently, most of the solid outlet due to the impulsion is the solid feed. That is the reason why the value of alpha is almost 0.8 when the feed flow rate is 25.85 g/min.

The appropriate level for the process should be to operate close to the Tee column and the amplitude of the impulsion should be small in order to purge the solid while minimizing solvent losses at the Tee column.

สถาบันวิทยบริการ  
จุฬาลงกรณ์มหาวิทยาลัย



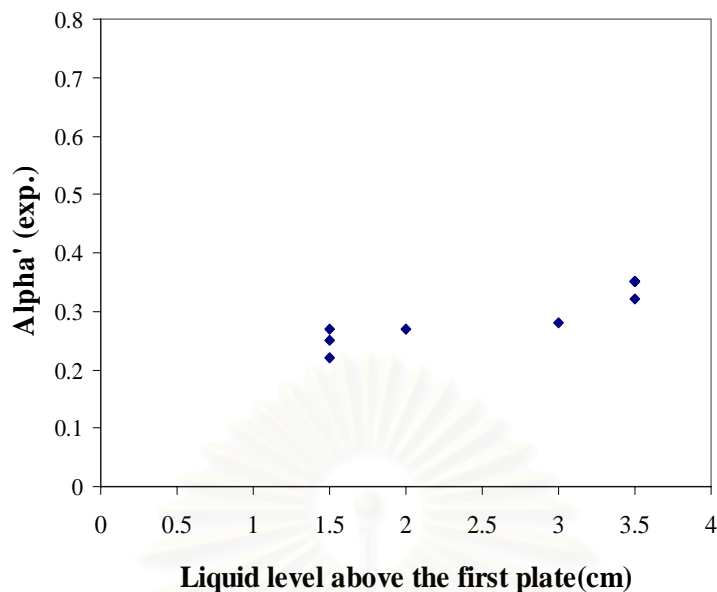


**Figure 4.18** Experimental results of  $\alpha_o'$  as a function of the initial liquid level

#### 4.2.2.3 Conclusions

During the experiments, we observed the behavior of the solid particles as a function of the percentage of ethanol.

1. The efficiency of separation is higher when using a higher percentage of ethanol.
2. For 95 percent of ethanol the sinking particles are mainly composed of leaves with some stem particles present.
3. For a percentage of ethanol smaller the 95 percent, the sinking part is only made up of leaves.
4. For a percentage of ethanol very much smaller the 95 percent, some leaves are present in the floating part.

However, it is quite difficult to determine accurately the value of  $\alpha_o'$  since the parameters are not measured directly from the experiments.

### 4.3 DYNAMIC EXPERIMENTAL RESULTS

This part deals with the characterization of the solid mass flowing inside the column (i.e. the active part of the column).

During these experiments the inlet liquid flow is turned on until the column is filled up with solvent and the level of the interface is then adjusted to a desired value. Then the pulsation and the inlet solid flow are started. The solid is fed into the column flowing currently with the ethanol solution. The measurement of the volume  $V_{SO}$  is done at the bottom of the column as a function of time. The relation between mass and volume (**Chapter 2.4.2**) is taken into account to obtain the mass solid outlet as a function of time.

#### 4.3.1 Typical experimental results

**Figure 4.19** shows a typical result from the experiment of solid mass at the bottom of the column  $m_{SO}$  as a function of time. The solid feed is interrupted at 23 min and started again at 37 min. The solid flow is measured until 53 min.

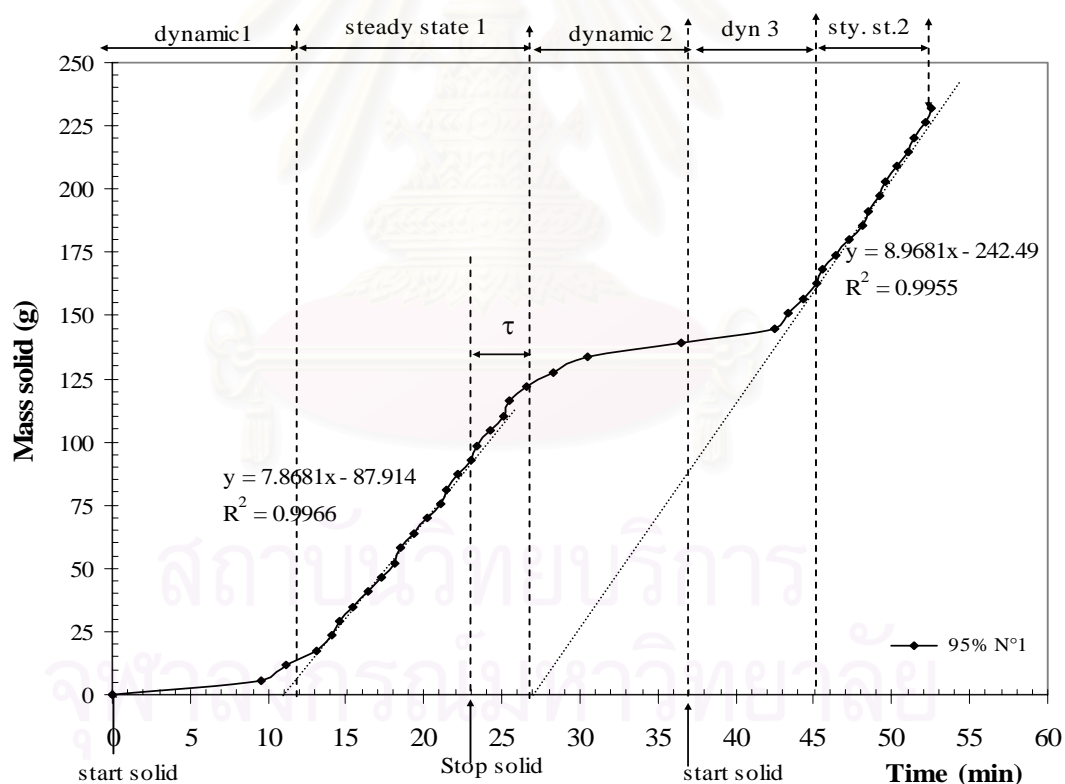


**Figure 4.19** A typical experiment showing mass solid outlet at the bottom of the column as a function of time

From this graph, it is possible to obtain information on:

- The solid mass outlet,
- The characteristic time of the dynamic state corresponds to the time when the solid feed inlet is started and the time at which the solid outlet flow rate is

considered as being constant (dynamic1 region and dynamic2 region in Figure 4.19).

- The accumulated mass is the mass of solid inside the column during the experiments. It is composed of two contributions:
  - A “dead mass” which stays all along the experiment on the discs and doughnuts,
  - A “moving mass” which goes down through the column,
- The mean residence time of the solid is directly derived from the time after which solid flow in is stopped until a plateau has been reached.

The data in Table 4.4 were estimated from Figure 4.19. The information on solid mass outlet, dynamic duration, accumulated mass, moving mass, dead mass and mean residence time will be detailed later. However, we can find the trend of the moving mass increasing with decreasing percentage of ethanol. It is expected that the dead mass should not vary so much at a constant solid input.

Exp. N°	$\dot{m}_{so}$ g.min <sup>-1</sup>	$\dot{m}_{so 2}$ g.min <sup>-1</sup>	Ethanol %	dynamic duration (min)		Accu. mass (g)	moving mass(g)	dead Mass (g)	$\tau$ (min)
				1	2				
1	8.83		95	11.0		99.37			
2	7.79	8.92	95	11.3	4.6	85.62	34.8	50.82	3.36
3	11.26		95	10.6		119.65	52.2	67.45	5.17
4	15.44		95	9.5		146.39	81.01	65.38	6.08
5	8.27	9.76	95	11.0	3.6	90.74	40.6	50.14	4.06
6	11.43		95	10.4		119			
7	7.96	8.12	70	13.8	6.4	110	46.4	63.6	6.1
8	10.39	11.94	70	13.5	3.9	115	52.2	62.8	
9	7.44	8.77	70	14.0	5.3	121.77			5.6
10	6.04	8.66	70	14.9	6.0	90.21	40.6	49.61	
11	5.94		50	19.2		94.02			8.8
12	8.04		50	18.4					
13	5.82	7.96	50	18.4	7.6	93.88	53.36	40.52	
14	4.45		30	20.9		64.06			
15	6.09		30	19.2		76.84			8.1

**Table 4.4** Estimated data from the graph of the mass solid outlet at the bottom of the column as a function of time

#### 4.3.2 Solid mass outlet

Figure 4.20 shows the rate of mass outlet of the solid at the bottom of the column  $\dot{M}_{so}$ , corresponding to experiments 2, 3 and 4 as a function of time. The rate of mass flow of solid increases with a mass solid feed increases.

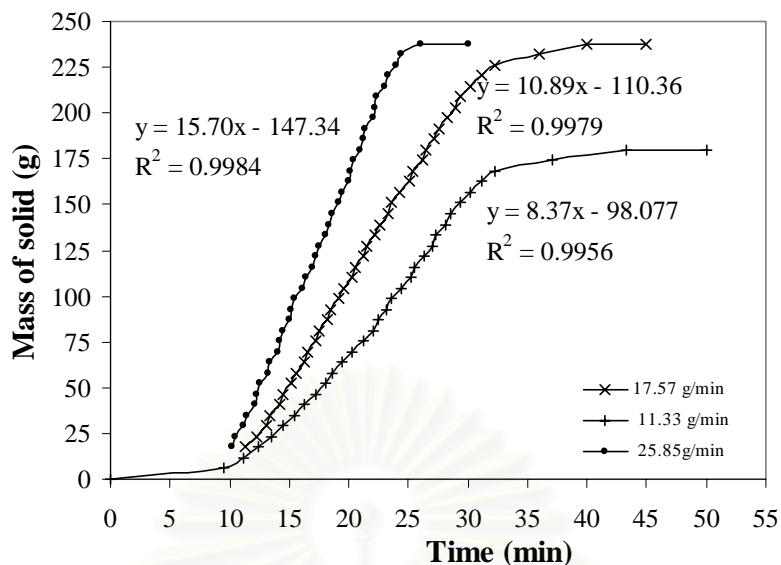


**Figure 4.20** The rate of mass out of the solid function of time for different mass solid input

#### 4.3.3 Transient regime (dynamic duration)

From **Figure 4.19** the dynamic duration is the time between start of solid flow until the solid outlet flow becomes constants. Dynamic duration1 is longer than dynamic duration2 because dynamic duration1 is the solid fill-up time in the column (on a disc and doughnut plate). Dynamic duration2 is the time after the solid is stopped, therefore excluding the effect of column fill-up.

**Figure 4.21** shows dynamic duration1 as a function of rate of mass solid flow at 95% ethanol which decreases as a function of rate of mass of solid flow at the outlet. It seems obvious that the transient regime is shorter when rate of solid mass flow increases.

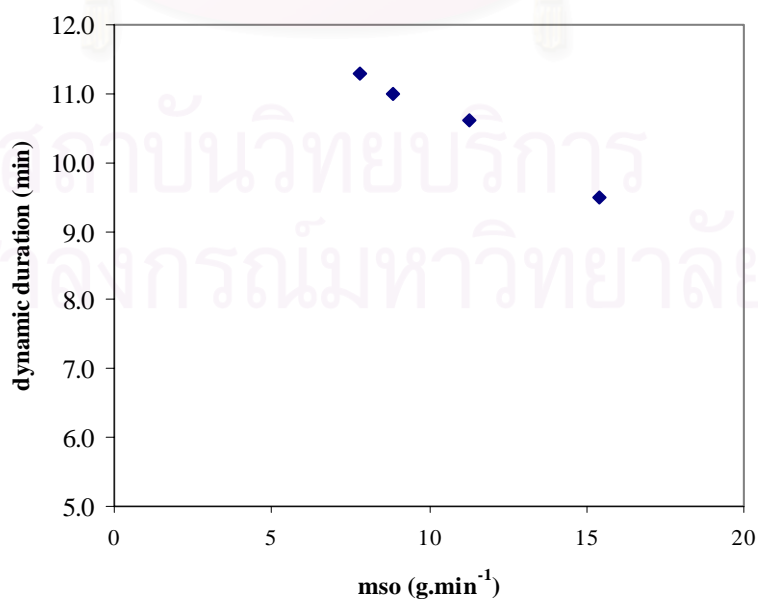


**Figure 4.21** The dynamic duration time function of mass solid outlet flow with 95% ethanol

Figure 4.22 shows dynamic duration as a function of percentage of ethanol at a mass solid inlet flow of  $11.3 \text{ g}\cdot\text{min}^{-1}$ . From the graph the dynamic duration decreases as percentage of ethanol increases.

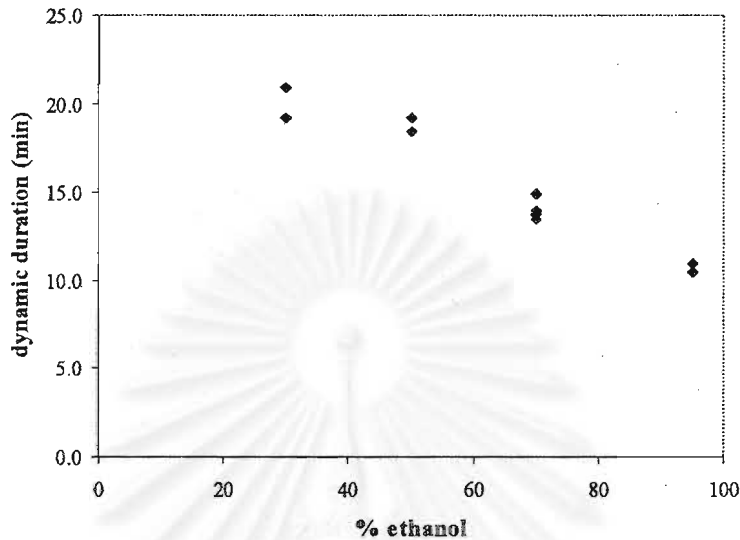


Figure 4.22 The dynamic duration time as a function ethanol concentration of a rate mass solid inlet of  $11.33 \text{ g}\cdot\text{min}^{-1}$

#### 4.3.4 Accumulated mass

The accumulated mass is the mass of solid which remains in the column during the experiment. The accumulated mass is composed of dead mass (the particle always stays on the disc and doughnut plate) and moving mass which is the mass of solid moving through the column.

Considering the accumulated mass with  $\dot{m}_{SO}$  instead of  $\dot{m}_{SI}$  as the experiment was measured at the bottom of the column, the accumulated mass can be calculated by:

$$m_{acc} = \dot{m}_{SO} \times \text{stop time} - m_{\text{stop time}} \quad (4.1)$$

$$m_{acc} = \text{dead mass} + \text{moving mass} \quad (4.2)$$

$m_{acc}$  : The accumulated mass,

$\dot{m}_{SO}$  : The mass flow solid at the bottom of the column,

$m_{\text{stop time}}$  : The mass at the stopped time.

The accumulated mass can be measured directly from the graph as shown in Figure 4.23.

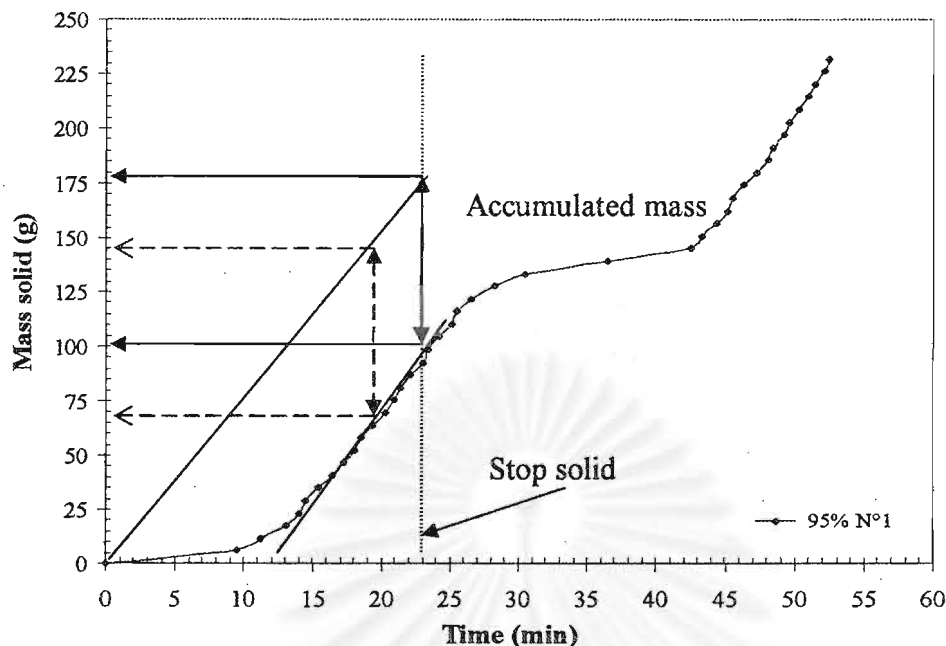


**Figure 4.23** The accumulated mass from the graph of rate of mass solid outlet at the bottom of the column  $\dot{m}_{SO}$  as a function of time

From equation 4.1, it is possible to calculate the accumulated mass as a function of time. **Figure 4.24** shows the accumulated mass function of time at 95% ethanol when changing the mass solid input (experiments 2, 3, 4, 5 in **Table 4.3**). From the graph, it is shown that the accumulated mass increases as the rate of mass solid input increases, as it is expected that the amount of solid that remains on the disc and doughnut plates is increasing.

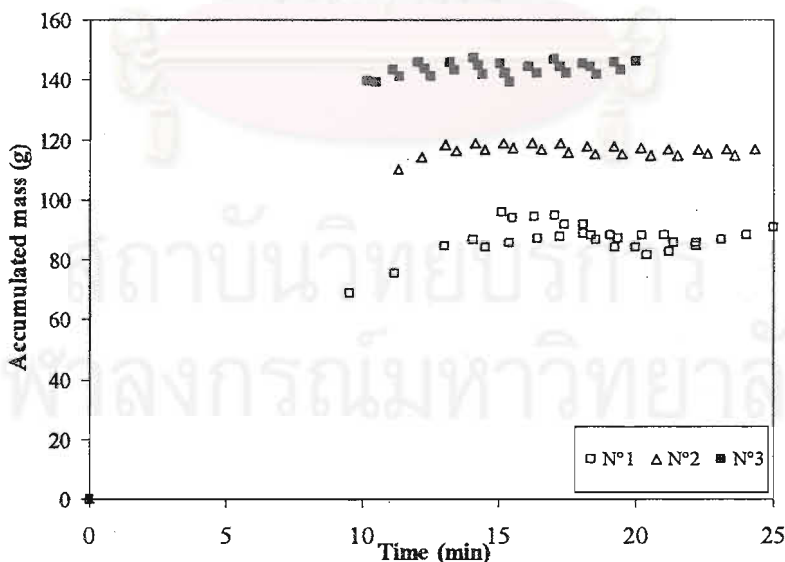


**Figure 4.24** The accumulated mass as a function of time when changing the mass solid input

**Figure 4.25** shows the accumulated mass as a function of time by varying the percentage of ethanol. The effect of the higher percentage of ethanol is that the separation of floating and sinking solid is better (**Chapter 2.4.1**). At identical solid

feed into the column, the amount of sinking solid is higher in the column when operating at 95%. On the other hand, the residence time of the solid particles when using 95% ethanol is smaller since the separation of the particle is better. **Figure 4.26** shows the mean accumulated mass of the solid in the column as a function of the percentage of ethanol. 70% ethanol operation corresponds to the highest value of accumulated mass.

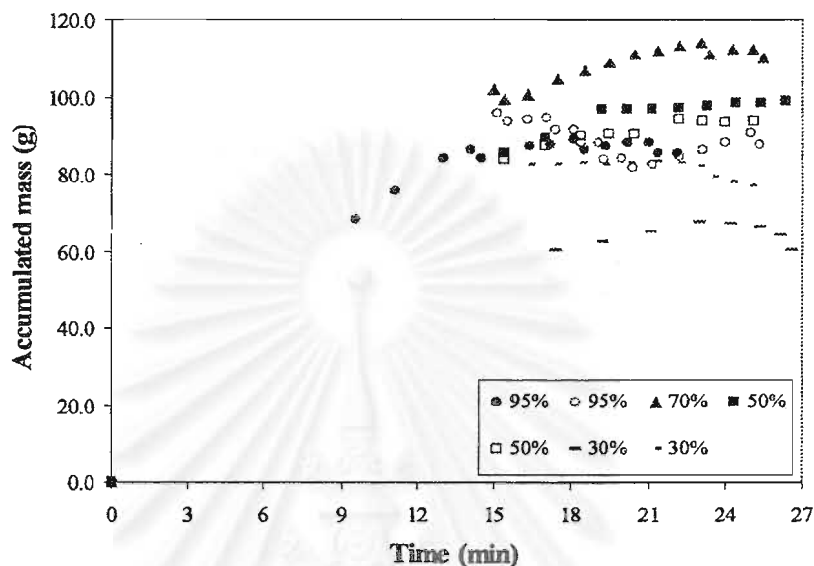


**Figure 4.25** The accumulated mass as a function of time  $m_{st}$  is  $11.33 \text{ g} \cdot \text{min}^{-1}$  with the percentage of ethanol as parameter

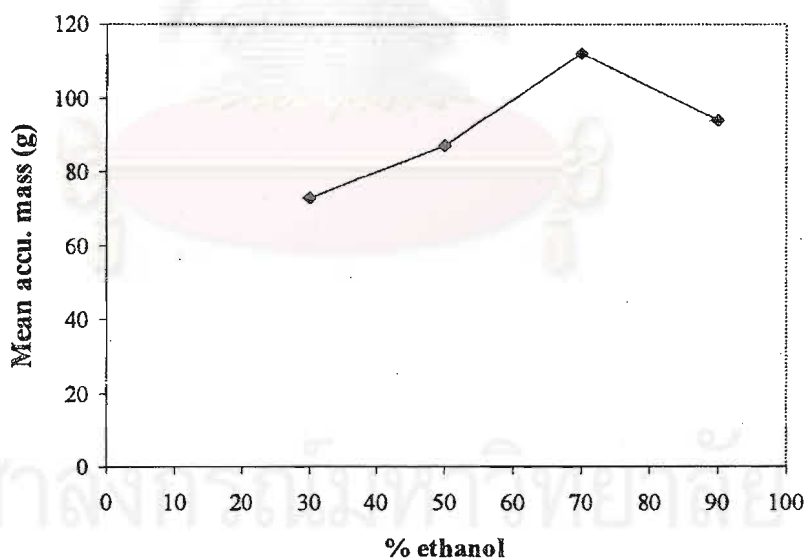


**Figure 4.26** The mean accumulated mass as a function of percentage of ethanol with the same mass solid input

**Figure 4.27** shows the mass solid outlet  $M_{so}$  as a function of time (experiments 9 and 10 in **Table 4.3**). The experiments were done with 70% ethanol, the rate of mass solid inlet being equal to  $11.33 \text{ g} \cdot \text{min}^{-1}$ , whereas the solid feed was stopped at 25 and 30 min for about 1 hr and 3 hours respectively without stopping the pulsation system and solvent flow. A few minutes, after the solid feed was stopped there was no more solid flow at the bottom of the column. This demonstrates the

presence of some accumulated solid mass always staying in the column. The residence time of the moving mass is about 5-6 min at a concentration of 70% ethanol.

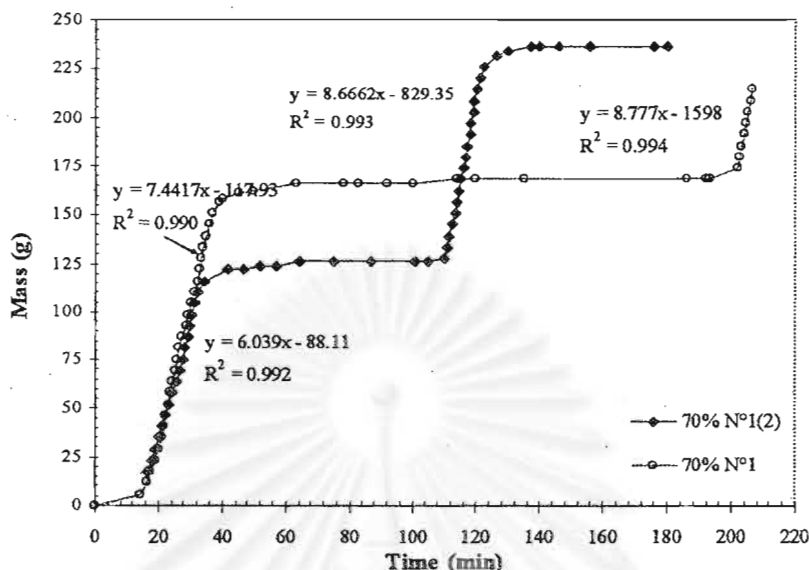


Figure 4.27 The mass solid outlet  $M_{SO}$  as a function of time using 70% ethanol

#### 4.3.5 Moving mass and dead mass

After the solid feed is stopped (Figure 4.2.8), there is a region until no more solid goes down through the column, this corresponds to the region steady state1 (after the solid feed is stopped) and dynamic2. This is a way to measure the moving mass.

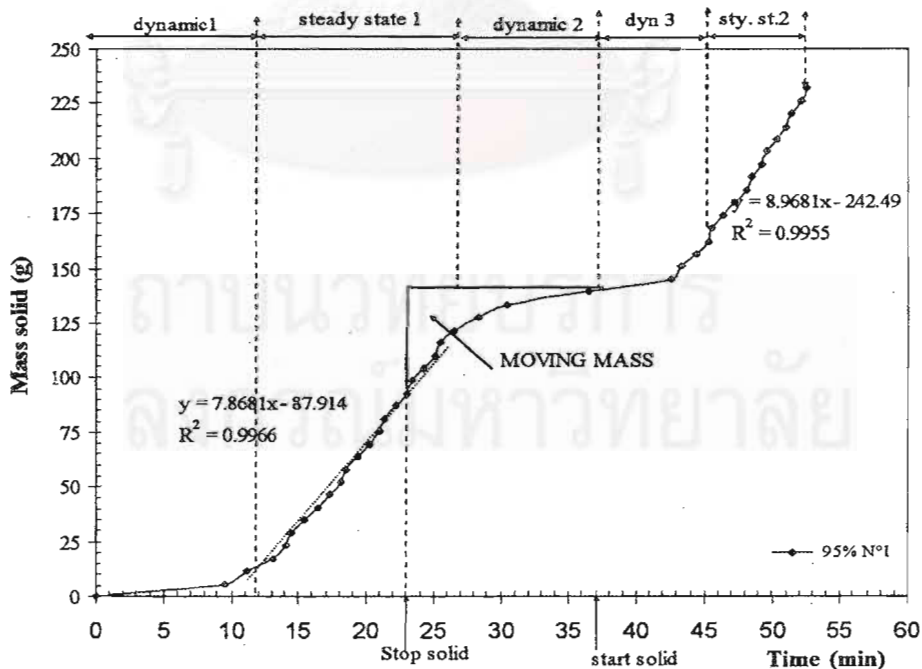


Figure 4.28 The moving mass from the graph of the mass solid outlet at the bottom of the column  $m_{SO}$  as a function of time



Figure 4.29 shows the mean moving mass as a function of mass solid flow at the outlet for 95% ethanol. The moving mass obviously increases with increasing mass solid input.

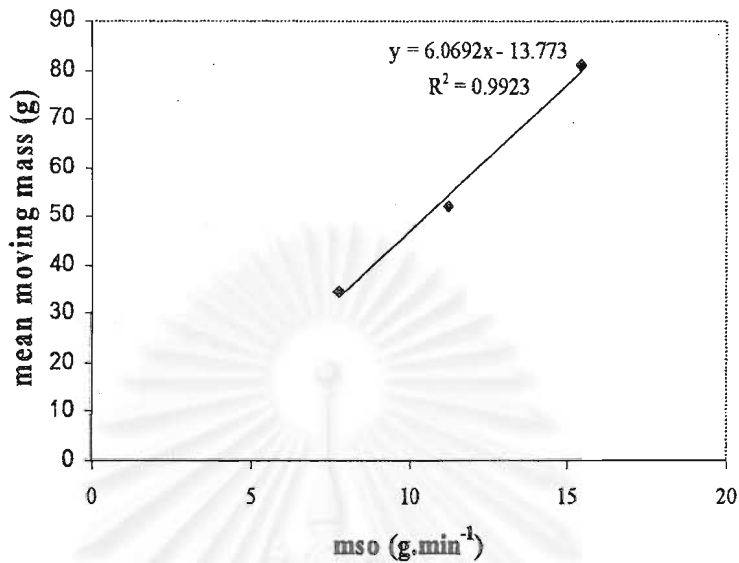


Figure 4.29 The mean moving mass as a function of mass solid flow at the outlet with 95% ethanol

Figure 4.30 shows the mean moving mass as a function of the percentage of ethanol at the same mass solid inlet. The moving mass decreases when the percentage of ethanol increases because the solid particle is very well wetted at higher percentages of ethanol.

The problem of floating particles is less difficult when working with higher percentages of ethanol. The experiment using 30% ethanol is quite difficult to analyze because at 30% ethanol flooding occurs with accumulation of the floating solids at the top of the column.

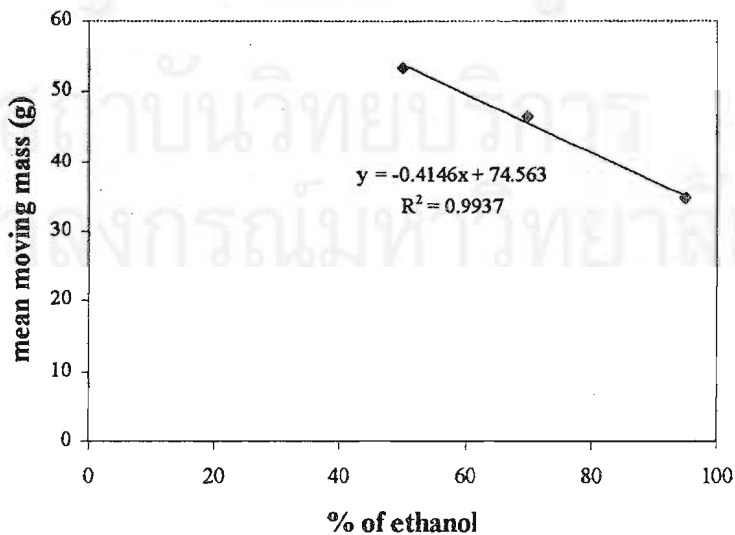
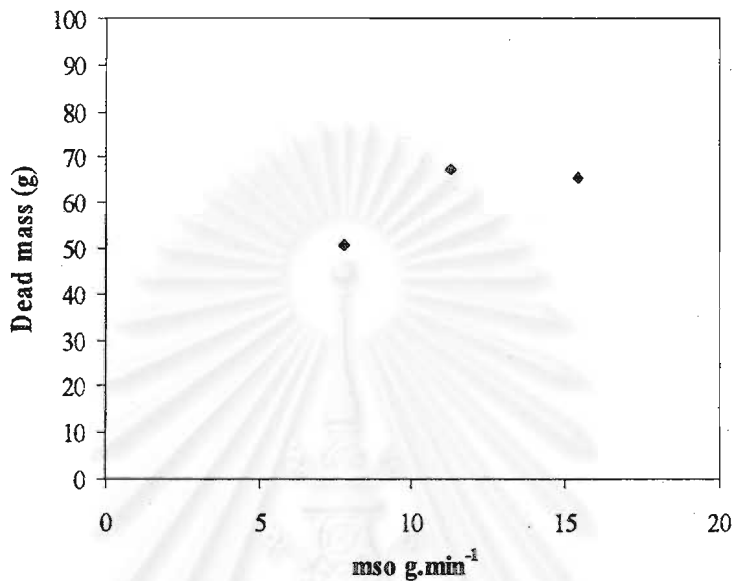


Figure 4.30 The mean moving mass as a function of percentage of ethanol  $m_{SI}$  is  $11.33 \text{ g.min}^{-1}$

As long as the accumulated mass and moving mass are determined, it is possible to estimate the dead mass. **Figure 4.31** shows the dead mass as a function of rate of mass solid outlet for 95% ethanol. The dead mass is more or less the same when the mass solid inlet varies from 17.57 to 25.85  $\text{g}\cdot\text{min}^{-1}$ . This indicates that the dead mass increases to a constant value even though the mass solid inlet increases further.



**Figure 4.31** The dead mass as a function of mass flow rate of solid outlet with 95% ethanol

**Figure 4.32** shows the dead mass as a function of ethanol percentage at the same  $\dot{m}_{SI}$  equal of 11.33  $\text{g}\cdot\text{min}^{-1}$ . The dead mass does not significantly depend on the percentage of ethanol.

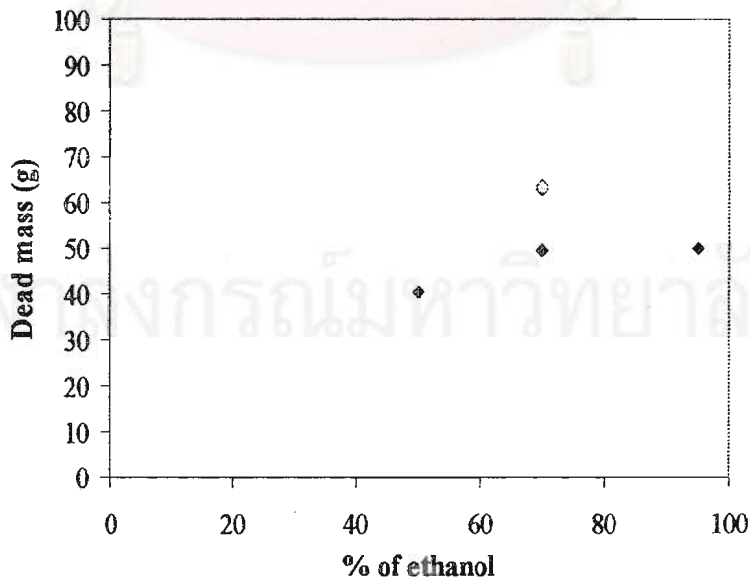


**Figure 4.32** The dead mass as a function of percentage of ethanol  $\dot{m}_{SI} = 11.33 \text{ g}\cdot\text{min}^{-1}$

### 4.3.6 Mean residence time

Figure 4.33 shows an example of characterization of the mean residence time from the mass flow rate of solid at the outlet as function of time.

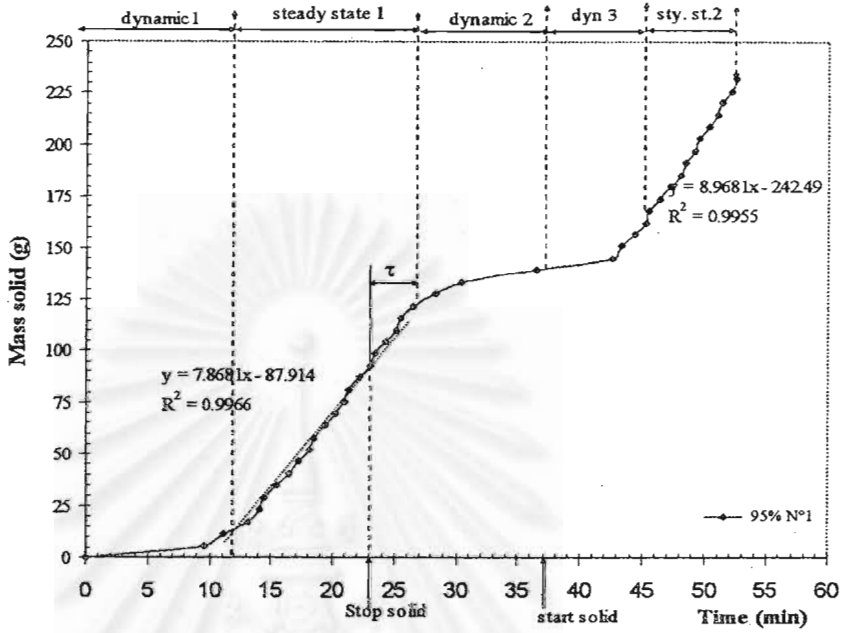


Figure 4.33 The mean residence time from the graph of the mass flow rate solid at the outlet at the bottom of the column  $\dot{m}_{SO}$  as a function of time

Figure 4.34 shows the mean residence time as a function of mass flow rate of solid at the outlet for 95% ethanol. The mean residence time increases when the mass flow rate of solid at the inlet increases.

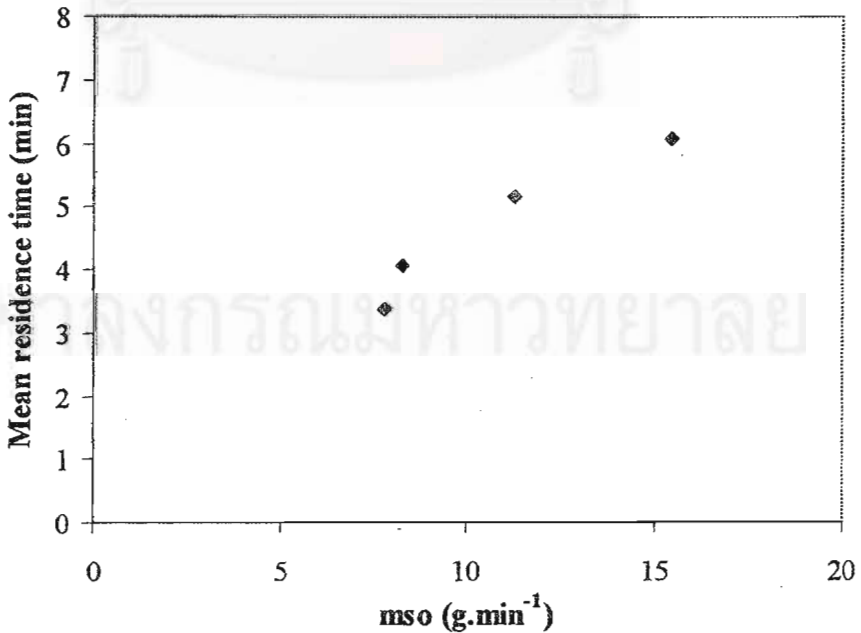


Figure 4.34 The mean residence time as a function of mass flow rate of solid at the outlet for 95% ethanol

Figure 4.35 shows the mean residence time as a function of percentage of ethanol for  $\dot{m}_{SI} = 11.33 \text{ g}\cdot\text{min}^{-1}$ . The mean residence time decreases when the percentage of ethanol increases, always for the same reason since the solid particle sinks very well at high percentage of ethanol.

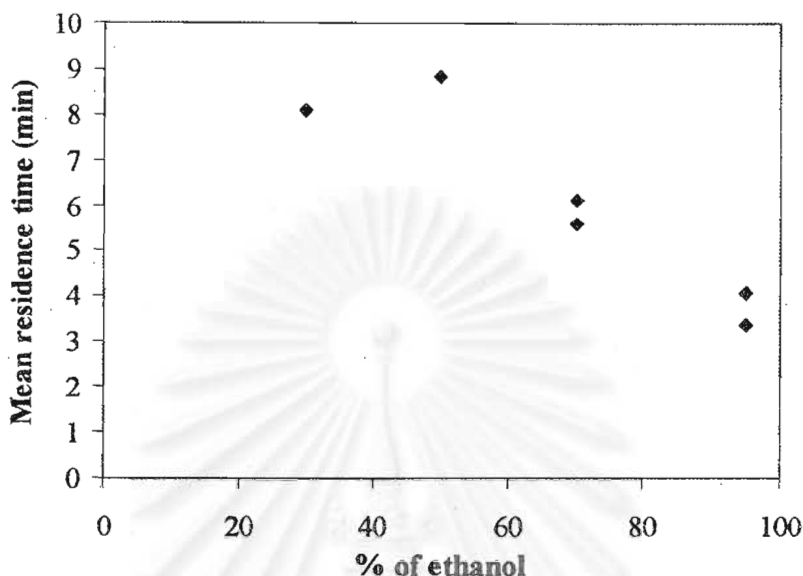


Figure 4.35 The mean residence time as a function of percentage of ethanol for  $\dot{m}_{SI} = 11.33 \text{ g}/\text{min}$

From the kinetics experiments it has been shown that the higher percentages of ethanol result in higher extracted andrographolide. Furthermore, it is expected that, the higher the contact time, the better the extraction yield. But, the residence time when using 95% ethanol is the smallest compared to 70%, 50% and 30 % ethanol respectively, because most of particles sink quickly down to the bottom of the column.

#### 4.4 EXTRACTION YIELDS AND RESIDENCE TIMES

The operating conditions of the extraction experiments with 95% ethanol are as follows:  $\dot{V}_L = 0.52 \text{ l}/\text{min}$ ,  $\dot{m}_L = 420 \text{ g}/\text{min}$ ,  $\dot{m}_{SI} = 11.33 \text{ g}/\text{min}$ , density,  $\rho = 810 \text{ g}/\text{cm}^3$ . The initial level of the liquid was 3 cm from the first disc. 2 samples were taken using the valve at the middle and at the bottom of the column at various times. The distance between the two valves was 130 cm. After sampling the solute was analyzed using the HPLC.

Since the solubility of the andrographolide presents no problems, it is possible to recycle the ethanol solvent. Figure 4.36 shows the andrographolide concentration as a function of time for 95% ethanol. The first experiment was completed within 2 hours. The same operating conditions were reproduced and presented in Figures 4.37 and 4.38 respectively with the recycling of the 95% ethanol.

Figures 4.36, 4.37 and 4.38 show the andrographolide concentrations at the middle and at the bottom of the column. The concentration profile increases at the beginning which corresponds to the solid filling up in the column as well as the

accumulation of solid on the discs and doughnuts plates (accumulated mass). Then, the concentration decreases until a plateau is reached, the dead mass being present and the residence time of the moving mass being of a few minutes. Obviously, the solute concentration is higher at the bottom than at the middle.

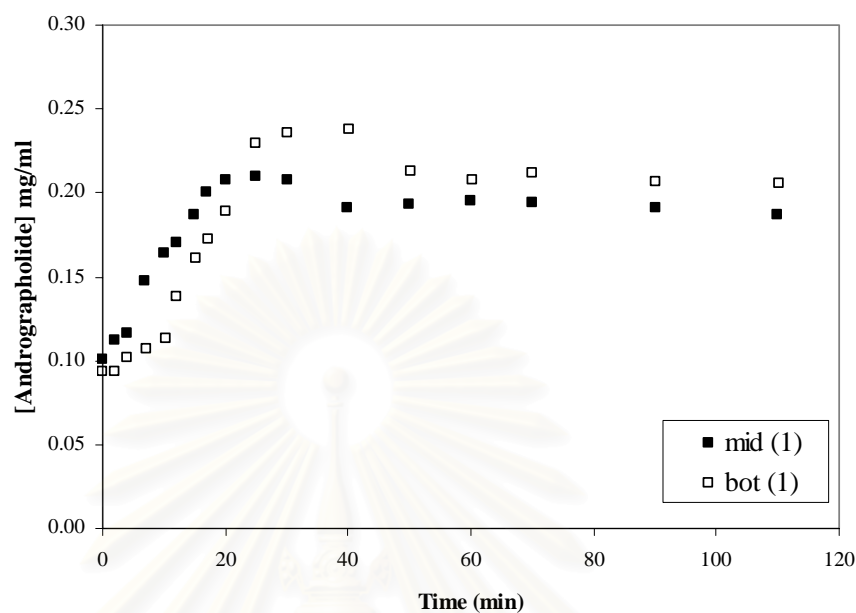


**Figure 4.36** The andrographolide concentration as a function of time with the recycled 95% ethanol

The rich solvent is then used for the next experiments (**Figures 4.37 and 4.38**). The used solvent is well mixed before being used again.

Due to the absorption by the solid, we have noticed that there is some loss of solvent. The curves and the conclusions from **Figures 4.37 and 4.38** are similar to those derived from **Figure 4.36**.

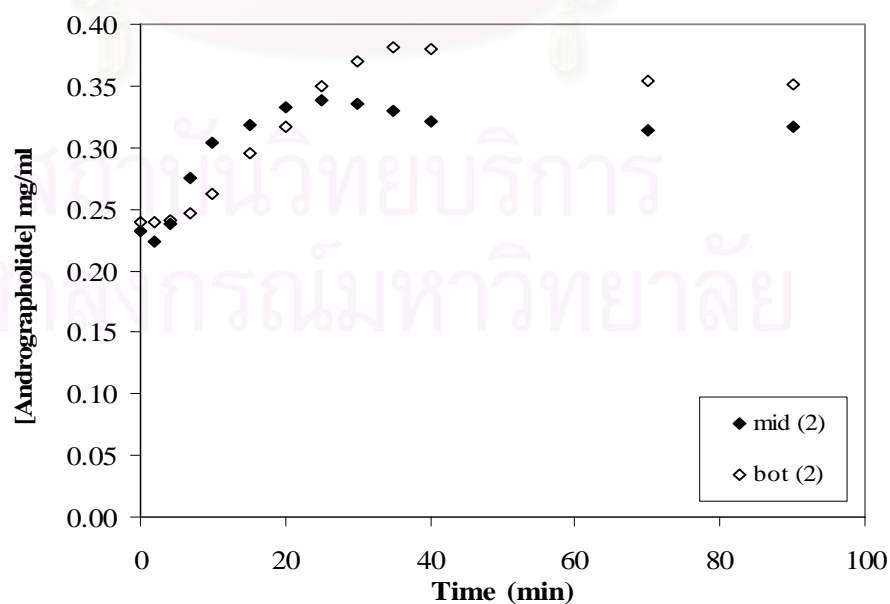


**Figure 4.37** The andrographolide concentration as a function of time with the recycled 95% ethanol

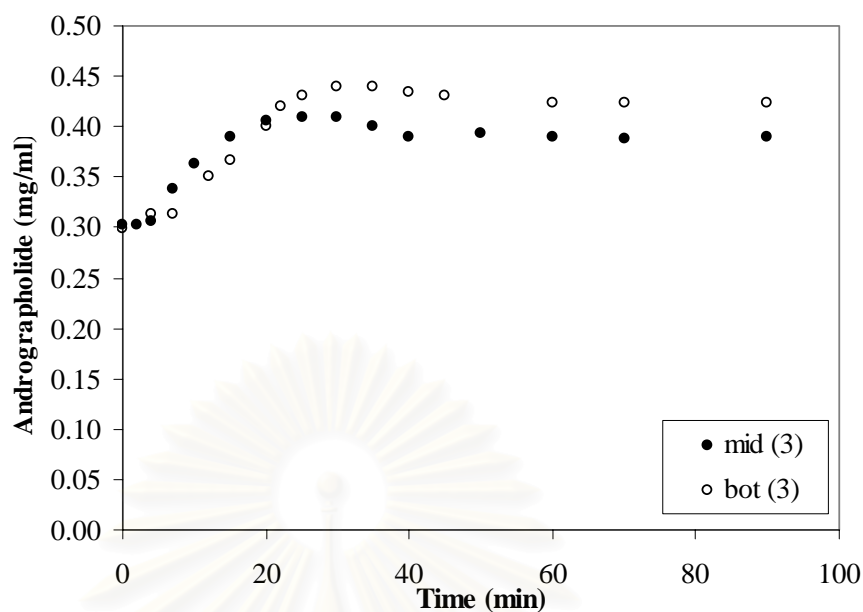


**Figure 4.38** The andrographolide concentration as a function of time with the recycled 95% ethanol

**Figures 4.39** and **4.40** summarize the andrographolide concentrations respectively at the middle and at the bottom of the column as a function of time. The final concentration is 0.087 mg/ml and 0.112 mg/ml, at the middle and at the bottom of the column respectively.

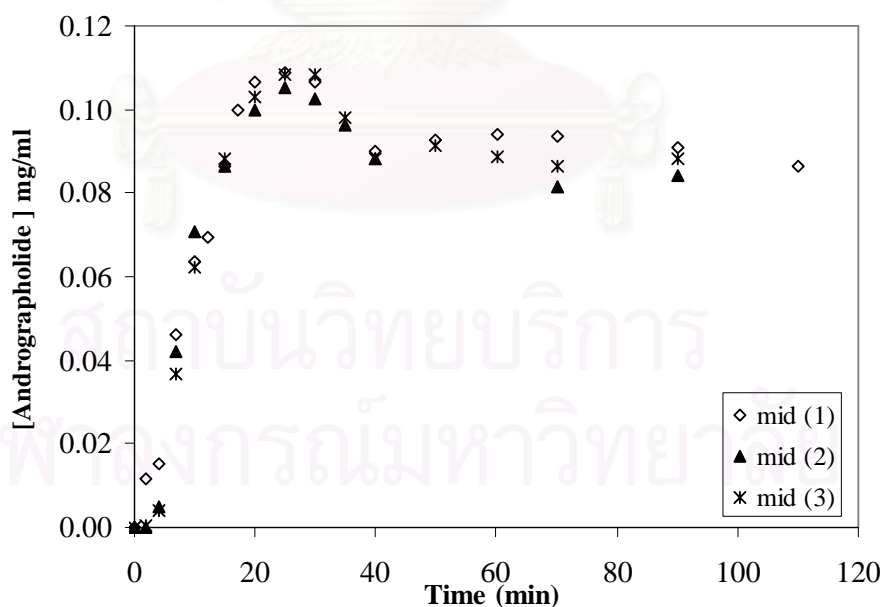


**Figure 4.39** The andrographolide concentration at the middle of the column as a function of time

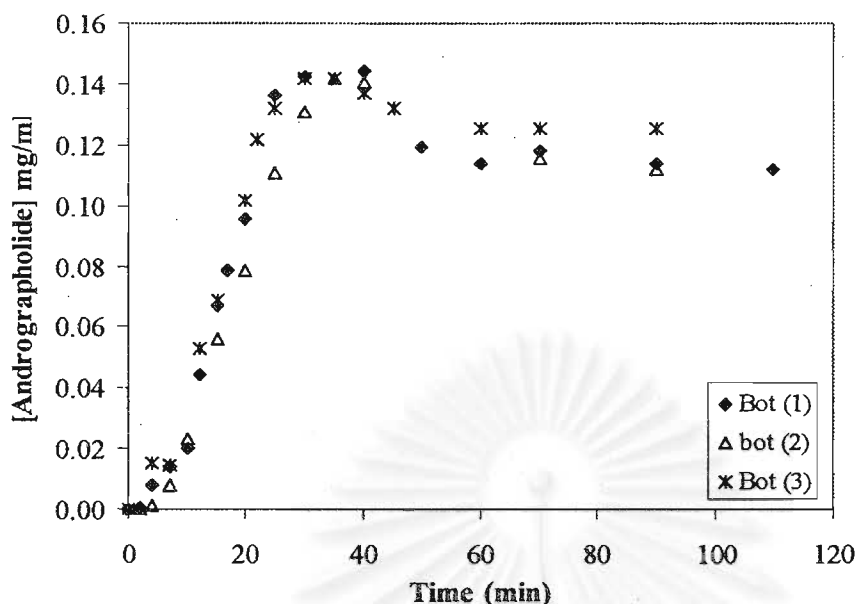


Figure 4.40 The andrographolide concentration at the bottom of the column as a function of time

We have now calculated the percentage of extraction and compared the results with the percentage of extraction in the batch experiments obtained in the Chapter II.

$$\dot{m}_{Andro} = Q_L \cdot C_A \quad \text{in liquid phase} \quad (4.3)$$

$$\dot{m}_{Andro} = Q_S \cdot C_i \quad \text{in solid phase} \quad (4.4)$$

$$\% \text{ of extraction} = \frac{\dot{m}_{Andro} \text{ (in liquid phase)}}{\dot{m}_{Andro} \text{ (in solid phase)}}$$

Table 4.5 shows that the percentage of extraction is about 30 percent for a 4 min residence time in the column (Table 4.4). This yield has to be compared with the batch experiment corresponding to 3-4 min. The results show that the extraction yield in the column is as efficient as in the batch experiments. The column can be considered as a fairly good plug flow. If one intends to increase the column performance, one has to increase the column height.

Exp N°	[Andro.] mg/ml		Andro. flow (g/min)		% extraction in the column		$\tau$ (min) comparing in batch experiment	
	Mid.	Bot.	Mid.	Bot.	Mid.	Bot.	Mid.	Bot.
1	0.087	0.112	45.24	58.24	22.18	28.56	< 2	3-4
2	0.084	0.112	43.68	58.24	21.42	28.56	< 2	3-4
3	0.088	0.126	45.76	65.52	22.44	32.13	< 2	3-4

Table 4.5 The residence time of the solid in the middle and at the bottom of the column

The parameters use are as follows:

$Q_L$  : The liquid flow rate (0.52 l/min),

$Q_S$  : The solid flow rate (11.33 g/min),

$\dot{m}_{Andro}$  : Mass flow of andrographolide in solid phase 203.94 mg/min,

$C_A$  : Concentration of andrographolide in liquid phase (0.087 and 0.112 mg/ml at middle and the bottom of the column respectively),

$C_i$  : Initial concentration of andrographolide when using 95% ethanol in batch experiment ( 18 mg of andrographolide/g of solid) **Figure 2.32 Chapter II**,

$\dot{m}_{Andro}$  : Mass flow rate of andrographolide in liquid phase 58.24 mg/min,

$\tau$  : Residence time (min).

## CONCLUSION

This chapter has presented the continuous process for extraction in a pulsed column with a pneumatic pulsation system.

The air pulsating system allowed changes the regular sinusoidal agitation. This system is more flexible and less energy consuming than a mechanical piston pulsation. The separation of the floating and sinking solids at the top of the column was studied and the results are encouraging. The problem of flooding due to floating particles can be solved using the method devised.

The hydrodynamic behaviour of the sinking particle strongly depends on the ethanol solvent. The residence time in the column is about 4 min in the 2.5 m column. In order to obtain a larger residence time, a longer column should be used.

In the next chapter, we will study extraction using a twin screw extruder, which can be also used for continuous solid-liquid extraction purposes. We will mention also some optimization of the operating conditions in the extraction column.

สถาบันวิทยบริการ  
จุฬาลงกรณ์มหาวิทยาลัย



## CHAPTER V

### TWIN SCREW EXTRUDER AND OPTIMIZATION

#### INTRODUCTION

This chapter is separated into two parts.

The first part is devoted to extraction studies performed with a twin-screw extruder, widely used in the food industry. This apparatus leads to physical and chemical transformations in one step of many plant materials. In this part, we are interested in the extraction of andrographolide from *Andrographis paniculata*, aiming to understand the operating principle and to compare the andrographolide extraction yields with those of the batch experiments. This study has to be considered as an alternative extraction method from the pulsed column.

The second part is focused on the optimization and on the global design of the extraction column. The information on the moving mass, accumulated mass, residence time and the rate of extraction are taken into account. These parameters allow the calculation of the optimal parameters of extraction.

The aim is to be able to compute the extraction yield with a simple approach.



สถาบันวิทยบริการ  
จุฬาลงกรณ์มหาวิทยาลัย

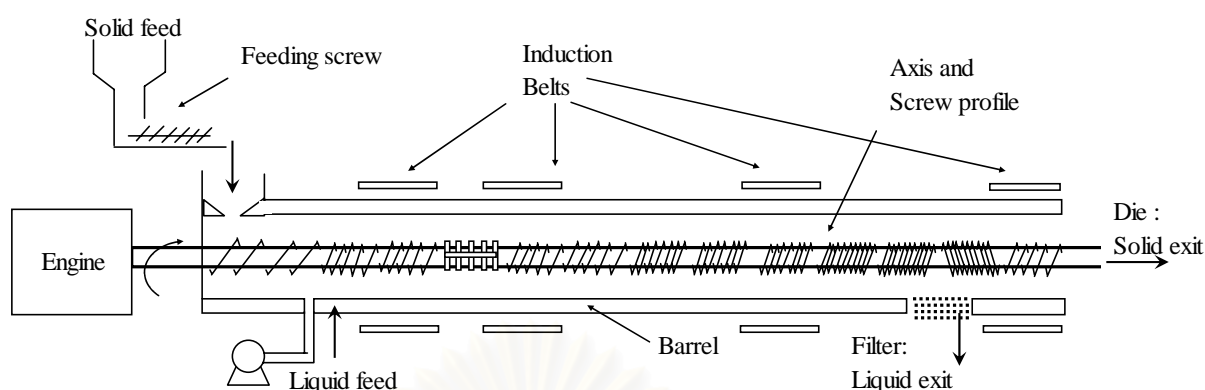
## 5.1 TWIN-SCREW EXTRUDER

The twin-screw extruder (TSE) is used as a thermo-mechano-chemical reactor. The plant material goes through a series of interrelated chemical and physical changes during its passage through the shearing and heating zones of the extruder. This system is suited for a range of mixing and extruding applications that are extended to many industries such as polymer modification and alloying, powder coating, catalytic reactive extrusion, polymer additive, pharmaceutical and agro-industry (Altomare, 1986; Isobe, 1992). The ability of TSE to carry out extraction and chemical reaction in a single continuous reactor makes TSE very valuable for the valorisation of agro-resource wastes (Rigal, 1996). The advantage of TSE is to obtain higher extraction efficiencies from plant materials. The use of TSE reduces contact time compared with a batch reactor such as in the case of the extraction of hemicelluloses that reaches 90% of maximum extraction (N'diaye, 1996). In addition, the liquid-solid ratio is six times less than with a batch reactor and the solid reaction time is much lower (N'diaye, 1996). We thought it would be valuable and of interest to perform the experiments on the plant extraction process with a TSE.

Prat (1998) proposed a description of the operation of the TSE for two phase processes, focusing on Residence Time Distributions (RTD) of the phases and on the relative contribution of the screw elements to the RTD under the influence of the operating parameter (feed rates, screw rotational speed, solvent concentration). In 2001, L. Prat presented one dimensional model for the solid transport along the TSE and a kinetic description of the solubilization process which was established from batch experiments.

In the present work, the application is the extraction of andrographolide from the *Andrographis paniculata* with ethanol as a solvent. We aim now to understand the principle of the twin screw extruder system and to compare the extraction result with the batch extraction experiments.

**Figure 5.1** shows the global process of a twin-screw extruder. The machine consists of a seven to eight-shaped elements barrel enclosing two corotating intermeshing screws. Four sections (B, C, E and G) heated by induction belts and cooled by water circulation. The 0.7 m long barrel, Four different kinds of elements is used in the axis profile: T2F (trapezoidal two-flight screw), C2F (two-flight screw), BB (bi-lobe kneading element) always positioned with a 90 degree shift and C2FC (reversed two-flight screw element). 50 mm length elements were used. The solid (plant) and liquid (ethanol solvent) are fed into the barrel by the first transport screws and are mixed together in the transport and kneading elements (BB). As the liquid is absorbed by the plant, the solute is liberated from the solid. Furthermore, reversed transport screw elements (RSE) cause severe compression of the plant material and allow the separation of the two phases. The liquid phase is then retrieved through a barrel filter located just up-stream from the RSE. The temperature is regulated with induction belts and cooled by water circulation. The filter element added at the end of the barrel extracts the liquid phase from the slurry.



	A		B		C		D		E		F		G	
Type	T2F	T2F	C2F	C2F	BB	C2F	C2F	C2F	C2F	C2F	C2F	C2F	C2FC	C2F
Pitch (mm)	50	50	33	33	25	100	33	25	25	25	16	16	-16	33
Length (mm)	50	50	50	50	50	50	50	50	50	50	50	50	50	50
Mixing	+	+	+	+	++++	+	+	+	+	+	+	+	++++	+
Shearing	+	+	+	+	0	+	+	+	+	+	+	+	++++	+
Conveying	+++	+++	+++	+++	+++	+++	+++	+++	+++	+++	+++	+++	---	+++

**Figure 5.1** Global process of the twin screw extruder

## 5.2 EXPERIMENT

The objective of the experiments was to evaluate the advantages of using a TSE for andrographolide extraction. The study is then not a complete study on the influences of the parameters. However, our aim was to study qualitatively the key-points of this technology.

### 5.2.1 Twin-screw extruder

Experiments were performed using the screw profile represented in **Figure 5.1**. This configuration was tested for our experimental investigation of the plant without any plugging or clogging at the counterscrew and with the solid extrudated obtained at the die being as dry as possible while the liquid filtrate was almost free of suspended solids.

The plant material is first conveyed and heated using a decreasing pitch screw in order to compact it, to remove air, then the ethanol solution was fed in the machine. The ethanol was carried out by the bilobal and excentric kneading paddles, respectively. Most of the mechanical effect is due to the reverse screw element which also forces the liquid phase through the filter.

The experiments were done with a 95% ethanol solution injected at a single point using a volumetric pump. The plant material was fed via a feeding screw at a constant flow rate (2.85 kg/h). The experiments temperature was 30°C. All data were taken 10 min after a steady state was reached.

The liquid and solid rates at the exit of the reactor were measured for every experiment and the samples of extracted solid were analyzed. The first experiments were done for a liquid/solid (L/S) ratio of 4, then we tried to decrease the liquid/solid ratio.

**Table 5.1** presents the operating conditions in terms of liquid/solid ratio (L/S), screw rotational speed  $N$ , solid feed inlet  $S_I$ , liquid feed inlet  $L_I$  etc.

Experiment N°	1	2	3	4	5
L/S	4	4	3	2	2
$N$ (rpm)	100	200	200	200	250
$S_I$ inlet (g/hr)	2850	2850	2850	2850	2850
$L_I$ inlet (g/hr)	11400	11400	8600	5700	5700
Response					
Time (min)	10	10	10	10	10
So outlet (g/hr)	x	1680	1740	x	1710
Lo outlet (g/hr)	x	12400	9500	x	6700

**Table 5.1** Operating data of the experiments conducted with the twin screw extruder

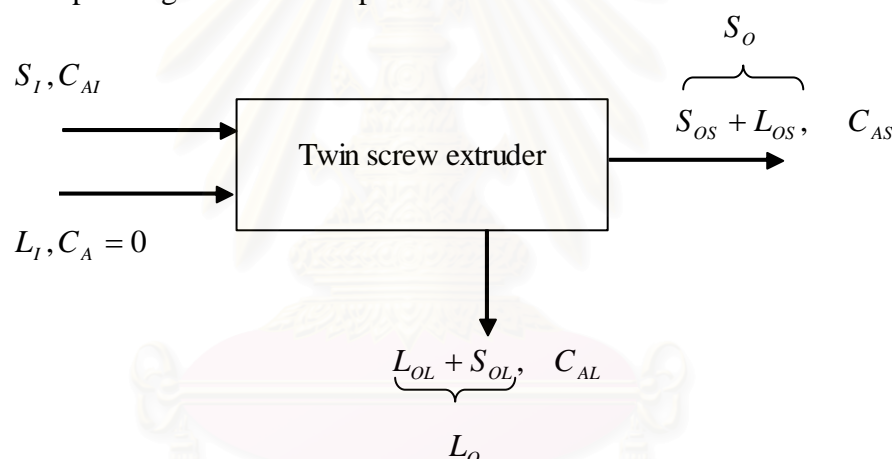


**Figure 5.2** The mass balance on the twin screw extruder

The parameters are as follows:

- $S_I$ : Solid feed inlet,
- $S_o$ : Solid and liquid outlet at the solid phase,
- $S_{OS}$ : Solid outlet at the solid phase,
- $S_{OL}$ : Solid outlet at the liquid phase,
- $L_I$ : Liquid feed inlet,
- $L_o$ : Liquid and solid outlet at the liquid phase,
- $L_{OL}$ : Liquid outlet at the liquid phase,
- $L_{OS}$ : Liquid outlet at the solid phase,
- $C_{AI}$ : Initial concentration of the andrographolide in the solid phase,
- $C_A$ : Initial andrographolide concentration in the liquid phase,

$C_{AS}$  : Andrographolide concentration in the solid phase,

$C_{AL}$  : Andrographolide concentration in the liquid phase,

$$\text{Global mass balance} \quad L_I + S_I = L_O + S_O \quad (5.1)$$

Partial mass balance

$$S_I \cdot C_{AI} + L_I \times 0 = (S_{OS} \times C_{AS} + L_{OS} \cdot C_{AL}) + (S_{OL} \times C_{AS} + L_{OL} \times C_{AL}) \quad (5.2)$$

$$S_I \cdot C_{AI} = S_O [(1-h)C_{AS} + hC_{AL}] + [S_I - S_O(1-h)]C_{AS} + [L_I - S_O h] \cdot C_{AL} \quad (5.3)$$

Where  $h$  : % humidity of solid outlet,  $L_{OS} = h(S_O)$ .

At the solid phase outlet,  $S_O$  was composed mostly of the solid  $S_{OS}$  and some of the liquid phases  $L_{OS}$  which was absorbed in the solid. In order to measure each respective phase, the following experiment was done: some sample of the solid outlet was separated into two parts. The first part was put in an oven at 70 °C within 24 h in order to determine the percentage humidity of the plant and the solid mass outlet  $S_{OS}$ . Then this allowed  $L_{OS}$ . The second part was put into a batch reactor with the ethanol solution within 24 hours in order to find the concentration of andrographolide in the solid phase outlet  $C_{AS}$ .

At the liquid phase outlet,  $L_O$  contained the liquid phase  $L_{OL}$  and some of the solid phase  $S_{OL}$ . During the experiment we observed that there is done solid phase in the liquid phase outlet. The amount of the solid phase in the liquid outlet was non negligible.  $S_{OL}$  and  $L_{OL}$  were calculated from the mass balance (**Table 5.2**). The sample of liquid phase was analyzed with an HPLC to determine the andrographolide concentration in the liquid phase  $C_{AL}$ .

**Table 5.2** shows the extraction yield obtained in the twin screw extruder. It allowed an extraction of 77% of the initial andrographolide with a liquid-solid ratio equal to 2. The residence time of the twin screw extruder is about 1 min with has to be compared which a batch of experiment 50 min yielding an 76.81% extraction! Moreover, the liquid/solid separation is more efficient in the case of the extruder.

The advantage of the TSE in comparison with the batch system is the fact that the extraction in an extruder is not controlled by mass transfer. The destructuring effects due the mechanical process prevail. The main benefit of the twin-screw extruder is that extraction and liquid/solid separation can be managed simultaneously in a very efficient manner. However, the cost of a TSE machine is very high in comparison with batch experiment equipment, and furthermore productivity is higher with a TSE.

Experiment N°	Measurement			Calculation		
	2	3	5	2	3	5
$S_I$ (g/hr)	2850	2850	2850	-	-	-
$L_I$ (g/hr)	11400	8600	5700	-	-	-
$C_{AI}$ (mg/g solid) Soxhlet	25-30	25-30	25-30	-	-	-
	Solid phase outlet					
$S_o = S_{os} + L_{os}$ (g/hr)	1680	1740	1710	-	-	-
$L_{OS} = h \cdot S_O$ (g/hr)	-	-	-	494.26	528.44	572.17
$S_{OS} = S_O(1-h)$ (g/hr)	-	-	-	1185.74	1211.56	1137.83
% humidity	29.42	30.37	33.46	-	-	-
$C_{AS}$ (mg/g solid) Batch	13.12	11.13	7.16	-	-	-
	Liquid phase outlet					
$L_O = L_{OL} + S_{OL}$ (g/hr)	12400	9500	6700	-	-	-
$S_{OL} = S_I - S_{OS}$ (g/hr)	-	-	-	1664.26	1638.44	1712.17
$L_{OL} = L_O - S_{OL}$ (g/hr)	-	-	-	10735.74	7861.56	4987.83
$CA_L$ (mg/ml)	3.19	6.17	12.07	-	-	-
$CA_L$ (g andrographolide)	-	-	-	34.25	48.51	60.20
Mean $CA_I$ (g andro initial)	78.38	78.38	78.38			
% mean extraction yield				<b>43.69</b>	<b>61.89</b>	<b>76.81</b>
	Extruder			Batch reactor		
Time in batch reactor (min)	≤1	≤1	≤1	<b>12</b>	<b>25</b>	<b>50</b>

**Table 5.2** Extraction yields from the twin screw extruder process

**Table 5.3** shows the global mass balance relative to the solid in the twin-screw extruder. Both solid phase outlet  $S_O$  and liquid outlet  $L_O$  were obtained from the experiments. From the table, the solid and liquid mass flow rate inlet equal to the solid and liquid mass flow rate outlet. However, there are some solid losses during the experiment.

There are many parameters influencing the partial mass balance. The initial concentration of andrographolide in the plant ( $C_{AI}$ ) was obtained using 10 g of solid sample with 500 ml of 95% ethanol in the soxhlet experiments. The andrographolide concentration can be varied from 0.5-0.6 mg/ml of ethanol or 25-30 mg/g solid, since the solid sample is composed of stems and leaves, with totally different concentration. The inlet mass was obtained by using the mean  $C_{AI}$  (27.5 mg/g).

Global mass balance (g/hr)	Inlet			Outlet		
	$S_I + L_I$			$S_O + L_O$		
	14250	11450	8550	14080	11240	8410
% error				1.19	1.83	1.64
Partial mass balance (g/hr)	$S_I \cdot C_{AI} + L_I \times 0$			$(S_{OS} \times C_{AS} + L_{OS} \cdot C_{AL}) + (S_{OL} \times C_{AS} + L_{OL} \times C_{AL})$		
	78.38	78.38	78.38	73.22	83.49	87.52
% error				6.59	-6.52	-11.66

**Table 5.3** Mass balance

### 5.3 OPTIMIZATION OF THE OPERATING CONDITIONS IN THE EXTRACTION COLUMN

From all the experimental results of parts II, III and IV, it is possible to evaluate the most appropriate operating parameters for an industrial extraction.

In previous chapters, it was possible to identify opposite effects of the operating parameters on the behaviour of the column, and on the global extraction yield. The percentage of ethanol allowed favourable kinetics of extraction and a better separation at the top of the column. But, it reduced the mean residence time in the column (the sinking of the particle is faster).

The objective of this part is to summarize the main results into a simple equation which can be solved via Excel.

The different steps will be as follows:

1. Identification of the equation of mass flow rate of the solid at the column bottom  $\dot{m}_{so}$ .
2. Identification of the equation of the moving mass.
3. Identification of the equation of the residence time.
4. Identification of the percentage of extraction and of the extraction yield.

A gradient method will be used to optimize the functioning point.

### 5.3.1 Determination of the equation of $\dot{m}_{SO}$

Table 5.4 shows the data concerning the ratio of mass flow rate of solid in the outlet and inlet mass flow rate of solid for the whole experiments. The operating conditions of all experiments are presented in the Table 4.3.

$\frac{\dot{m}_{SO}}{\dot{m}_{SI}(\text{exp.})}$ : The mass solid flow which is going throughout the column during the experiment

Experiment	% Ethanol	$\dot{m}_{SI}$ exp.	$\dot{m}_{SO} / \dot{m}_{SI}(\text{exp.})\%$		
			$\dot{m}_{SI} = 11.33$ g/min (1)	$\dot{m}_{SI} = 17.53$ g/min (2)	$\dot{m}_{SI} = 25.85$ g/min (3)
1	95	10.62	83.05		
2	95	10.29			
3	95	17.10		65.85	
4	95	28.02			55.12
5	95				
6	95	13.63	83.82	83.82	
7	70	9.95	83.14		
8	70	10.68	74.19		
9	70	14.18	73.30		
10	70	no			
11	50	9.94			
12	50	11.35	70.84		
13	50	8.14	71.58		
14	30	8.01			
15	30	8.87	68.66		

Table 5.4 Solid output-solid input ratio according to the solid feed.

Figure 5.3 shows the relation between this ratio and the ethanol percentage. The curves were correlated via a simple linear equation.

Regression for solid flow:

$$\text{Flow } \dot{m}_{SI} = 11.33 \text{ g/min: } y = 0.2411 * x + 59.317 \quad (5.4)$$

$$\text{Flow } \dot{m}_{SI} = 17.53 \text{ g/min: } y = 0.0257 * x + 63.407 \quad (5.5)$$

$$\text{Flow } \dot{m}_{SI} = 25.85 \text{ g/min: } y = 0.0093 * x + 54.233 \quad (5.6)$$



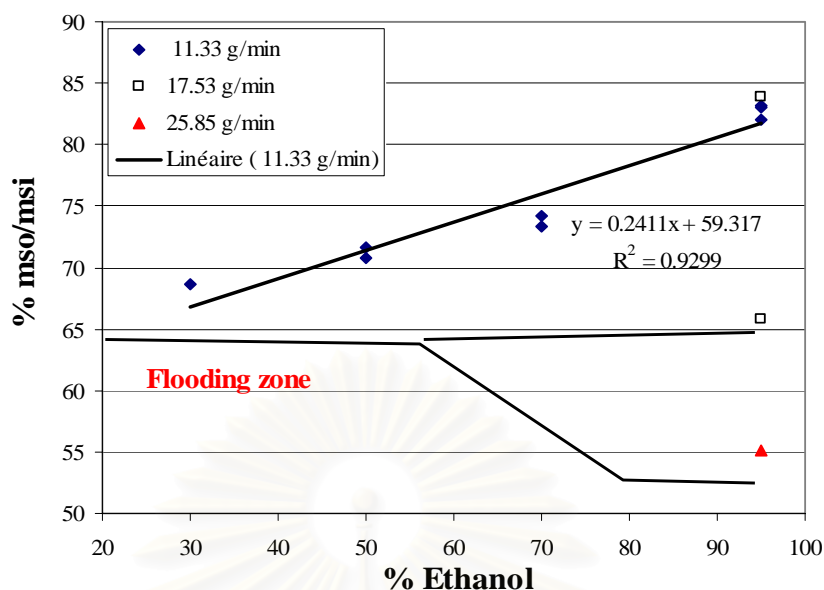


**Figure 5.3** The percent of the outlet mass flow rate of solid at the bottom of the column with the inlet mass flow rate of the solid as a function of ethanol percentage

### 5.3.2 Determination of the equation relative to the moving mass

As it has been explained previously (**Chapter 4.3.5**), the moving mass is the mass of solid passing the active part (or dynamic zone) of the column (considering the extraction). **Table 5.4** shows the experimental results of the estimated moving mass for the solid feed corresponding to a inlet solid mass flow rate of  $11.33 \text{ g}\cdot\text{min}^{-1}$ . All experiments are shown in **Appendix III**.

Moving mass (experiment)			
Experiment	% ethanol	Moving mass (g)	Average
1	95	29.00	
2	95	34.80	34.80
3	95		
4	95		
5	95	40.60	
6	95		
7	70	46.40	
8	70	52.20	
9	70		46.40
10	70	40.60	
11	70		
12	50	46.40	53.36
13	50	60.32	
14	30		
15	30	29	

**Table 5.5** Experimental results on the moving mass

Figure 5.4 shows the moving mass of the solid as a function of ethanol concentration. The moving mass of the solid in the column decreases when the percentage of ethanol increases.

The linear relation is:  $y = -0.4146x + 74.56$  (5.7)

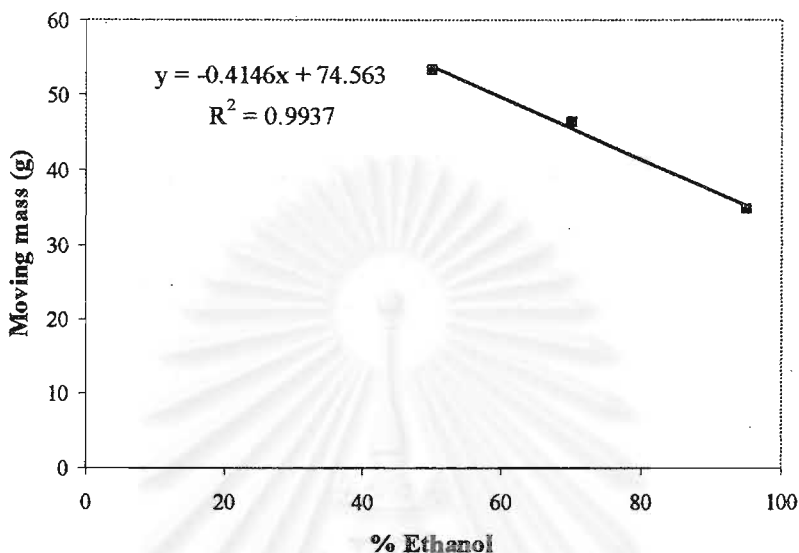


Figure 5.4 The moving mass as a function of ethanol percentage

The comparison between the linear model of the moving mass and the experiments leads to an error of only 1.07%

% Ethanol	Mass flow (g/min)	Moving mass (g)	Moving mass (model)	Error
95	8.5	34.8	35.17	1.07%

### 5.3.3 Determination of the residence time

The mean residence time is obtained by dividing the moving mass by  $\dot{m}_{SO}$ :

$$\tau = \frac{m_{moving}}{\dot{m}_{SO}} \quad (5.8)$$

This result is obtained for the 2.5 m in height experimental column.

From the mass flow rate of solid in the column ( $\dot{m}_{SO}$ ) and the moving mass in the column, it was possible to get the residence time of the solid in the column as follow.

% Ethanol	Mass flow (g/min)	Moving mass (g)	$\tau$ (min)
95	9.316	35.17	3.78

From the calculation, the residence time for 95% ethanol is 3.78 min. Despite of the important simplifications on the moving mass and the flow rate  $\dot{m}_{SO}$ , the calculated mean residence time is in a good agreement with the batch experiments.

### 5.3.4 Determination of the extraction rate

We intend now to establish a correlation to represent the extraction rate.

We know that the extraction rate in the column can be derived from the extraction in the batch reactor. Therefore, the extraction results in the batch reactor were taken into account for the calculation. We will try to fit the curve that permits to compute the percentage of extraction (y) depending on the percentage of ethanol (x).

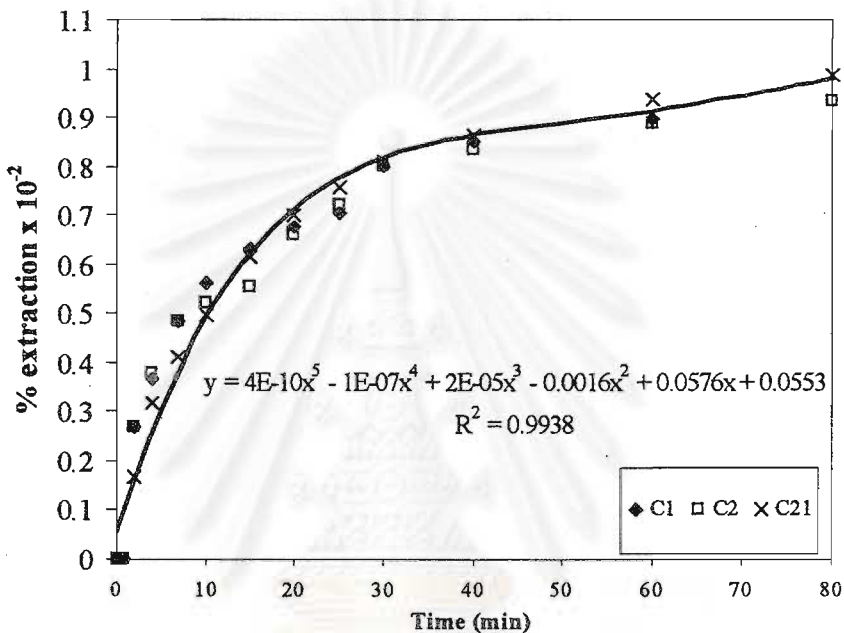


Figure 5.5 The extraction yield as a function of time when using  $C_1=80\%$ ,  $C_2 = 70\%$  and  $C_{21} = 60\%$  ethanol respectively

Figure 5.5 shows the curve fitting, yielding the following correlation:

$$y = 4 \cdot 10^{-10} x^5 - 1 \cdot 10^{-7} x^4 + 2 \cdot 10^{-5} x^3 - 1.6 \cdot 10^{-3} x^2 + 0.0576x + 0.0553 \quad (5.9)$$

We assume that there is no significant difference on the extraction rate due to the percentage of ethanol. Furthermore, this equation will be used for up to 90% of the extraction.

### 5.3.5 Determination of the extraction yield

Some examples of calculation of extraction yields are given at different ethanol compositions:

For 60% in the 2.5 m column with  $\dot{m}_{SI} = 11.33$  g/min

$\dot{m}_{SO}$ (g/min)	Moving Mass (g)	Residence time (min)	% Extraction in batch reactor
8.360	49.69	5.94	34.52%

For 95% ethanol, in the 2.5m column with  $\dot{m}_{SI} = 11.33$  g/min

$\dot{m}_{SO}$ (g/min)	Moving Mass (g)	Residence time (min)	% Extraction in batch reactor
9.316	35.18	3.78	25.11%

$\dot{m}_{SO}$  is calculated from equations (5.4-5.6), the moving mass is calculated from equation (5.7), the residence time is defined by (moving mass/ $\dot{m}_{SO}$ ) and % of extraction is calculated from equation (5.9) based on the batch experiments at the time corresponding to the residence time.

As an illustration of the importance of all the contributions (S/L separation of the top, kinetics of extraction and hydrodynamics in the column), we only considered the kinetics and the residence time.

Figure 5.6 shows the percentage of extraction as a function of ethanol concentrate when considering only the moving mass and the mass flow rate of the solid in the column. The percentage of extraction decreases when the percentage of ethanol increases. Note that ethanol concentration influences directly the amount of moving mass in the column.

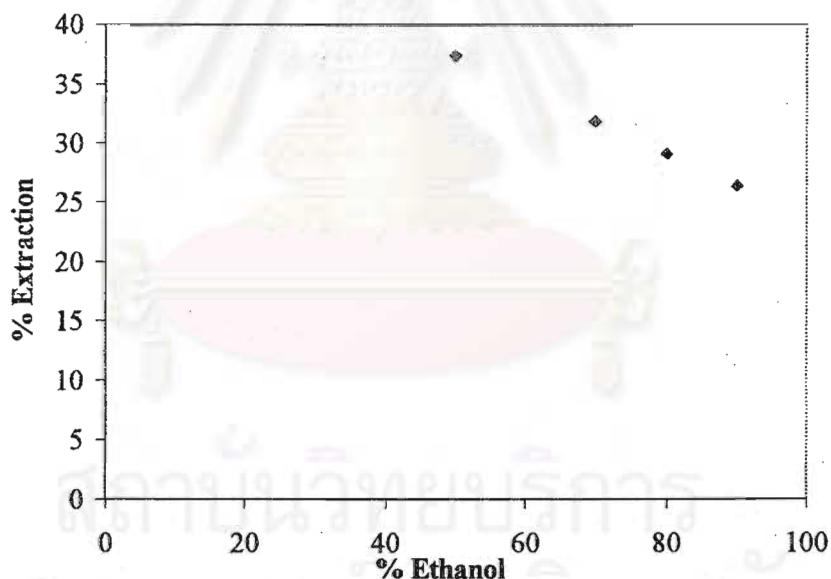


Figure 5.6 The percentage of extraction as a function of ethanol percentage

### 5.3.6 Determination of the equilibrium

In addition to the rate of extraction, the equilibrium at infinite time was needed to calculate the extracted mass of andrographolide.

The extraction yield can be defined as the quantity of the active principle extracted compared with the theoretical quantity. From Chapter II, with the soxhlet experiments, we found that the mixture of the solid is composed of 80% leaves and

20% stems. The active principle is mainly located in the leaves. We also assume that only the leaves are flowing throughout the column, the floating part being separated at the top of the column with the impulsion.

In order to calculate the maximal quantity of extract, the results of the soxhlet experiments that determined the maximum quantity of extracted active principle were used.

The maximum concentration of andrographolide is:

Leaves: 44.38 mg/g solid

Stem: 15.2 mg/g solid

(Chapter 2.1.5)

From Figure 2.17, it is possible to derive the equation of the final concentration (y) as a function of the percentage of ethanol (x). The relation is:

$$\text{The final concentration} = 0.2 \times \% \text{ of ethanol} + 15.678 \quad (5.10)$$

It is then possible to evaluate the extraction yield in the column:

For 60% ethanol in the 2.5 m column, with  $\dot{m}_{SI} = 11.33$  g/min

Maximum extract (mg/g)	27.674	equation (5.10)	(1)
Quantity maximum per min	231.341	(1)* $\dot{m}_{SO} = (2)$	(2)
Extracted (mg)	79.861	(2)*% extraction	(3)
Extract solid (mg/g solid)			
0.8 leave, 0.2 stem	38.544	(0.2*15.2+0.8*44.2)	(4)
Quantity total possible(mg/min)	436.704	(4) * $\dot{m}_{SI}$	(5)
Extraction yield	0.183	(3)/(5)	(6)

For 95% ethanol, in the 2.5 m column, with  $\dot{m}_{SI} = 11.33$  g/min

Maximum extract (mg/g)	34.674	equation (5.10)	(1)
Quantity maximum per min	323.009	(1)* $\dot{m}_{SO} = (2)$	(2)
Extracted (mg)	81.088	(2)*% extraction	(3)
Extract solid (mg/g solid)			
0.8 leaves, 0.2 stem	38.544	(0.2*15.2+0.8*44.2)	(4)
Quantity total possible(mg/min)	436.704	(4) * $\dot{m}_{SI}$	(5)
Extraction yield	0.186	(3)/(5)	(6)

Figure 5.7 shows the extraction yield as a function of the percentage of ethanol in the 2.5 m column. The curve shows a maximum in the extraction yield due to the opposite effect of ethanol on the final concentration and on the residence time. The maximum value is 0.1877 with 81.54 % ethanol.

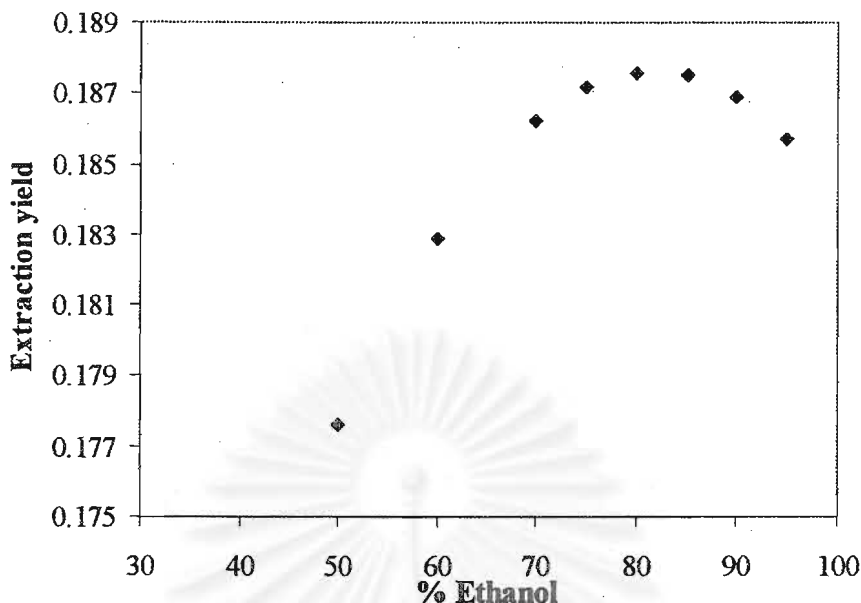


**Figure 5.7** The extraction yield as a function of the ethanol percentage with the 2.5 m column

The approach developed, despite of the important assumptions used, allows representation of the system in a correct way and to take into account the different parameters. It is a simple tool which can be used to design an industrial installation and optimize the operating parameters according to an economical criterion.

### 5.3.7 Example of design

In order to increase the extraction yield in the extraction column, the column height of extraction column should be increased in order to obtain the proper residence times of the solid in the column.

An example of calculation of the maximum amount extract of andrographolide and of the extraction yield when changing the column height is presented. The extraction yield increases when the column height increases.

For = 2.5 m column using 95% of ethanol, the parameters obtained are:

$\dot{m}_{so}$ (g.min <sup>-1</sup> )	Moving Mass (g)	Residence time (min)	% Extraction
9.316	35.18	3.78	25.11%

For = 5 m column using 95% of ethanol, the parameters obtained are:

$\dot{m}_{so}$ (g.min <sup>-1</sup> )	Moving Mass (g)	Residence time (min)	% Extraction
9.316	70.365	7.55	40.74%

Maximum extract (mg/g)	34.674	equation (5.10)	(1)
Quantity maximum per min	323.009	(1)* $\dot{m}_{so} = (2)$	(2)
Extracted (mg)	131.575	(2)*% extraction	(3)
Extract solid (mg/g solid)			
0.8 leaves, 0.2 stem	38.544	(0.2*15.2+0.8*44.2)	(4)
Quantity total possible(mg/min)	436.704	(4) * $\dot{m}_{sl}$	(5)
Extraction yield	0.30	(3)/(5)	(6)

For = 10 m column using 95% of ethanol, the parameters obtained are:

$\dot{m}_{so}$ (g.min <sup>-1</sup> )	Moving Mass (g)	Residence time (min)	% Extraction
9.316	140.73	15.11	62.44%

Maximum extract (mg/g)	34.674	equation (5.10)	(1)
Quantity maximum per min	323.009	(1)* $\dot{m}_{so} = (2)$	(2)
Extracted (mg)	201.656	(2)*% extraction	(3)
Extract solid (mg/g solid)			
0.8 leaves, 0.2 stem	38.544	(0.2*15.2+0.8*44.2)	(4)
Quantity total possible(mg/min)	436.704	(4) * $\dot{m}_{sl}$	(5)
Extraction yield	0.46	(3)/(5)	(6)

Figure 5.8 shows the extraction yield as a function of the column height when changing the percentage of ethanol. The extraction is quite the same when the column height is less than 10 m. If the column height is less than 10 m recycling the ethanol is not an important factor as regards to the extraction yield. With higher columns, the longer residence time in the column makes the influence of the solvent composition more relevant.

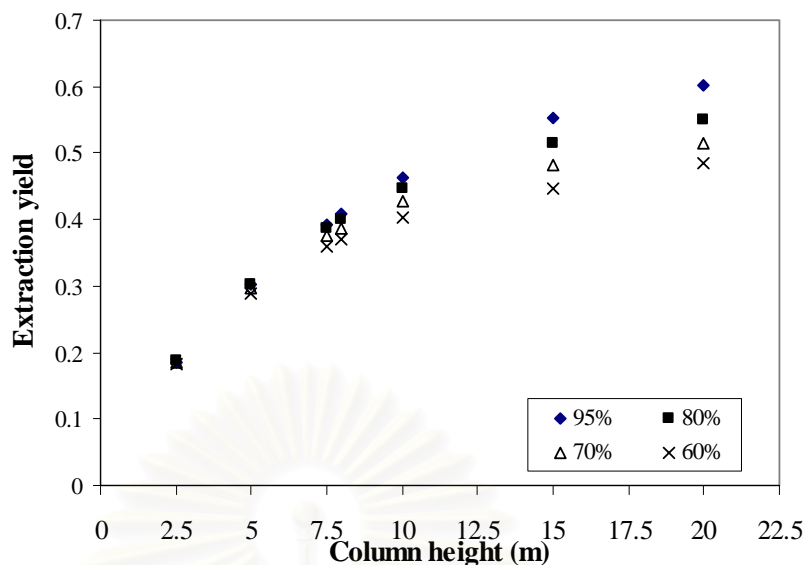


**Figure 5.8** The extraction yield of the solid as a function of the column height

However, there are many factors that are to be considered for determination of optimal conditions. It depends on the capital costs, operating cost, operating process, security etc. For example, the higher percentages of ethanol solution are favourable for the extraction of the active principle. On the other hand, with the higher percentages of the ethanol, there is less moving solid mass in the column, the price of the solvent is high and the safety issue relates to storage of solvent should be considered. Since there is no problem of solubility of andrographolide in the ethanol solution, this allows the solvent to be recycled.

## CONCLUSION

In this chapter were presented some of the characteristic of a twin-screw extruder and the extraction yields of the solute using the twin screw extruder. We found that the twin-screw extruder allowed a 77% extraction of the initial andrographolide with a residence time in the reactor of only 1 min. The liquid-solid ratio is much less than in the case of a batch reactor. An efficient liquid-solid separation is obtained. The main advantage of the twin-screw extruder is that extraction and liquid/solid separation can be achieved simultaneously in a very efficient manner. However, the choice of the plants for experiment with screw extruders has to be considered. In addition, the extracted substance should have high-values compared to the instrument costs of such a device.

The second part was devoted to the assembly of the diffusion model obtained from the batch experiments in **Chapter II** with the experimental results of **Chapter IV** on the hydrodynamic behaviour of the solid in the column. This allowed an optimization to be done and allowed operating conditions in the column to be determined by using a simple linear regression from the experimental results.



## GENERAL CONCLUSIONS

This work was to develop an extraction process of the andrographolide from the *Andrographis paniculata* Nees plant which is used as traditional medicinal plant in Thailand. In this particular process, the active principle extracted is a medicine used to cure for diarrhea in pigs which are considered to be the main source of protein for Thai and Chinese people. This development of a continuous extraction process will be useful for related industries.

This work is composed of two main parts: the batch study and the continuous process.

Firstly the structure and composition of the plants were analyzed. The influence of the main operating parameters such as the solid mass flow rates, percentage of ethanol solvent, size of particles and temperature were studied as well as the influence of high temperatures, age and storage of plant that may lead to destruction of the active principle.

The results of the batch experiments are as follows:

- The sizes of the particles were shown to have very little effect on both extraction kinetics and final concentration. On the contrary, the particle shape (stem and leaf) did show a strong influence on kinetic and final concentration.
- The percentage of ethanol has also no effect on the kinetics of extraction but the final concentration increases with the percentage of ethanol.
- Both the final concentration and the extraction kinetics increase with temperature. However, the reaction of destruction of the solute is activated at high temperatures.

From the kinetics of the extraction, residence times of 15 to 30 min allow extraction yields to attain 60 to 80 %.

The andrographolide concentration decreases in plants stored for 2 years after harvest and dramatically decreases when fermentation attacks the plant. The plant should therefore be kept as dry as possible.

The mass transfer model emphasizes the 2 different shapes of the particles. The plane shape refers to the leaves and the cylindrical shape refers to the stems. The experimental results are used to identify the diffusion coefficients in both stems and leaves. The diffusion coefficients of the andrographolide in the plant were measured to be  $8.43 \times 10^{-14} \text{ m}^2 \cdot \text{s}^{-1}$  for the 60 percent of ethanol solution at ambient temperature. The diffusion coefficient can reach up to  $52 \times 10^{-14} \text{ m}^2 \cdot \text{s}^{-1}$  with 60% ethanol at 60°C.

The batch results allow choosing the operating conditions of the continuous process.

The second part is devoted to the continuous process through a hydrodynamic study. Classically, a disc and doughnut pulsed column was used, but with a co-current

operation mode, with the knowledge that one theoretical stage is sufficient (there is no limit of action principle solubility). Such a co-current mode normally allows for easier entrainment of the particles by the carrier flow, leading to higher throughputs than with a counter-current mode.

Despite the choice of co-current flow, some of the particles still tend to float at the feed inlet at the top of the column. Subsequently, our own work focused on solving this practical problem by way of a new mode of agitation, alternating between a pulsation cycle and an impulsion, in order to drain out the accumulated floating particles at the top. With this good in mind, a new pulsation system was developed, based on a pneumatically air pulsed system, which is more flexible than using a mechanical system. The way, we obtained a good separation of the floating and sinking solid parts at the top of the column. The problem of flooding due to floating particles was solved with the air pulsating system.

The solid hydro-dynamical behavior was intensively studied. Some information on mass balance, transient regime, residence time, moving mass, accumulated mass and dead mass were obtained.

The main results are as follows:

- The moving mass, transient regime and the residence time decrease when the percentage of ethanol increases.
- The moving mass, transient regime and the residence time increase with the mass solid at the inlet increase.
- The residence time was about 4 min with 95% ethanol.
- The dead mass does not depend on the percentage of ethanol, but depends strongly on mass solid inlet flow. The dead mass increases with the mass solid inlet increase, until a plateau is reached.

The extraction yield in the column was about 28% which corresponds to the extraction yield in batch experiments at 3-4 min. This extraction yield in the column is therefore in good agreement with the batch yield. This confirms that the column acts similarly to a plug flow system. Furthermore, the continuous process obviously presents advantages of safety in comparison with a batch process where large amounts of solvents are used.

However, the hydrodynamic behaviour of the sinking particles strongly depends on the ethanol solvent. In order to increase the residence time in the column, it will be necessary to increase the column height or to increase the amplitude of mixing in the column.

The hydrodynamic behavior of the solid in the column and the batch experiments were coupled in order to determine the most appropriate operating conditions. The extraction yield depends on the ethanol percentage and the amount of moving solid as well: the higher the ethanol percentage, the smaller amount of the moving solid in the column. These two main effects allow the optimization to be done as well as the global design of the column by using a simple regression based on experimental results. The overall extraction yield in the column is caused by two major contributions, the solid separation at the top of the column and the extraction yield in the active part of the column.

A good solid separation was obtained by using a non sinusoidal pulsation. This is the major technological improvements of this work. This study also developed a global methodology to predict the extraction yield in the column. This methodology was successfully applied to the andrographolide extraction.

Finally, one set of experiments was done using the twin screw extruder, which was used as continuous solid-liquid extraction equipment. The twin screw extruder has grown very rapidly in the last 10 years as a promising reactor for continuous extraction from the plant materials. We found that the twin screw extruder allowed 77% extraction of the initial andrographolide with a residence time in the reactor of only 1 min. The liquid solid ratio is much less than the ratio used in a batch reactor. An efficient liquid-solid separation was obtained. However, the extracted substance should be high valued because equipment cost is high for TSE systems.



สถาบันวิทยบริการ  
จุฬาลงกรณ์มหาวิทยาลัย

## REFERENCES

- Akbarsha, M. A., B. Manivanan, K.S. Hamid, and B. Vijayan. 1990. Antifertility effect of *Andrographis paniculata* (Nees) in male albino rat. Indian. Journal of Experimental Biology 28: 421 – 426.
- Altamore, R.E., P. Ghossi,. 1986. An analysis of residence time distribution pattern in a twin screw cooking extruder. Biotechnol. Prog. 2, 3:157-163.
- Anderson, J.L. 1973. Prediction of the concentration dependence of macromolecular diffusion coefficients. Ind. Eng. Chem. Fundam. 12, 4: 488-490.
- Azbel, D. 1981. Two – phase flows in chemical engineering. 1st ed. Cambridge University Press: Cambridge.
- Bacon, J . 1936. Frankln Inst. 221: 251.
- Baird, M.H.I. 1966. Vibrations and pulsations. British. Chemical. Engineering 11, 1: 20.
- Baird, M.H.I. 1967. Water blow pulsation. British. Chemical. Engineering. 12, 12: 1877.
- Baird, M.H.I. and J.H. Garstang. 1967. Power Consumption and Gas Hold-Up in a Pulsed Column. Chemical Engineering Science 22: 1663-1673.
- Baird, M.H.I., Gloyne, A.R., and Meghant, M.A.N. 1968. Solvent extraction in an air-pulsed packed column. The Canadian Journal of Chemical Engineering 46: 249.
- Berger, R., W.Leuckel, and D.Wolf ,. 1978. Chem. Ind. p. 760.
- Berger, R. 2000. Liquid – liquid extraction. Ullmann's Encyclopedia of Industrial Chemistry Wiley-VCH Verlag, Article Online Posting Date: June 15.
- Bichsel, B. 1979. Diffusion phenomena during the decaffeination of coffee Beans. Fd. Chem. 4: 53-61.
- Calabrese, C.; Berman, S. H., et al. 2000. A phase. I trial of andrographolide in HIV positive patients and normal volunteers. Phytotherapy research 14: 333-338.
- Chantry, W.A., R.L. Von, and H.F. Wiegandt,. 1955. Application of pulsation to Liquid-liquid extraction. Industrial and engineering chemistry 47,6: 1153.
- Charnprasert, C. and Pecharaply, D. 1988. The cultivation of *Andrographis paniculata* Nees for medical uses. Bull. Dept. Med. Sci. Thailand., 30, 4: 315-320.

- Chen, B.H., Khana, R., and Douglas, W.J.M. 1965. 15th Canadian Chemical Engineering Conference, October, Quebec City.
- Coloured atlas of the Chinese material medical specified in pharmacopoeia of the People's Republic of China. 1995. Pharmacopoeia Commission of the Ministry of Public Health P. R. of China, pp.347-348.
- Danckwerts, P.V. 1951. Process development. Industrial and Engineering Chemistry 43: 1460-1467
- Division of medical plants research and development department of medical science ministry of public health. 1990. Handbook of Medicinal plant for Primary Public Health Text and Journal Corporation. Bangkok. p. 53 (Thai language).
- Dousse, R. 1978. Utilisation de l'extraction solide liquide par diffusion dans la technologie des fruits et légumes. Doctoral dissertation. Ecole Polytechnique Fédérale de Zurich.
- Edwards, R.B., and G.H. Beyer,. 1956. AICHE J. 2:148.
- Einstein, A. 1956. Investigation on the theory of the brownian movement. New York: Dover. (cited in Aaderson, 1973)
- Galaya Srisuwan. 1988. Extraction solide - liquide en colonne pulsé a disques et couronnes : modélisation et application au cas du tanin. Doctoral dissertation, Institut National Polytechnique de Toulouse, France.
- Geier, R.G. 1957. USAEC Report TID-7534, Book 1: 107.
- Geier, R.G. 1958. Proceedings of the 2<sup>nd</sup> Conference on Peaceful Uses of Atomic Energy 17, Geneva, paper 515.
- Ghai, R. K.; Ertl, H., and Dullien, F.A.L. 1973. Liquid diffusion of non electrolytes: Part I. A.I.Ch.E Journal 19, 5: 881-900
- Giovammo, A. 1967. Mass transfer with chemical reaction. 1 st ed. Elsevier Publishing. New York.
- Godfrey, J. C., and Slater, M.J. 1994. Liquid-Liquid extraction equipment. 1st ed. JOHN WILEY & SONS, 772.
- Grimmett, E.S.; Brown, B.P. 1962. A Pulsed column for counter current liquid-solid flow. Industrial and Engineering Chemistry 11:54.
- Gupta, S., Choudhry, M.A., Yadava, J.N.S., and Srivastava, V. 1990. Antidiarrheal activity of diterpenes of *Andrographis paniculata* (Kalmegh) against *Escherichia Coli* enterotoxin in *Vivo* models. Int. J. Crude Drug Res. 28; 4 : 273-83.
- HANRATTY, T.J. 1935. Trans. AIChE 31 : 365.

- Haunold, C. 1991. Extraction de pyr  thrines analyse du proc  d   discontinu et de l'influence des ultrasons mod  lisation et mise en oeuvre d'un proc  d   continu. Doctoral dissertation. Institut National Polytechnique de Toulouse, France.
- Higbie, R. 1935. Transactions of the American Institute of Chemical Engineers 31: 365-89.
- Hildebrand, J.H., Prausnitz, J.M., and Scott, R.L. 1970. Regular and related solutions. van Nostrand, New York.
- Isobe, S., F. Zuber, K. Uemura, and A. Nogushi,. 1992. A new twin –screw press design for oil extraction of dehulled sunflower seeds. J. Am. Oil Chem. Soc. 69, 9: 884-889.
- Jealous, A., and Johnson, F. 1955. Power requirements for pulsed generation in pulse columns. Industrial and Engineering Chemistry 47, 6: 1159-1166.
- Kakuji, T., Miyanami, K., and Takeo, Y. 1975. Behaviour of suspended solid particles in a multistage vibrating disk column with Cocurrent Solids-Liquid Flow. Power Technology 12: 239-245.
- Kasetklangklung. 1996. Andrographis paniculata. Thai Medicinal Plant Journal Transfer Tech. Agric 2, 14: 6-17. (Thai language)
- Laidler, K. J. 1950. Chemical Kinetics. 1 st ed. INC: McGRAW-Hill pp.3-7.
- Lalou, A. 1995. Mise au Point d'un Proc  de d'Extraction des H  micelluloses a partir d'un Substrat V  g  tal Ligno - Cellulosique : Application au cas des Coques de Tournesol. Doctoral dissertation, Institut National Polytechnique de Toulouse, France : 1995.
- Lane Et Riggle,. 1959. Chem. Eng. Prog. Symp.Ser. 55:127
- Laws, D.R.J., and others. 1977. J. Inst. Brew. London 3, 1:39.
- Lee, Yeun Chung. 1986. Analysis of continuous countercurrent solid-liquid extractors. Doctoral dissertation, University of Massachusetts.
- Levich, L.G. 1962. Physicochemical Hydrodynamics Prentice-Hall: Englewood Cliffs N.J., Section 6.
- Lewis, W.K., and Whitman, W.G. 1924. Industrial and Engineering Chemistry 16: 1215-20
- Leybros, J.; Fremeayx, P. 2002. Extraction solide - liquide sspct th  oriques : trait   g  nie et proc  d  s chimiques. Techniques de l'ing  nieur J2780-8.
- Li, J.C.M., and Chang, P. 1955. Self – diffusion coefficient and viscosity in liquids. The journal of chemical physics 23, 3: 518-520.

- Mahaverawat, N. 1992. Determination of Diterpenoid Contents in the Leaves of *Andrographis paniculata* Nees. Master's Thesis, Department of Pharmaceutical Sciences, Chulalongkorn University, 1992
- McCabe, W.L., Julian, C. S., and P. Harriott,. 1993. Unit operation of chemical engineering. 5 th ed. McGraw – Hill Chemical Engineering Series.
- Medicinal plant research institute, department of medical science, ministry of public health. 1999. Standard of Thai Herbal Medicine: *Andrographis paniculata* (Burm.f.) Nees. The war Veterans Organization Press: Bangkok. p.66. (Thai language).
- Milburn, C.R., and Baird, M.H.I. 1970. Flow pulsation generator for pilot-scale studies. Ind. Eng. Chem. Process Des. Develop 9, 4: 629.
- Naiyana Tipakorn . 2000. Effect of *Andrographis paniculata* (BRUM.F.) NEE on performance, mortality and coccidiosis in broiler chickens. Doctoral Dissertation, Institute of animal physiology and animal nutrition, Gottingen, Germany.
- N'diaye, S., L. Rigal, P. Larocque, and P. F. Vidal,. 1996. Extraction of hemicelluloses from poplar, *Populus Tremuloides*: using and extruder – type twin – screw reactor : a feasibility Study. Bioresource Technology 57: 61-67.
- Office of medicinal plant data. 1989. Fha-Ta-Lai step on medicinal plant. Book 1. Faculty of Pharmacy, Mahidol University. Bangkomol Press. Bangkok. pp.171-178.
- Poole, J.B., and Doyle, D. 1966. Solid-liquid separation. Her majesty's stationery office.
- Prat, L. 1998. Modélisation d'un réacteur thermo - mécano - chimique bi -vis utilise en fractionnement de la matière végétale. Doctoral dissertation, Institut National Polytechnique de Toulouse, France.
- Prat, L., Guiraud, P., Rigal, L., and Gourdon, C. 1999. Solid-liquid reactive extraction with raw plant substrate. Comm.2<sup>nd</sup> European Congress on Chemical Engineering ECCE2, MONTPELLIE, France, in CD-ROM.
- Prat, L., Guiraud, P., Rigal, L., and Gourdon, C. 1999. Two phase residence time distribution in a modified twin screw extruder. Chemical Engineering and Processing 38: 73-83.
- Prat, L., Guiraud, P., Rigal, L., and Gourdon, C. 2002. A one dimensional model for the prediction of extraction yield in a two phases modified twin-screw extruder. Chemical Engineering and Processing 41: 743-751.

- Rajani, M., Shrivastava, N., Ravishankara, M. N. 2000. A rapid method for isolation of andrographolide from *Andrographis paniculata* Nees (Kalmegh). Pharmaceutical Biology 38, 3: 204-209.
- Research review. 1997. *Andrographis* vs the common cold. The Journal of the America Botanical Council and the Herb Research Foundation 40: 18.
- Richardson, G. 1961. USAEC Report HW-SA-2083.
- Rigal, L. 1996. Technologie d'extrusion bi - vis et fractionnement de la matière végétale, 40 ans d'extraction bi - vis chez CLEXTRAL. Recueil de Conférences Firminy 8-10 October, France.
- Sandberg, F. 1994 *Andrographidis herba Chuanxinlian: A review* Gothenburg, Sweden: Swedish herbal Institute, Available from the American Botanical Council (USA)
- Saxena, S. et al. 1998. Chemistry and pharmacology of *Andrographis* species. Indian Drugs 35, 8.
- Scheibel, E.G. 1954. Ind. Eng. Chem. 46: 2007. (cited in Skelland, 1974)
- Sege, G., and Woodfield, W. 1954. Chem. Eng. Progress 50, 8: 396-402.
- Sege, G., and Woodfield, W. 1954. Pulse column variables. Chemical Engineering Progress 50, 8: 380.
- Seikova, I. ; Guiraud, P.; Mintchev, A. Nikolov,. 1999. Influences of the shape and size polydispersion of the solid phase upon the kinetic of extraction from vegetable materials. 3<sup>rd</sup> . Eur. Conf. Chem. Eng. 5-7 October, Montpellier, France.
- Sichuan Chinese herb research institute. 1973. Review of chemical studies on *A. paniculata*. Journal of New Medicine and New Drugs : 23-30.
- Sharma, A., L. Krishan, and S.S. Handa,. 1992. Standardization of the Indian crude drug kalmegh by high pressure liquid chromatographic determination of Andrographolide. Phytochemical analysis 3: 129-31.
- Simeonov, E., I. Tsibranska, and A. Minchev,. 1999. Solid-liquid extraction from plants –experimental kinetics and modeling. Chemical Engineering Journal 73: 255-259.
- Skelland, A.H.P. 1974. Diffusional mass transfer. London and New York Academic press, 1.
- Somkiat Ngamprasertsith. 1993. Extraction par solvant a partir de matières végétales en colonne pulsée a disques et couronnes. Doctoral dissertation, Institut National Polytechnique de Toulouse, France.



- Spiro, M., and David, S.J. 1982. Kinetics and equilibria of tea infusion. Part 3., rotating disc experiments interpreted by a steady-stage model. J. Chem. Soc. Faraday Trans I. 78: 295-305.
- Spiro, M., and Page, C.M. 1981. The kinetics and equilibria of tea infusion, kinetics of extraction of theaflavins, thearubigins and caffeine in Koonsong Broken Pekoe. J. Sci. Food Agric.32: 1135-1139.
- Spiro, M., Selwood, R.M. 1984. The kinetics and mechanism of caffeine infusion coffee: the effect of particle size. J. Sci. Food Agric. 35: 915-924.
- Spiro, M., and Siddique, S. 1981. Kinetics and equilibria of tea infusion: analysis and partition constants of theaflavins, thearubigins and caffeine in Koonsong Broken Pekoe. J. Sci. Food Agric. 32: 1027-1032.
- Srisomporn Preeprame. 1992. Physicochemical properties of chemical constituents in *Andrographis paniculata* Nees. Master's Thesis, Department of Pharmaceutical Sciences, Chulalongkorn University.
- Sutham Sukmanee. 1984. Echange d'Ion en colonne pulsée a disques et couronnes hydrodynamique et échange d'Ion. Doctoral dissertation, Institut National Polytechnique de Toulouse, France.
- Suwanbareerak, K., and C. Chaichantipyuth,. 1991. Num-Lai-Pung-Porn, *Andrographis paniculata*. J. Med. Pla. Thailand Soc. 7, 1: 3-9.
- Tayeb, J., Vergnes, B., and Della Valle, G. 1989. A basic model for a twin screw extruder. J. Food Sci. 54: 207-214.
- Thai pharmacopoeia. 1995. Bangkok: Prachachon. Vol. 1.(Thai language).
- Thai pharmacopoeia. 1997. Bangkok: Pt. 1. P.A. Living. Vol. 2, p. 2064-3065. (Thai language)
- Thornton, J.D. 1954. Chem. Eng. Progr. Symp. Seri 13: 39.
- Thornton, J.D. 1957. Transact. Inst. Chem. Eng. 35: 316.
- Thornton, J.D. 1992. Process chemistry and extraction operation in the hydrometallurgical nuclear pharmaceutical and food industries. oxford science publication, Volume 2.
- Treybal, R.E. 1963. Liquid extraction. London: McGraw-Hill.
- Tuwiner. 1962. Diffusion and membrane technology. New York: Rheinhold.
- Uhle, K. 1970. Chem.Ing.Tech. 42: 841.
- Van dijck, W.J.D. 1935. Process and apparatus for intimately contacting Fluids.U.S. Patent. 2011186 (August 13).

- Wade, L.G.Jr. 1987. Organic chemistry.-3 rd ed. Prentice hall international editions, pp.396-400.
- Weech, M.E., and B.E. Knight,. 1967. Design of air pulsers for pulse column application. I&EC Process Design and Development 6, 4:481.
- Weibo, L. 1995. Prospect for study on treatment of AIDS with traditional Chinese medicine. J. Trad. Chinese Med. 15, 1: 3-9.
- Wilkie, C.R., and Chang, P. 1955. A.I.Ch.E J. 1: 264.
- Yin, J., and L. Guo,. 1993. Contemporary traditional Chinese medicine. Beijing: Xie Yuan.

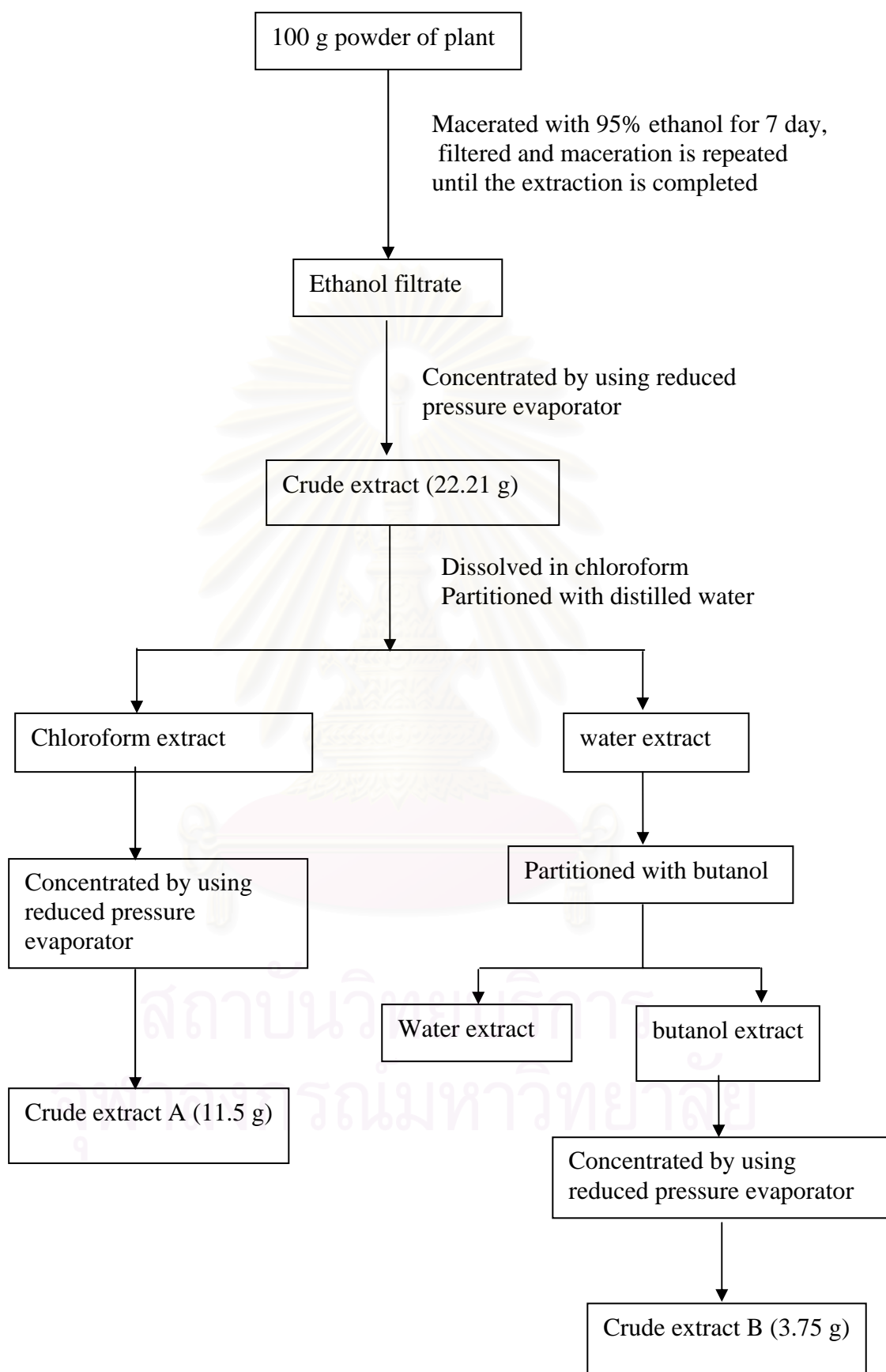


สถาบันวิทยบริการ  
จุฬาลงกรณ์มหาวิทยาลัย



## APPENDICES

สถาบันวิทยบริการ  
จุฬาลงกรณ์มหาวิทยาลัย

**Appendix I** The technique of extraction of *Andrographis paniculata*The scheme of extraction of *Andrographis paniculata*

## GENERAL TECHNIQUE FOR ISOLATION

### 1 Column chromatography

#### 1.1 Open column chromatography

Column size: 3 inch x 10 inch, 2 inch x 14 inch, 1 cm x 50 cm.

Adsorbent: silica gel 60 particle size 0.040-0.063 mm (E. Merck)

Packing: Adsorbent is mixed with the solvent system into a slurry then poured into the column

Sample loading: The portion of crude extract is dissolved in small volume of solvent used for packing the column and gently applied on top of the adsorbent. If the crude extract was insoluble in solvent used for packing column.

The crude extract is dissolved in a small volume of volatile solvent then mixed with small amount of silica gel 60 used in column chromatography. The mixture should be kept in a vacuum desiccator. The dried mixture is applied on top of the adsorbent

Solvent: n – Hexane (E. Merck), Chloroform (E. Merck), Methanol, Ethyl acetate

#### 1.2 Quick column chromatography

Column size: 5 inch x 8 inch, 3.5 inch x 4.5 inch, 3 inch x 2 inch.

Adsorbent: silica gel 60 particle size 0.015-0.040 mm

Packing: The Adsorbent is packed into the column in a single portion for 2-3 cm in height. The column is clamped and connected to the suctioned flask. A low viscosity solvent (petroleum ether, hexane is poured carefully over the adsorbent then suction pump is started. The solvent would rapidly flow pass through the column. The adsorbent would be packed. The top of the adsorbent bed should be flattened.

Sample loading: The portion of crude extract is mixed with silica gel 60 used in column chromatography in the ratio 1: 2. The dried mixture is applied on top of the adsorbent and flattened.

Solvent: n-Hexane, Chloroform, Ethyl acetate, Methanol

### 2 Crystallization techniques

The purification of impure crystalline compounds is usually effected by crystallisation from a suitable solvent. The crystallisation process consists of :

1. Dissolving the impure substance in some suitable solvent at or near the boiling point.
2. Filtering the hot solution.
3. Allowing the hot solution to cool.
4. Adding the second solvent in case crystals are not formed.
5. Separating the crystal from the solution.

The resulting solid was tested for purity after drying through melting point determination and thin layer chromatography and if found impure is again recrystallised.

The process is repeated until a pure compound is obtained.

**Appendix II.I** Concentration of andrographolide in mg/ml of solvent experiment from batch reactor

date	19/06/2001	19/06/2001	05/06/2001	05/06/2001	18/07/2001
% Ethanol	80	70	60	0	60
Volume solvent (ml)	500	500	500	500	500
Mass initial (g)	10	10	10	10	10
Temp (°C)	20-22	20-22	20-22	20-22	20-22
Size (mm)	0.6-0.8	0.6-0.8	0.6-0.8	0.6-0.8	0.45-0.6
Time (min)/sample	C1	C2	C3	C4	C5
0	0.00	0.00	0.00	0.00	0.00
2	0.17	0.16	0.12		0.16
4	0.23	0.23	0.23	0.04	0.25
7	0.30	0.29	0.29	0.10	0.32
10	0.35	0.31	0.34	0.14	0.36
15	0.40	0.33	0.39	0.17	0.43
20	0.43	0.39	0.43	0.23	0.47
25	0.44	0.43	0.46	0.24	0.49
30	0.50	0.48	0.48	0.27	0.51
40	0.53	0.50	0.50	0.28	0.56
60	0.56	0.53	0.55	0.31	0.63
80	0.60	0.56	0.56	0.34	0.64
100	0.61	0.58	0.57	0.36	0.67
120	0.61	0.58	0.59	0.37	0.68
150	0.63	0.60	0.58	0.38	0.68
$D \times 10^{12}$ (m <sup>2</sup> /min)	6.63	5.43	5.56	0.73	7.31
$D \times 10^{14}$ (m <sup>2</sup> /sec)	<b>11.05</b>	<b>9.05</b>	<b>9.26</b>	<b>1.22</b>	<b>12.18</b>
criteria	6.26E-07	1.72E-07	1.50E-07	-1.00E-06	6.09E-07

สถาบันวิทยบริการ  
จุฬาลงกรณ์มหาวิทยาลัย

date	23/05/2001	23/05/2001	05/06/2001	05/06/2001	05/06/2001
% Ethanol	60	70	0	0	0
Volume solvent (ml)	500	500	500	500	500
Mass initial (g)	10	10	10	20	30
Temp (°C)	20-23	20-23	21	21	21
Size (mm)	0.3-0.45	0.3-0.45	0.45-0.6	0.45-0.6	0.45-0.6
Time (min)/sample	C6	C7	C8	C9	C10
0	0.00	0.00	0.00	0.00	0.00
2	0.23	0.24	0.04	0.15	0.23
4	0.32	0.29	0.09	0.23	0.35
7	0.46	0.44	0.14	0.30	0.47
10	0.45	0.49	0.17	0.39	0.54
15	0.52	0.50	0.20	0.45	0.62
20	0.61	0.51	0.23	0.49	0.68
25	0.63	0.51	0.28	0.52	0.70
30	0.65	0.51	0.30	0.54	0.72
40	0.66	0.55	0.32	0.56	0.73
60	0.66	0.70	0.36	0.59	0.74
80	0.68	0.70	0.37	0.61	0.78
100	0.76	0.72	0.39	0.60	0.79
120	0.76	0.73	0.40	0.61	0.79
150	0.78	0.74	0.40	0.62	0.80
$D \times 10^{12} \text{ (m}^2/\text{min)}$	13.01	7.72	3.48	7.97	10.60
$D \times 10^{14} \text{ (m}^2/\text{sec)}$	<b>21.68</b>	<b>12.87</b>	<b>5.8</b>	<b>13.28</b>	<b>17.67</b>
criteria	9.78E-07	4.67E-07	-1.33E-07	1.051E-07	8.64E-08

สถาบันวิทยบริการ  
จุฬาลงกรณ์มหาวิทยาลัย

date	05/06/2001	05/06/2001	05/06/2001	23/05/2001	23/05/2001
% Ethanol	0	0	0	60	60
Volume solvent (ml)]	500	500	500	500	500
Mass initial (g)	10	20	30	10	20
Temp (°C)	22	22	22	20-22	20-22
Size (mm)	0.6-0.8	0.6-0.8	0.6-0.8	0.6-0.8	0.6-0.8
Time (min)/sample	C11	C12	C13	C14	C15
0	0.00	0.00	0.00	0.00	0.00
1					
2	0.04	0.10	0.13	0.15	0.30
4	0.10	0.20	0.25	0.24	0.52
7	0.14	0.26	0.38		0.59
10	0.17	0.31	0.48	0.26	0.67
15	0.23	0.38	0.51	0.28	0.77
20	0.24	0.44	0.63	0.39	0.81
25	0.27	0.47	0.65	0.41	0.86
30	0.28	0.51	0.72	0.43	0.89
40	0.31	0.54	0.76	0.47	0.95
60	0.34	0.58	0.80	0.52	1.01
80	0.36	0.62	0.82	0.54	1.05
100	0.37	0.62	0.82	0.56	1.10
120	0.38	0.63	0.83	0.58	1.10
150	0.38	0.62	0.83	0.59	1.12
$D \times 10^{12} (\text{m}^2/\text{min})$	3.79	4.87	5.35	5.87	5.06
$D \times 10^{14} (\text{m}^2/\text{sec})$	<b>6.31</b>	<b>8.11</b>	<b>8.92</b>	<b>9.78</b>	<b>8.43</b>
Criteria	-2.73E-07	-2.549E-07	-2.303E-07	-9.67E-08	6.60E-07



date	23/05/2001	23/05/2001	05/06/2001	18/07/2001	05/06/2001
% Ethanol	60	60	60	60	0
Volume solvent (ml)]	500	500	500	500	500
Mass initial (g)	5	10	10	10	20
Temp (°C)	20-22	20-22	20-22	20-22	22
Size (mm)	0.6-0.8	0.1-0.3	0.6-0.8	0.3-0.45	0.45-0.6
Time (min)/sample	C16	C17	C18	C19	C20
0	0.00	0.00	0.00	0.00	0.00
1		0.12		0.21	
2	0.08		0.12		0.15
4	0.11	0.23	0.23	0.22	0.23
7	0.12	0.36	0.29	0.28	0.30
10	0.14	0.46	0.34	0.30	0.39
15	0.17	0.50	0.39	0.39	0.45
20	0.18	0.56	0.43	0.40	0.49
25	0.19	0.59	0.46	0.45	0.52
30	0.20	0.58	0.48	0.52	0.54
40	0.21	0.59	0.50	0.55	0.56
60	0.23	0.63	0.55	0.58	0.59
80	0.24	0.64	0.56	0.60	0.61
100	0.25	0.65	0.57	0.61	0.60
120	0.25	0.65	0.59	0.61	0.61
150	0.25	0.66	0.58	0.61	0.62
$D \times 10^{12} (\text{m}^2/\text{min})$	6.38	7.37	6.63	6.56	1.26
$D \times 10^{14} (\text{m}^2/\text{sec})$	<b>10.63</b>	<b>12.28</b>	<b>11.05</b>	<b>10.93</b>	<b>2.1</b>
Criteria	4.24E-07	6.51E-07	4.19E-07	3.16E-08	-4.27E-07

date	05/06/2001	05/06/2001	05/06/2001	05/06/2001	01/01/2001
% Ethanol	0	0	0	0	60
Volume solvent (ml)	500	500	500	500	500
Mass initial (g)	20	10	10	10	10
Temp (°C)	22	22	22	22	40
Size (mm)	0.6-0.8	0.3-0.45	0.45-0.6	0.6-0.8	0.6-0.8
Time (min)/sample	C21	C22	C23	C24	C25
0	0.00	0.00	0.00	0.00	0.00
2	0.10				0.27
4	0.20	0.15	0.04	0.04	0.32
7	0.26	0.23	0.09	0.10	
10	0.31	0.26	0.14	0.14	0.37
15	0.38	0.29	0.17	0.17	0.40
20	0.44	0.32	0.20	0.23	
25	0.47	0.34	0.24	0.24	0.42
30	0.51	0.35	0.28	0.27	
40	0.54	0.38	0.30	0.28	
45					0.46
60	0.58	0.40	0.32	0.31	
65					0.45
80	0.62	0.41	0.36	0.34	
100	0.62	0.40	0.37	0.36	
105					0.48
120	0.63	0.41	0.40	0.38	
150	0.62	0.41	0.40	0.38	
$D \times 10^{12} (\text{m}^2/\text{min})$	0.95	0.78	2.41	2.81	23.55
$D \times 10^{14} (\text{m}^2/\text{sec})$	<b>1.58</b>	<b>1.3</b>	<b>4.02</b>	<b>4.68</b>	<b>39.25</b>
criteria	8.01E-07	9.81E-07	-7.95E-07	-4.619E-07	7.99E-07

สถาบันวิทยบริการ  
จุฬาลงกรณ์มหาวิทยาลัย

date	01/01/2001	01/01/2001	19/06/2001	04/09/2001	04/09/2001
% Ethanol	60	60	0	60	60
Volume solvent(ml)	500	500	500	500	500
Mass initial (g)	10	10	10	10	10
Temp (°C)	50	60	23	23	23
Size (mm)	0.6-0.8	0.6-0.8	0.3-0.45	0.6-0.8	0.6-0.8
Time (min)/sample	C26	C27	C28	C29	C30
0	0.00	0.00	0.00	0	0
2	0.31	0.44	0.06	0.14	0.14
4	0.39	0.47	0.15	0.22	0.22
7			0.16	0.31	0.31
10	0.46	0.55	0.23	0.34	0.34
15	0.47	0.56	0.26	0.39	0.39
20			0.27	0.43	0.43
25	0.48	0.57	0.30	0.47	0.47
30			0.36		
40			0.39	0.50	0.5
45	0.55	0.61			
60			0.42	0.60	0.6
65	0.59	0.62			
80			0.43	0.64	0.64
100			0.44	0.66	0.66
105	0.59	0.65			
120			0.45	0.66	0.66
150			0.47	0.66	0.66
Dx10 <sup>12</sup> (m <sup>2</sup> /min)	17.17	31.26	4.43	5.42	6.04
	<b>28.62</b>	<b>52.1</b>	<b>7.38</b>	<b>9.03</b>	<b>10.07</b>
criteria	1.30E-07	1.78E-07	-9.09E-08	-6.78E-08	8.92E-07

**Appendix II.II** Concentration of andrographolide in mg/ml of solvent experiment from batch reactor (Batch B)

Volume (ml)	500	500
% ethanol	95	95
Mass initial (g)	20	10
Time (min)/ sample (mg/ml)	B.1	B.2
0	0.00	0.00
2	0.17	0.10
4	0.21	0.14
7	0.24	0.13
10	0.28	0.15
15	0.32	0.18
20	0.36	0.19
25	0.41	0.21
30	0.44	0.23
35	0.45	0.25
40	0.47	0.28
60	0.54	0.30
80	0.59	0.32
100	0.61	0.35
120	0.64	0.36
150	0.65	0.36

APPENDIX III Experiments of extraction column

Experiment N°1

Initial liquid level before pulsation = 0 cm of disc plate

$\dot{m}_{SI}$  (g/min) = 11.33

Theory:  $f_m = 1/1.2$   $f_i = 1/38 \text{ sec}^{-1}$

$\dot{m}_{LI}$  (g/min) = 431.6

Graph:  $f_m = 1/1.19$   $f_i = 1/37.9 \text{ sec}^{-1}$

95% ethanol

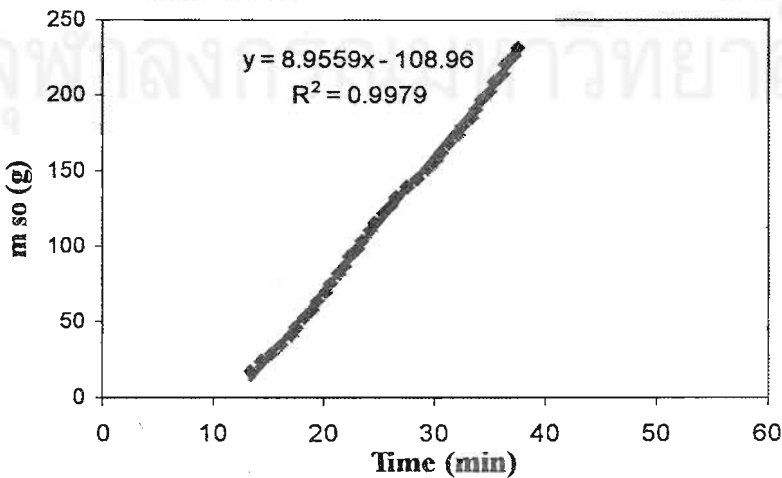
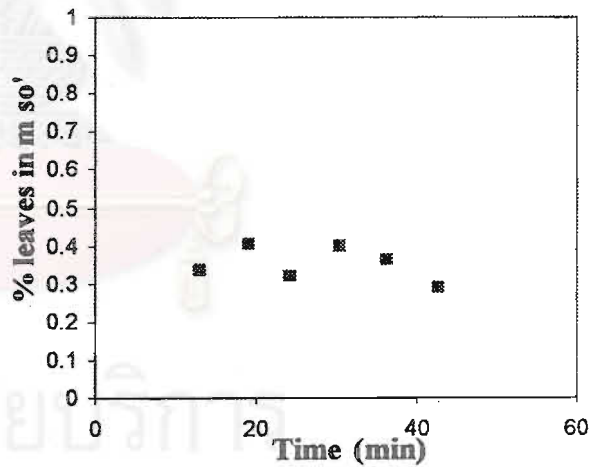
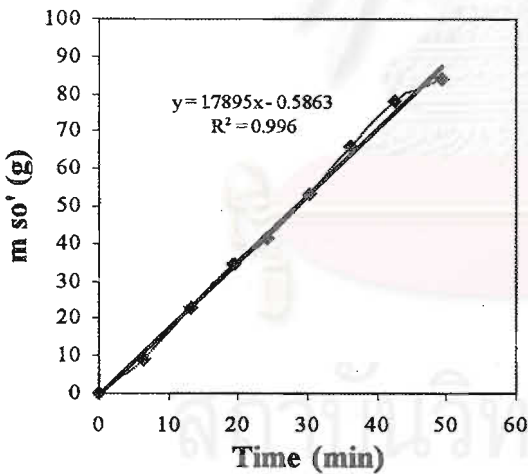
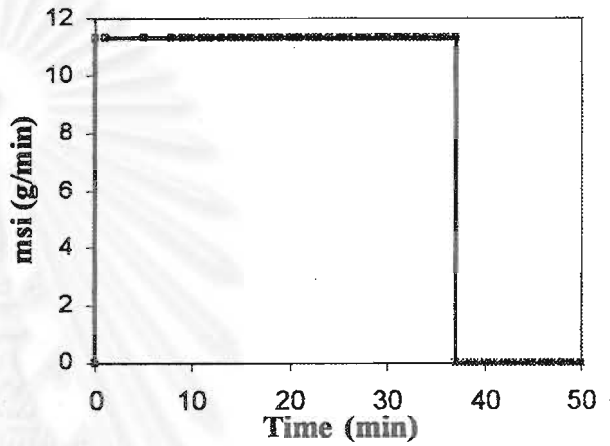
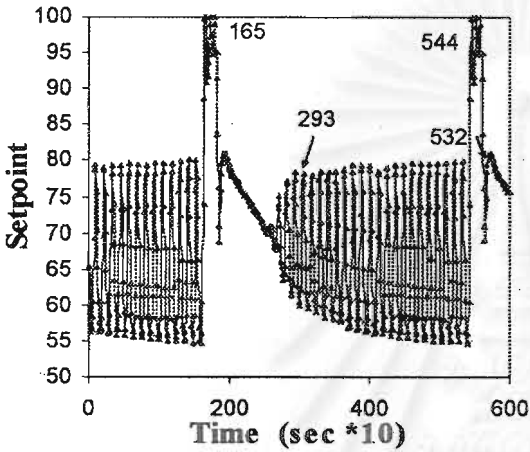
$A_m = 25$   $A_i = 44$  (70-100 psi)

$\alpha' = 0.32$

density = 830 g/cm<sup>3</sup>

Stop solid 37 min

Stop liquid 50 min



Experiment N°2

Initial liquid level before pulsation = 0 cm of disc plate

$\dot{m}_{sl}$  (g/min) = 11.33

Theory:  $f_m = 1/1.2$   $f_i = 1/38 \text{ sec}^{-1}$

$\dot{m}_{ll}$  (g/min) = 431.6

Graph:  $f_m = 1/1.14$   $f_i = 1/37.9 \text{ sec}^{-1}$

95% ethanol

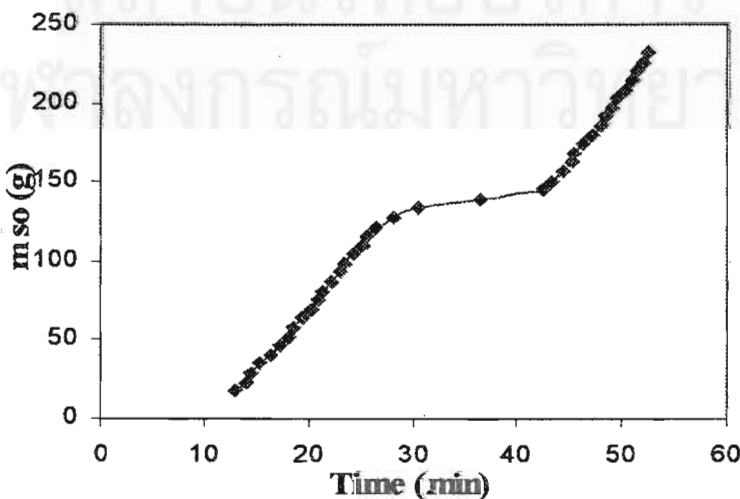
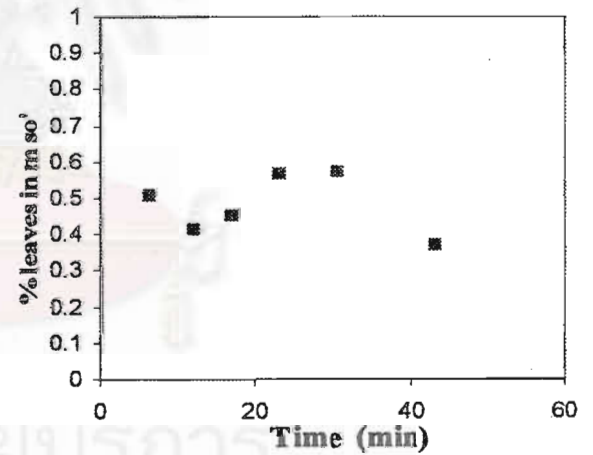
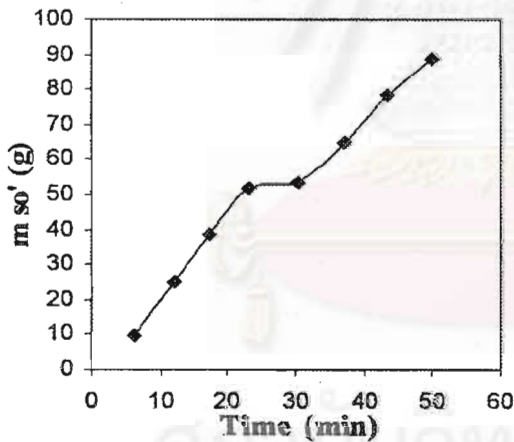
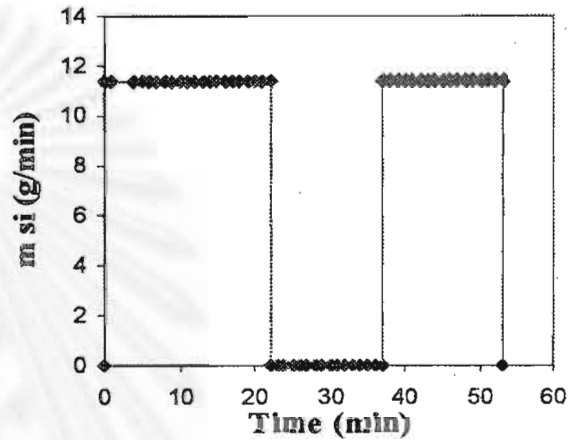
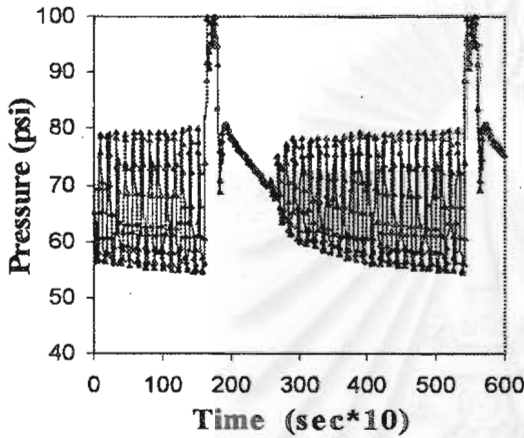
$A_m = 25$   $A_i = 44$

$\alpha' = 0.32$ , density =  $830 \text{ g/cm}^3$

Stop solid 22 min Start solid 37 min

Stop solid 53 min

Stop liquid 53 min



Experiment N°3

Initial liquid level before pulsation = 0 cm of disc plate

$\dot{m}_{sl}$  (g/min) = 11.33

Theory:  $f_m = 1/1.2$   $f_i = 1/38 \text{ sec}^{-1}$

$\dot{m}_L$  (g/min) = 431.6

Graph:  $f_m = 1/1.14$   $f_i = 1/37.9 \text{ sec}^{-1}$

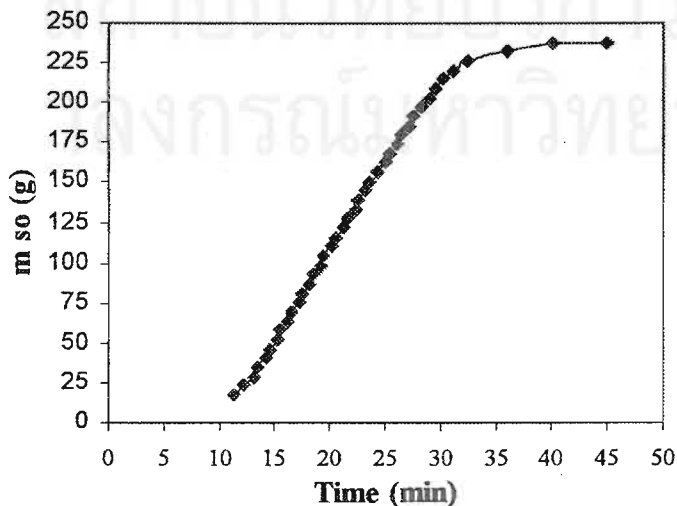
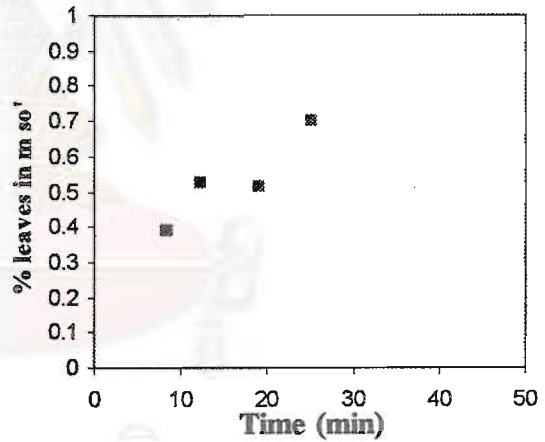
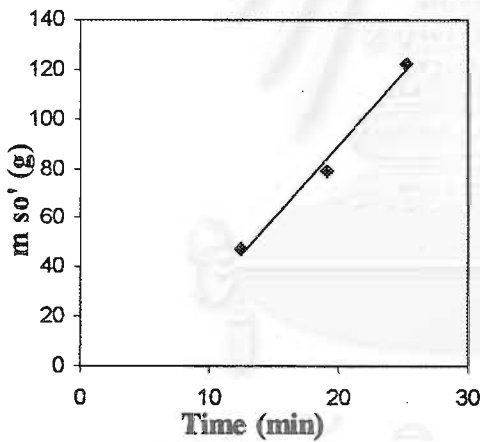
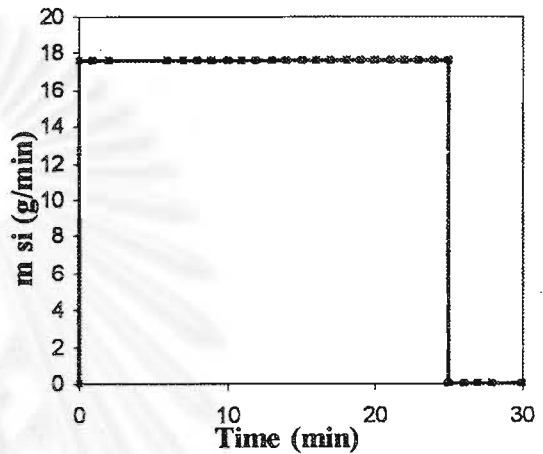
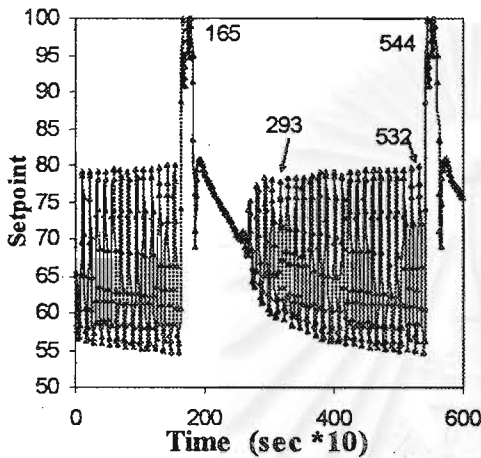
95% ethanol

$A_m = 25$   $A_i = 44$

$\alpha' = 0.53$ , density = 830 g/cm<sup>3</sup>

Stop solid 25 min

Stop liquid 50 min



Experiment N°4

Initial liquid level before pulsation = 0 cm of disc plate

$\dot{m}_{sl}$  (g/min) = 25.85

Theory:  $f_m = 1/1.2$   $f_i = 1/26 \text{ sec}^{-1}$

$\dot{m}_{ll}$  (g/min) = 452.35

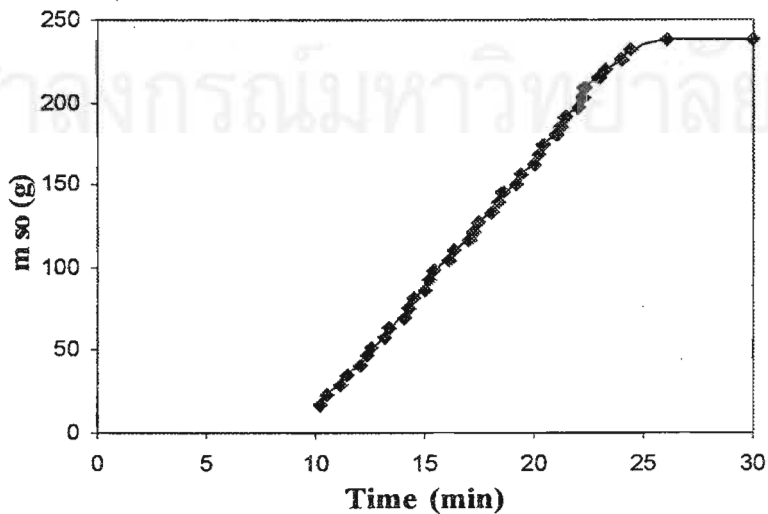
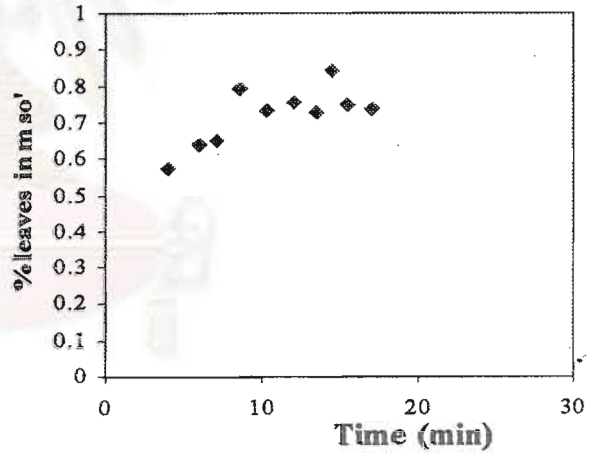
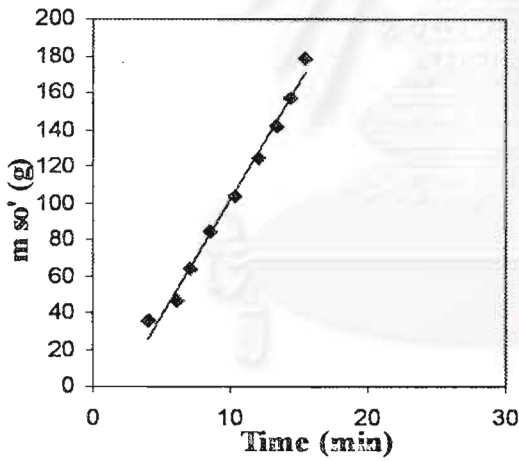
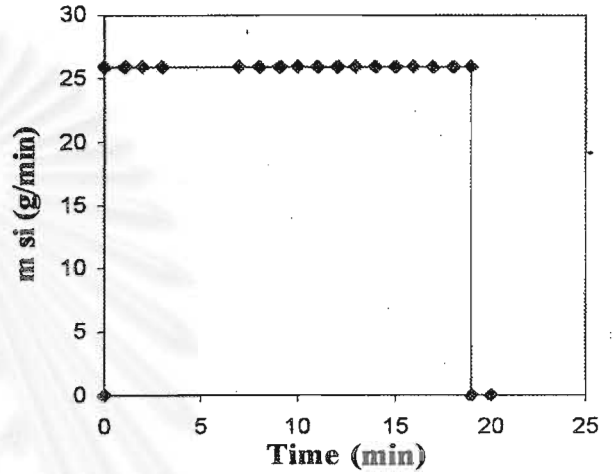
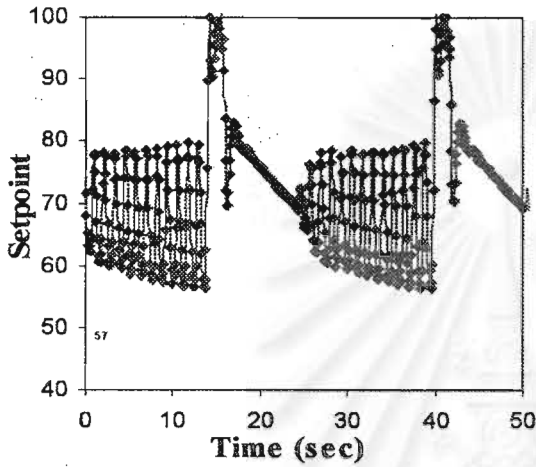
Graph:  $f_m = 1/1.0$   $f_i = 1/25.7 \text{ sec}^{-1}$

95% ethanol

$A_m = 21$   $A_i = 43$

$\alpha' = 0.72$ , density =  $830 \text{ g/cm}^3$

Stop solid 19 min  
Stop liquid 30 min





## Experiment N°5

Initial liquid level before pulsation = +1.5 cm of disc plate

$$\dot{m}_{sl} \text{ (g/min)} = 11.33$$

$$\text{Theory: } f_m = 1/1.2 \quad f_i = 1/38 \text{ sec}^{-1}$$

$$\dot{m}_{ll} \text{ (g/min)} = 419.15$$

$$\text{Graph: } f_m = 1/1.15 \quad f_i = 1/38.1 \text{ sec}^{-1}$$

95% ethanol

$$A_m = 21 \quad A_i = 33$$

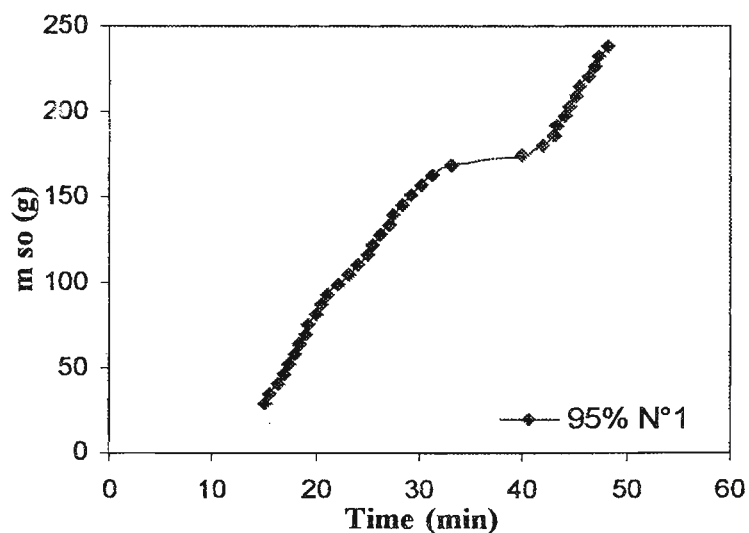
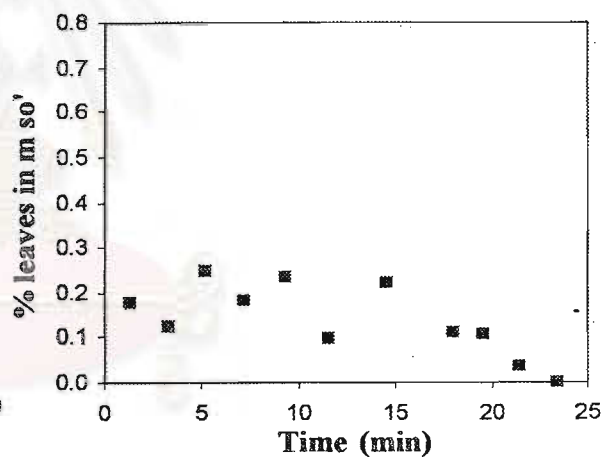
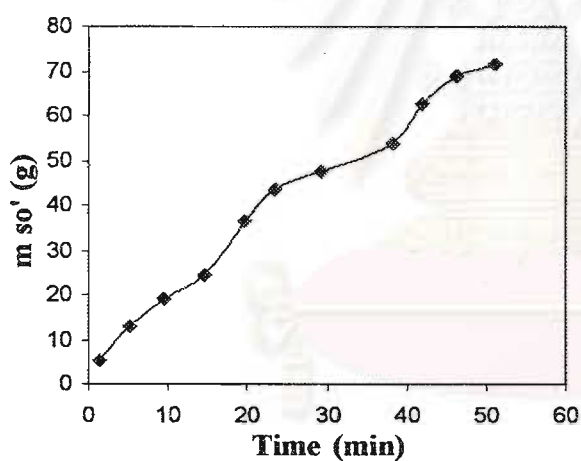
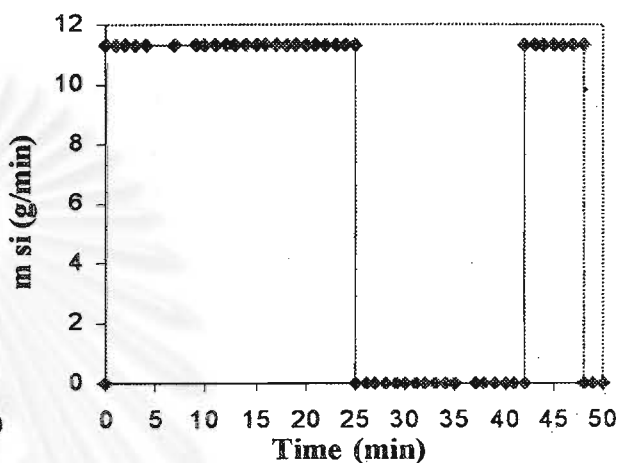
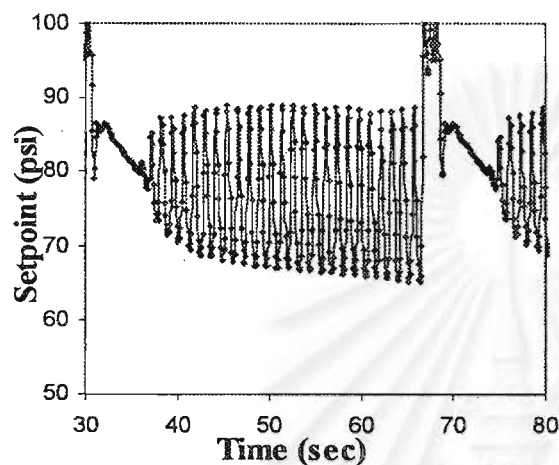
$$\alpha' = 0.15, \text{ density} = 837 \text{ g/cm}^3$$

Stop solid 25 min

Start solid again 42 min

Stop solid 48 min

Stop liquid 51 min



## Experiment N°6

Initial liquid level before pulsation = +1.5 cm of disc plate

$$\dot{m}_{sl} \text{ (g/min)} = 17.57$$

$$\text{Theory: } f_m = 1/1.2 \quad f_i = 1/38 \text{ sec}^{-1}$$

$$\dot{m}_L \text{ (g/min)} = 431.6$$

$$\text{Graph: } f_m = 1/1.15 \quad f_i = 1/38.1 \text{ sec}^{-1}$$

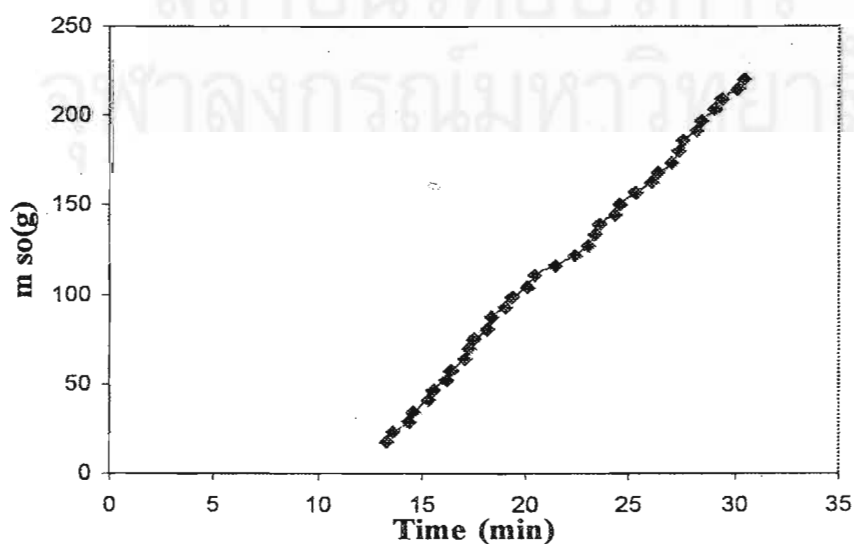
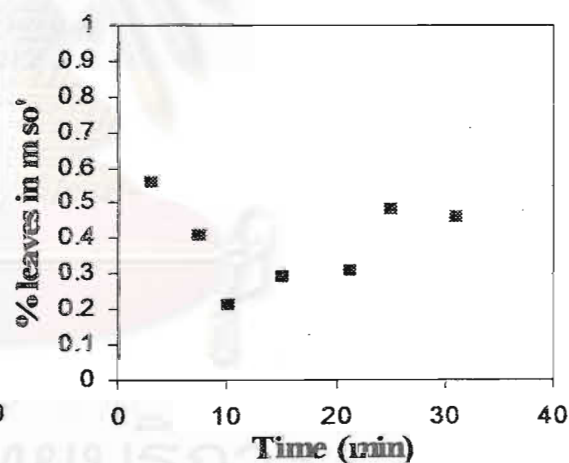
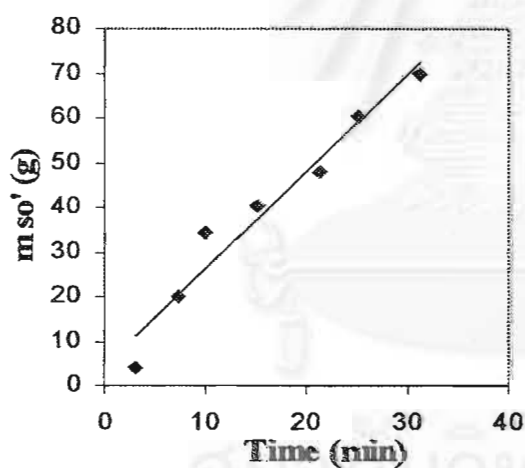
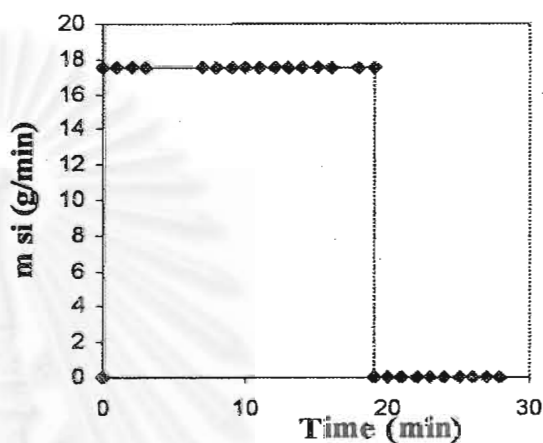
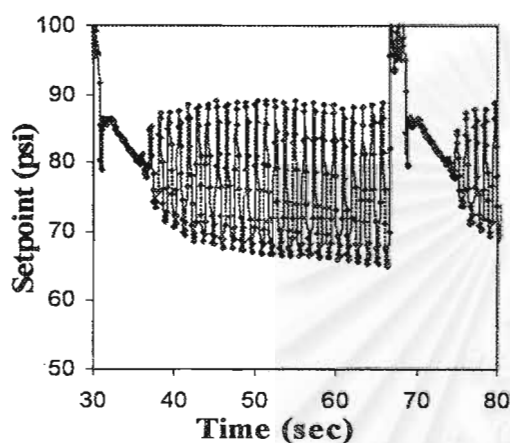
95% ethanol

$$A_m = 21 \quad A_i = 33$$

$$\alpha' = 0.31$$

Stop solid 19 min

Stop liquid 24.3 min



Experiment N°7

Initial liquid level before pulsation = +1.5 cm of disc plate

$\dot{m}_{SI}$  (g/min) = 11.33

Theory:  $f_m = 1/1.2$   $f_i = 1/38 \text{ sec}^{-1}$

$\dot{m}_{LI}$  (g/min) = 368.28

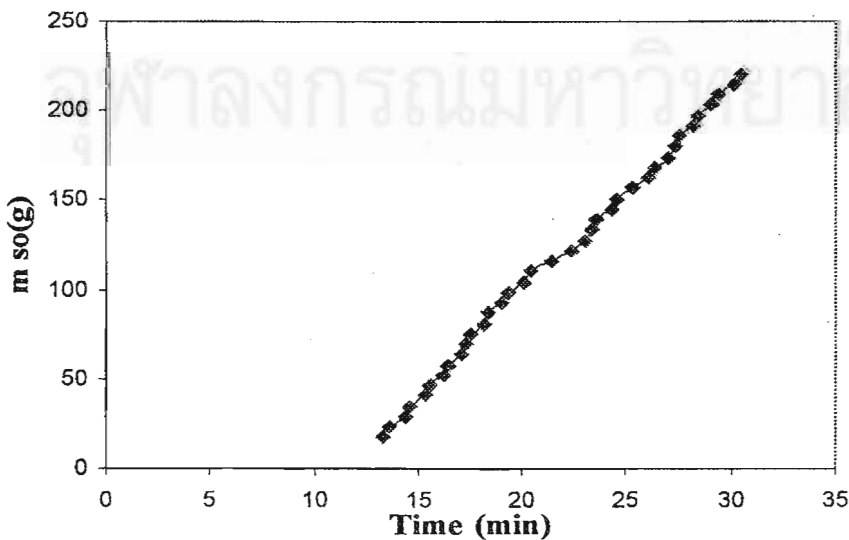
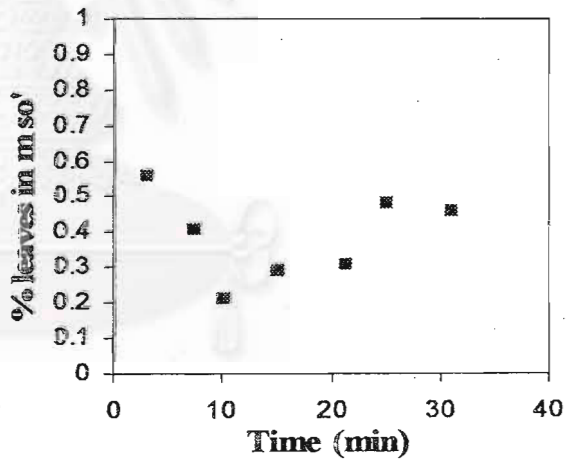
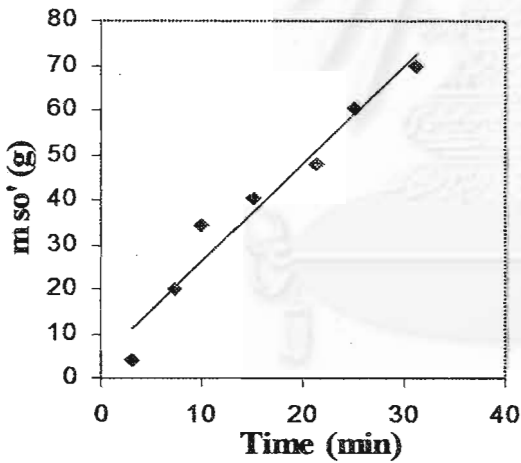
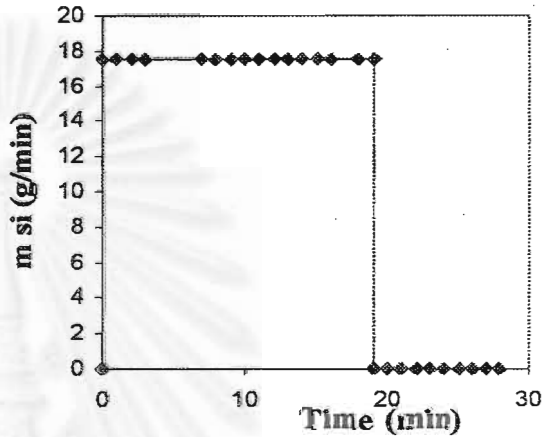
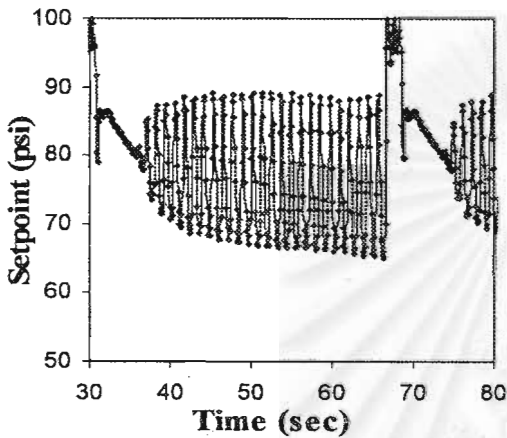
Graph:  $f_m = 1/1.14$   $f_i = 1/37.9 \text{ sec}^{-1}$

70% ethanol

$A_m = 23.5$   $A_i = 44$

$\alpha' = 0.22$ , density  $890 \text{ g/cm}^3$

Stop solid 26 min Start solid again 36.15 min  
 Stop solid 40 min Stop liquid 50.52 min



Experiment N°8

Initial liquid level before pulsation = +3 cm of disc plate

$\dot{m}_{SI}$  (g/min) = 17.57

Theory:  $f_m = 1/1.2$      $f_i = 1/38 \text{ sec}^{-1}$

$\dot{m}_L$  (g/min) = 545.35

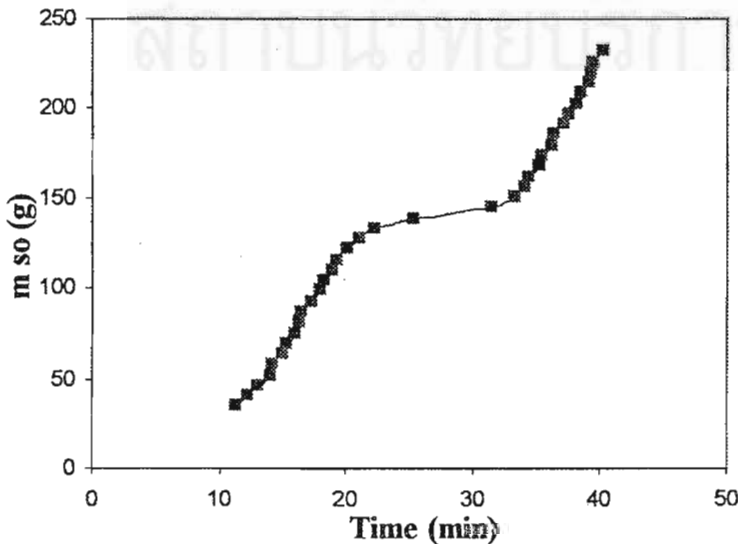
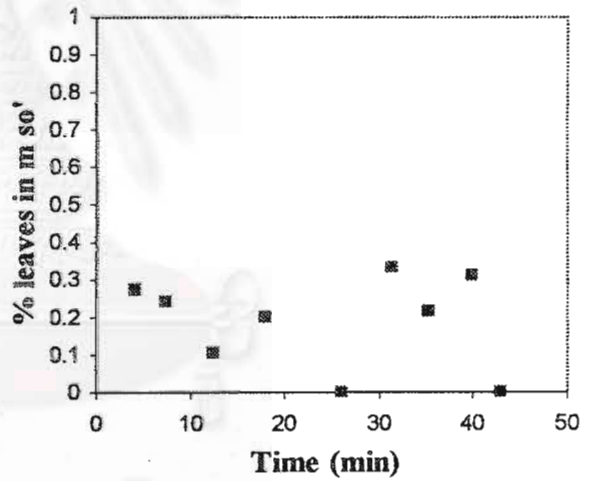
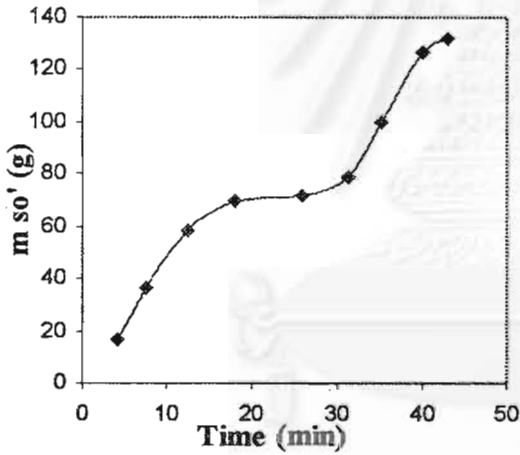
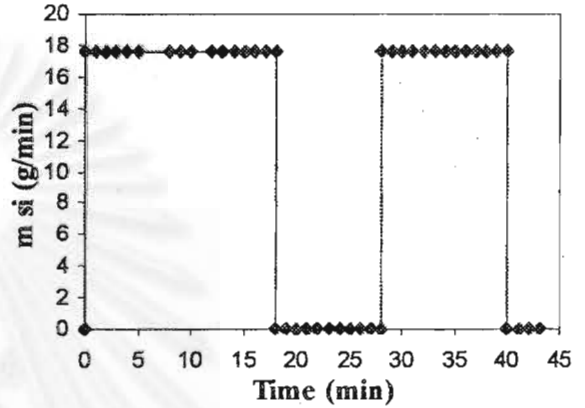
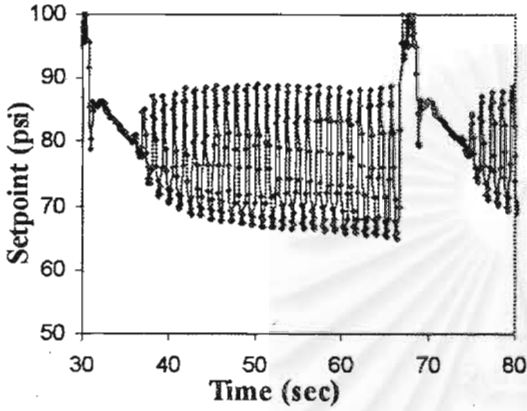
Graph:  $f_m = 1/1.14$      $f_i = 1/38.1 \text{ sec}^{-1}$

70% ethanol

$A_m = 21$      $A_i = 33$

$\alpha' = 0.28$ , density 890 g/cm<sup>3</sup>

Stop solid 17.35 min Start solid again 28 min  
 Stop solid 40 min    Stop liquid 43 min



Experiment N°9

Initial liquid level before pulsation = +1.5 cm of disc plate

$\dot{m}_{sl}$  (g/min) = 11.33

Theory:  $f_m = 1/1.2$   $f_i = 1/38 \text{ sec}^{-1}$

$\dot{m}_{Li}$  (g/min) = 431.6

Graph:  $f_m = 1/1.15$   $f_i = 1/38.1 \text{ sec}^{-1}$

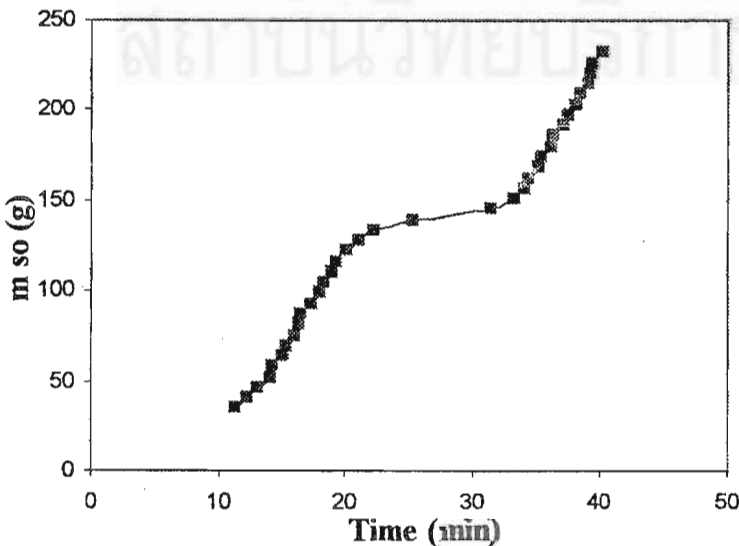
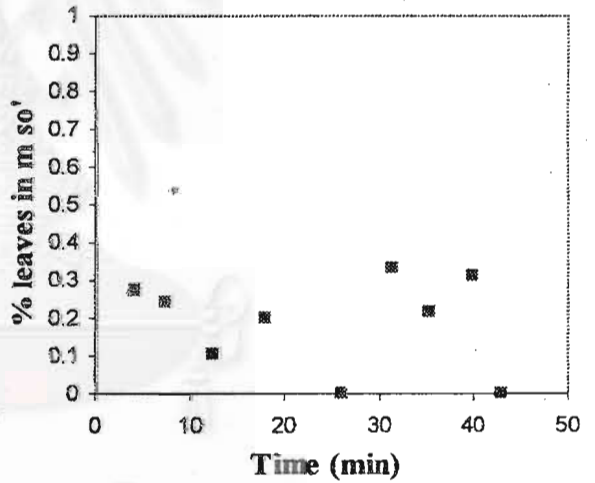
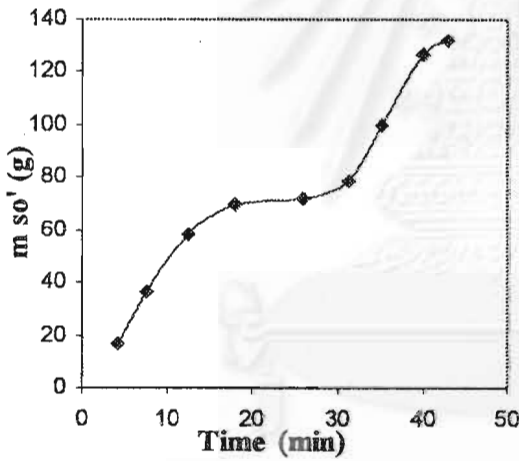
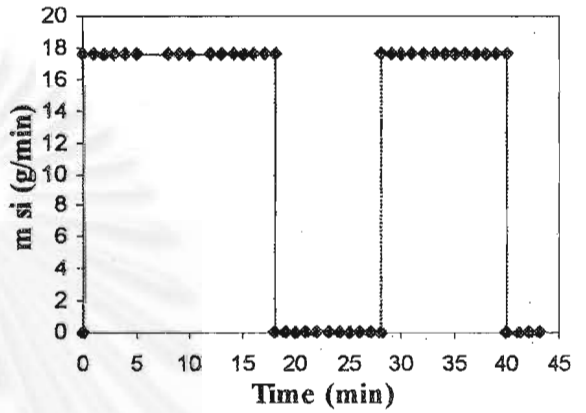
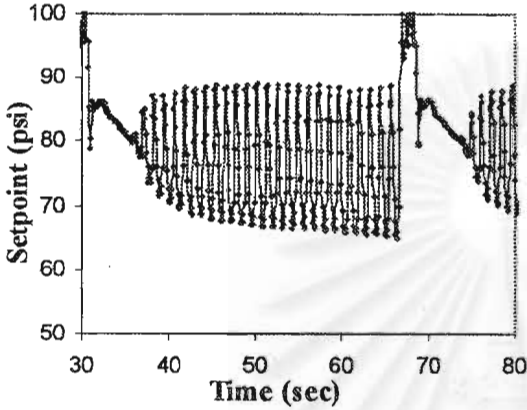
70% ethanol

$A_m = 21$   $A_i = 33$  (80-100psi)

$\alpha' = 0.25$

Stop solid 30 min Start solid again 3 hr 15 min

Stop solid 3hr 25 min Stop liquid 3 hr 30 min



Experiment N°10

Initial liquid level before pulsation = +2 cm of disc plate

$\dot{m}_{sl}$  (g/min) = 11.33

Theory:  $f_m = 1/1.2$   $f_i = 1/38 \text{ sec}^{-1}$

$\dot{m}_{Ll}$  (g/min) = 431.6

Graph:  $f_m = 1/1.15$   $f_i = 1/38.1 \text{ sec}^{-1}$

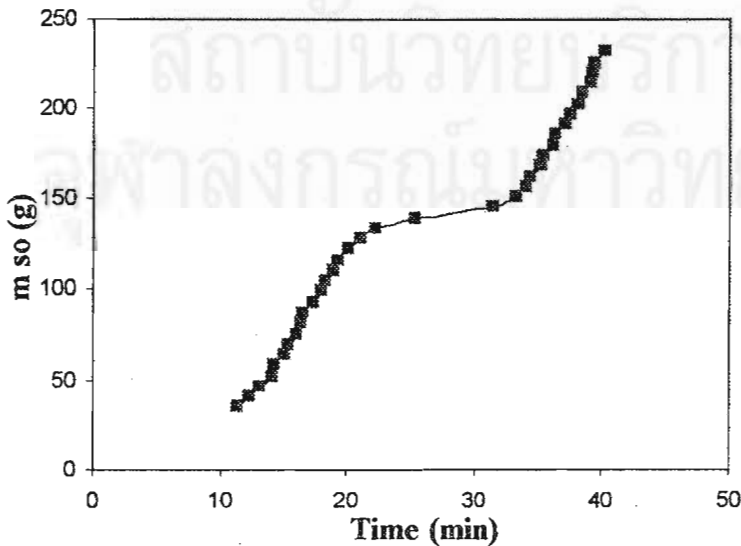
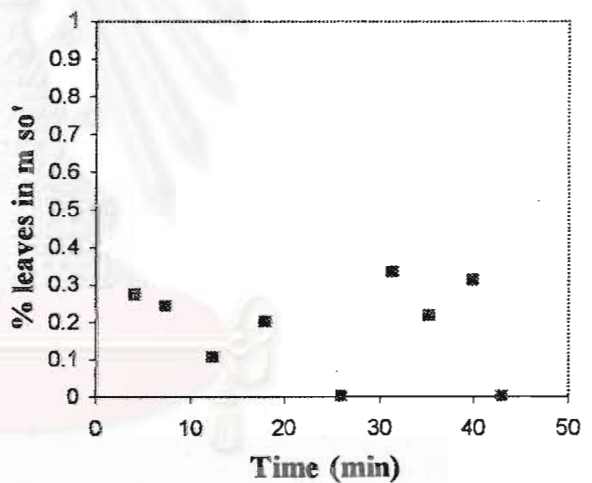
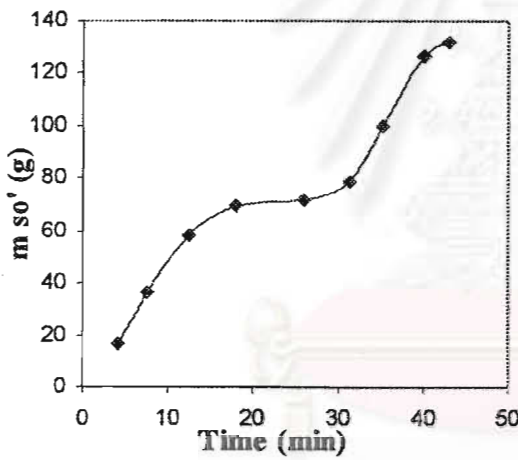
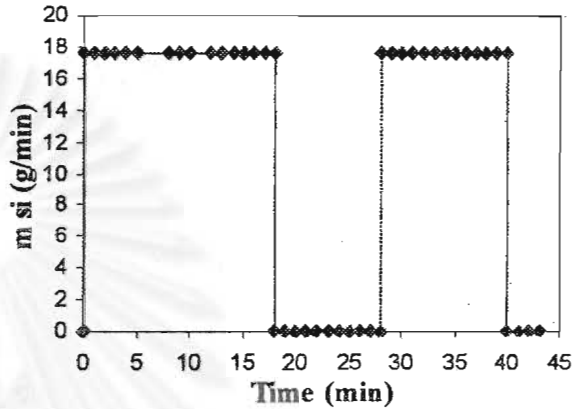
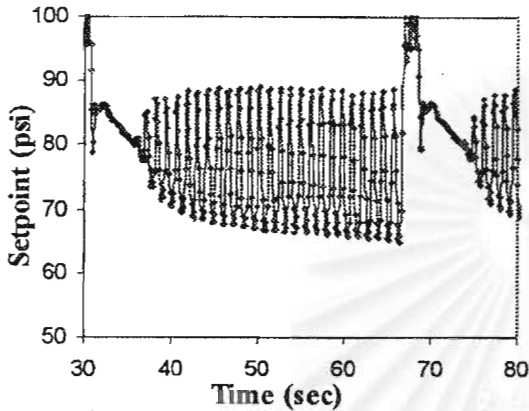
70% ethanol

$A_m = 21$   $A_i = 33$  (80-100psi)

$\alpha' = 0.27$

Stop solid 26 min Start solid again 105 min

Stop solid 116 min Stop liquid 180 min



Experiment N°11,12

Initial liquid level before pulsation = +3.5 cm of disc plate

$\dot{m}_{sl}$  (g/min) = 11.33

Theory:  $f_m = 1/1.2$   $f_i = 1/38 \text{ sec}^{-1}$

$\dot{m}_{Ll}$  (g/min) = 501.4

Graph:  $f_m = 1/1.15$   $f_i = 1/38.1 \text{ sec}^{-1}$

50% ethanol

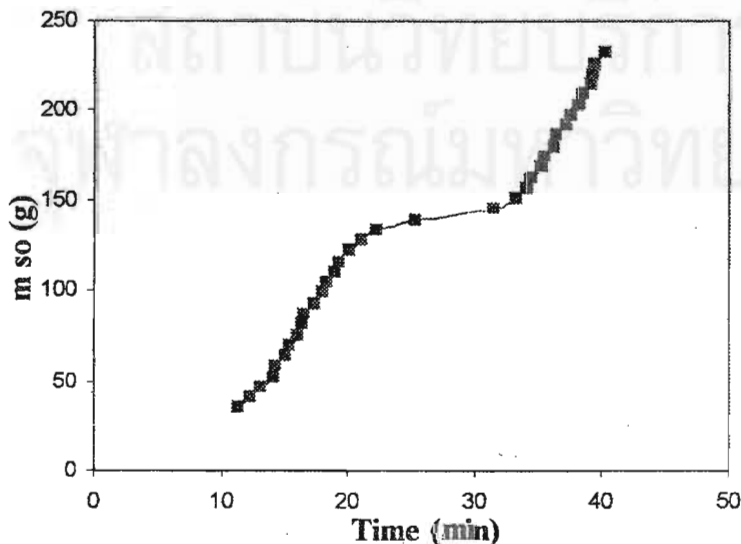
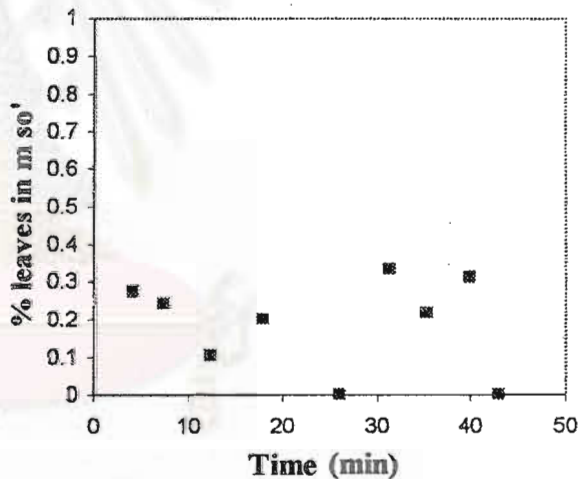
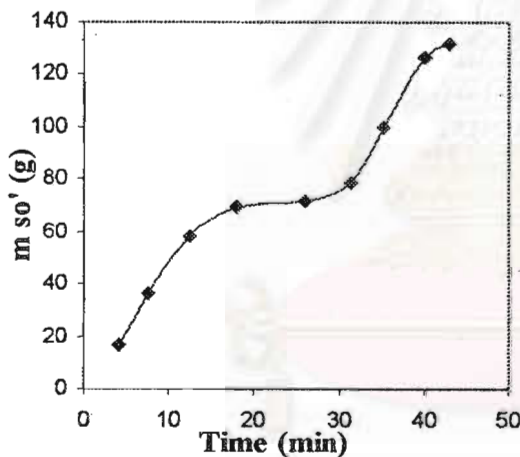
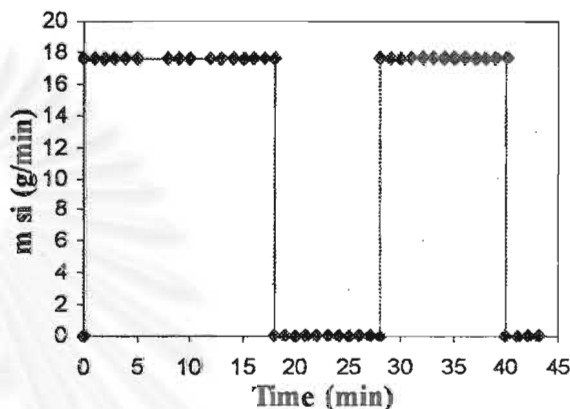
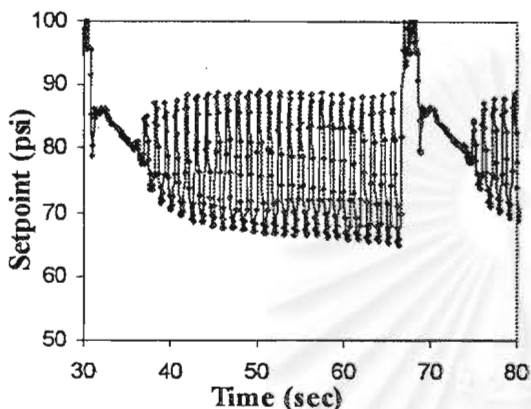
$A_m = 21$   $A_i = 33$  (80-100psi)

$\alpha' = 0.35$

Stop solid 14.20 min Start solid 16.45 min

\* mean  $\dot{m}_{so}$ , and  $\dot{m}_{so}$

Stop solid 29.50 min Stop liquid 60 min



Experiment N°13

Initial liquid level before pulsation = +3.5 cm of disc plate

$\dot{m}_{SI}$  (g/min) = 11.33

Theory:  $f_m = 1/1.2$   $f_i = 1/38 \text{ sec}^{-1}$

$\dot{m}_L$  (g/min) = 482.54

Graph:  $f_m = 1/1.15$   $f_i = 1/38.1 \text{ sec}^{-1}$

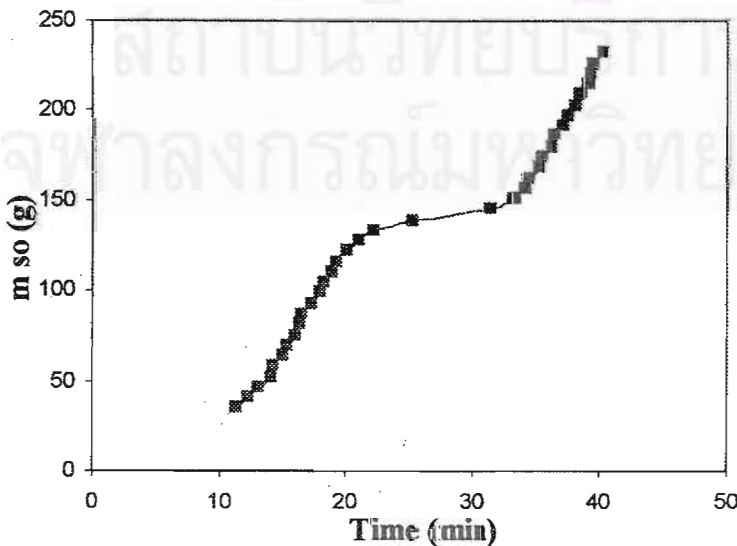
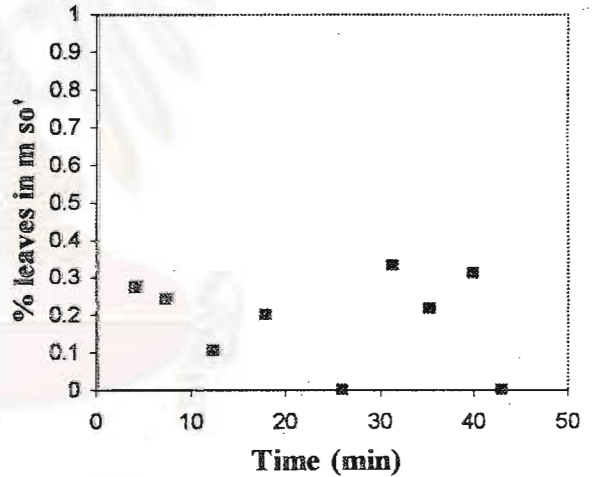
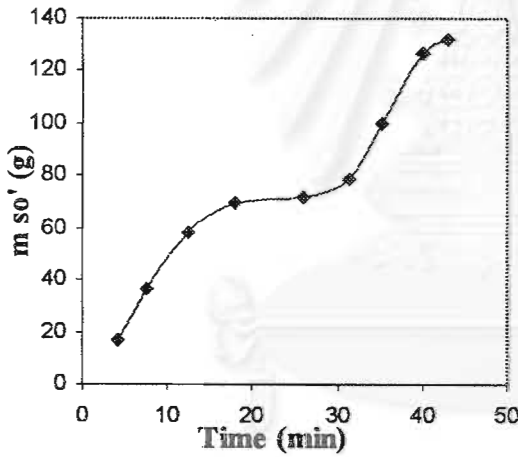
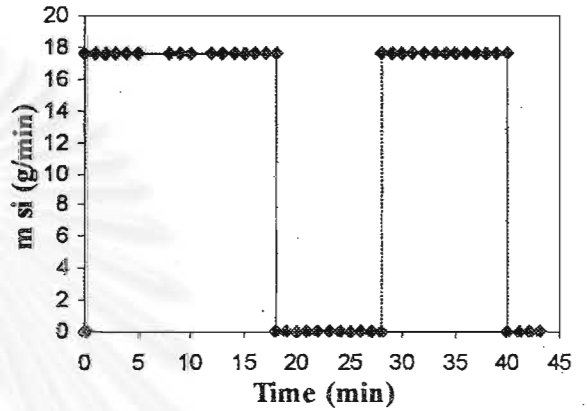
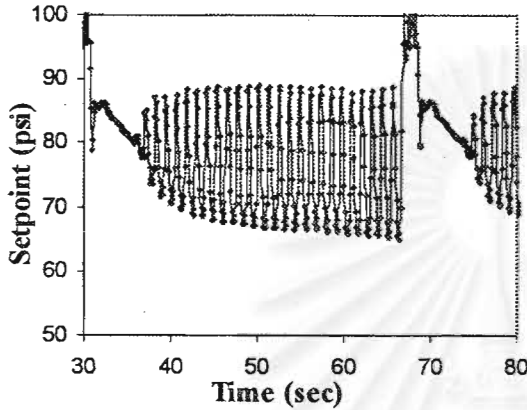
50% ethanol

$A_m = 21$   $A_i = 33$  (80-100psi)

$\alpha' = 0.32$

Stop solid 25.1 min Start solid 92.33 min

Stop solid 105.1 min Stop liquid 190 min





Experiment N°14

Initial liquid level before pulsation = +3.5 cm of disc plate

$\dot{m}_{sl}$  (g/min) = 11.33

$\dot{m}_{Ll}$  (g/min) = 456.01

30% ethanol

$\alpha' = 0.35$

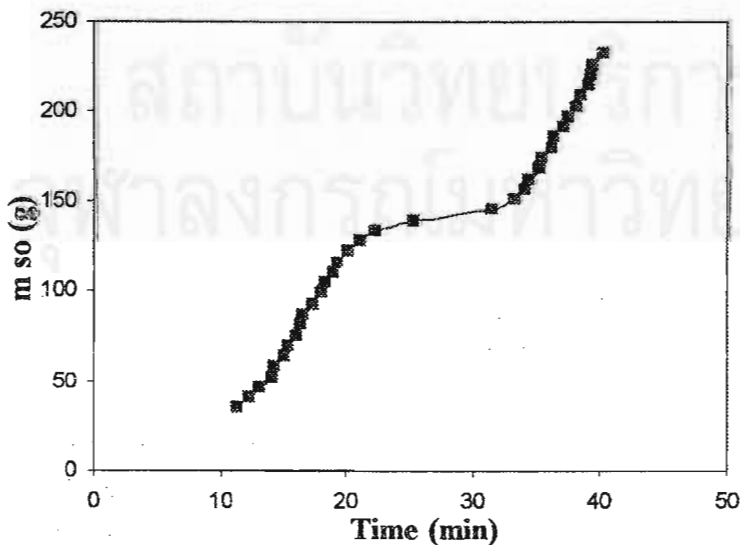
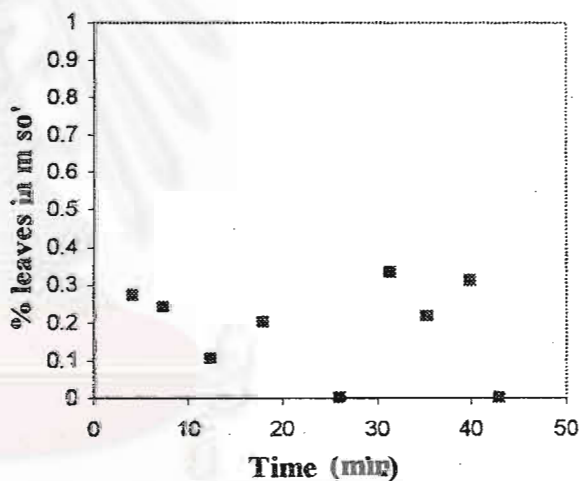
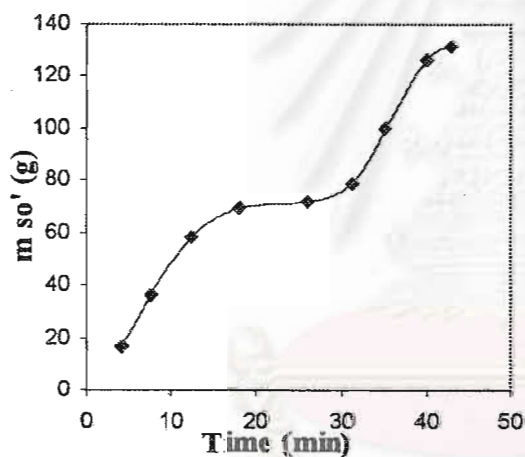
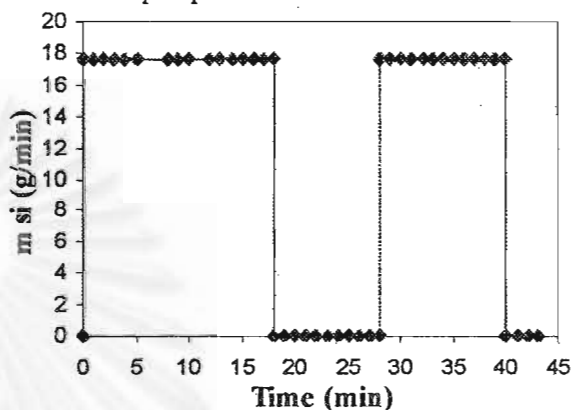
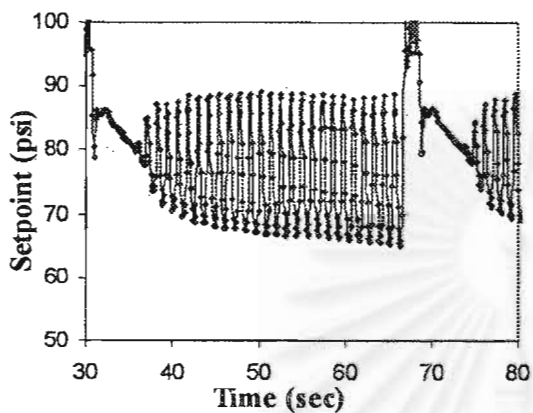
Theory:  $f_m = 1/1.2$      $f_i = 1/38 \text{ sec}^{-1}$

Graph:  $f_m = 1/1.15$      $f_i = 1/38.1 \text{ sec}^{-1}$

$A_m = 21$      $A_i = 33$  (80-100psi)

Start solid 31 min

Stop liquid 50 min



Experiment N°15

Initial liquid level before pulsation = +3.5 cm of disc plate

$\dot{m}_{sl}$  (g/min) = 11.33

$\dot{m}_{Ll}$  (g/min) = 463.18

30% ethanol

$\alpha' = 0.35$

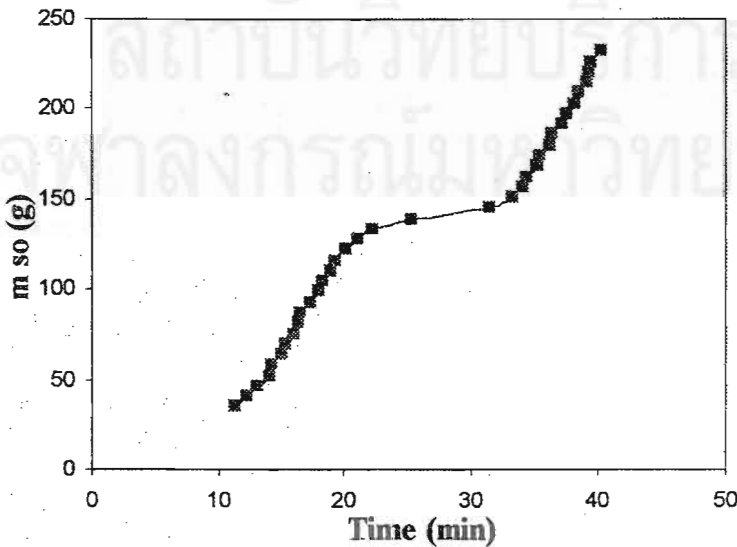
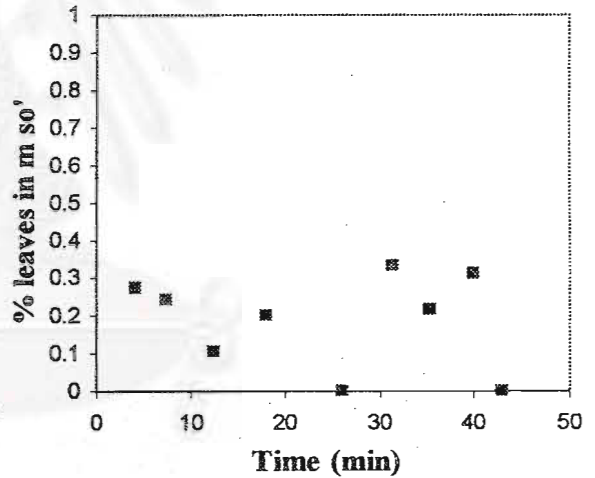
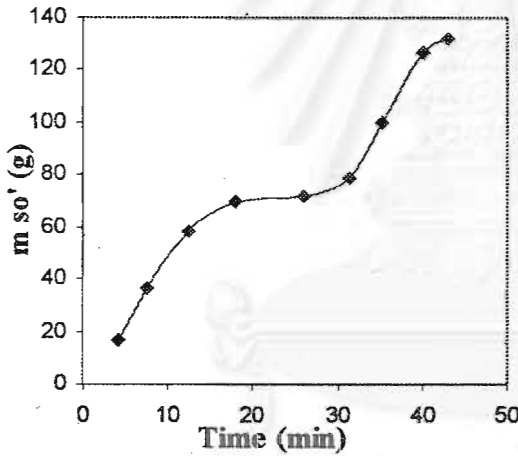
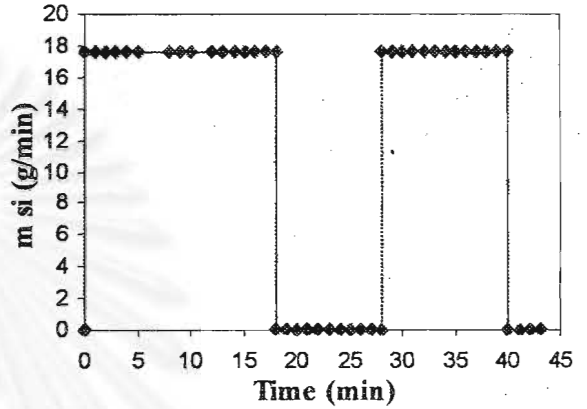
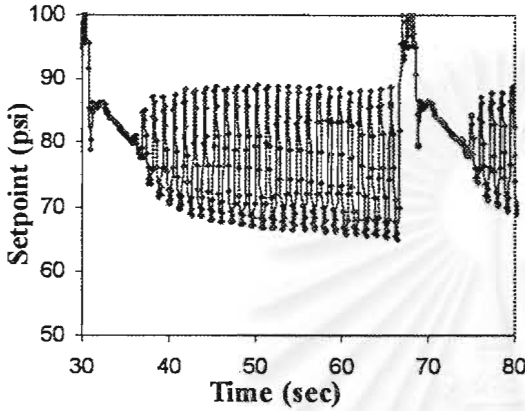
Theory:  $f_m = 1/1.2$   $f_i = 1/38 \text{ sec}^{-1}$

Graph:  $f_m = 1/1.15$   $f_i = 1/38.1 \text{ sec}^{-1}$

$A_m = 21$   $A_i = 33$  (80-100psi)

Start solid 23.35 min

Stop liquid 45 min



## CURRICULUM VITAE

Name: Miss Rutchadaporn Wongkittipong  
 Address: 1730/17 M.6 U-Thong, Suphanburi, 72160 Thailand  
 Date of Birth: June 10, 1977  
 Telephone number: 00 66 (0)35 55 16 53  
 E-mail address: rutchadaporn\_w@hotmail.com

### Education

2000 – Present: PHD RESEARCH FELLOW, Chemical & processes engineering ENSIACET in Toulouse-France.

1999 - Present: PH.D. COURSE at Department of Chemical Technology Faculty of Science, Chulalongkorn University, Thailand.

1995-1998: BACHELORS, Chemical Engineering, Chulalongkorn University Thailand. (Second Honor)

1992 -1994: M.6 Certificate, U-Thong School, Suphanburi, Thailand

1989-1991: M.3 Certificate, U- Thong School, Suphanburi, Thailand

### Training Experiences

1996: Valence Company, Ayutthaya, Thailand  
 1997: Royal Chitralada, Bangkok, Thailand

### Publications

R. Wongkittipong, L. Prat; S. Damronglerd, C. Gourdon, Solid-liquid extraction of Andrographolide from plants, 9th International Summer School of Chemical Engineering, 18-24 September 2001, BULGARIA.

R. Wongkittipong, L. Prat; S. Damronglerd, C. Gourdon, Solid-liquid extraction of Andrographolide from plants experimental study and model, 15th International congress of Chemical and Process Engineering, 25-29 August, 2002, Praha, CZECH REPUBLIC.

R. Wongkittipong, L. Prat; S. Damronglerd, C. Gourdon, Solid-liquid extraction of Andrographolide from plants experimental study, kinetic reaction and model was accepted by Separation and Purification Technology

R. Wongkittipong, L. Prat; S. Damronglerd, C. Gourdon, A new pulsation policy of the solid-liquid extraction in Disc and Doughnut pulsed column, Conference of Thai students in France and Europe, 7-10 November, 2003, Grenoble, FRANCE.